Dissertation zur Erlangung des Doktorgrades
der Fakultät für Chemie und Pharmazie
der Ludwig-Maximilians-Universität München

TCR signals in the identity and function of mature NKT and regulatory T cells

Johann Christoph Vahl

aus

Hannover

2013

Erklärung

Diese Dissertation wurde im Sinne von § 7 der Promotionsordnung vom 28. November 2011 von Herrn Prof. Dr. Klaus Förstemann betreut.

Eidesstattliche Versicherung

Diese Dissertation wurde eigenständig und ohne unerlaubte Hilfe erarbeitet.

München, am 07. Juli 2013

Johann Christoph Vahl

Dissertation eingereicht am

1. Gutachter: Prof. Dr. Klaus Förstemann

2. Gutachter: Prof. Dr. Ludger Klein

Mündliche Prüfung am

Table Of Contents

1. List Of Publications

This thesis is based on the following publications, which are referred to in the text by their Roman numerals (I-III):

I. **Vahl J.C.**, Heger K., Knies N., Hein M.Y., Boon L., Yagita H., Polic B. and Schmidt-Supprian M. (2013). NKT cell-TCR expression activates conventional T cells in vivo, but is largely dispensable for mature NKT cell biology. *PLOS Biology* 11(6): e1001589. doi: 10.1371/journal.pbio.1001589.

II. **Vahl J.C.**, Heger K., Ohkura N., Hein M.Y., Kretschmer K., Prazeres da Costa O., Buch T., Polic O., Sakaguchi S. and Schmidt-Supprian M. TCR ablation leads to loss of regulatory T cell identity. *Manuscript in preparation*.

III. Chu Y., **Vahl J.C.**, Kumar D., Heger K., Bertossi A., Wójtowicz E., Soberon V., Schenten D., Mack B., Reutelshöfer M., Beyaert R., Amann K., van Loo G. and Schmidt-Supprian M. (2011). B cells lacking the tumor suppressor TNFAIP3/A20 display impaired differentiation and hyperactivation and cause inflammation and autoimmunity in aged mice. *Blood* 117: 2227–2236.

2. Abbreviations

AIRE	autoimmune regulator
APC	antigen-presenting cell
BCR	B cell receptor
cTec	cortical thymic epithelial cell
CTLA-4	cytotoxic T lymphocyte associated antigen 4
DC	dendritic cell
DN	double negative
DNA	deoxyribonucleic acid
ER	endoplasmic reticulum
FADD	Fas-associated via death domain
FoxP3	forkhead box P3
HLA	human leukocyte antigen
HSC	hematopoietic stem cell
ICOS	T cell inducible co-stimulator
IFN-γ	interferon-γ
Ii	invariant chain
IL	interleukin
IPEX	immune dysregulation, poly-endocrinopathy, enteropathy, X-linked
LAG-3	lymphocyte activation gene 3
LPS	lipopolysaccharide
MHC	major histocompatibility complex
mRNA	messenger RNA
mTec	medullary thymic epithelial cell
NK cell	natural killer cell
NKT cell	natural killer T cell
PLZF	promyelocytic leukemia zinc finger protein
pT_{reg}	peripherally-derived regulatory T
RAG	recombinase activating gene
RNA	ribonucleic acid
RSS	recombination signal sequences
SP	single-positive
T_C cell	cytotoxic T cell
TCR	T cell receptor
Tdt	terminal deoxynucleotidyl transferase
Tet	ten-eleven-translocation
T_H cell	helper T cell
TNF	tumor necrosis factor
TRAIL	TNF-related apoptosis-inducing ligand
T_{reg}	regulatory T cell
TSA	tissue-specific antigen
tT_{reg}	thymus-derived regulatory T

3. Summary

B cells and T cells, which compose the cells of the adaptive immune system, express highly variable B cell receptors (BCRs) or T cell receptors (TCRs) on their surface. The generation of these receptors through the almost random rearrangement of gene segments during B and T cell development is a tightly controlled process to prevent the occurrence of self-reactive cells that could cause autoimmune diseases. Nevertheless, some T cell subsets, most prominently natural killer T (NKT) cells and regulatory T (T_{reg}) cells, are selected for the expression of autoreactive TCRs that enable them to recognize self-ligands during development. However, to what extent TCR-mediated signals are required to maintain the identity and functional capabilities of mature NKT cells and T_{reg} cells remained incompletely understood.

In **Paper I**, we analyzed the importance and consequences of TCR signals for mature NKT cells by TCR ablation and TCR switch experiments. The vast majority of NKT cells express a semi-invariant TCR, which is composed of the same Vα14i-TCRα-chain for all of these cells, together with a limited set of TCRβ-chains. As expected, we found that transgenic expression of the Vα14i-TCR at the physiological time point during thymic T cell development resulted in the generation of large numbers of bona fide NKT cells. Subsequently, we could show by employing a TCR switch approach that replacing the endogenous TCR repertoire with a Vα14i-TCR on conventional T cells in the immunological periphery is not sufficient to reprogram these cells towards the NKT cell lineage. However, the Vα14i-TCR-expressing formerly conventional T cells were significantly activated, indicating that NKT cells constantly receive autoreactive TCR signals at these locations. Finally, to examine whether these autoreactive TCR signals are important for NKT cell homeostasis and effector function, we ablated TCR expression on a fraction of NKT cells and followed their fate over time. Since NKT cell lineage identity, homeostasis and their innate rapid cytokine secretion abilities were virtually unchanged upon TCR ablation, our results indicate that peripheral NKT cells become unresponsive to and thus are independent of their continuously autoreactive TCR.

T_{reg} cells are indispensable to prevent the development of autoimmune diseases. Similar to NKT cells, T_{reg} cells are selected upon auto-antigen recognition during thymic development, although not much is known about the nature of the selecting ligands. Furthermore, accumulating evidence suggests that T_{reg} cells still receive stronger TCR signals

than conventional CD4 T cells upon emigration to the periphery. In order to examine the impact of these signals, we inducibly ablated the TCR from T_{reg} cells and monitored the homeostasis, gene expression and suppressive function of TCR-deficient T_{reg} cells (**Paper II**). Interestingly, T_{reg} cell biology is strongly changed upon the loss of TCR expression. The TCR-deficient T_{reg} cells decayed quickly, lost a substantial proportion of their typical gene expression pattern, and furthermore lost the expression of several key suppressor proteins. Therefore, we could show that in striking contrast to NKT cells, T_{reg} cells rely on tonic signals received through their autoreactive TCR to maintain their cellular identity and functionality.

In addition to TCR signals, T cell behavior can also be heavily influenced through immunomodulatory cytokines. The deletion of the ubiquitin-editing enzyme A20, a negative regulator of the NF-κB signaling cascade, specifically in B cells led to cellular expansion and activation of T cells as well as myeloid cells (**Paper III**). We present evidence that this expansion was most likely caused by the spontaneous release of pro-inflammatory cytokines, prominently IL-6, through A20-deficient B cells. Interestingly, under these conditions T_{reg} cells were also expanded, and might keep the sterile inflammation initially at bay.

In summary, we could demonstrate that for two inherently autoreactive T cell subsets, NKT cells and T_{reg} cells, the dependence on autoreactive signals for homeostasis, gene expression and function is fundamentally different. On the one hand, NKT cells become completely independent from their autoreactive TCR during their development, similar to receptors of cells of the innate immune system. In contrast, T_{reg} cells that do not receive continuous TCR signals quickly lose their suppressive potential as well as a large part of their signature gene expression, and they also rapidly decay.

4. Introduction

The human body is under constant attack from various pathogens, disease-causing agents, such as bacteria, viruses, fungi, protozoa and parasites. During evolution, an immune system has developed that is able to efficiently protect us. Broadly, it can be separated into two parts: the innate and the adaptive immune system [1,2]. The innate immune system is composed of cells that recognize pathogen-associated foreign structures with germline-encoded receptors. B cells and T cells constitute the adaptive arm of the immune system. In contrast to receptors of the innate immune system, each of these latter cells assembles a unique receptor from many gene segments in a randomized process during their development – the B cell receptor (BCR) or T cell receptor (TCR) [3,4]. This resulting huge repertoire of receptor specificity guarantees that at least in principle, an adaptive immune response against every pathogen can be generated. Upon activation by their cognate antigen, individual B and T cells enormously expand in order to effectively combat pathogenic invaders.

4.1. T cell biology

T cells are named after the thymus, a primary lymphoid organ in which most steps of T cell development take place. The structure and function of the thymus are conserved in animals harboring an adaptive immune system [5].

T cells recognize antigen through their heterodimeric T cell receptor (TCR), which is expressed on the cell surface [6,7]. It consists of TCRα and TCRβ polypeptide chains in more than 85 % of all T cells, which are linked through a disulfide bond (**Figure 1**). This subset is called α/β T cells [8]. Few T cells express TCRγ/TCRδ chains and will not be discussed here in more detail [8-10]. TCRα-/TCRβ-chains have short cytoplasmic tails, consisting of around 5-12 amino acids, which cannot transduce signals to the cytosol [6,10]. Instead, they are associated with the non-polymorphic CD3 complex, composed of CD3γ, CD3δ, CD3ε and CD3ζ, which induces intracellular signaling pathways upon TCR receptor binding [11-15].

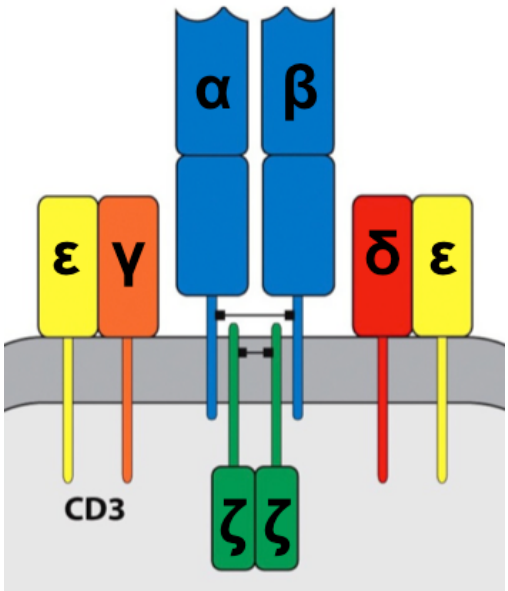

Figure 1 α/β T cells recognize antigen through their heterodimeric T cell receptor. Upon T cell receptor crosslinking, CD3 molecules mediate intracellular signaling. Figure is adapted from [1].

4.1.1. Antigen presentation to T cells

The vast majority of T cells recognize peptide antigens, presented through major histocompatibility complex (MHC) proteins. In the human, the system is called human leukocyte antigen (HLA), and constitutes the most polymorphic region of the whole genome, with over 7000 allelic variants over the population [16]. In both man and mice, two classes of MHC molecules can be found, termed MHCI and MHCII, which vary in their function, loading and cellular expression [10,16].

The main role of MHCI is to present intracellular peptides. Thereby, virus- or bacteria-infected cells, or cells that are oncogenic, can be recognized and destroyed by the immune system. MHCI is composed of the MHCI α-chain and β_2-microglobulin [10]. It is expressed on the surface of all nucleated cells. Nuclear or cytoplasmic proteins are constantly being degraded through proteasomes, the resulting fragments are shuttled to the endoplasmic reticulum (ER) and loaded onto MHCI [10]. Usually, these peptides are rather short, with around 8-14 amino acids [16]. Only upon successful loading of a peptide, the peptide-MHCI complex is presented on the cell surface.

In contrast to MHCI, MHCII mainly presents peptides derived from endocytic pathways. Thereby, immune responses against extracellular pathogens can be mounted [10,17]. Importantly, MHCII is almost exclusively expressed on the surface of antigen-presenting cells (APCs), such as dendritic cells (DCs), B cells and macrophages, as well as on thymic epithelial cells [10,17]. Still, in some conditions, such as inflammation, MHCII expression can be also induced in other cells [10]. Peptide fragments presented by MHCII are at least 13 amino acids long, but they can also be much longer [10]. MHCII is composed of an MHCIIα and MHCIIβ chain. In the ER, these molecules form a complex together with a third protein, the invariant chain (Ii). The Ii stabilizes the MHCII dimer and inhibits loading of other peptides [10]. Furthermore, the invariant chain is thought to play a role in targeting MHCII to late endosomes, where it finally dissociates from MHCII to allow loading of exogenous peptides [10].

However, exceptions to this strict separation have been demonstrated. In some conditions like viral infections, dendritic cells (DCs) are able to engulf infected cells and present processed peptides of these cells over MHCI, a process which is called cross-presentation [9,10]. Furthermore, endogenous peptides derived from autophagy may also be presented via MHCII [10,18].

4.1.2. T cell co-receptors

CD4 and CD8 are both designated as co-receptors, as they were shown to bind together with the TCR to peptide-MHCII or peptide-MHCI complexes, respectively [12,19]. The simultaneous binding to the same peptide-MHC molecule has been shown to strongly increase the signaling intensity in comparison to TCR binding alone [12]. CD4 is a single-chain protein, consisting of four immunoglobulin-like domains (**Figure 2**). CD8 is usually a heterodimer of the CD8α/CD8β-chain, which each contain one immunoglobulin-like domain. Few T cells also express CD8α-homodimers.

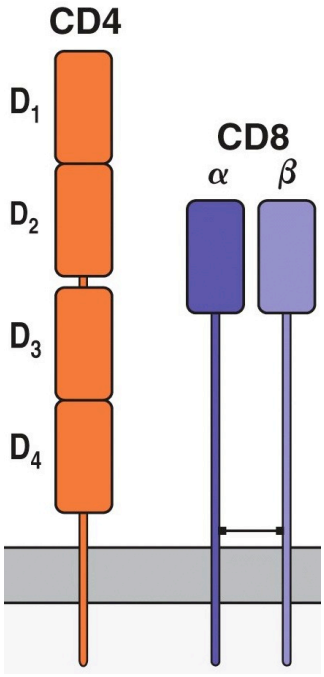

Figure 2 The CD4 and CD8 co-receptors are composed of Ig domains. Figure is adapted from [1].

4.1.3. T cell receptor rearrangements

T cell development is a stepwise process. Hematopoietic stem cells (HSCs) in the bone marrow constantly generate T cell progenitors, which leave the bone marrow and enter the thymus [17,20]. There, developing T cells can be distinguished by their distinct expression pattern. Early T cell-precursors do not express CD4 or CD8 on their surface; this is called the double-negative (DN) stage [8,17]. These cells can further be distinguished by surface expression of the proteins CD25, the α-chain of the high affinity receptor for the cytokine IL-2, and the adhesion molecule CD44, into DN1 (CD44+ CD25-), DN2 (CD44+ CD25+), DN3 (CD44- CD25+) and DN4 (CD44- CD25-) [8,17].

A crucial process during thymic T cell development is the generation of a functional and diverse TCR repertoire. This is accomplished through V(D)J recombination, sometimes also called somatic recombination. In this process, each one of the various variable (V), joining (J) and in the case of the TCRβ-chain also diversity (D) gene segments are joined together and put in close proximity of the constant (C) exons of these genes [21]. The parts of the TCR encoded by V, D and J segments contact the antigen/MHC complex, whereas the constant region encodes the part that anchors the polypeptide in the cell membrane (**Figure 3**).

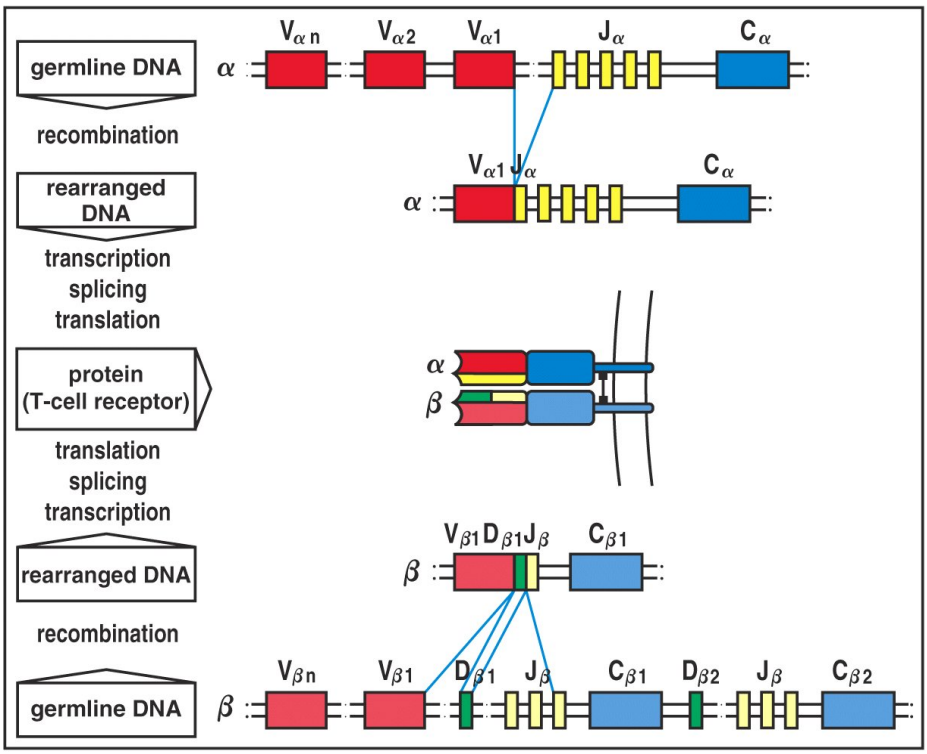

Figure 3 During V(D)J recombination, the germline V, (D in the case of the TCRβ chain) and J segments are joined together in an almost random process. Expression of these variable TCR chains yields a highly diverse TCR repertoire. Figure is adapted from [1].

In the human, the TCRβ locus consists of around 47 V, 13 J, 2 D and 2 C genes, whereas the TCRα locus consists of 70 V genes, 61 J genes and one C gene [13]. The main enzymes involved in V(D)J recombination are two recombinases, called recombination activating gene-1 (RAG-1) and RAG-2. These enzymes recognize recombination signal sequences (RSS) flanking the V(D)J gene segments [4]. During recombination, RAG molecules introduce DNA double-strand breaks, which are reassembled together by non-homologous end joining [3,4].

It has been shown that both enzymes are expressed in two waves in developing T cells [22,23]. First, RAG-1 and RAG-2 are expressed at the DN2 (CD44+ CD25+) stage, when rearrangements of the TCRβ-chain take place. If the rearrangement of the TCRβ-chain was successful, meaning that no stop codon was introduced during recombination and a full-length protein can be generated, the TCRβ-chain is expressed on the cell surface together with a germline-encoded pre-Tα chain [17]. Once the cell receives signals through this pre-TCR, expression of both recombinases is stopped and the cells undergo 6-8 divisions [17,23]. Subsequently, the cells upregulate CD4 and CD8 to become double-positive (DP) thymocytes, and re-express RAG-1 and RAG-2 to rearrange the TCRα chain in a similar manner [17,23]. However, in contrast to the generation of the TCRβ-chain, T cells can

undergo several rounds of rearrangements, termed secondary rearrangements, of the TCRα chain locus on one chromosome [24] (**Figure 4**). Primary rearrangements were shown to start at the 3' Vα segments and 5' Jα segments of the TCR. If these do not lead to positive selection of the developing T cell, secondary rearrangements of flanking 5' Vα segments and 3' Jα take place, thereby optimizing the generation of mature T cells by allowing them to test several possible TCRα chains during thymic selection [24].

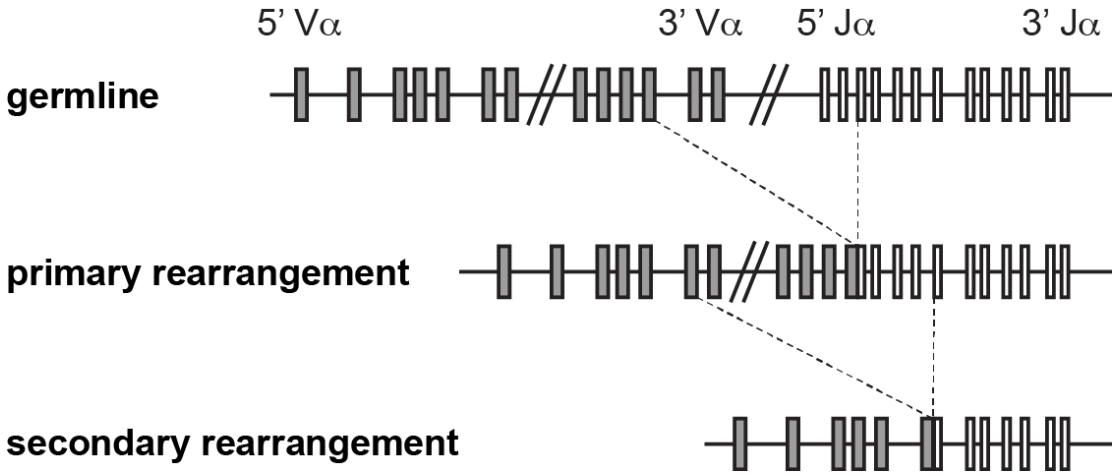

Figure 4 The structure of the TCRα-locus allows several sequential rounds of V(D)J recombination, termed secondary rearrangements.

Theoretically, T cells are capable to express one out of more than 10^{15} different receptors [16,25], although the actual repertoire found in the periphery of mice (~ 2 x 10^6) and humans (~ 2.5 x 10^8) is much smaller [25,26]. One factor how this high TCR diversity is accomplished is the random selection of different segments during V(D)J recombination. Moreover, the diversity is further increased through imprecise joining of the segments at the junctions, and also through the random removal or addition of nucleotides through the enzyme terminal deoxynucleotidyl transferase (TdT) [25,27].

4.1.4. T cell selection

During T cell development, it is on the one hand of importance that the newly generated TCR is able to recognize MHC-presented peptides [16]. On the other hand, the development of self-reactive T cells that could cause pathology has to be strictly prevented [28]. To meet both requirements, T cells undergo strict selection processes in the thymus before they are released in the periphery [17-19,28]. These processes mostly take place at two different anatomical locations in the thymus, an outer part called cortex, and an inner part called medulla [17,18,28].

T cell progenitors enter the thymus and undergo V(D)J recombination in the cortex [8,17] (**Figure 5**). Upon TCR surface expression, DP T cells are tested for their ability to recognize self-peptides presented by MHCI and MHCII on cortical thymic epithelial cells (cTECs) [18,28]. In this interaction, the vast majority of T cells does not receive a sufficient stimulus through their newly developed TCR to survive, causing "death through neglect" [17,18,28]. Only those T cells expressing a potentially useful TCR with sufficient affinity for self-antigen-MHC complexes are positively selected and allowed to survive [19]. Depending on whether the recognized antigen is presented via MHCI or MHCII, T cell commitment towards the CD8- or CD4-lineage takes place at this developmental stage, and the cells downregulate expression of either CD4 or CD8 to become single-positive (SP) T cells [19,29,30].

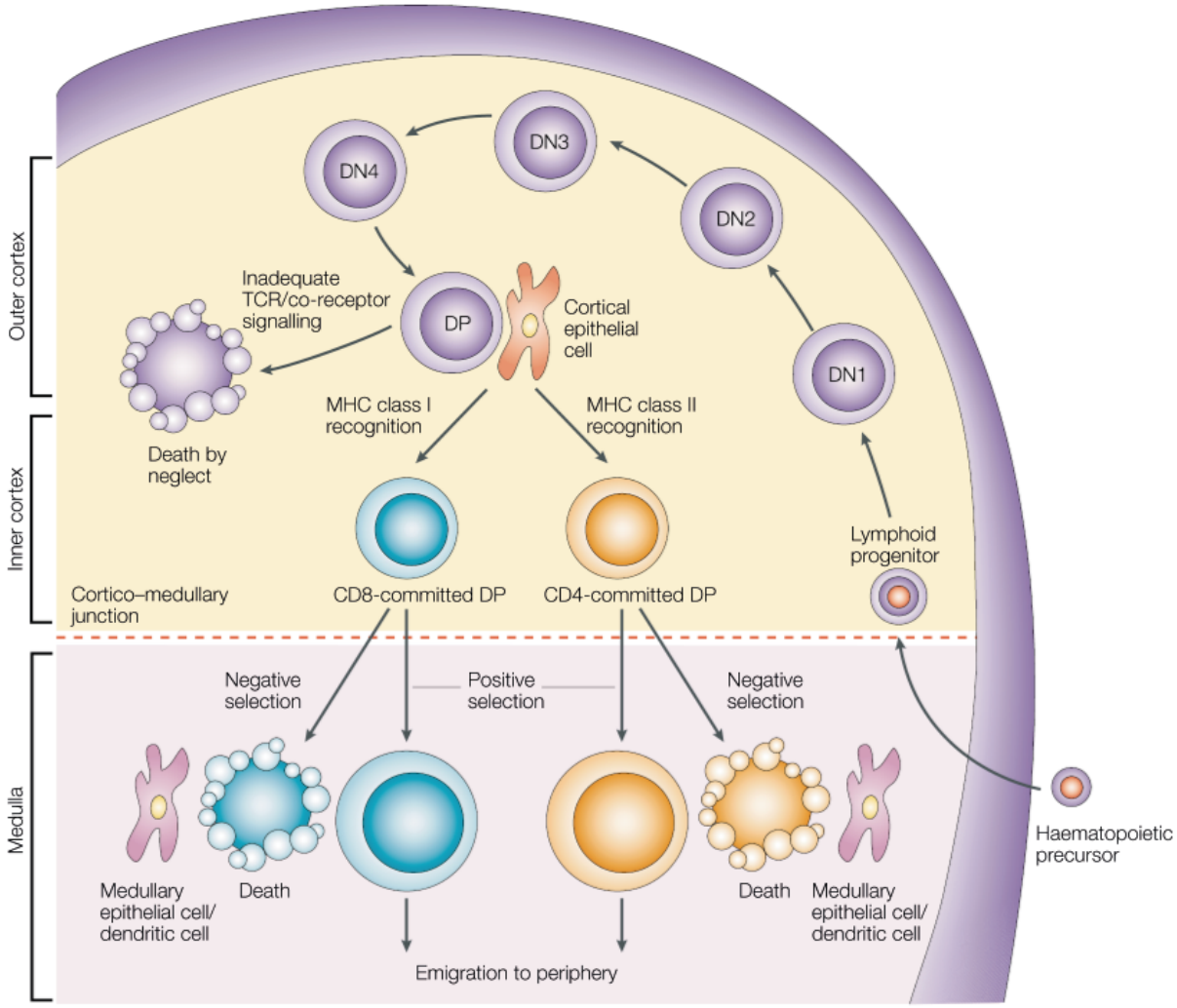

Figure 5 Overview of thymic T cell development. T cell progenitors migrate from the bone marrow into the thymus. There, they start to rearrange their T cell receptor. Upon surface expression, these cells undergo positive and negative selection mechanisms before they finally leave the thymus as naïve mature T cells. Figure is adapted from [17].

The final steps of thymic T cell development take place in the thymic medulla. Here, autoreactive T cells recognizing self-peptides are deleted from the repertoire. It has been shown that medullary thymic epithelial cells (mTECs) are able to present tissue-specific antigens (TSA) due to the actions of a protein called autoimmune regulator (AIRE) [31]. Furthermore, additional self-peptides, and also antigens derived from the commensal gut flora and the food, are presented by immigrant dendritic cells [32]. T cells that can be activated upon recognition of these peptides could be harmful for the host if they were released into the periphery. Therefore, these cells quickly undergo apoptosis upon strong activation, a process called negative selection [18,28]. Only those cells with weak affinity for self-peptide/MHC complexes are finally allowed to leave the thymus.

Collectively, the mechanism that prevent autoimmune T cell activation during early T cell development before the mature T cell leaves the thymus are called central tolerance [18,28]. Still, the elimination of autoreactive cells through central tolerance mechanisms is incomplete, amongst other things because not all possible self-antigens are presented by mTECs and DCs in the thymus. To control autoreactive T cells in the immunological periphery, several peripheral tolerance mechanisms have evolved. These include protection through regulatory T cells that are able to directly suppress autoreactive T cells in trans, but also cell-intrinsic pathways such as anergy, a hypo-responsive state that is induced through chronic self-antigen recognition [18,28].

4.1.5. Naïve, effector and memory T cells

After their selection, T cells leave the thymus as mature naïve, antigen-inexperienced cells. These cells express specific homing receptors, most importantly CD62L, and chemokine receptors such as CCR7, which allow them to migrate through the bloodstream to the secondary lymphoid organs, spleen and lymph nodes, where they eventually encounter their antigen [33,34]. Naïve T cells are not able to immediately react upon primary activation through antigen encounter. Instead, antigen encounter rapidly induces a developmental program towards the so-called effector T cells [33,35,36]. These effector cells express homing and chemokine receptors that allow them to migrate to the sites of infection [36]. Furthermore, they start to produce specific effector molecules, e.g. immuno-modulatory cytokines, chemokines and cytotoxic substances, which allow them to fight the infection once they encounter their antigen for the second time [33]. Due to the huge amount and variability of possible antigens that have to be recognized, only few T cells are able to recognize a specific antigen. Therefore, this population has to vigorously expand upon antigen encounter

to mount an effective immune response [35]. It was shown that during an immune response, more than 10 000 effector T cells can be generated from one mother cell [35]. At the end of the immune response, 90-95 % of these effector cells die in the so-called contraction phase [35,36]. Nevertheless, a pool of long-lived memory cells remains that is able to quickly protect the body in case of another infection with the same pathogen, which is the hallmark of adaptive immunity [33-36].

4.1.6. Conventional T cell subsets

As previously noted, the presentation of intracellular and extracellular pathogen-derived antigens is predominantly separated on two different MHC molecule classes. This separation is essential to allow the immune system to mount pathogen-specific responses. In this line, functionally different T cell subsets specific for MHCI and MHCII have evolved. Broadly, these can be separated in CD4+ helper T (T_H) cells and CD8+ cytotoxic T (T_C) cells [12,37].

Cells that harbor intracellular bacteria or that are infected with a virus need to be destroyed in order to eradicate the infection and to prevent further spreading of the disease. As previously noted, these cells will eventually present peptides derived from their intracellular pathogen via MHCI to CD8+ cytotoxic T cells [10]. Activated cytotoxic T cells are able to directly kill infected cells through two distinct mechanisms. First, CD8+ T cells start to produce and store various cytotoxic and pro-apoptotic molecules in secretory vesicles upon their activation, which they directly release on their target cells through exocytosis [38]. Among these secreted molecules, the two most prominent members are perforins and granzymes. Perforins are pore-forming, membranolytic proteins that directly integrate in the target cell plasma membrane [38,39]. Thereby, perforin facilitates the entry of granzymes, which are serine proteases that induce programmed cell death into the target cell [39].

The second pathway to trigger the direct destruction of infected cells is called FADD (Fas-associated via death domain) [7,38]. Activated cytotoxic CD8+ T cells upregulate the expression of the ligands for the FAS, TNF (tumor necrosis factor) and TRAIL (TNF-related apoptosis inducing ligand) receptors on their surface. Once these ligands bind to their respective receptors on their target cells, an intracellular signaling cascade is induced that ultimately triggers caspase activation and apoptosis [7,38].

The main role of CD4+ helper T cells in immune responses is not to kill other cells, but to modulate and control the function of various other cells of the immune system. Naïve CD4+ T cells may differentiate into one of several helper T cell subsets. Initially, these were

separated into T_H1 T cells that elicit cell-mediated, pro-inflammatory immune responses, and T_H2 T cells that control antibody-mediated humoral immunity [40].

However, the T_H1/T_H2 model eventually turned out to be an oversimplification [41,42]. Through IFN-γ production, T_H1 T cells also effect humoral immune responses by inducing B cells to switch their antibody isotypes towards those that help with the phagocytosis of microbes [43]. Furthermore, several additional CD4+ T cell subsets have been discovered over the last years. At the moment, it is believed that a naïve CD4+ T cell can differentiate into one of at least five different subsets: T_H1, T_H2, T_H17, peripherally-derived regulatory T (pT_{reg}) or follicular helper T (T_{FH}) cells [44].

T_H1 T cells produce several chemokines and cytokines, most importantly interferon-γ (IFN-γ), upon activation. Thereby, they recruit macrophages to sites of inflammation and activate these cells [45]. Activated macrophages consequently engulf and destroy microbes [45]. Thus, T_H1 T cells play a main role in the defense against intracellular pathogens [46].

T_H2 T cells are crucial in immune responses against extracellular parasites, and also to help B cells to produce antibodies. They influence the production of specific antibody classes by B cells, mostly through release of the cytokines interleukin-4 (IL-4) and IL-5 [45]. IL-4 elicits an isotype switch towards IgE antibodies, which are important in mast cell- and basophil-mediated responses against extracellular parasites and toxins. Furthermore, they are able to control the generation, recruitment and activation of eosinophils by producing the cytokine IL-5 [47].

A third subset was found to produce the cytokines IL-17A and IL-17F during immune responses and consequently called T_H17 T cells [48,49]. In addition, they also produce IL-22 [46]. These cytokines have a broad effect on various different cells types, but the main role of T_H17 T cells seems to lie in the defense against fungi and some bacteria strains [46,50].

Follicular helper T (T_{FH}) cells are the newest addition to the growing list of helper T cells subsets. They can be found in germinal centers, where they aid B cells undergoing class-switch recombination and somatic hypermutation reactions [51]. The existence of further helper T cell subsets, including T_H9 and T_H22 T cells, was proposed, but it is not clear at the moment whether these cells represent separate lineages [51].

Two additional CD4+ T cell subsets that are essential to maintain immune homeostasis, natural killer T (NKT) cells and regulatory T (T_{reg}) cells, do not develop from conventional CD4+ naïve T cells, but instead are generated as separate lineages during thymic T cell development [52]. Both of these cells were the main topic of my PhD thesis research and are

discussed below in more detail. However, it was found that peripheral naïve CD4+ T cells have the ability to differentiate into cells with a similar function and gene expression as thymus-derived regulatory T cells. To distinguish both lineages, a new nomenclature was recently proposed [53]. Thymus-derived T_{reg} cells should be called thymic T_{reg} cells (tT_{reg}), whereas those that differentiate from naïve T cells in the periphery should be called peripherally-derived T_{reg} (pT_{reg}) cells.

The differentiation of naïve CD4+ T cells into one of the different effector lineages depends on the strength of TCR signaling, as well as the presence of distinct cytokines, during activation. In a recent paper, it was demonstrated that although a single T cell clone gives rise to various effector T cells during an immune response, the fate of these cells seems to be predominantly determined through their TCR [54]. Nevertheless, at least *in vitro*, the addition of cytokines during T cell activation also significantly influences their effector fate. IL-12 and IFN-γ induce development towards the T_H1 lineage, whereas IL-4 directs T cells towards the T_H1 effector T cells [51]. Similarly, TGF-β together with IL-6 or IL-21 induces differentiation towards T_H17 cells, whereas pT_{reg} cells can be induced through IL-2 and TGF-β [51].

4.2. Natural killer T cells

Over 20 years ago, a subset of T cells in mice expressing the natural killer (NK) cell surface marker NK1.1 was first described [55]. Shortly afterwards, a similar T cell population was also identified in the human [56,57]. In addition to NK1.1, these T cells can express several other receptors typically associated with NK cells [58-60]. Although a variety of different names have been proposed over the last years, most commonly these cells are called natural killer T (NKT) cells [61]. Nevertheless, it is important to mention that not all NKT cells express NK1.1 or other NK cell markers, and some CD8+ conventional T cells also express NK1.1 upon activation [61-63].

In mice, NKT cells represent about 2.5 % of T cells in the spleen, 0.5 % in the blood and peripheral lymph nodes, and up to 30 % of T cells in the liver [64]. They appear about 10 fold less frequent in the human, but their numbers are very variable between individuals [64]. In contrast to peptide-recognizing conventional T cells, NKT cells recognize glycolipids, presented by the MHCI-like molecule CD1d [65]. The vast majority, called type-I-NKT cells, express a peculiar T cell receptor [64], which is composed of the invariant Vα14–Jα18 (Vα14i) rearrangement of the TCRα-chain in mice [66]. Importantly, the Vα14i protein derived from this rearrangement is the same for all NKT cells [63]. This Vα14i-TCRα-chain

is expressed together with a limited set of TCRβ-chains that predominantly contain Vβ8, Vβ7 or Vβ2 [66,67]. In man, a similar group of NKT cells expresses the homologous Vα24-Jα18 rearrangement, together with a Vβ11-containing TCRβ-chain [58,66]. Interestingly, the interaction of NKT cell TCRs and glycolipids presented by CD1d is strongly conserved among different species, with mice NKT cells recognizing glycolipids presented by human CD1d and vice versa [68]. Type-II-NKT cells, which do not express the Vα14i-TCR, but also recognize glycolipids presented by CD1d, are very rare [69]. These cells are much less understood, and will not be discussed here in further detail.

4.2.1. CD1d mediates antigen presentation to NKT cells

Early on, it was discovered that CD1d plays a critical role in the selection and function of NKT cells [67,70]. Hence, NKT cells do not develop in mice deficient for CD1d [71]. In the human, the CD1 family consists of five members, CD1a, CD1b, CD1c, CD1d and CD1e, which all present glycolipids to different T cell subsets with the exception of CD1e [72]. In rodents, only CD1d is expressed due to the deletion of the other genes during evolution [72,73]. The most efficient loading of glycolipids on CD1d molecules takes place in lysosomes and late endosomes [73,74]. Still, CD1d can also be loaded directly at the cell surface [73]. In contrast to MHCI, which is expressed on the surface of all nucleated cells, CD1d is only expressed on antigen-presenting cells (DCs, B cells and macrophages), cortical thymocytes and activated hepatocytes [64].

In mice, most NKT cells express CD4 and few are DN (CD4- CD8-), whereas in the human, also some CD8+ NKT cells are present [75,76]. However, CD4 and CD8 do not directly bind to CD1d and do not act as co-receptors on NKT cells as opposed to their role in the interactions of conventional T cells with MHC molecules [75,76]. Thus, the functional role of CD4 and CD8 on NKT cells is still unclear.

4.2.2. Thymic NKT cell development

Currently, it is believed that NKT cells diverge from conventional T cells at the DP stage in the thymus [59,77]. The assembly of a Vα14i-TCR through V(D)J recombination is a stochastic event in T cell development, with an estimated incidence of about 1 in 10^6 cells [78]. In mice, NKT cells first appear around day 5 after birth [79], whereas conventional α/β T cells are already present at birth [11]. The delayed emergence is due to the fact the Vα14-Jα18 rearrangement is always a secondary rearrangement, because Jα18 is a rather distal gene segment close to the 3' end of the Jα locus, and rearrangements generally progress from the

5’ end to the 3’ end at the Jα locus [76]. In line with this, gene mutations that shorten the life span of T cells undergoing rearrangements of the TCRα-chain, and thereby impair secondary rearrangements, show strongly decreased numbers of developing NKT cells [77,80]. In contrast, transgenic mice expressing a rearranged Vα14i-TCRα-chain contain significantly increased NKT cell numbers [81-84].

The thymic selection process of NKT cells differs in several aspects from that of conventional T cells. First, Vα14i-TCR-expressing DP T cells are not positively selected by thymic epithelial cells (TECs), but instead by other DP thymocytes that express CD1d on their surface [85,86]. Restricting CD1d expression to DP thymocytes was sufficient to allow NKT cell development [85,86]. A possible reason why thymic epithelial cells fail to select NKT cells is that homotypic interactions of members of the SLAM family (SLAMf) of surface receptors, which are not present on thymic epithelial cells, are obligatory during NKT cell selection [83]. However, CD1d is expressed on TECs as well as on thymic DCs, and these cells were suggested to play a role in negative selection of NKT cells [75].

An additional major difference between conventional T cells and NKT cells is the TCR signal strength during thymic development. As discussed in the previous section, autoreactive T cells could be harmful for the host and are therefore deleted from the repertoire through negative selection. Still, some T cell subsets, including NKT cells and regulatory T cells, are instead selected for their ability to recognize specific self-antigens, which is known as agonist selection [52,87] (**Figure 6**). This recognition triggers a comparably strong TCR downstream signal, as it was recently demonstrated by using reporter mice for TCR signaling strength [88]. How TCR- and also SLAMf-generated signals are merged to direct these cells towards the NKT cell lineage is just beginning to be understood. Recently, it was observed that Egr1 and Egr2, two transcription factors induced by TCR signaling, are significantly higher expressed at early NKT cell development stages in comparison to conventional T cells [89]. Furthermore, it was shown that Egr2 is directly able to bind to the promoter and to induce the expression of the transcription factor promyelocytic leukemia zinc finger protein (PLZF) [89]. PLZF itself controls the maturation and effector differentiation of NKT cells and is considered to be a key lineage-defining transcription factor [90,91].

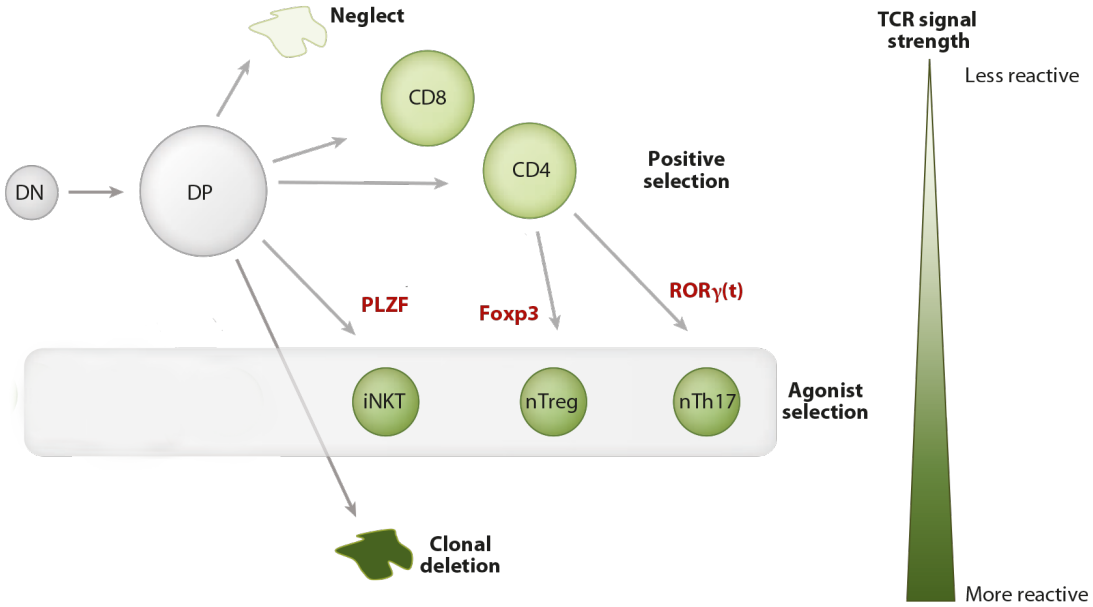

Figure 6 During T cell development, differences in TCR signal strength can lead to fundamental different developmental fates. Conventional T cells are positively selected through rather weak signals. In contrast, NKT cells and regulatory T cells are selected for their ability to recognize self-antigen, which induces strong TCR signals. Figure is adapted from [52].

4.2.3. NKT cell maturation

After selection by auto-antigenic activation, thymic NKT cells undergo a series of maturation steps. The first stage that can be identified by flow cytometry is called stage 0. These cells are characterized by the expression of CD24, a marker of immature T cells [92], and express neither CD44 nor NK1.1 [78]. Stage 1 NKT cells have downregulated CD24 and do proliferate vigorously, thereby increasing the pool of NKT cells after positive selection. Progression from stage 1 to stage 2 is characterized by increased CD44 expression, and these cells are still actively cycling [93]. The majority of stage 2 NKT cells exit the thymus to undergo their final maturation step, the upregulation of NK1.1 and other NK cell markers to become stage 3 NKT cells, in the periphery [79,93]. However, few long-lived NKT cells can also fully mature in the thymus [79]. Furthermore, NKT cells acquire a surface marker phenotype reminiscent of activated/memory T cells with low expression of CD62L, and high expression CD44, CD69, CD122 and ICOS, during their maturation [67,90,94].

4.2.1. Antigen recognition and activation of NKT cells

The first antigen that was described to activate NKT cells and still the most potent one up to date is the glycolipid α-galactosyl-ceramide (αGalCer), which was discovered in a screen for novel compounds with anti-tumor activity [65,95]. Originally, αGalCer was isolated from a sample of the marine sponge *Agelas mauritianus* [95], but it is now believed that it was

derived from bacteria colonizing the sponge [64]. NKT cell reactivity towards bacterial glycolipids has been demonstrated for several strains such as *Streptococcus pneumoniae* [96], some *Sphingomonas* species [97,98] and *Borrelia burgdorferi* [99].

However, NKT cells were shown not only recognize pathogen-derived lipids, but also display reactivity towards self-antigens. It is believed that NKT cells are "autoreactive by design" [100], and this autoreactivity is fundamental during development, as NKT cells are selected upon self-antigen recognition in the thymus [74,101,102]. In mice containing a mutated CD1d not able to target endosomal/lysosomal compartments for endogenous lipid loading, the development of NKT cells was strongly impaired [74]. At the moment, although some plausible candidates have been put forward [101,102], the exact nature of the endogenous ligand(s) involved in thymic NKT cell selection is still unclear.

Moreover, also mature peripheral NKT cells display autoreactivity. When NKT cells were co-cultured *in vitro* with antigen-presenting cells in the absence of additional stimulatory lipids, they were activated to some extent, which was abrogated through the addition of CD1d blocking antibodies [58,103]. This inherent autoreactivity of NKT cells was shown to be important for NKT cell activation in several diseases. Infection of mice with *Salmonella typhimurium*, a bacterium that does not contain NKT cell antigen, led to NKT cell activation that was partially blocked by antibodies against CD1d [103]. Similar observations of CD1d-dependent presentation of self-lipids to NKT cells were described for mice infected with influenza A virus [104]. Lastly, CD1d-dependent NKT cell activation in the absence of foreign antigen was also reported to be crucial for cancer rejection [105].

In these disease settings, altered lipid metabolism in antigen-presenting cells was shown to induce the presentation of self-lipids with a stronger potential to activate NKT cells [106,107]. Using self-lipids as "danger signals" to activate NKT cells might be a useful mechanism for the immune system to elicit NKT cell responses in a broad range of immune responses [106,107].

For several microbial lipids [108], synthetic lipids [109] and self-lipids [110], the binding of the Vα14i-TCR to lipid-loaded CD1d has been analyzed so far. Despite the structural difference of these lipid antigens, the binding mode of the Vα14i-TCR was surprisingly similar for all complexes [111]. The only variable region of the Vα14i-TCR, a part of the TCRβ-chain, was never in direct contact with the lipid antigen, but just contacted CD1d [87,111]. Only the invariable Vα14i-TCRα-chain could ligate the presented lipid. This conserved binding mode of the Vα14i-TCR is very similar to pattern recognition receptors of

the innate immune system [87].

In addition to TCR-derived signals, also pro-inflammatory cytokines are able to induce NKT cell activation during immune responses (**Figure 7**). The best-described cytokine in this context is IL-12, and in contrast to naïve conventional T cells, NKT cells express high amounts of the IL-12 receptor in the steady state [103,112]. Likewise, IL-18 has been shown

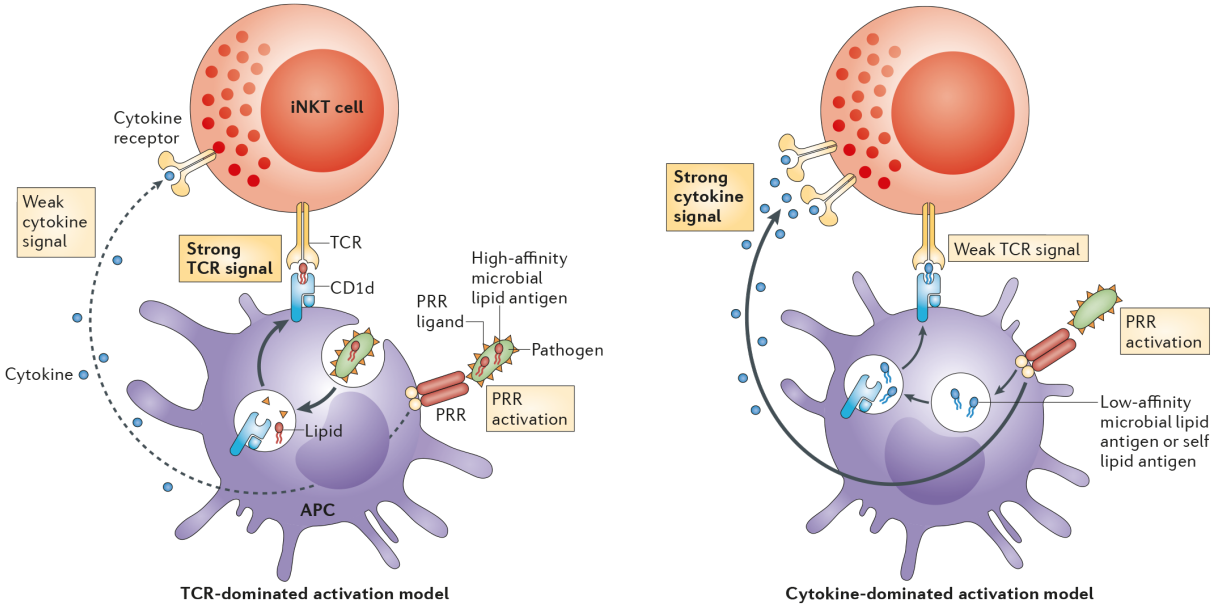

Figure 7 Depending on the type of the pathogen, NKT cell activation is either dominated by TCR-generated signals, or by cytokines released from antigen-presenting cells. Figure is adapted from [115].

to directly induce NKT cell activation [113]. These cytokines are mainly produced by dendritic cells activated by innate immune pathways such as toll-like receptor signals [113,114]. In some extreme cases, cytokine-derived signals alone were proposed to be sufficient to fully activate NKT cells in the absence of additional TCR stimulation [112,113]. However, in most disease settings, TCR-dependent recognition of (self)antigen, together with cytokine signals, cooperatively mediate NKT cell activation [112,115].

4.2.2. NKT cell functions in disease

Once activated, the most distinguishing feature of NKT cells is their rapid production and secretion of a large set of immuno-modulatory cytokines [94,116]. NKT cells comprise the only T cell subset that is able to simultaneously produce proinflammatory T_H1 cytokines such as IFN-γ and TNF, as well as T_H2 cytokines such as IL-4 and IL-13 [94,116]. Interestingly, the basis for their fast cytokine release during immune responses appears to be their ability to store large pools of untranslated cytokine mRNA, which can be quickly mobilized upon activation [117,118]. An additional important function of NKT cells is the release of

chemokines in order to recruit other immune cells to the sites of infection [119]. Similar to cytokine mRNA, NKT cells are also able to store mRNAs for several of these chemokines to allow an accelerated response [120]. Finally, NKT cells are able to employ cytotoxic mechanisms to directly kill other cells through perforin/granzyme-release as well as through the FADD pathway [120].

NKT cells are critical regulators of several immune responses, as it has been demonstrated through the analysis of diverse mouse models, but also the empirical investigations of human patients [64,121]. On the one hand, NKT cell have a protective role against microbial infection [97,99,122], autoimmune disease development [121] and cancer [105,121]. On the other hand, due to their potent immunoregulatory functions, inappropriate activation of NKT cells is implicated in the pathogenesis of atherosclerosis and allergies [64,121].

4.3. Regulatory T cells

The first indication for a suppressive T cells subset was found over 40 years ago. It was described that extraction of the thymus, a process called thymectomy, led to a destruction of ovaries when it was performed three days, but not seven days after birth in mice [123]. While this phenotype was primarily speculated to be due to the absence of hormones produced by the thymus, follow-up experiments showed that thymectomy triggers various autoimmune diseases in mice and in rats [124-127]. Furthermore, this pathology was caused by autoreactive T cells, as T cell transfer could transmit the disease to other animals [126,127]. Importantly, disease onset could be prevented upon transfer of either thymocytes or splenocytes from adult mice [128]. These findings indicated the existence of two distinct T cell populations in these animals: First, a subset of effector T cells that is causative for disease onset and also elicits the disease upon transfer into other animals. Secondly, a subset of suppressive T cells that is able to control autoimmunity, but is not generated until 3 days after birth [129].

Over the years, these suppressive cells were further characterized through experiments in which the transferred cells were depleted or enriched for cells expressing certain cell surface markers. In this way, it was shown that suppressive T cells predominantly expressed the cell surface markers CD4 [128], high levels of CD5 [130] and low amounts of CD45RB [131]. Furthermore, suppressive cells were found to express high amounts of CD25, the α-chain of

the high-affinity receptor for the cytokine IL-2 [132]. From thereon, these cells were called regulatory T (T_{reg}) cells [132,133].

4.3.1. FoxP3 is the signature T_{reg} cell transcription factor

A major breakthrough in the understanding of T_{reg} cells came in 2003, when several groups found that the forkhead box P3 (FoxP3) protein is specifically expressed by T_{reg} cells [134-136]. FoxP3 is a forkhead/winged-helix family transcription factor located on the X chromosome [137-139]. Mutations in the *Foxp3* gene were initially found to be causative for the rare human autoimmune disease IPEX (immune dysregulation, polyendocrinopathy, enteropathy, X-linked), to which patients succumb during infancy [138,139]. A similar phenotype was observed in mice harboring the *scurfy* mutation, which is a loss of function mutation of the *Foxp3* gene [137]. FoxP3 expression, which is confined to T cells, is crucial for T_{reg} cell development, as these cells were shown to be absent in mice lacking FoxP3 [134], and T cell-specific FoxP3 inactivation reproduced the *scurfy* phenotype [140]. Importantly, ectopic expression of FoxP3 in activated CD4+ conventional T cells partially induced the T_{reg} cell gene signature and also conferred suppressive abilities [134,135,141].

Recently, it has been shown that FoxP3 can both induce and suppress target gene expression [141-143]. However, FoxP3 binds directly to less than 10 % of FoxP3-regulated genes [142]. Instead, FoxP3 was shown to control gene expression as part of large transcriptional complexes that can contain several hundred co-factors [144].

4.3.2. Regulatory T cell development

Thymus-derived regulatory T (tT_{reg}) cells are thought to branch off from the other T cell lineages at the DP stage in the thymus. However, in contrast to conventional T cells, which are present at birth [11], tT_{reg} cell development is delayed during ontogeny [145]. Mature tT_{reg} cells are rarely found in the thymus before day 3 after birth [145], explaining the previously observed differential outcomes of neonatal thymectomy on day 3 and day 7 [123]. The vast majority of tT_{reg} cells express the co-receptor CD4 and accordingly recognize peptides presented by MHCII, and tT_{reg} cells are not found in mice deficient for MHCI/MHCII [140]. Although the TCR repertoire of tT_{reg} cells is partially shared with that of conventional CD4+ T cells, most TCRs are different [146,147]. Importantly, tT_{reg} cells are thought to express autoreactive TCRs and are selected by agonist ligand, similar to NKT cells [52,146,147]. Still, agonists selecting tT_{reg} cells have not been identified yet, but will probably include rare tissue-specific antigen [148].

The proposed autoreactive nature of tT_{reg} cells is based on several experimental observations. First, the majority of tT_{reg} cells have a surface phenotype that is reminiscent of recently activated T cells, with high expression of CD25, CD122, GITR, and Ox40 [142,149]. Second, in mice expressing a transgenic TCR, tT_{reg} cells only developed once the cognate antigen was expressed as a second transgene [150]. Finally, in a mouse model that reports TCR signaling strength, tT_{reg} cells consistently displayed higher signaling strength in comparison to conventional T cells in the thymus, and also in the periphery [88].

The thymic generation of tT_{reg} cells is a multistep process. The observations that in addition to TCR signaling strength, interleukin-2 (IL-2) signaling is of critical importance for tT_{reg} cell development [151,152], and that $CD25^{high}$ FoxP3– T cells are the direct precursors of FoxP3+ tT_{reg} cells [152], were recently combined in a two-step model for tT_{reg} cell differentiation [152]. According to this model, strong TCR signals upon self-antigen recognition induce the surface expression of CD25 [152]. This is thought to increase the sensitivity for IL-2, which induces FoxP3 expression in a second (TCR-independent) stage [152].

However, despite its undeniable importance, FoxP3 expression alone is not sufficient to induce the characteristic T_{reg} cell gene expression profile [141,153]. In mice in which GFP was inserted in an disrupted FoxP3 locus, the surface marker phenotype of GFP-expressing T cells resembled that of wild-type T_{reg} cells despite the absence of FoxP3 [154]. An interesting explanation for this finding is the recent discovery that in addition to FoxP3 expression, a second prerequisite for T_{reg} cell development is the establishment of a specific DNA hypomethylation pattern (T_{reg}-Me) [153]. Covalent methylation of cytosines, which is mainly found at clusters of CpG dinucleotides, is an epigenetic DNA modification that is connected to heterochromatin and transcriptional silencing [33]. In contrast, demethylation of CpG islands is connected to open chromatin structure and enhanced gene expression [33]. In T_{reg} cells, the loci of five genes that are highly expressed in these cells, including FoxP3, were found to be significantly hypomethylated in comparison to conventional T cells [153]. Importantly, also T_{reg}-Me induction is TCR signaling-dependent and progressively established through continuous TCR signaling over days [153]. This demethylation is an active process which acts independently of cell proliferation [155]. Altogether, the TCR-dependent induction of both FoxP3 expression as well as T_{reg}-Me is a crucial process during thymic T_{reg} cell commitment, since both play largely non-redundant roles in controlling T_{reg} cell gene expression.

4.3.3. Regulatory T cell subsets

Similar to the previously discussed conventional T cells, T_{reg} cells can be broadly separated into naïve and effector subsets [156,157]. The majority of T_{reg} cells in lymphoid organs usually express the surface markers CD62L and CCR7 resembling naïve T cells, which allow them efficient cycling between lymph nodes and spleen [156-158]. On the other hand, T_{reg} cell migration into non-lymphoid tissues is usually accompanied with downregulation of both markers [156-158]. Instead, these T_{reg} cells express receptors that can also be found on effector T cells, such as homing and chemokine receptors [157,158] as well as additional activation markers [156]. Interestingly, it was recently demonstrated that during immune responses, effector T_{reg} cell subsets are generated that share the expression of specific transcription factors and surface receptors with the conventional helper T cells they suppress [159-161], which is crucial for optimal T_{reg} cell function in distinct disease settings [162,163].

4.3.4. Regulatory T cell functions

Throughout the lifetime of mice, T_{reg} cells are needed to prevent aberrant autoimmune/inflammatory responses, as it was shown that deletion of these cells in mature animals led to death within 2-3 weeks [164]. T_{reg} cells mainly act as suppressive cells, and are able to modulate the behavior of various other cell types, including T cells, B cells, DCs and NK cells. Due to the variety of immune responses and immune cells that have to be controlled, T_{reg} cells possess several different suppressor mechanisms (**Figure 8**) [165,166].

First, most T_{reg} cells express high levels of CD25 on their surface, which is not only indispensable for their development [152] and their homeostasis [167], but also for the control of immune responses. High CD25 expression enables T_{reg} cells to efficiently outcompete effector T cells for IL-2 [168]. It is believed that T_{reg} cells can act as a "sink" for IL-2, causing effector T cell death due to withdrawal of IL-2 [168]. Furthermore, T_{reg} cells are able to disrupt target cell metabolism through increasing the amount of extracellular adenosine, which inhibits T cell responses [169]. They do so through the surface coexpression of CD39 and CD73, two ectoenzymes that in concert hydrolyze nucleotides to nucleosides [169].

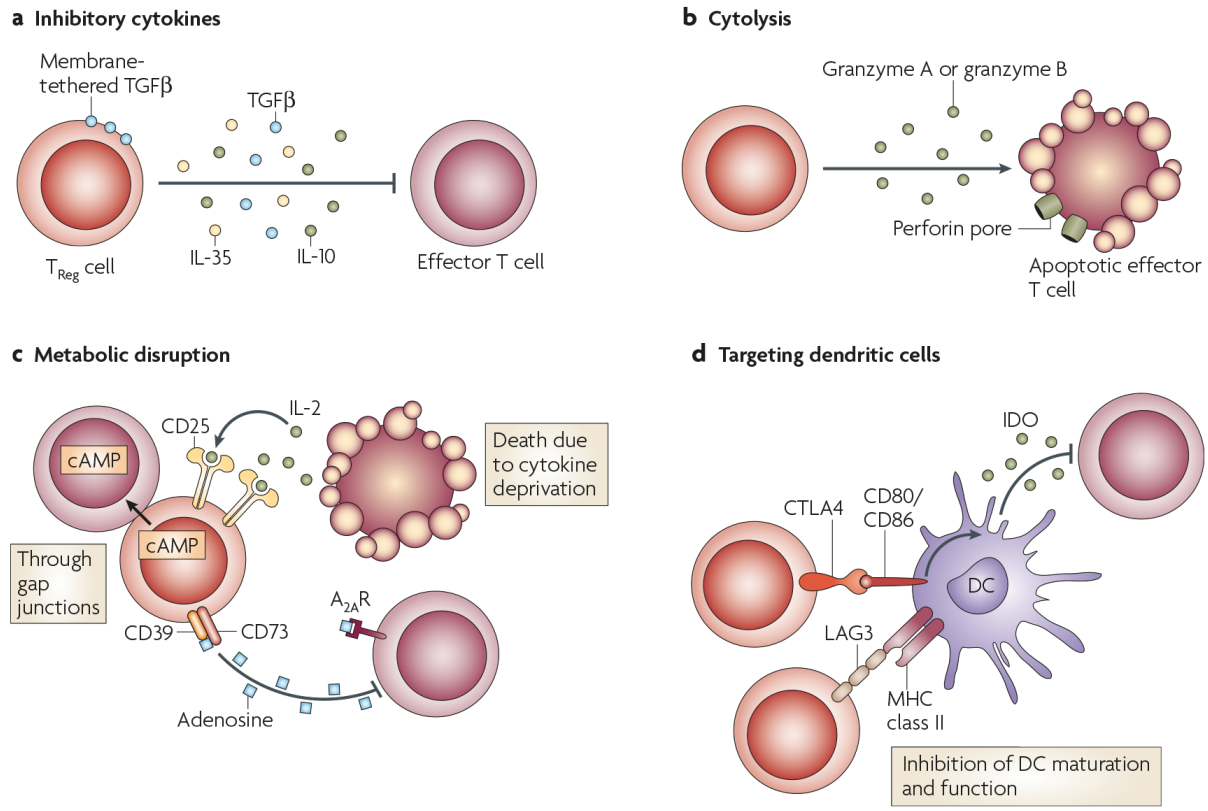

Figure 8 To control immune responses, T_{reg} cells employ various suppressive mechanisms, including the release of cytokines or cytotoxic molecules, metabolic disruption as well as the modulation of dendritic cell function. Figure is adapted from [165].

A second suppressive mechanism of T_{reg} cells is cytolysis. Similar to cytotoxic CD8+ T cells and NKT cells, T_{reg} cells are able to directly induce target cell lysis through the release of granzymes and perforin [170,171]. To this date, T_{reg} cell-mediated killing of effector T cells [170], B cells [171] as well as dendritic cells [172] has been demonstrated.

A third important suppressive mechanism of T_{reg} cells is the release of inhibitory cytokines. Early on, it was discovered that IL-10 is produced by T_{reg} cells [173], which is able to dampen inflammatory cytokines production of innate immune cells during immune responses. Accordingly, in mice with T_{reg} cell-specific deletion of the *IL-10* gene, the control of immune responses at the colon and the lungs was impaired [174]. Recently, a novel cytokine, IL-35, has been found, which is mainly expressed by T_{reg} cells and directly inhibits the proliferation of effector T cells [175].

Finally, T_{reg} cells are able to control immune response by interfering with the maturation and function of antigen-presenting DCs. Cytotoxic T lymphocyte associated antigen 4 (CTLA-4) is constitutively expressed on the surface of T_{reg} cells, and has been shown to block DC costimulation through removing costimulatory ligands from the surface of DCs by trans-

endocytosis [176,177]. Furthermore, during direct interactions of T_{reg} cells and DCs, binding of lymphocyte activation gene 3 (LAG-3) to MHCII on DCs blocks DC maturation [178].

Several T_{reg} cell-specific knockout mice of putative suppressor molecules have been generated up to date, but none of these animals did develop systematic autoimmunity similar to that which is observed in T_{reg} cell-ablated or FoxP3-deficient animals [129,179]. The most dramatic autoimmune symptoms were found in mice with CTLA-4 ablation in BALB/c T_{reg} cells [176], but a less severe phenotype was observed when a similar analysis was performed in C57BL76 mice [129]. Therefore, it is believed that none of these suppressive mechanisms is indispensable for T_{reg} cell function, and depending on the type of immune response, one or several act complementary in a non-redundant fashion [129,179].

5. Aim of the thesis

In addition to the innate immune system that operates with germline-encoded receptors, each cell of the adaptive immune system employs one of a large variety of different receptors for antigen recognition. This diversity is generated early in T cell or B cell development through the almost random rearrangement of certain gene segments, which together constitute the full-length T cell receptor (TCR) or B cell receptor. Upon TCR surface expression, several mechanisms of tolerance take place to prevent the development of autoreactive cells that could induce immune responses against cells of the own body. In contrast, few T cell subsets, including natural killer T (NKT) and regulatory T (T_{reg}) cells, are instead selected for their ability to recognize self-antigens during thymic development. However, the role of this inherent autoreactivity for mature NKT cells or T_{reg} cell biology was not well understood.

In the course of this thesis, we experimentally addressed the following important questions:

1. Do mature peripheral NKT cells receive autoreactivity signals through their lipid-recognizing Vα14i-TCR in the immunological periphery? If yes, to which degree does NKT cell gene signature, homeostasis and effector function rely on these signals? (**Paper I**)
2. Are mature T_{reg} cell homeostasis, gene expression and suppressive function affected if these cells lose persistent autoreactive TCR signals? (**Paper II**)
3. How does the spontaneous secretion of inflammatory cytokines by A20-deficient B cells influence splenic T cell subsets? (**Paper III**)

6. Brief summaries of the publications

Paper I:

Vahl et al., 2013. NKT Cell-TCR Expression Activates Conventional T Cells in Vivo, but Is Largely Dispensable for Mature NKT Cell Biology. *PLOS Biology* 11(6): e1001589.

The T cell receptor (TCR) is a heterodimer, and almost each conventional T cell expresses a different TCR. This diverse TCR repertoire is generated in a randomized process during T cell development. In contrast to peptide-recognizing conventional T cells, most natural killer T (NKT) cells express a semi-invariant, glycolipid-recognizing TCR that is called Vα14i. This receptor is composed of the same Vα14i TCRα-chain for all NKT cells, which is expressed together with a limited set of TCRβ-chains. During thymic T cell development, the rare cells that randomly express the Vα14i-TCR are selected to become NKT cells upon recognition of self-glycolipid antigens.

In order to define the importance of the Vα14i-TCR and its inherent autoreactivity for NKT cell maintenance, cellular identity and function, we generated mice harboring a $Vα14i^{StopF}$ knock-in allele, which allows inducible expression of the invariant Vα14i-chain under endogenous control. In mice that expressed this knock-in transgene at the physiological expression time point during thymic T cell development, significantly higher numbers of NKT cells could be found in thymus, spleen and lymph nodes in comparison to littermate controls. These transgenic NKT cells showed, in comparison to wild-type NKT cells, similar expression patterns of important NKT cell markers and transcription factors, and furthermore a similar release of cytokines upon activation.

To study the consequence of Vα14i-TCR expression and to examine its autoreactivity in the periphery, we developed a genetic switch system that enabled us to exchange the TCRα-repertoire, present on naïve T cells, for a Vα14i-restricted TCR repertoire. We could show that Vα14i-TCR expression was not sufficient to convert naïve conventional T cells into NKT cells. However, the TCR-switched cells were significantly activated. Furthermore, we found evidence for ongoing sterile inflammation in these mice, altogether indicating that NKT cells receive autoreactive TCR signals not only in the thymus, but also in the periphery.

Finally, to address the importance of this autoreactivity for NKT cells, we ablated the NKT cell-TCR from mature NKT cells *in vivo* and followed the fate of these cells over time.

We observed that homeostasis, gene expression and effector cytokine expression were unaltered in comparison to TCR-expressing NKT cells.

In summary, we concluded that after thymic NKT cell selection by self-lipids, NKT cells become independent from constitutive signals received through their autoreactive TCR.

In this study, I performed all experiments, except for the generation of the Vα14i^{StopF} mouse, which was performed by Marc Schmidt-Supprian. I received experimental help from Klaus Heger and Nathalie Knies with the analysis of the switched animals and the cytokine secretion, respectively. Furthermore, I analyzed all data presented in this study together with Marc Schmidt-Supprian, and we received help from Marco Y. Hein with the generation of the heatmap shown in Figure 8. Louis Boon, Hideo Yagita and Bojan Polic provided blocking antibodies or mice. Moreover, I wrote the paper together with Marc Schmidt-Supprian.

Paper II:

Vahl et al., 2013. TCR ablation leads to loss of regulatory T cell identity. *Manuscript in preparation*.

Regulatory T (T_{reg}) are indispensable to protect humans and mice from the occurrence of spontaneous autoimmunity during their lifetime. At first glance, it seems rather astonishing that an intrinsic feature of T_{reg} cells is their high reactivity towards self-antigens. During thymic T cell development, the vast majority of T cells whose newly generated T cell receptor (TCR) displays self-reactivity are deleted from the repertoire to avoid the onset of immune responses targeted at the own body. However, this is not the case for T_{reg} cells, which are instead selected for their high self-reactivity. Additionally, T_{reg} cells are believed to receive persistent autoreactive TCR signals in the periphery upon emigration from the thymus, but it remained unclear to which extent T_{reg} cells rely on these signals.

To study the role of autoreactive TCR signals for mature peripheral T_{reg} cells, we conditionally ablated their TCR and monitored the behavior of these cells. Interestingly, TCR-deficient T_{reg} cell counts quickly decreased, which was due to impaired proliferation as well as impaired survival in absence of tonic TCR signals. Furthermore, we showed that the activated/effector phenotype of T_{reg} cells, as well as a large part of their signature gene expression pattern, depends on continuous TCR signals. However, the recently discovered T_{reg} cell-specific demethylation pattern of four important T_{reg} cell markers was unaltered in TCR-deficient Treg cells, and fittingly the expression of these markers was only mildly

affected. Finally, we could demonstrate that TCR-deficient T_{reg} cells lose a large proportion of their proteins implicated in their suppressive function.

In summary, we showed that TCR signals are the basis for a stable T_{reg} cell lineage, and in their absence, T_{reg} cell homeostasis, signature gene expression and suppressive function are severly impaired.

In this study, I performed and analyzed the majority of experiments. I received experimental help from Klaus Heger with the analysis of the cytokine secretion upon activation. The analysis of the methylation pattern was performed by Naganari Ohkura in the laboratory of Shimon Sakaguchi. Furthermore, the Affymetrix microarrays were run in the laboratory of Thorsten Buch, and we received help from Karsten Kretschmer and Olivia Prazeres da Costa with the analysis. Marco Y. Hein helped with the generation of the heatmap shown in the Supplementary Figure 2. Bojan Polic provided the $C\alpha^{F/F}$ mice. Moreover, I wrote the paper together with Marc Schmidt-Supprian.

Paper III:

Chu et al., 2011. B cells lacking the tumor suppressor TNFAIP3/A20 display impaired differentiation and hyperactivation and cause inflammation and autoimmunity in aged mice. *Blood* 117, 2227-2236.

Various stimuli, most prominently B cell receptor (BCR) or T cell receptor (TCR) ligation, as well as toll-like receptor engagement, activate the nuclear factor-κB (NF-κB) signaling pathway in adaptive immune cells. One important regulator of this pathway is the ubiquitin-editing enzyme A20, which restricts NF-κB activation through a negative feedback loop. Polymorphisms and mutations of A20 have been found in patients suffering from autoimmune diseases connected to aberrant antibody secretion by B cells, including rheumatoid arthritis and system lupus erythematosus. Furthermore, A20 is frequently functionally inactivated in human B cell lymphoma.

To study the role of A20 in B cell development and B cell-mediated autoimmunity, we ablated A20 specifically in B cells. Herein, we observed that A20 deficiency did not impair early B cell development. Yet, the mature recirculating B cell in the bone marrow as well as splenic B1 B cells subsets were reduced, whereas the numbers of marginal zone B cells and immature B cells were increased. Moreover, these mice showed an enlarged splenic cellularity, which was mostly due to significantly increased numbers of effector and

regulatory T cells, as well as of several myeloid cell subsets. This expansion could be attributed, amongst other possibilities, to the spontaneous release of pro-inflammatory cytokines, primarily IL-6, by A20-deficient B cells. Interestingly, the analysis of an aged cohort revealed even more pronounced effects of B cell-specific A20 deletion. These animals showed splenomegaly due to an even further increased expansion of T cells and myeloid cells. Moreover, we detected massive expansion of plasma cells, tissue-specific class-switched autoantibodies in the serum, as well as IgG immune complex deposition in the kidney.

In summary, we concluded that A20 is a critical regulator of B cell activation in mice. In its absence, spontaneous cytokine production of B cells leads to chronic inflammation, which exacerbates with age and finally ends in autoimmune disease states.

My contribution to this study was the analysis of T cells and myeloid cells in both young and aged animals.

7. Acknowledgements

This thesis would not have been possible without the help and support of many people.

First of all, I would like to express my sincere gratitude to my supervisor, Dr. Marc Schmidt-Supprian, for choosing me as a Ph.D. student and always being an excellent mentor with great support, patience, and brilliant ideas. Furthermore, I would like to thank him for teaching me not only about science but also about life, a lot of fun and lasting friendship.

I express my gratitude to Prof. Klaus Förstemann for accepting to act as my principal supervisor at the LMU Munich, and for all of his nice support. Furthermore, I would like to thank Prof. Dr. Ludger Klein for accepting to be the second referee. I would also like to thank the other members of the thesis committee, Prof. Dr. Vigo Heissmeyer, PD Dr. Dietmar E. Martin, Prof. Dr. Karl-Peter Hopfner and Prof. Dr. Martin Biel, for taking the time to review my work.

Special thanks to our collaborating scientists Prof. Dr. Ludger Klein and Prof. Dr. Vigo Heissmeyer for their nice support of our work and many fruitful discussions. Moreover, I would like to thank Prof. Dr. Reinhard Fässler for hosting and supporting the Schmidt-Supprian lab and for his helpful comments.

Furthermore, I would like to thank all present and former members of the Schmidt-Supprian group, Arianna, Barbara, Yuanyuan, Klaus, Valeria, Dilip, Julia, David and Maike, and also of other groups, especially Raphael, Korana, Ajla, Marco, Guru, Marsilius, Michail, Katharina, Martin, Ksenija and Maria for friendship, a fun working atmosphere, fruitful discussions and experimental help. I would also like to thank Carmen Schmitz, Ines Lach-Kusevic, Dr. Walter Göhring, Klaus Weber and Dr. Armin Lambacher for technical and administrative support, and our animal caretakers, especially Mia, Bianca and Jens.

Additionally, I would like to thank the Ernst Schering Foundation for personal and financial support.

My love and gratitude go to Nathalie, my family and all friends who are always there for me. To them, I dedicate this thesis.

8. Curriculum Vitae

Education

Ludwig-Maximilians-University
Munich

PhD studies	Since 07/2008
Max-Planck-Institute of Biochemistry	
Topic: „ TCR signals in the identity and function of mature NKT and regulatory T cells“	
Research Areas: Immunology/Genetics/Molecular Biology	

Free University
Berlin

Study of Biochemistry	10/2002 – 05/2008
Majors: Biochemistry/Immunology/Biophysics	
Diploma in Biochemistry	22nd of May 2008
Final Degree: 1.0	
Intermediate Diploma in Biochemistry	5th of April 2005
Intermediate Diploma in Biology	4th of October 2004

Leibniz University
Hanover

Study of Applied Computer Science	10/2000 – 09/2002

ADDITIONAL QUALIFICATIONS

Stays Abroad

Harvard University

Diploma Thesis Research 08/2007 – 04/2008

Topic: "Role of the IκB kinases in B cell development & functions"

Research Areas: Immunology/Oncology

Harvard University

Research Internship 08/2006 – 11/2006

Topic: "Selection and evolution of enzymes from a partially randomized non-catalytic scaffold"

Research Areas: In-vitro-Evolution/Genetics

Awards

DAAD Travel Grant (For the symposium in Chicago/U.S.A.) 09/2011

Doctoral Fellowship of the Ernst Schering Foundation 03/2009 – 02/2011

Keystone Symposia Scholarship (Travel Grant) 01/2011

DAAD Travel Grant (For the internship in Boston/U.S.A.) 08/2006

Selected Publications

Vahl JC, Heger K, Knies N, Hein MY, Boon L, Yagita H, Polic B, Schmidt-Supprian M. NKT Cell-TCR Expression Activated Conventional T Cells in Vivo, but Is Largely Dispensable for Mature NKT Cell Biology. (2013). *PLOS Biology* 11(6): e1001589

Chu Y, **Vahl JC**, Kumar D, Heger K, Bertossi A, Wójtowicz E, Soberon V, Schenten D, Mack B, Reutelshöfer M, Beyaert R, Amann K, van Loo G, Schmidt-Supprian M. B cells lacking the tumor suppressor TNFAIP3/A20 display impaired differentiation and hyperactivation and cause inflammation and autoimmunity in aged mice. (2011). *Blood* 117(7): 2227-36.

Derudder E, Cadera EJ, **Vahl JC**, Wang J, Fox CJ, Zha S, van Loo G, Pasparakis M, Schlissel MS, Schmidt-Supprian M, Rajewsky K. Development of immunoglobulin lambda-chain-positive B cells, but not editing of immunoglobulin kappa-chain, depends on NF-kappaB signals. (2009). *Nat Immunol* 10, 647-654.

Personal Interests

Tennis/Soccer/Road Racing/Playing the Guitar/Cooking

9. References

1. Murphy KP, Travers P, Walport M, Janeway C (2008) Janeway's immunobiology. Garland Pub. 1 pp.

2. Van Kaer L, Parekh VV, Wu L (2011) Invariant natural killer T cells: bridging innate and adaptive immunity. Cell and tissue research 343: 43–55. doi:10.1007/s00441-010-1023-3.

3. Krangel MS (2009) Mechanics of T cell receptor gene rearrangement. Curr Opin Immunol 21: 133–139. doi:10.1016/j.coi.2009.03.009.

4. Roth DB (2003) Restraining the V(D)J recombinase. Nat Rev Immunol 3: 656–666. doi:10.1038/nri1152.

5. Boehm T (2012) Self-renewal of thymocytes in the absence of competitive precursor replenishment. J Exp Med 209: 1397–1400. doi:10.1084/jem.20121412.

6. Clevers H, Alarcon B, Wileman T, Terhorst C (1988) The T cell receptor/CD3 complex: a dynamic protein ensemble. Annu Rev Immunol 6: 629–662. doi:10.1146/annurev.iy.06.040188.003213.

7. Glimcher LH, Townsend MJ, Sullivan BM, Lord GM (2004) Recent developments in the transcriptional regulation of cytolytic effector cells. Nat Rev Immunol 4: 900–911. doi:10.1038/nri1490.

8. Starr TK, Jameson SC, Hogquist KA (2003) Positive and negative selection of T cells. Annu Rev Immunol 21: 139–176. doi:10.1146/annurev.immunol.21.120601.141107.

9. Vyas JM, Van Der Veen AG, Ploegh HL (2008) The known unknowns of antigen processing and presentation. Nat Rev Immunol 8: 607–618. doi:10.1038/nri2368.

10. Neefjes J, Jongsma MLM, Paul P, Bakke O (2011) Towards a systems understanding of MHC class I and MHC class II antigen presentation. Nat Rev Immunol 11: 823–836. doi:10.1038/nri3084.

11. Strominger JL (1989) Developmental biology of T cell receptors. Science 244: 943–950.

12. Janeway CA (1992) The T cell receptor as a multicomponent signalling machine: CD4/CD8 coreceptors and CD45 in T cell activation. Annu Rev Immunol 10: 645–674. doi:10.1146/annurev.iy.10.040192.003241.

13. Hodges E, Krishna MT, Pickard C, Smith JL (2003) Diagnostic role of tests for T cell receptor (TCR) genes. J Clin Pathol 56: 1–11.

14. Malissen B, Malissen M (1996) Functions of TCR and pre-TCR subunits: lessons from gene ablation. Curr Opin Immunol 8: 383–393.

15. Dave VP (2009) Hierarchical role of CD3 chains in thymocyte development. Immunol Rev 232: 22–33. doi:10.1111/j.1600-065X.2009.00835.x.

16. Sewell AK (2012) Why must T cells be cross-reactive? Nat Rev Immunol 12: 669–677. doi:10.1038/nri3279.

17. Germain RN (2002) T-cell development and the CD4-CD8 lineage decision. Nat Rev Immunol 2: 309–322. doi:10.1038/nri798.

18. Klein L, Hinterberger M, Wirnsberger G, Kyewski B (2009) Antigen presentation in the thymus for positive selection and central tolerance induction. Nat Rev Immunol 9: 833–844. doi:10.1038/nri2669.

19. Jameson SC, Hogquist KA, Bevan MJ (1995) Positive selection of thymocytes. Annu Rev Immunol 13: 93–126. doi:10.1146/annurev.iy.13.040195.000521.

20. Bhandoola A, Sambandam A (2006) From stem cell to T cell: one route or many? Nat Rev Immunol 6: 117–126. doi:10.1038/nri1778.

21. Fugmann SD, Lee AI, Shockett PE, Villey IJ, Schatz DG (2000) The RAG proteins and V(D)J recombination: complexes, ends, and transposition. Annu Rev Immunol 18: 495–527. doi:10.1146/annurev.immunol.18.1.495.

22. Wilson A, Held W, MacDonald HR (1994) Two waves of recombinase gene expression in developing thymocytes. J Exp Med 179: 1355–1360.

23. Kuo TC, Schlissel MS (2009) Mechanisms controlling expression of the RAG locus during lymphocyte development. Curr Opin Immunol 21: 173–178. doi:10.1016/j.coi.2009.03.008.

24. Huang C, Kanagawa O (2001) Ordered and coordinated rearrangement of the TCR alpha locus: role of secondary rearrangement in thymic selection. J Immunol 166: 2597–2601.

25. Nikolich-Zugich J, Slifka MK, Messaoudi I (2004) The many important facets of T-cell repertoire diversity. Nat Rev Immunol 4: 123–132. doi:10.1038/nri1292.

26. Morris GP, Allen PM (2012) How the TCR balances sensitivity and specificity for the recognition of self and pathogens. Nat Immunol 13: 121–128. doi:10.1038/ni.2190.

27. Landau NR, Schatz DG, Rosa M, Baltimore D (1987) Increased frequency of N-region insertion in a murine pre-B-cell line infected with a terminal deoxynucleotidyl transferase retroviral expression vector. Mol Cell Biol 7: 3237–3243.

28. Xing Y, Hogquist KA (2012) T-cell tolerance: central and peripheral. Cold Spring Harb Perspect Biol 4. doi:10.1101/cshperspect.a006957.

29. Park J-H, Adoro S, Guinter T, Erman B, Alag AS, et al. (2010) Signaling by intrathymic cytokines, not T cell antigen receptors, specifies CD8 lineage choice and promotes the differentiation of cytotoxic-lineage T cells. Nat Immunol 11: 257–264. doi:10.1038/ni.1840.

30. Singer A, Adoro S, Park J-H (2008) Lineage fate and intense debate: myths, models and mechanisms of CD4- versus CD8-lineage choice. Nat Rev Immunol 8: 788–801. doi:10.1038/nri2416.

31. Mathis D, Benoist C (2009) Aire. Annu Rev Immunol 27: 287–312. doi:10.1146/annurev.immunol.25.022106.141532.

32. Li J, Park J, Foss D, Goldschneider I (2009) Thymus-homing peripheral dendritic cells constitute two of the three major subsets of dendritic cells in the steady-state thymus. J Exp Med 206: 607–622. doi:10.1084/jem.20082232.

33. Weng N-P, Araki Y, Subedi K (2012) The molecular basis of the memory T cell response: differential gene expression and its epigenetic regulation. Nat Rev Immunol 12: 306–315. doi:10.1038/nri3173.

34. Sallusto F, Geginat J, Lanzavecchia A (2004) Central memory and effector memory T cell subsets: function, generation, and maintenance. Annu Rev Immunol 22: 745–763. doi:10.1146/annurev.immunol.22.012703.104702.

35. Harty JT, Badovinac VP (2008) Shaping and reshaping CD8+ T-cell memory. Nat Rev Immunol 8: 107–119. doi:10.1038/nri2251.

36. Pepper M, Jenkins MK (2011) Origins of CD4(+) effector and central memory T cells. Nat Immunol 12: 467–471.

37. Swain SL (1983) T cell subsets and the recognition of MHC class. Immunol Rev 74: 129–142.

38. Russell JH, Ley TJ (2002) Lymphocyte-mediated cytotoxicity. Annu Rev Immunol 20: 323–370. doi:10.1146/annurev.immunol.20.100201.131730.

39. Thiery J, Keefe D, Boulant S, Boucrot E, Walch M, et al. (2011) Perforin pores in the endosomal membrane trigger the release of endocytosed granzyme B into the cytosol of target cells. Nat Immunol. doi:10.1038/ni.2050.

40. Mosmann TR, Cherwinski H, Bond MW, Giedlin MA, Coffman RL (1986) Two types of murine helper T cell clone. I. Definition according to profiles of lymphokine activities and secreted proteins. J Immunol 136: 2348–2357.

41. Gor DO, Rose NR, Greenspan NS (2003) TH1-TH2: a procrustean paradigm. Nat Immunol 4: 503–505. doi:10.1038/ni0603-503.

42. Nakayamada S, Takahashi H, Kanno Y, O'shea JJ (2012) Helper T cell diversity and plasticity. Curr Opin Immunol 24: 297–302. doi:10.1016/j.coi.2012.01.014.

43. Snapper CM, Paul WE (1987) Interferon-gamma and B cell stimulatory factor-1 reciprocally regulate Ig isotype production. Science 236: 944–947.

44. Murphy KM, Stockinger B (2010) Effector T cell plasticity: flexibility in the face of changing circumstances. Nat Immunol 11: 674–680. doi:10.1038/ni.1899.

45. Abbas AK, Murphy KM, Sher A (1996) Functional diversity of helper T lymphocytes. Nature 383: 787–793. doi:10.1038/383787a0.

46. Zhu J, Paul WE (2008) CD4 T cells: fates, functions, and faults. Blood 112: 1557–1569. doi:10.1182/blood-2008-05-078154.

47. Coffman RL, Seymour BW, Hudak S, Jackson J, Rennick D (1989) Antibody to interleukin-5 inhibits helminth-induced eosinophilia in mice. Science 245: 308–310.

48. Harrington LE, Hatton RD, Mangan PR, Turner H, Murphy TL, et al. (2005) Interleukin 17-producing CD4+ effector T cells develop via a lineage distinct from the T helper type 1 and 2 lineages. Nat Immunol 6: 1123–1132. doi:10.1038/ni1254.

49. Park H, Li Z, Yang XO, Chang SH, Nurieva R, et al. (2005) A distinct lineage of CD4 T cells regulates tissue inflammation by producing interleukin 17. Nat Immunol 6: 1133–1141. doi:10.1038/ni1261.

50. Korn T, Bettelli E, Oukka M, Kuchroo VK (2009) IL-17 and Th17 Cells. Annu Rev Immunol. doi:10.1146/annurev.immunol.021908.132710.

51. Zhu J, Yamane H, Paul WE (2010) Differentiation of effector CD4 T cell populations (*). Annu Rev Immunol 28: 445–489. doi:10.1146/annurev-immunol-030409-101212.

52. Stritesky GL, Jameson SC, Hogquist KA (2012) Selection of self-reactive T cells in the thymus. Annu Rev Immunol 30: 95–114. doi:10.1146/annurev-immunol-020711-075035.

53. Abbas AK, Benoist C, Bluestone JA, Campbell DJ, Ghosh S, et al. (2013) Regulatory T cells: recommendations to simplify the nomenclature. Nat Immunol 14: 307–308. doi:10.1038/ni.2554.

54. Tubo NJ, Pagán AJ, Taylor JJ, Nelson RW, Linehan JL, et al. (2013) Single Naive CD4(+) T Cells from a Diverse Repertoire Produce Different Effector Cell Types during Infection. Cell 153: 785–796. doi:10.1016/j.cell.2013.04.007.

55. Arase H, Arase N, Ogasawara K, Good RA, Onoé K (1992) An NK1.1+ CD4+8- single-positive thymocyte subpopulation that expresses a highly skewed T-cell antigen receptor V beta family. Proc Natl Acad Sci USA 89: 6506–6510.

56. Porcelli S, Yockey CE, Brenner MB, Balk SP (1993) Analysis of T cell antigen receptor (TCR) expression by human peripheral blood CD4-8- alpha/beta T cells demonstrates preferential use of several V beta genes and an invariant TCR alpha chain. J Exp Med 178: 1–16.

57. Dellabona P, Padovan E, Casorati G, Brockhaus M, Lanzavecchia A (1994) An invariant V alpha 24-J alpha Q/V beta 11 T cell receptor is expressed in all individuals by clonally expanded CD4-8- T cells. J Exp Med 180: 1171–1176.

58. Exley M, Garcia J, Balk SP, Porcelli S (1997) Requirements for CD1d recognition by human invariant Valpha24+ CD4-CD8- T cells. J Exp Med 186: 109–120.

59. Gapin L, Matsuda JL, Surh CD, Kronenberg M (2001) NKT cells derive from double-positive thymocytes that are positively selected by CD1d. Nat Immunol 2: 971–978. doi:10.1038/ni710.

60. McNab FW, Pellicci DG, Field K, Besra GS, Smyth MJ, et al. (2007) Peripheral NK1.1 NKT cells are mature and functionally distinct from their thymic counterparts. J Immunol 179: 6630–6637.

61. Godfrey DI, Macdonald HR, Kronenberg M, Smyth MJ, Kaer LV (2004) NKT cells: what's in a name? Nat Rev Immunol 4: 231–237. doi:10.1038/nri1309.

62. Kronenberg M (2005) Toward an understanding of NKT cell biology: progress and paradoxes. Annu Rev Immunol 23: 877–900. doi:10.1146/annurev.immunol.23.021704.115742.

63. Matsuda JL, Mallevaey T, Scott-Browne JP, Gapin L (2008) CD1d-restricted iNKT cells, the "Swiss-Army knife" of the immune system. Curr Opin Immunol 20: 358–368. doi:10.1016/j.coi.2008.03.018.

64. Bendelac A, Savage PB, Teyton L (2007) The Biology of NKT Cells. Annu Rev Immunol 25: 297–336.

65. Kawano T, Cui J, Koezuka Y, Toura I, Kaneko Y, et al. (1997) CD1d-restricted and TCR-mediated activation of valpha14 NKT cells by glycosylceramides. Science 278: 1626–1629.

66. Lantz O, Bendelac A (1994) An invariant T cell receptor alpha chain is used by a unique subset of major histocompatibility complex class I-specific CD4+ and CD4-8- T cells in mice and humans. J Exp Med 180: 1097–1106.

67. Bendelac A, Killeen N, Littman DR, Schwartz RH (1994) A subset of CD4+ thymocytes selected by MHC class I molecules. Science 263: 1774–1778.

68. Brossay L, Chioda M, Burdin N, Koezuka Y, Casorati G, et al. (1998) CD1d-mediated recognition of an alpha-galactosylceramide by natural killer T cells is highly conserved through mammalian evolution. J Exp Med 188: 1521–1528.

69. Gapin L, Godfrey DI, Rossjohn J (2013) Natural Killer T cell obsession with self-antigens. Curr Opin Immunol. doi:10.1016/j.coi.2013.01.002.

70. Bendelac A, Lantz O, Quimby M, Yewdell J, Bennink J, et al. (1995) CD1 recognition by mouse NK1+ T lymphocytes. Science 268: 863–865.

71. Smiley ST, Kaplan MH, Grusby MJ (1997) Immunoglobulin E production in the absence of interleukin-4-secreting CD1-dependent cells. Science 275: 977–979.

72. Mori L, De Libero G (2012) T cells specific for lipid antigens. Immunol Res 53: 191–199. doi:10.1007/s12026-012-8294-6.

73. Girardi E, Zajonc DM (2012) Molecular basis of lipid antigen presentation by CD1d and recognition by natural killer T cells. Immunol Rev 250: 167–179. doi:10.1111/j.1600-065X.2012.01166.x.

74. Chiu Y-H, Park S-H, Benlagha K, Forestier C, Jayawardena-Wolf J, et al. (2002) Multiple defects in antigen presentation and T cell development by mice expressing cytoplasmic tail-truncated CD1d. Nat Immunol 3: 55–60. doi:10.1038/ni740.

75. Godfrey DI, Berzins SP (2007) Control points in NKT-cell development. Nat Rev Immunol 7: 505–518. doi:10.1038/nri2116.

76. Engel I, Hammond K, Sullivan BA, He X, Taniuchi I, et al. (2010) Co-receptor choice by V alpha14i NKT cells is driven by Th-POK expression rather than avoidance of CD8-mediated negative selection. J Exp Med 207: 1015–1029. doi:10.1084/jem.20090557.

77. Egawa T, Eberl G, Taniuchi I, Benlagha K, Geissmann F, et al. (2005) Genetic evidence supporting selection of the Valpha14i NKT cell lineage from double-positive thymocyte precursors. Immunity 22: 705–716. doi:10.1016/j.immuni.2005.03.011.

78. Benlagha K, Wei DG, Veiga J, Teyton L, Bendelac A (2005) Characterization of the early stages of thymic NKT cell development. J Exp Med 202: 485–492. doi:10.1084/jem.20050456.

79. Pellicci DG, Hammond KJL, Uldrich AP, Baxter AG, Smyth MJ, et al. (2002) A natural killer T (NKT) cell developmental pathway iInvolving a thymus-dependent NK1.1(-)CD4(+) CD1d-dependent precursor stage. J Exp Med 195: 835–844.

80. Bezbradica JS, Hill T, Stanic AK, Van Kaer L, Joyce S (2005) Commitment toward the natural T (iNKT) cell lineage occurs at the CD4+8+ stage of thymic ontogeny. Proc Natl Acad Sci USA 102: 5114–5119. doi:10.1073/pnas.0408449102.

81. Bendelac A, Hunziker R, Lantz O (1996) Increased interleukin 4 and immunoglobulin E production in transgenic mice overexpressing NK1 T cells. J Exp Med 184: 1285–1293.

82. Wakao H, Kawamoto H, Sakata S, Inoue K, Ogura A, et al. (2007) A novel mouse model for invariant NKT cell study. J Immunol 179: 3888–3895.

83. Griewank K, Borowski C, Rietdijk S, Wang N, Julien A, et al. (2007) Homotypic interactions mediated by Slamf1 and Slamf6 receptors control NKT cell lineage development. Immunity 27: 751–762. doi:10.1016/j.immuni.2007.08.020.

84. Thapa P, Das J, McWilliams D, Shapiro M, Sundsbak R, et al. (2013) The transcriptional repressor NKAP is required for the development of iNKT cells. Nat Commun 4: 1582. doi:10.1038/ncomms2580.

85. Wei DG, Lee H, Park S-H, Beaudoin L, Teyton L, et al. (2005) Expansion and long-range differentiation of the NKT cell lineage in mice expressing CD1d exclusively on cortical thymocytes. J Exp Med 202: 239–248. doi:10.1084/jem.20050413.

86. Schümann J, Pittoni P, Tonti E, Macdonald HR, Dellabona P, et al. (2005) Targeted expression of human CD1d in transgenic mice reveals independent roles for thymocytes and thymic APCs in positive and negative selection of Valpha14i NKT cells. J Immunol 175: 7303–7310.

87. Gapin L (2010) iNKT cell autoreactivity: what is “self” and how is it recognized? Nat Rev Immunol 10: 272–277. doi:10.1038/nri2743.

88. Moran AE, Holzapfel KL, Xing Y, Cunningham NR, Maltzman JS, et al. (2011) T cell receptor signal strength in Treg and iNKT cell development demonstrated by a novel fluorescent reporter mouse. J Exp Med 208: 1279–1289. doi:10.1084/jem.20110308.

89. Seiler MP, Mathew R, Liszewski MK, Spooner C, Barr K, et al. (2012) Elevated and sustained expression of the transcription factors Egr1 and Egr2 controls NKT lineage differentiation in response to TCR signaling. Nat Immunol 13: 264–271. doi:10.1038/ni.2230.

90. Kovalovsky D, Uche OU, Eladad S, Hobbs RM, Yi W, et al. (2008) The BTB–zinc finger transcriptional regulator PLZF controls the development of invariant natural killer T cell effector functions. Nat Immunol 9: 1055–1064. doi:10.1038/ni.1641.

91. Savage AK, Constantinides MG, Han J, Picard D, Martin E, et al. (2008) The transcription factor PLZF directs the effector program of the NKT cell lineage. Immunity 29: 391–403. doi:10.1016/j.immuni.2008.07.011.

92. Marodon G, Rocha B (1994) Generation of mature T cell populations in the thymus: CD4 or CD8 down-regulation occurs at different stages of thymocyte differentiation. Eur J Immunol 24: 196–204. doi:10.1002/eji.1830240131.

93. Benlagha K, Kyin T, Beavis A, Teyton L, Bendelac A (2002) A thymic precursor to the NK T cell lineage. Science 296: 553–555.

94. Matsuda JL, Naidenko OV, Gapin L, Nakayama T, Taniguchi M, et al. (2000) Tracking the response of natural killer T cells to a glycolipid antigen using CD1d tetramers. J Exp Med 192: 741–754.

95. Kobayashi E, Motoki K, Uchida T, Fukushima H, Koezuka Y (1995) KRN7000, a novel immunomodulator, and its antitumor activities. Oncol Res 7: 529–534.

96. Kinjo Y, Illarionov P, Vela JL, Pei B, Girardi E, et al. (2011) Invariant natural killer T cells recognize glycolipids from pathogenic Gram-positive bacteria. Nat Immunol 12: 966–974. doi:10.1038/ni.2096.

97. Kinjo Y, Wu D, Kim G, Xing G-W, Poles MA, et al. (2005) Recognition of bacterial glycosphingolipids by natural killer T cells. Nature 434: 520–525. doi:10.1038/nature03407.

98. Mattner J, Debord KL, Ismail N, Goff RD, Cantu C, et al. (2005) Exogenous and endogenous glycolipid antigens activate NKT cells during microbial infections. Nature 434: 525–529. doi:10.1038/nature03408.

99. Kinjo Y, Tupin E, Wu D, Fujio M, Garcia-Navarro R, et al. (2006) Natural killer T cells recognize diacylglycerol antigens from pathogenic bacteria. Nat Immunol 7: 978–986. doi:10.1038/ni1380.

100. Bendelac A, Bonneville M, Kearney J (2001) Autoreactivity by design: innate B and T lymphocytes. Nat Rev Immunol 1: 177–186.

101. Facciotti F, Ramanjaneyulu GS, Lepore M, Sansano S, Cavallari M, et al. (2012) Peroxisome-derived lipids are self antigens that stimulate invariant natural killer T cells in the thymus. Nat Immunol 13: 474–480. doi:10.1038/ni.2245.

102. Zhou D, Mattner J, Cantu C, Schrantz N, Yin N, et al. (2004) Lysosomal glycosphingolipid recognition by NKT cells. Science 306: 1786–1789.

103. Brigl M, Bry L, Kent SC, Gumperz JE, Brenner MB (2003) Mechanism of CD1d-restricted natural killer T cell activation during microbial infection. Nat Immunol 4: 1230–1237. doi:10.1038/ni1002.

104. De Santo C, Salio M, Masri SH, Lee LY-H, Dong T, et al. (2008) Invariant NKT cells reduce the immunosuppressive activity of influenza A virus-induced myeloid-derived suppressor cells in mice and humans. J Clin Invest 118: 4036–4048. doi:10.1172/JCI36264.

105. Crowe NY, Smyth MJ, Godfrey DI (2002) A critical role for natural killer T cells in immunosurveillance of methylcholanthrene-induced sarcomas. J Exp Med 196: 119–127.

106. Darmoise A, Teneberg S, Bouzonville L, Brady RO, Beck M, et al. (2010) Lysosomal alpha-galactosidase controls the generation of self lipid antigens for natural killer T cells. Immunity 33: 216–228. doi:10.1016/j.immuni.2010.08.003.

107. Brennan PJ, Tatituri RVV, Brigl M, Kim EY, Tuli A, et al. (2011) Invariant natural killer T cells recognize lipid self antigen induced by microbial danger signals. Nat Immunol. doi:10.1038/ni.2143.

108. Li Y, Girardi E, Wang J, Yu ED, Painter GF, et al. (2010) The Vα14 invariant natural killer T cell TCR forces microbial glycolipids and CD1d into a conserved binding mode. J Exp Med 207: 2383–2393. doi:10.1084/jem.20101335.

109. Pellicci DG, Patel O, Kjer-Nielsen L, Pang SS, Sullivan LC, et al. (2009) Differential recognition of CD1d-alpha-galactosyl ceramide by the V beta 8.2 and V beta 7 semi-invariant NKT T cell receptors. Immunity 31: 47–59. doi:10.1016/j.immuni.2009.04.018.

110. Pellicci DG, Clarke AJ, Patel O, Mallevaey T, Beddoe T, et al. (2011) Recognition of β-linked self glycolipids mediated by natural killer T cell antigen receptors. Nat Immunol 12: 827–833. doi:10.1038/ni.2076.

111. Rossjohn J, Pellicci DG, Patel O, Gapin L, Godfrey DI (2012) Recognition of CD1d-restricted antigens by natural killer T cells. Nat Rev Immunol 12: 845–857. doi:10.1038/nri3328.

112. Brigl M, Tatituri RVV, Watts GFM, Bhowruth V, Leadbetter EA, et al. (2011) Innate and cytokine-driven signals, rather than microbial antigens, dominate in natural killer T cell activation during microbial infection. J Exp Med 208: 1163–1177. doi:10.1084/jem.20102555.

113. Nagarajan NA, Kronenberg M (2007) Invariant NKT cells amplify the innate immune response to lipopolysaccharide. J Immunol 178: 2706–2713.

114. Brigl M, Brenner MB (2010) How invariant natural killer T cells respond to infection by recognizing microbial or endogenous lipid antigens. Semin Immunol 22: 79–86. doi:10.1016/j.smim.2009.10.006.

115. Brennan PJ, Brigl M, Brenner MB (2013) Invariant natural killer T cells: an innate activation scheme linked to diverse effector functions. Nat Rev Immunol. doi:10.1038/nri3369.

116. Coquet JM, Chakravarti S, Kyparissoudis K, McNab FW, Pitt LA, et al. (2008) Diverse cytokine production by NKT cell subsets and identification of an IL-17-producing CD4-NK1.1- NKT cell population. Proc Natl Acad Sci USA 105: 11287–11292. doi:10.1073/pnas.0801631105.

117. Matsuda JL, Gapin L, Baron JL, Sidobre S, Stetson DB, et al. (2003) Mouse V alpha 14i natural killer T cells are resistant to cytokine polarization in vivo. Proc Natl Acad Sci USA 100: 8395–8400. doi:10.1073/pnas.1332805100.

118. Stetson DB, Mohrs M, Reinhardt RL, Baron JL, Wang Z-E, et al. (2003) Constitutive cytokine mRNAs mark natural killer (NK) and NK T cells poised for rapid effector function. J Exp Med 198: 1069–1076. doi:10.1084/jem.20030630.

119. Chang Y-J, Huang J-R, Tsai Y-C, Hung J-T, Wu D, et al. (2007) Potent immune-modulating and anticancer effects of NKT cell stimulatory glycolipids. Proc Natl Acad Sci USA 104: 10299–10304. doi:10.1073/pnas.0703824104.

120. Matsuda JL, Zhang Q, Ndonye R, Richardson SK, Howell AR, et al. (2006) T-bet concomitantly controls migration, survival, and effector functions during the development of Valpha14i NKT cells. Blood 107: 2797–2805. doi:10.1182/blood-2005-08-3103.

121. Berzins SP, Smyth MJ, Baxter AG (2011) Presumed guilty: natural killer T cell defects and human disease. Nat Rev Immunol 11: 131–142. doi:10.1038/nri2904.

122. Kinjo Y, Ueno K (2011) iNKT cells in microbial immunity: recognition of microbial glycolipids. Microbiology and immunology. doi:10.1111/j.1348-0421.2011.00338.x.

123. Nishizuka Y, Sakakura T (1969) Thymus and reproduction: sex-linked dysgenesia of the gonad after neonatal thymectomy in mice. Science 166: 753–755.

124. Kojima A, Prehn RT (1981) Genetic susceptibility to post-thymectomy autoimmune diseases in mice. Immunogenetics 14: 15–27.

125. Penhale WJ, Farmer A, McKenna RP, Irvine WJ (1973) Spontaneous thyroiditis in thymectomized and irradiated Wistar rats. Clin Exp Immunol 15: 225–236.

126. Sakaguchi S, Takahashi T, Nishizuka Y (1982) Study on cellular events in postthymectomy autoimmune oophoritis in mice. I. Requirement of Lyt-1 effector cells for oocytes damage after adoptive transfer. J Exp Med 156: 1565–1576.

127. Taguchi O, Nishizuka Y (1980) Autoimmune oophoritis in thymectomized mice: T cell requirement in adoptive cell transfer. Clin Exp Immunol 42: 324–331.

128. Sakaguchi S, Takahashi T, Nishizuka Y (1982) Study on cellular events in post-thymectomy autoimmune oophoritis in mice. II. Requirement of Lyt-1 cells in normal female mice for the prevention of oophoritis. J Exp Med 156: 1577–1586. doi:10.1084/jem.156.6.1577.

129. Josefowicz SZ, Lu L-F, Rudensky AY (2012) Regulatory T cells: mechanisms of differentiation and function. Annu Rev Immunol 30: 531–564. doi:10.1146/annurev.immunol.25.022106.141623.

130. Sakaguchi S, Fukuma K, Kuribayashi K, Masuda T (1985) Organ-specific autoimmune diseases induced in mice by elimination of T cell subset. I. Evidence for the active participation of T cells in natural self-tolerance; deficit of a T cell subset as a possible cause of autoimmune disease. J Exp Med 161: 72–87.

131. Morrissey PJ, Charrier K, Braddy S, Liggitt D, Watson JD (1993) CD4+ T cells that express high levels of CD45RB induce wasting disease when transferred into congenic severe combined immunodeficient mice. Disease development is prevented by cotransfer of purified CD4+ T cells. J Exp Med 178: 237–244.

132. Sakaguchi S, Sakaguchi N, Asano M, Itoh M, Toda M (1995) Immunologic self-tolerance maintained by activated T cells expressing IL-2 receptor alpha-chains (CD25). Breakdown of a single mechanism of self-tolerance causes various autoimmune diseases. J Immunol 155: 1151–1164.

133. Sakaguchi S (2011) Regulatory T cells: history and perspective. Methods Mol Bio 707: 3–17. doi:10.1007/978-1-61737-979-6_1.

134. Fontenot JD, Gavin MA, Rudensky AY (2003) Foxp3 programs the development and function of CD4+CD25+ regulatory T cells. Nat Immunol 4: 330–336. doi:10.1038/ni904.

135. Hori S, Nomura T, Sakaguchi S (2003) Control of regulatory T cell development by the transcription factor Foxp3. Science 299: 1057–1061. doi:10.1126/science.1079490.

136. Khattri R, Cox T, Yasayko S-A, Ramsdell F (2003) An essential role for Scurfin in CD4+CD25+ T regulatory cells. Nat Immunol 4: 337–342. doi:10.1038/ni909.

137. Brunkow ME, Jeffery EW, Hjerrild KA, Paeper B, Clark LB, et al. (2001) Disruption of a new forkhead/winged-helix protein, scurfin, results in the fatal lymphoproliferative disorder of the scurfy mouse. Nat Genet 27: 68–73. doi:10.1038/83784.

138. Chatila TA, Blaeser F, Ho N, Lederman HM, Voulgaropoulos C, et al. (2000) JM2, encoding a fork head-related protein, is mutated in X-linked autoimmunity-allergic disregulation syndrome. J Clin Invest 106: R75–R81. doi:10.1172/JCI11679.

139. Wildin RS, Ramsdell F, Peake J, Faravelli F, Casanova JL, et al. (2001) X-linked neonatal diabetes mellitus, enteropathy and endocrinopathy syndrome is the human equivalent of mouse scurfy. Nat Genet 27: 18–20. doi:10.1038/83707.

140. Fontenot JD, Rasmussen JP, Williams LM, Dooley JL, Farr AG, et al. (2005) Regulatory T cell lineage specification by the forkhead transcription factor foxp3. Immunity 22: 329–341. doi:10.1016/j.immuni.2005.01.016.

141. Hill JA, Feuerer M, Tash K, Haxhinasto S, Perez J, et al. (2007) Foxp3 Transcription-Factor-Dependent and -Independent Regulation of the Regulatory T Cell Transcriptional Signature. Immunity 27: 786–800. doi:10.1016/j.immuni.2007.09.010.

142. Zheng Y, Josefowicz SZ, Kas A, Chu T-T, Gavin MA, et al. (2007) Genome-wide analysis of Foxp3 target genes in developing and mature regulatory T cells. Nature 445: 936–940. doi:10.1038/nature05563.

143. Marson A, Kretschmer K, Frampton GM, Jacobsen ES, Polansky JK, et al. (2007) Foxp3 occupancy and regulation of key target genes during T-cell stimulation. Nature 445: 931–935. doi:10.1038/nature05478.

144. Rudra D, Deroos P, Chaudhry A, Niec RE, Arvey A, et al. (2012) Transcription factor Foxp3 and its protein partners form a complex regulatory network. Nat Immunol. doi:10.1038/ni.2402.

145. Fontenot JD, Dooley JL, Farr AG, Rudensky AY (2005) Developmental regulation of Foxp3 expression during ontogeny. J Exp Med 202: 901–906. doi:10.1084/jem.20050784.

146. Hsieh C-S, Liang Y, Tyznik AJ, Self SG, Liggitt D, et al. (2004) Recognition of the peripheral self by naturally arising CD25+ CD4+ T cell receptors. Immunity 21: 267–277. doi:10.1016/j.immuni.2004.07.009.

147. Hsieh C-S, Zheng Y, Liang Y, Fontenot JD, Rudensky AY (2006) An intersection between the self-reactive regulatory and nonregulatory T cell receptor repertoires. Nat Immunol 7: 401–410. doi:10.1038/ni1318.

148. Hsieh C-S, Lee HM, Lio C-WJ (2012) Selection of regulatory T cells in the thymus. Nat Rev Immunol. doi:10.1038/nri3155.

149. McHugh RS, Whitters MJ, Piccirillo CA, Young DA, Shevach EM, et al. (2002) CD4(+)CD25(+) immunoregulatory T cells: gene expression analysis reveals a functional role for the glucocorticoid-induced TNF receptor. Immunity 16: 311–323.

150. Jordan MS, Boesteanu A, Reed AJ, Petrone AL, Holenbeck AE, et al. (2001) Thymic selection of CD4+CD25+ regulatory T cells induced by an agonist self-peptide. Nat Immunol 2: 301–306. doi:10.1038/86302.

151. Burchill MA, Yang J, Vogtenhuber C, Blazar BR, Farrar MA (2007) IL-2 receptor beta-dependent STAT5 activation is required for the development of Foxp3+ regulatory T cells. J Immunol 178: 280–290.

152. Lio C-WJ, Hsieh C-S (2008) A two-step process for thymic regulatory T cell development. Immunity 28: 100–111. doi:10.1016/j.immuni.2007.11.021.

153. Ohkura N, Hamaguchi M, Morikawa H, Sugimura K, Tanaka A, et al. (2012) T Cell Receptor Stimulation-Induced Epigenetic Changes and Foxp3 Expression Are Independent and Complementary Events Required for Treg Cell Development. Immunity. doi:10.1016/j.immuni.2012.09.010.

154. Gavin MA, Rasmussen JP, Fontenot JD, Vasta V, Manganiello VC, et al. (2007) Foxp3-dependent programme of regulatory T-cell differentiation. Nature 445: 771–775. doi:10.1038/nature05543.

155. Toker A, Engelbert D, Garg G, Polansky JK, Floess S, et al. (2013) Active Demethylation of the Foxp3 Locus Leads to the Generation of Stable Regulatory T Cells within the Thymus. J Immunol. doi:10.4049/jimmunol.1203473.

156. Fisson S, Darrasse-Jèze G, Litvinova E, Septier F, Klatzmann D, et al. (2003) Continuous activation of autoreactive CD4+ CD25+ regulatory T cells in the steady state. J Exp Med 198: 737–746. doi:10.1084/jem.20030686.

157. Huehn J, Siegmund K, Lehmann JCU, Siewert C, Haubold U, et al. (2004) Developmental stage, phenotype, and migration distinguish naive- and effector/memory-like CD4+ regulatory T cells. J Exp Med 199: 303–313. doi:10.1084/jem.20031562.

158. Lee JH, Kang SG, Kim CH (2007) FoxP3+ T cells undergo conventional first switch to lymphoid tissue homing receptors in thymus but accelerated second switch to nonlymphoid tissue homing receptors in secondary lymphoid tissues. J Immunol 178: 301–311.

159. Koch MA, Tucker-Heard G, Perdue NR, Killebrew JR, Urdahl KB, et al. (2009) The transcription factor T-bet controls regulatory T cell homeostasis and function during type 1 inflammation. Nat Immunol 10: 595–602. doi:10.1038/ni.1731.

160. Wang Y, Su MA, Wan YY (2011) An Essential Role of the Transcription Factor GATA-3 for the Function of Regulatory T Cells. Immunity. doi:10.1016/j.immuni.2011.08.012.

161. Chung Y, Tanaka S, Chu F, Nurieva RI, Martinez GJ, et al. (2011) Follicular regulatory T cells expressing Foxp3 and Bcl-6 suppress germinal center reactions. Nat Med. doi:10.1038/nm.2426.

162. Campbell DJ, Koch MA (2011) Phenotypical and functional specialization of FOXP3+ regulatory T cells. Nat Rev Immunol 11: 119–130. doi:10.1038/nri2916.

163. Cretney E, Kallies A, Nutt SL (2012) Differentiation and function of Foxp3(+) effector regulatory T cells. Trends Immunol. doi:10.1016/j.it.2012.11.002.

164. Kim JM, Rasmussen JP, Rudensky AY (2007) Regulatory T cells prevent catastrophic autoimmunity throughout the lifespan of mice. Nat Immunol 8: 191–197. doi:10.1038/ni1428.

165. Vignali DAA, Collison LW, Workman CJ (2008) How regulatory T cells work. Nat Rev Immunol 8: 523–532. doi:10.1038/nri2343.

166. Shevach EM (2009) Mechanisms of foxp3+ T regulatory cell-mediated suppression. Immunity 30: 636–645. doi:10.1016/j.immuni.2009.04.010.

167. Setoguchi R, Hori S, Takahashi T, Sakaguchi S (2005) Homeostatic maintenance of natural Foxp3(+) CD25(+) CD4(+) regulatory T cells by interleukin (IL)-2 and induction of autoimmune disease by IL-2 neutralization. J Exp Med 201: 723–735. doi:10.1084/jem.20041982.

168. Pandiyan P, Zheng L, Ishihara S, Reed J, Lenardo MJ (2007) CD4+CD25+Foxp3+ regulatory T cells induce cytokine deprivation-mediated apoptosis of effector CD4+ T cells. Nat Immunol 8: 1353–1362. doi:10.1038/ni1536.

169. Deaglio S, Dwyer KM, Gao W, Friedman D, Usheva A, et al. (2007) Adenosine generation catalyzed by CD39 and CD73 expressed on regulatory T cells mediates immune suppression. J Exp Med 204: 1257–1265. doi:10.1084/jem.20062512.

170. Gondek DC, Lu L-F, Quezada SA, Sakaguchi S, Noelle RJ (2005) Cutting edge: contact-mediated suppression by CD4+CD25+ regulatory cells involves a granzyme B-dependent, perforin-independent mechanism. J Immunol 174: 1783–1786.

171. Zhao D-M, Thornton AM, Dipaolo RJ, Shevach EM (2006) Activated CD4+CD25+ T cells selectively kill B lymphocytes. Blood 107: 3925–3932. doi:10.1182/blood-2005-11-4502.

172. Boissonnas A, Scholer-Dahirel A, Simon-Blancal V, Pace L, Valet F, et al. (2010) Foxp3+ T cells induce perforin-dependent dendritic cell death in tumor-draining lymph nodes. Immunity 32: 266–278. doi:10.1016/j.immuni.2009.11.015.

173. Asseman C, Mauze S, Leach MW, Coffman RL, Powrie F (1999) An essential role for interleukin 10 in the function of regulatory T cells that inhibit intestinal inflammation. J Exp Med 190: 995–1004.

174. Rubtsov YP, Rasmussen JP, Chi EY, Fontenot J, Castelli L, et al. (2008) Regulatory T cell-derived interleukin-10 limits inflammation at environmental interfaces. Immunity 28: 546–558. doi:10.1016/j.immuni.2008.02.017.

175. Collison LW, Workman CJ, Kuo TT, Boyd K, Wang Y, et al. (2007) The inhibitory cytokine IL-35 contributes to regulatory T-cell function. Nature 450: 566–569. doi:10.1038/nature06306.

176. Wing K, Onishi Y, Prieto-Martin P, Yamaguchi T, Miyara M, et al. (2008) CTLA-4 control over Foxp3+ regulatory T cell function. Science 322: 271–275. doi:10.1126/science.1160062.

177. Qureshi OS, Zheng Y, Nakamura K, Attridge K, Manzotti C, et al. (2011) Trans-endocytosis of CD80 and CD86: a molecular basis for the cell-extrinsic function of CTLA-4. Science 332: 600–603. doi:10.1126/science.1202947.

178. Liang B, Workman C, Lee J, Chew C, Dale BM, et al. (2008) Regulatory T cells inhibit dendritic cells by lymphocyte activation gene-3 engagement of MHC class II. J Immunol 180: 5916–5926.

179. Benoist C, Mathis D (2012) Treg cells, life history, and diversity. Cold Spring Harb Perspect Biol 4: a007021. doi:10.1101/cshperspect.a007021.

10. Supplements

In the following, paper I, II and III are reprinted.

Paper I

Vahl J.C., Heger K., Knies N., Hein M.Y., Boon L., Yagita H., Polic B. and Schmidt-Supprian M. (2013). NKT cell-TCR expression activates conventional T cells in vivo, but is largely dispensable for mature NKT cell biology.
PLOS Biology 11(6): e1001589. doi: 10.1371/journal.pbio.1001589.

OPEN ACCESS Freely available online

PLOS BIOLOGY

NKT Cell-TCR Expression Activates Conventional T Cells in Vivo, but Is Largely Dispensable for Mature NKT Cell Biology

J. Christoph Vahl[1], Klaus Heger[1], Nathalie Knies[1¤a], Marco Y. Hein[1¤b], Louis Boon[2], Hideo Yagita[3], Bojan Polic[4], Marc Schmidt-Supprian[1]*

1 Molecular Immunology and Signaltransduction, Max Planck Institute of Biochemistry, Martinsried, Germany, **2** Bioceros, Yalelaan 46, Utrecht, The Netherlands, **3** Juntendo University School of Medicine, Tokyo, Japan, **4** University of Rijeka School of Medicine, Rijeka, Croatia

Abstract

Natural killer T (NKT) cell development depends on recognition of self-glycolipids via their semi-invariant Vα14i-TCR. However, to what extent TCR-mediated signals determine identity and function of mature NKT cells remains incompletely understood. To address this issue, we developed a mouse strain allowing conditional Vα14i-TCR expression from within the endogenous *Tcrα* locus. We demonstrate that naïve T cells are activated upon replacement of their endogenous TCR repertoire with Vα14i-restricted TCRs, but they do not differentiate into NKT cells. On the other hand, induced TCR ablation on mature NKT cells did not affect their lineage identity, homeostasis, or innate rapid cytokine secretion abilities. We therefore propose that peripheral NKT cells become unresponsive to and thus are independent of their autoreactive TCR.

Citation: Vahl JC, Heger K, Knies N, Hein MY, Boon L, et al. (2013) NKT Cell-TCR Expression Activates Conventional T Cells in Vivo, but Is Largely Dispensable for Mature NKT Cell Biology. PLoS Biol 11(6): e1001589. doi:10.1371/journal.pbio.1001589

Academic Editor: Philippa Marrack, National Jewish Medical and Research Center/Howard Hughes Medical Institute, United States of America

Received December 14, 2012; **Accepted** May 7, 2013; **Published** June 18, 2013

Funding: This study was supported by the DFG through an Emmy Noether grant and SFB 1054 to MS-S. The Vα14iStopF mice were generated with support from a Sandler Foundation for Asthma Research grant to Klaus Rajewsky. JCV and KH received PhD stipends from the Ernst Schering Foundation and the Boehringer Ingelheim Fonds, respectively. The funders had no role in study design, data collection and analysis, decision to publish, or preparation of the manuscript.

Competing Interests: The authors have declared that no competing interests exist.

Abbreviations: α-GalCer, α-Galactosylceramide; DN, double-negative; Egr2, early growth response protein 2; GATA-3, GATA binding protein 3; ICOS, inducible T-cell co-stimulator; NKT, natural killer T; PLZF, promyelocytic leukemia zinc finger; ROR-γt, Retinoic acid-related Orphan Receptor Gamma; SLAMf, SLAM family; T-bet, T-box expressed in T cells; tg, transgenic; Th-POK, T-helper-inducing POZ/Krüppel-like factor; Va14i, Vα14-Jα18.

* E-mail: supprian@biochem.mpg.de

¤a Current address: Institut für Klinische Chemie und Pathobiochemie, Klinikum rechts der Isar, Technische Universität München, Munich, Germany.
¤b Current address: Proteomics and Signal Transduction, Max Planck Institute of Biochemistry, Martinsried, Germany.

Introduction

Natural Killer T (NKT) cells represent a subset of T cells in mice and humans that express NK cell markers and recognize a small class of glycolipid (auto-) antigens [1,2]. Most mouse NKT cells express an invariant Vα14-Jα18 (Vα14i) TCRα rearrangement (Vα24-Jα18 in humans). In principle, all TCRβ-chains are able to pair with this Vα14i-TCR chain [3]. However, the selection of NKT cells by endogenous glycolipids presented by the monomorphic MHC class I-like CD1d induces a strong bias towards TCRs containing Vβ8, Vβ7, or Vβ2 [1,3], which is abrogated in the absence of selection [3,4]. Recently, crystallographic analysis demonstrated a conserved binding mode of the NKT cell TCR to various glycolipids, where only germline-encoded residues were in direct antigen contact, reminiscent of innate pattern-recognition receptors [5]. Moreover, several observations suggest that this receptor is inherently auto-reactive [1,2] and thereby determines NKT cell identity and influences their function. The expression of several inhibitory NK cell receptors on NKT cells was suggested to control their self-reactivity and avoid autoimmune activation [6,7].

During development in the thymus, the few T cells expressing a Vα14i-TCR are selected upon recognition of self-lipids on double-positive thymocytes. Although several good candidates have been put forward [8–10], the exact nature of the selecting glycolipids remains controversial. Homotypic interactions involving the SLAM family (SLAMf) receptors 1 and 6 are additionally required for NKT cell differentiation [11]. Auto-reactive activation during thymic selection is thought to induce a substantially stronger TCR stimulus in comparison to that during the development of conventional T cells [12,13]. As a consequence, expression of the transcription factors Egr1 and Egr2 is strongly increased [13], which in turn directly induce PLZF, the key transcription factor controlling NKT cell differentiation, migration, and functions [13].

Interestingly, the homeostatic proliferation of NKT cells after adoptive transfer was similar in CD1d-deficient and wild-type mice, indicating that this process is mostly cytokine-driven and does not depend on continued TCR-mediated self-lipid-recognition [14,15]. However, as the transferred cells contained CD1d, a role for antigen could not be completely excluded. In addition, tonic antigen-independent TCR signals might contribute to NKT cell maintenance and phenotype. During immune responses, NKT cell activation depends mostly on two parameters: engagement of the TCR and the presence of proinflammatory cytokines released from antigen-presenting cells activated by innate immune path-

Author Summary

Immune system natural killer T (NKT) cells help to protect against certain strains of bacteria and viruses, and suppress the development of autoimmune diseases and cancer. However, NKT cells are also central mediators of allergic responses. The recognition of one's own glycolipid antigens (self-glycolipids) in the thymus via the unique Vα14i T cell receptor, Vα14i-TCR, triggers the NKT cell developmental program, which differs considerably from that of conventional T cells. We generated a mouse model to investigate whether the Vα14i-TCR on mature NKT cells constantly recognizes self-glycolipids and to assess whether this TCR is required for survival and continued NKT cell identity. Switching the peptide-recognizing TCR of a mature conventional T cell to a glycolipid-recognizing Vα14i-TCR led to activation of the T cells, indicating that this TCR is also autoreactive on peripheral T cells or can signal autonomously. But TCR ablation did not affect the half-life, characteristic gene expression or innate functions of mature NKT cells. Therefore, the inherently autoreactive Vα14i-TCR is dispensable for the functions of mature peripheral NKT cells after instructing thymic NKT cell development. Thus the Vα14i-TCR serves a similar function to pattern-recognition receptors, in mediating immune recognition of foreign invasion or diseased cells.

ways such as toll-like receptor (TLR) signals. Lipids derived from different bacteria [16–19] were shown to directly activate mouse and human NKT cells in a TLR- and IL-12-independent manner, and NKT cells are required for productive immune responses against these pathogens. NKT cells can also be activated indirectly through cytokines such as IL-12, IL-18, or type I interferons (IFNs) [20]. However, it remains controversial whether, depending on the strength of the cytokine signal, weak responses to self-antigens presented by CD1d are an additional obligate requirement. In one study, CD1d-dependent signals were found to be necessary for full NKT cell activation in response to all tested pathogens [20]. In contrast, others reported that IL-12-dependent NKT cell activation after LPS injection [21] or MCMV infection [22] is independent of either foreign or self-glycolipid antigen presentation by CD1d.

Upon activation, the most distinguishing feature of NKT cells is their ability to rapidly produce and secrete large amounts of cytokines (Th1 and Th2 cytokines, among others). Their fast, effector-like response could be based on steady-state expression of cytokine mRNA in mice [23,24] that was suggested to be a consequence of tonic self-reactive activation [2]. Recently, it was reported that human NKT cells do not constitutively express cytokine mRNAs. Instead, rapid cytokine-induced innate IFNγ production by NKT cells was suggested to rely on obligate continuous recognition of self-lipids, which retains histone acetylation patterns at the *IFNG* locus that favor transcription [25]. Another characteristic feature of NKT cells, their surface marker expression reminiscent of memory or recently activated T cells, was also connected to their inherent autoreactivity [2].

To thoroughly address the open questions regarding the nature and importance of TCR signaling for NKT cells, we generated a novel mouse model that allowed us to study the extent of Vα14i-TCR-mediated auto-antigen recognition in the periphery and its relevance for NKT cell identity. Furthermore, we monitored the fate of NKT cells after TCR ablation. Our results prove the inherent self-reactivity of the NKT cell TCR and demonstrate that although essential for positive selection, tonic TCR signaling is not required for NKT cell homeostasis, lineage identity, and rapid cytokine secretion.

Results

Correct Timing and Endogenous Control of Vα14i-TCR Expression Produces Large Numbers of Bona Fide NKT Cells

In order to produce large numbers of NKT cells in a physiological manner and to manipulate the expression of the semi-invariant Vα14i-TCR in a conditional fashion, we generated *Vα14i*^{StopF} knock-in mice. To this end we cloned a productive *Vα14-Jα18* rearrangement, including the *Vα14* leader exon, intron and 1.8 kb of upstream regulatory sequence, and 0.2 kb intronic sequence downstream of *Jα18*. These elements were inserted by homologous recombination 3′ of *Jα1* upstream of the *Cα* constant region of the *Tcrα* locus (Figure 1A). Expression of putative upstream rearrangements is aborted by four SV40 polyA sites at the 5′ end of the construct, and expression of Vα14i is rendered conditional through a loxP-flanked STOP cassette. We obtained over 80% (271 of 325) homologous recombinant ES cell clones during gene targeting, indicating an unusually high targeting efficiency of our construct (Figure S1A). The development of conventional T and NKT cells, identified by staining with mouse CD1d-PBS57-tetramers (tetramer+), occurs unperturbed in *Vα14i*^{StopF}*/wt* heterozygous mice. In homozygous *Vα14i*$^{StopF/F}$ mice, T cell development is abolished due to transcriptional termination of TCRα expression before the Cα exons (Figure 1B). We bred *Vα14i*^{StopF} to *CD4-Cre* mice, in order to express the inserted Vα14i-chain in double-positive thymocytes, mimicking the physiological timing of TCRα-chain rearrangement and expression [26,27]. On average 23 times more thymic and 43 times more splenic NKT cells were generated in these, compared to wild-type mice (Figures 1B and 2A–E). Around 9% of the tetramer+ T cells in *CD4-Cre Vα14i*^{StopF}*/wt* mice expressed the CD8 co-receptor (over 80% as CD8αβ heterodimer; Figures 1C and S1B,C), which is also expressed by some human NKT cells, but normally not in mice [28]. The proportions of CD4− CD8− double negative (DN) and CD4+ cells were comparable between transgenic (tg) and wild-type NKT cells (Figure 1C). Furthermore, the tgNKT cells were largely comparable to wild-type NKT cells with respect to Vβ-chain bias (Figure 1D) and surface phenotype (Figure 1E). Finally, we found that NKT cells from *CD4-Cre Vα14i*^{StopF}*/wt* animals expressed the critical transcription factors promyelocytic leukemia zinc finger (PLZF), GATA binding protein 3 (GATA-3), and T-helper-inducing POZ/Krüppel-like factor (Th-POK) (Figure 1F) [28,29]. Interestingly, we also detected a substantial proportion of the recently described NKT17 subset in the transgenic animals. These DN NK1.1^{-} NKT cells express the transcription factor ROR-γt and were shown to produce the cytokine IL-17 upon activation (Figure 1F) [29,30].

Timing of Transgenic Vα14i-TCR Expression Is Critical for Normal NKT Cell Development

Premature TCRα expression leads to aberrant T cell development in transgenic mouse models [26,27]. To directly compare the consequence of premature to CD4-Cre-mediated timely Vα14i-TCRα-chain expression in our knock-in approach, we bred our mice to a germline *Cre-deleter* strain (*Nestin-Cre*) [31]. Compared to CD4-Cre-induced Vα14i-TCRα-chain expression, premature expression in *Cre-deleter Vα14i*^{StopF}*/wt* led to significantly reduced numbers of NKT cells in thymus and spleen, especially of CD4+ NKT cells (Figure 2A–C). In addition, we

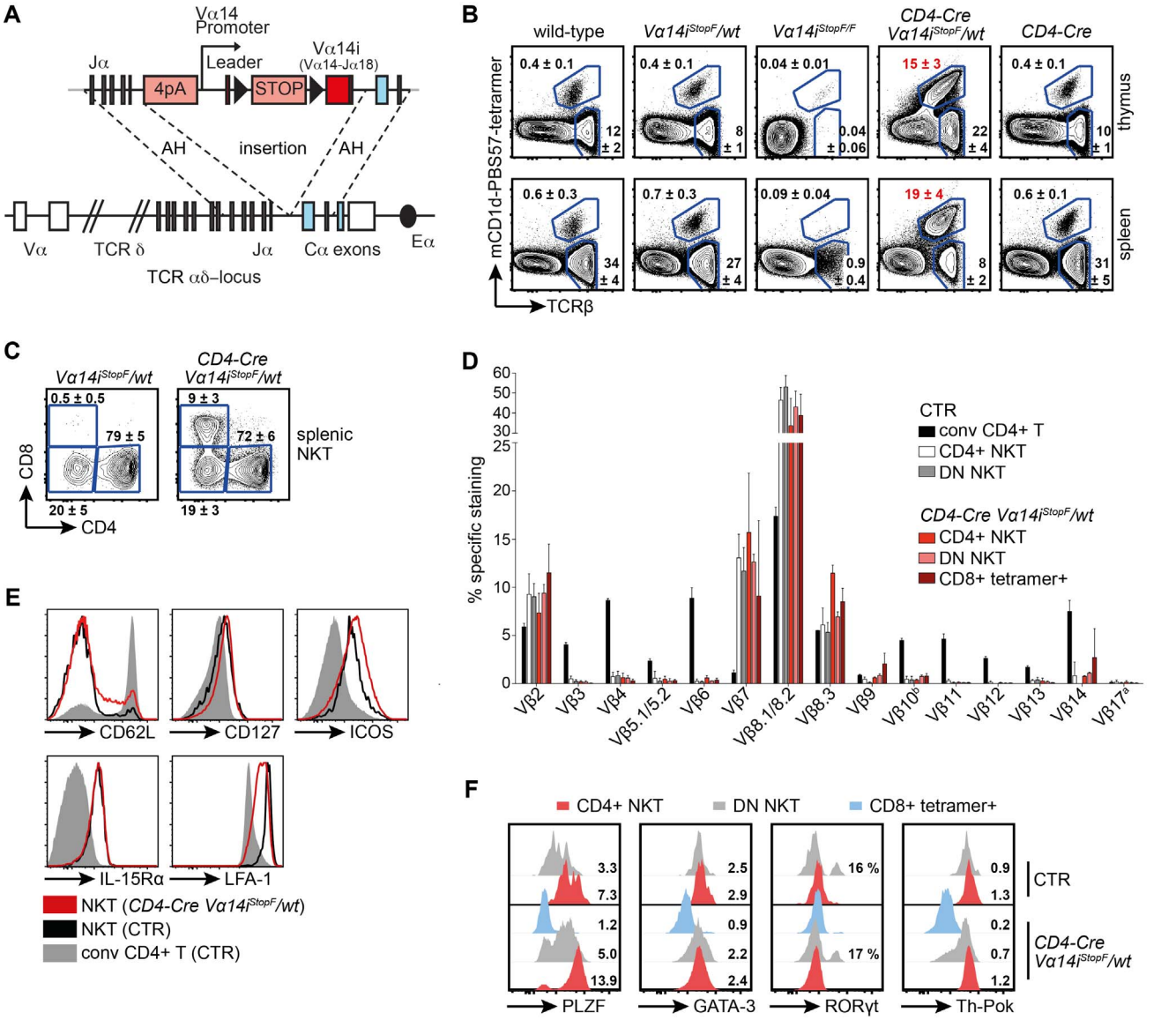

Figure 1. The Vα14i-TCR knock-in mouse produces large numbers of correctly selected, bona fide NKT cells. (A) Schematic representation of the knock-in transgene. The *Vα14* promoter, *loxP* (triangle)-flanked STOP cassette, and pre-rearranged *Vα14i* (Vα14-Jα18, red square) sequences were inserted 3′ of *Jα1* and 5′ of the first *Cα* exon (coding exons are highlighted in blue); 4pA = 4 SV40 polyadenylation sites. AH, arms of homology. *Eα*, enhancer (black oval). (B) Representative proportions of NKT cells and conventional T cells of total lymphocytes in thymus and spleen. Numbers indicate mean percentages ± SD of at least seven age-matched mice per genotype. (C) Representative proportions of splenic CD4+, CD8+, and DN (CD4− CD8−) NKT cells. Numbers indicate mean percentages ± SD of seven mice per genotype. (D) The Vβ repertoires of splenic NKT cells of the indicated genotypes. Bars indicate means and error bars SD of three independent experiments. (E) Representative flow cytometric analysis of the indicated cell-surface proteins on conventional CD4+ T cells and NKT cells. (F) Intracellular flow cytometric staining of PLZF, GATA-3, ROR-γt, and Th-POK in the depicted NKT cells. Numbers indicate means of the median fluorescence intensities (MFIs), normalized to CD4+ tetramer− T cells of CTR animals, or percentage of ROR-γt+ cells among DN NKT cells; calculated from three animals per genotype. Histograms are representative of three independent experiments with eight mice in total. Throughout the figure, NKT cells were gated as tetramer+ TCRβ+, conventional (conv) T cells as tetramer− TCRβ+; CTR, *CD4-Cre* or *Vα14i*^{StopF}*/wt*.

doi:10.1371/journal.pbio.1001589.g001

found reduced thymocyte counts and a significant increase of most likely lineage-"confused" DN (CD4− CD8−) tetramer-negative T cells (Figure 2D,E). In fact *Cre-deleter Vα14i*^{StopF}*/wt* mice strongly resemble the "first generation" Vα11 promoter-driven (Vα11p) *Vα14i* transgenic mice in these respects (Table S1) [32]. Moreover, in *Cre-deleter Vα14i*^{StopF}*/wt* mice, we observed increased proportions of Vβ9-, Vβ10-, and Vβ14-containing Vα14i-TCRs, which can recognize α-GalCer-loaded tetramers, but most likely not endogenous self-glycolipids [3,4], pointing to perturbed positive selection (Figure 2F). *CD4-Cre Vα14iStop*^{F}*/wt* mice produce more NKT cells than any of the previously reported models, including mice with a *Vα14i* allele derived from a NKT cell nuclear transplantation experiment [11,32–35]. A comparison of different *Vα14i*-transgenic models demonstrates that both the correct timing and endogenous control of TCR expression control favor NKT cell development (Table S1). Our analyses therefore showed that physiological timing of Vα14i-TCRα-expression at endogenous levels in *CD4-Cre Vα14i*^{StopF}*/wt*

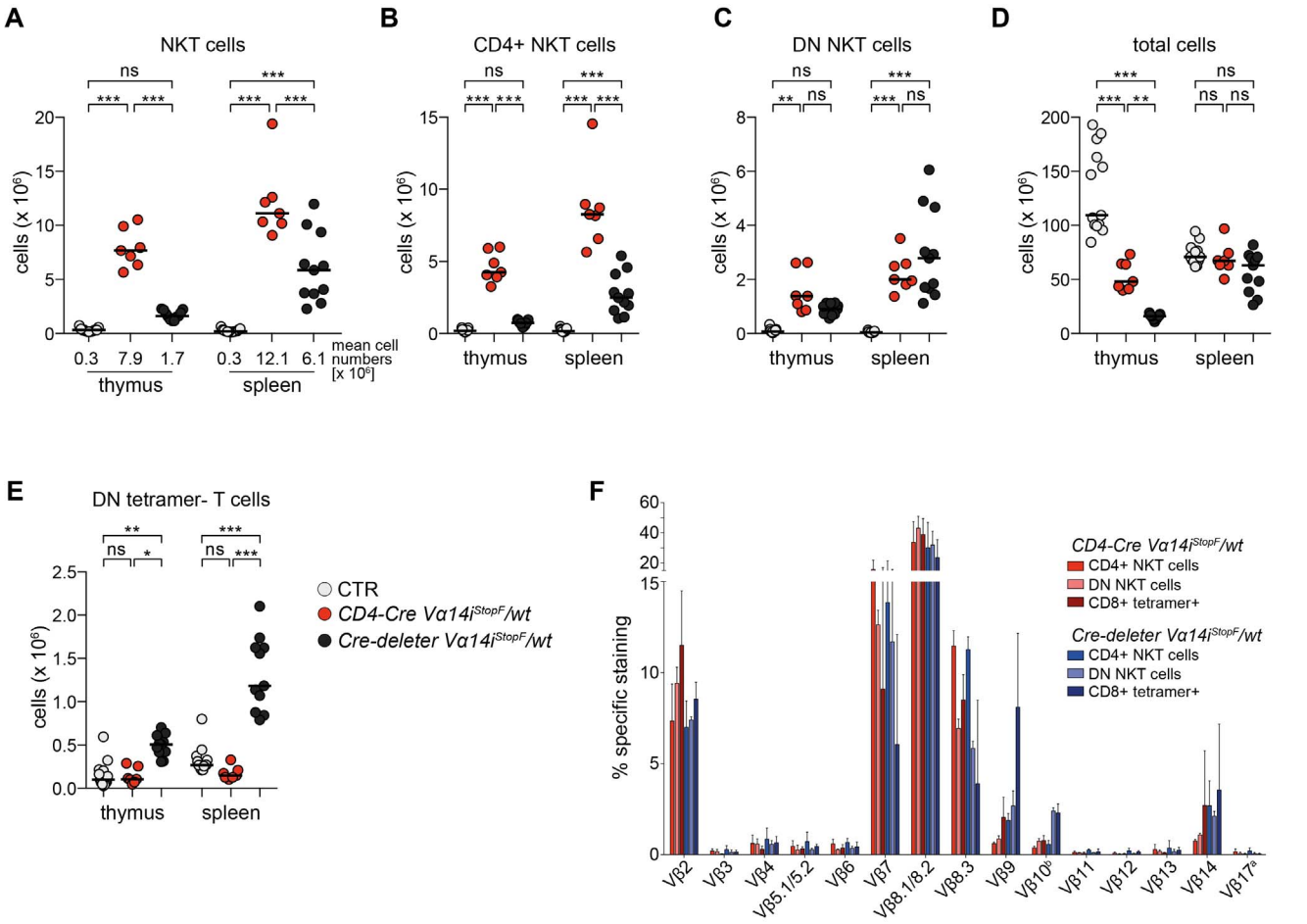

Figure 2. Premature Vα14i-TCR expression impairs NKT and conventional T cell development. (A–E) Absolute cell numbers in thymus and spleen of 7–13 mice of the indicated genotypes: NKT cells (A), CD4+ NKT cells (B), DN NKT cells (C), total cells (D), and DN tetramer− T cells (E). Bars indicate medians. *** $p<0.001$; ** $p<0.01$; * $p<0.05$; ns, not significant; one-way ANOVA. (A) Mean cell numbers are depicted below the scatter blot. (F) The Vβ repertoires of splenic NKT cells of the depicted animals. Data for *CD4-Cre Vα14i*^{StopF}*/wt* are the same as shown in Figure 1D. Bars indicate means and error bars SD of 3–4 mice per genotype of 3–4 independent experiments. Throughout the figure, NKT cells were gated as tetramer+ TCRβ+, conventional (conv) T cells as tetramer− TCRβ+; CTR, *CD4-Cre* or *Vα14i*^{StopF}*/wt*.
doi:10.1371/journal.pbio.1001589.g002

mice contributes to the production of large numbers of correctly selected, bona fide NKT cells.

NKT Cell Maturation in *CD4-Cre Vα14i*^{StopF}*/wt* Animals

To test the functionality of our transgenic NKT cells, we injected *CD4-Cre Vα14i*^{StopF}*/wt* mice with the NKT cell ligand α-Galactosylceramide (α-GalCer) and determined their cytokine production directly ex vivo. The transgenic NKT cells were able to mount a rapid and robust cytokine response. Although a reduced proportion of transgenic NKT cells responded, in absolute cell numbers there was a 6–10-fold increase compared to wild-type NKT cells (Figure 3A). We did not observe significant steady-state cytokine production by transgenic or control NKT cells, and we detected only minor increases in cytokine levels in the serum of some of these mice (Figure S1D). Since cytokine production also varies with NKT cell maturation, we analyzed NKT cell development in *CD4-Cre Vα14i*^{StopF}*/wt* mice in more detail. This revealed a strong bias toward immature fractions in the thymus, due to the dramatic increase in NKT cell progenitors. In the periphery, 20% of NKT cells fully matured, as judged by the expression of NK1.1 and other NK cell markers (Figure 3B,C). This view is further supported by the reduced proportion of CD69 and T-bet-expressing NKT cells in *CD4-Cre Vα14i*^{StopF}*/wt* compared to wild-type mice (Figure 3D). The expression of both CD69 and T-bet strongly correlated with NK1.1 surface levels (Figure S1E,F). This also explains the higher intracellular PLZF expression in CD4+ and DN NKT cells of *CD4-Cre Vα14i*^{StopF}*/wt* animals in comparison to control animals (Figure 1F), as it was shown that PLZF expression is downregulated during NKT cell development [36]. Reduced maturation seems to be a common feature in mice with overabundance of NKT cells (Figure S1G and Table S1) [33]. Indeed, a comparison of different Vα14i-tg mice suggests that independently of the total number of NKT cells generated, the size of the homeostatic niche for mature NKT cells appears to be around two million cells (Table S1).

IL-15 is critical for the final maturation of NKT cells [37] and together with IL-7 required for their peripheral maintenance [14,38]. NKT cells compete with NK cells for these resources [38]. The halved number of NK cells in *CD4-Cre Vα14i*^{StopF}*/wt* mice (Figure 3E) suggests that the availability of these and maybe other cytokines might be insufficient due to the dramatically increased NKT cell numbers. The fact that a similar effect was observed in Vα11p-*Vα14itg* mice (Figure 3E) underscores this notion. These results let us conclude that while large amounts of NKT cells can

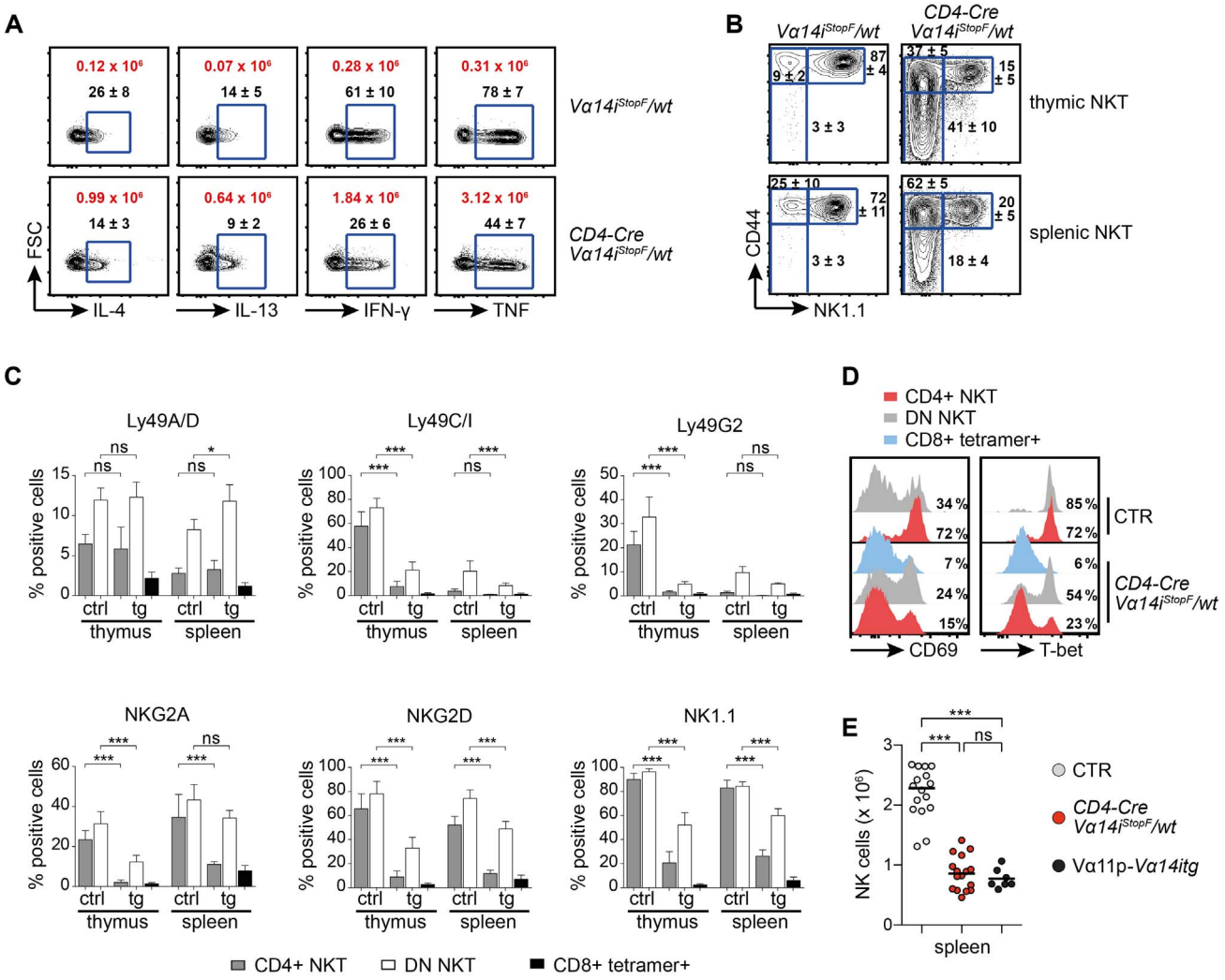

Figure 3. NKT cell overproduction affects their maturation and NK cell homeostasis. (A) Intracellular IL-4, IL-13, IFN-γ, and TNF expression of splenic CD4+ NKT cells isolated from the depicted animals 90 min after αGalCer injection. Cells were stained directly ex vivo without addition of brefeldin or monensin. Black numbers indicate mean percentages ± SD, and red numbers indicate mean total NKT cell counts expressing the respective cytokine. Data are from three animals per genotype; FSC, forward scatter. (B) Representative proportions of stage 1 (CD44^{low} NK1.1^{low}), stage 2 (CD44^{high} NK1.1^{low}), and stage 3 (CD44^{high} NK1.1^{high}) thymic and splenic NKT cells. Numbers indicate mean percentages ± SD of 10 mice per genotype. (C) Flow cytometric analysis of the depicted markers on thymic and splenic, transgenic, and control NKT cells. Bars indicate means and error bars SD calculated from 4–7 mice. (D) Extracellular and intracellular flow cytometric stainings of CD69 and T-bet in the depicted NKT cell subpopulations. Numbers in representative histogram indicate percentage of CD69^{high} or T-bet+ cells among the indicated NKT cells calculated from eight animals per genotype (CD69) or three animals per genotype (T-bet). Histograms are representative of at least three independent experiments with each at least seven mice in total. (E) Absolute splenic NK cell numbers (NK1.1+ TCRβ− tetramer−) of age-matched 6–12-wk-old animals (7–16 per genotype). Bars indicate medians. *** $p<0.001$; ns, not significant; one-way ANOVA. Throughout the figure, NKT cells were gated as tetramer+ TCRβ+, conventional (conv) T cells as tetramer− TCRβ+; CTR, *CD4-Cre* or *Vα14i^{StopF}/wt*.
doi:10.1371/journal.pbio.1001589.g003

be produced in mice, depending on the mode of Vα14i expression, the number of fully mature NKT cells is restricted by homeostatic constraints, some of which are shared with NK cells.

The Exchange of the Endogenous TCR Repertoire for a Vα14i-Restricted One on Mature Conventional T Cells Leads to a Significant Population of Tetramer+ T Cells

The strong self-lipid-induced TCR stimulus that early NKT cell progenitors receive in the thymus can be visualized through high GFP expression under the control of the *Nur77* gene locus, reporting TCR signal strength [12]. However, the subsequent loss of GFP in mature NKT cells suggests that these cells are either not exposed to or not responsive to self-antigens. In order to answer this question and to study NKT cell TCR-autoreactivity in the periphery, we investigated the consequences of Vα14i-TCR signals for conventional naïve T cells. We wondered whether Vα14i-TCR expression on naïve T cells, lacking inhibitory receptors and generally a NKT cell "identity", would lead to activation upon (self-)lipid recognition and what cellular fate(s) are elicited by such activation.

To this end, we generated mice enabling us to exchange the endogenous TCR-repertoire present on naïve peripheral T cells for a Vα14i-restricted TCR repertoire. The induction of Cre expression in *Mx-Cre Cα^{F}/Vα14i^{StopF}* mice inactivates the *Cα^{F}* allele and simultaneously turns on the *Vα14i^{StopF}* allele, leading to substitution of endogenous TCRα-chains with the Vα14i TCRα-

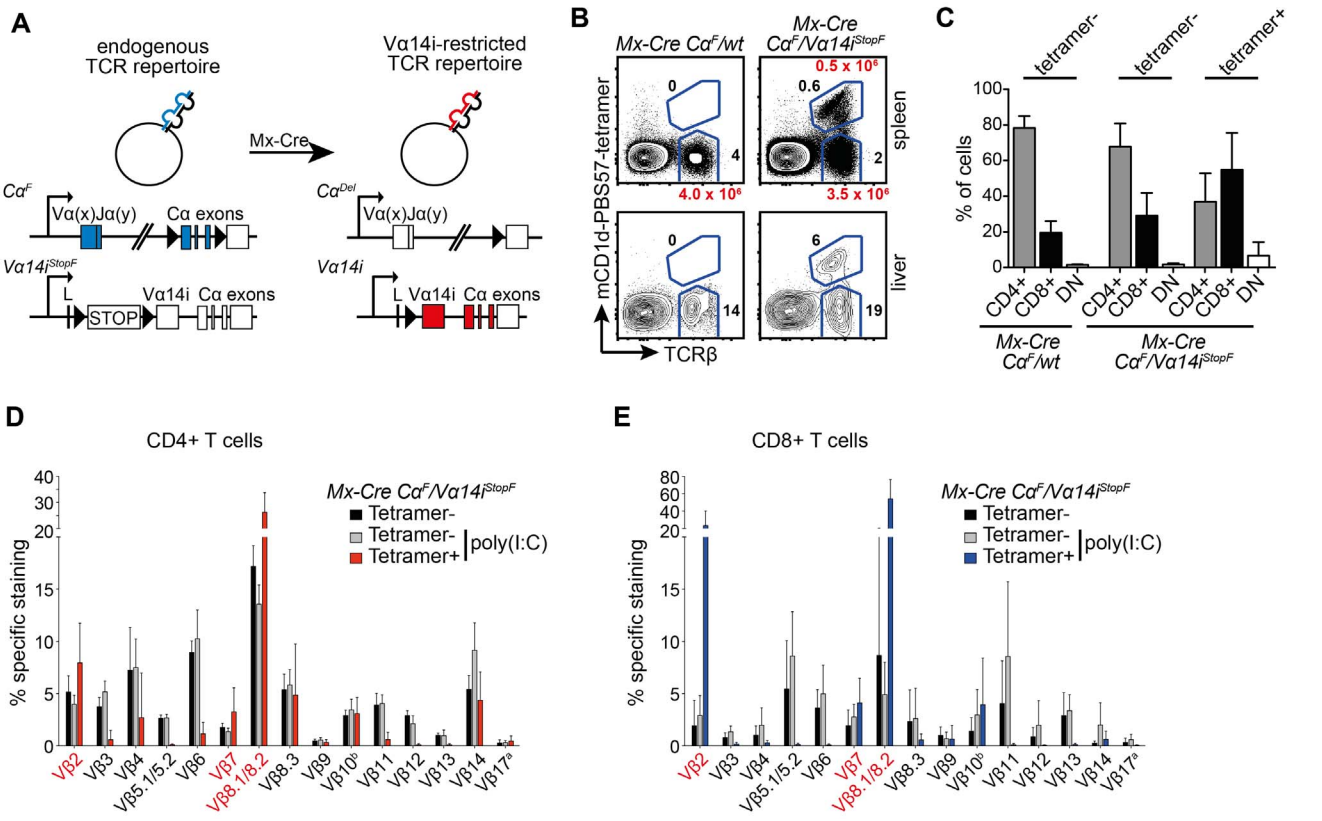

Figure 4. TCR switch on mature conventional T cells. (A) Genetic set-up of the TCR switch experiment. In *Mx-Cre* $C\alpha^F/V\alpha14i^{StopF}$ mice, the endogenous TCRα-chains (Vα(x)Jα(y)) are exclusively expressed from the $C\alpha^F$ allele. Cre-mediated recombination leads to termination of expression from the $C\alpha^F$ allele, and simultaneous start of expression of the Vα14i-TCRα-chain from the $V\alpha14i^{StopF}$ allele. (B) T-cell-deficient mice were reconstituted with NKT cell-depleted splenocytes of the indicated genotypes. After 2 wk, the TCR switch was induced by poly(I:C) injection. Eight weeks later, percentages of tetramer+ and tetramer− T cells (TCRβ+) were analyzed in spleen and liver. Black numbers indicate percentages of total lymphocytes, red numbers absolute cell number calculated from 9–17 animals. (C) Bars indicate means and SD (error bars) of CD4+, CD8+, or DN (CD4− CD8−) cells among tetramer− and tetramer+ T cells, calculated from at least nine mice per genotype. (D, E) The Vβ repertoires of the depicted splenic CD4+ (D) or CD8+ (E) T cell subsets isolated from T-cell-deficient animals that received NKT cell-depleted *Mx-Cre* $C\alpha^F/V\alpha14i^{StopF}$ splenocytes. Some of these mice were injected with poly(I:C) 2 wk later to induce the TCR switch. Eight weeks after poly(I:C) injection, the Vβ repertoires were analyzed. Data represent means and SD (error bars) of two independent experiments with a total of three mice (tetramer− without poly(I:C) injection) or eight mice (poly(I:C) injected) per T cell population. Vβs typical for glycolipid selection of NKT cells are highlighted in red.
doi:10.1371/journal.pbio.1001589.g004

chain (Figure 4A). As mentioned above, the Vα14i-chain can pair with all TCRβ-chains [3], although only Vβ2-, Vβ7-, and Vβ8-containing Vα14i-TCRs can recognize endogenous lipids such as iGb3 [3,4]. Since TCRs containing one of these Vβ-chains constitute approximately 30% of the CD4+ and CD8+ peripheral T cell pool (Figure 1D and unpublished data), we predicted that our genetic switch experiment should generate sufficient numbers of T cells able to recognize self-lipids.

In *Mx-Cre* transgenic mice, Cre expression can be induced through injection of dsRNA, such as poly(I:C) [39]. However, low-level "leaky" recombination occurs also in absence of an inducer [39,40], leading to increased numbers of tetramer+ T cells in naive *Mx-Cre* $C\alpha^F/V\alpha14i^{StopF}$ mice (Figure S2A). Therefore, splenocytes were depleted of tetramer+ T cells by magnetic cell separation (MACS, Figure S2A), and 20×10^6 purified cells were injected intravenously (i.v.) into recipient animals lacking conventional αβ T cells and NKT cells ($C\alpha^{-/-}$ or $V\alpha14i^{StopF/F}$). After cells were allowed to engraft for 2 wk, the TCR switch was induced by poly(I:C) injection. Importantly, except for a short-term activation of the immune system, poly(I:C) injection in *Mx-Cre* mice per se has no significant long-lasting effect on peripheral conventional T cells [40,41] or on the number and phenotype of NKT cells (unpublished data). To definitely exclude any effect of poly(I:C) injection on our results, we waited 2–4 mo before analyzing the animals after the induced TCR switch.

We found significant numbers of tetramer+ CD4+ and CD8+ T cells as a result of this switch experiment (Figure 4B–E). "Unloaded" tetramers did not stain these cells, demonstrating that they were not reactive against CD1d itself (Figure S2B). The TCR-switched tetramer+ T cells were predominantly enriched in cells expressing Vβ-chains that are associated with high avidity auto-antigen binding: Vβ2, Vβ8.1/8.2, and Vβ7 (Figure 4D,E) [3,4,42]. The exceptions were CD8+ TCR-switched tetramer+ T cells, in which Vβ7-expressing cells were not enriched. The bias toward tetramer+ CD8+ T cells (Figure 4C) is most likely due to more efficient Mx-Cre-mediated recombination in these cells [40].

Sterile Inflammation in Mice Containing TCR-Switched T Cells

Animals containing TCR-switched tetramer+ T cells, but not controls, displayed splenomegaly (Figure 5A,B), characterized by increased numbers of macrophages/monocytes, neutrophils, and Ter119+ erythroid progenitor cells, suggesting an inflammatory state (Figure 5C–E). In line with these findings, we could detect

elevated serum TNF in more than half of these mice (Figure 5F). Elevated levels of other cytokines, such as IL-2, IL-4, IL-5, IL-6, IL-10, IL-17, and IFN-γ, were not found in the sera of these mice (unpublished data). Interestingly, we found that 6 (highlighted in red throughout the figure) of 17 spleens containing TCR-switched T cells were almost completely devoid of B cells (Figure 5G) as well as dendritic cells (DCs, Figure 5H), which present lipid antigens to NKT cells via CD1d [1]. Furthermore, tetramer- "conventional" T cells were also strongly reduced in these animals (unpublished data). Together, these results suggest that induced expression of the Vα14i-TCR on conventional naïve T cells causes sterile inflammation, possibly due to autoimmune activation.

Vα14i-TCR Signaling Induces Cellular Activation, But Not NKT Cell Differentiation of TCR-Switched Tetramer+ T Cells

The appearance of tetramer+ cells displaying a Vβ bias similar to antigen-selected NKT cells, together with signs of inflammation upon TCR switch and the absence of CD1d-expressing B cell and DCs in some cases, suggested auto-antigen-mediated activation of TCR-switched cells. To verify that the newly assembled Vα14i-TCR on conventional T cells is functional, we injected recipients of *Mx-Cre* $C\alpha^{F}/V\alpha14i^{StopF}$ and control cells with α-GalCer or PBS 2 mo after switch induction. Ninety minutes after α-GalCer, but not PBS, injection, CD4+ and CD8+ tetramer+ T cells produced IFN-γ and TNF (Figure 6A), demonstrating the functionality of the newly assembled Vα14i-TCR. In comparison to NKT cells from wild-type or *CD4-Cre* $V\alpha14i^{StopF}/wt$ animals, a smaller proportion of tetramer+ T cells produced cytokines (Figures 6A and S2C). Tetramer+ TCR-switched T cells could also be activated in vitro through α-GalCer-pulsed A20 cells overexpressing CD1d (unpublished data) [43].

To study the consequences of Vα14i-TCR expression on tetramer+ TCR-switched T cells in more detail, we analyzed their surface phenotype and transcription factor expression. Absence of NK cell markers (Figures 6B and S2D) and PLZF expression (Figure 6C) indicated that the Vα14i-TCR signals are not sufficient to induce NKT cell differentiation of mature conventional T cells. However, the TCR-switched tetramer+ T cells expressed signifi-

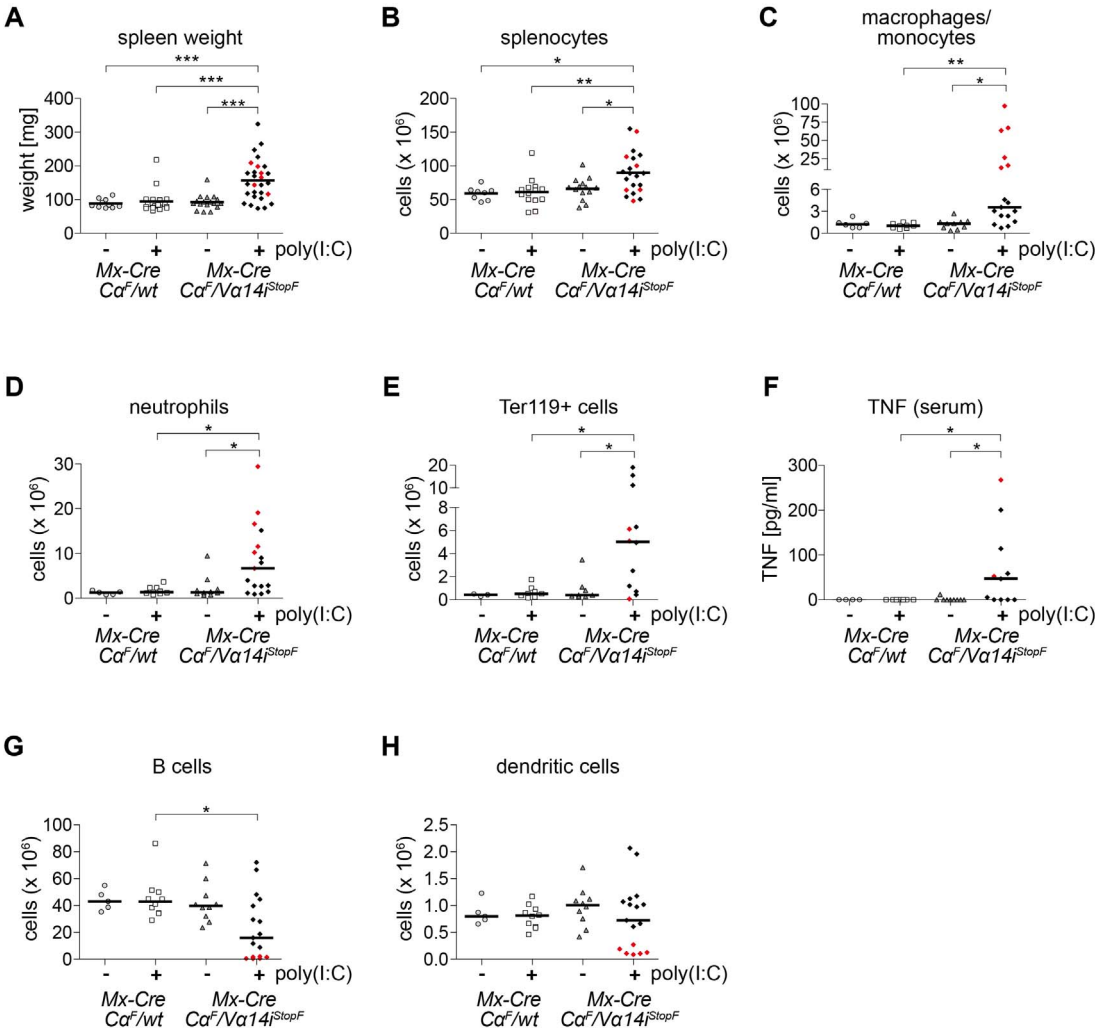

Figure 5. Signs of sterile inflammation in mice harboring TCR-switched T cells. T-cell-deficient mice were reconstituted with NKT-cell-depleted splenocytes of the indicated genotypes. Spleen weight (A), absolute splenic cell numbers (B–E, G, H), and serum TNF levels (F) of 3–28 mice per genotype were determined 8 wk after poly(I:C) administration where indicated. Bars indicate medians. Red points show six animals with near absence of B cells and dendritic cells. (B) Total splenocytes; (C) Macrophages/monocytes (Mac1+ $Gr1^{int}$ SiglecF−); (D) Neutrophils (Mac1+ $Gr1^{high}$ SiglecF−); (E) Erythroblasts (Ter119+); (G) B cells (B220+ TCRβ−); (H) Dendritic cells (CD11c+). *** $p<0.001$; ** $p<0.01$; * $p<0.05$, one-way ANOVA.
doi:10.1371/journal.pbio.1001589.g005

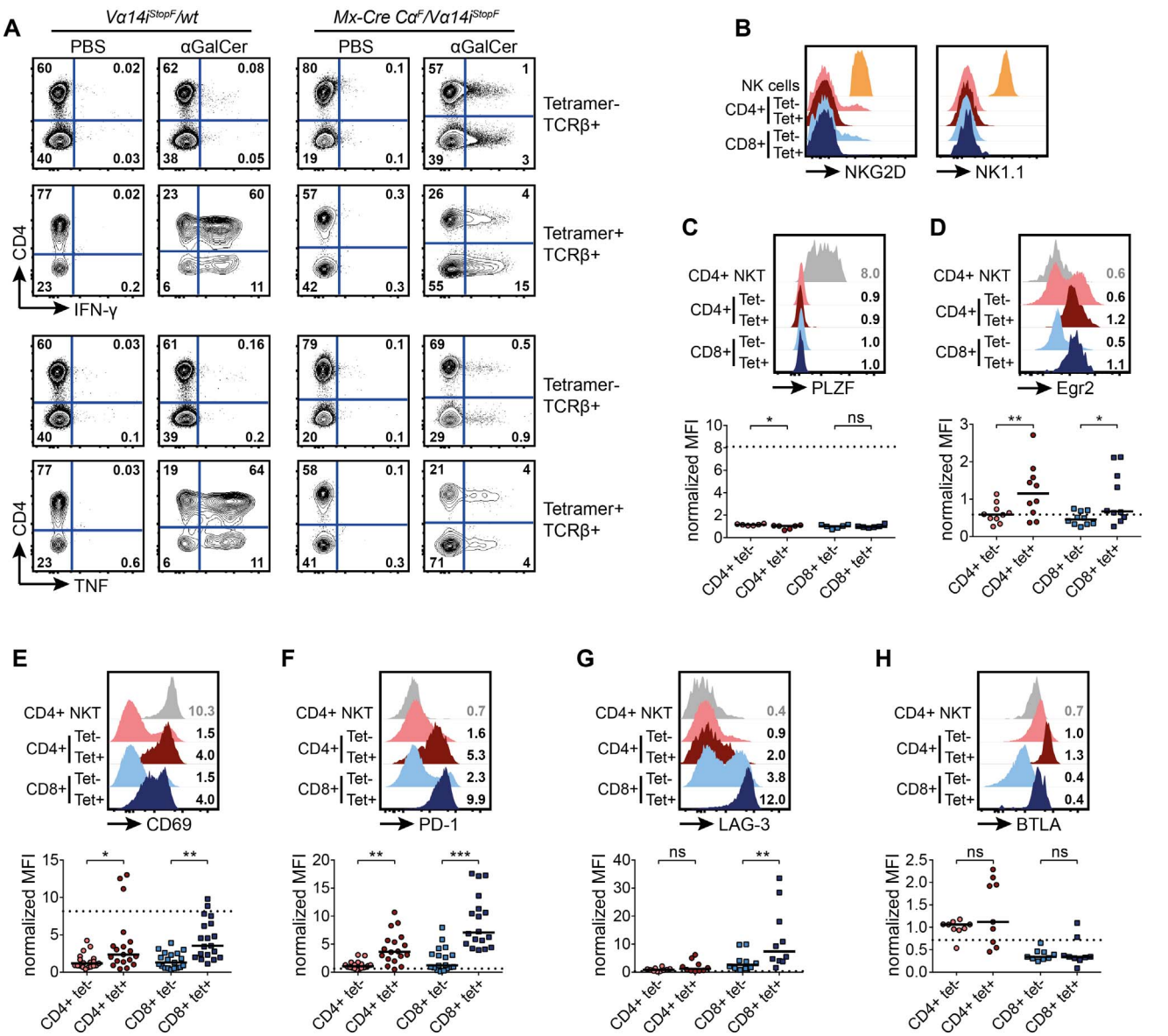

Figure 6. TCR-switched tetramer+ T cells display an activated/exhausted phenotype, but no signs of NKT cell differentiation. T-cell-deficient mice were reconstituted with NKT-cell-depleted splenocytes of the indicated genotypes. The TCR switch was induced by poly(I:C) administration. Eight weeks later, the animals were analyzed. (A) Expression of intracellular IFN-γ or TNF ex vivo 90 min after αGalCer injection of the indicated mice. Data are representative of two independent experiments with two animals each. (B) Representative histograms of flow cytometric analyses. Surface expression of NKG2D and NK1.1 on T cells (TCRβ+) of the indicated surface phenotypes in comparison to NK cells (NKG2D+ TCRβ− CD5− or NK1.1+ TCRβ− CD5−) are shown. Histograms are representative for at least three independent experiments with at least one mouse each. (C–H) Representative histograms of flow cytometric analyses. T cells (TCRβ+) of the indicated surface phenotypes, and of wild-type splenic CD4+ NKT cells, are shown. Numbers in representative histograms indicate means of the median fluorescence intensities (MFIs), normalized to CD4+ tetramer− T cells of animals that received NKT-cell-depleted *Mx-Cre* $C\alpha^{F}$*/wt* splenocytes, 8 wk after poly(I:C) injection. Means were calculated from 6–25 mice. Scatter plots display normalized MFI. Bars indicate medians. Dotted lines indicate medians of the median fluorescence intensities of control CD4+ wild-type NKT cells calculated from 2–6 mice. (C, D) Intracellular PLZF (C) and Egr2 (D) expression. (E–H) Extracellular expression of CD69 (E), PD-1 (F), LAG-3 (G), BTLA (H); *** $p<0.001$; ** $p<0.01$; * $p<0.05$; ns, not significant; one-way ANOVA.
doi:10.1371/journal.pbio.1001589.g006

cantly higher levels of Egr2 in comparison to tetramer− T cells in the same animals (Figure 6D), suggesting that the switched cells receive stronger TCR signals [13]. TCR-switched T cells showed further signs of cellular activation, as they expressed elevated levels of CD69 (Figure 6E). Interestingly, these T cells displayed also significantly increased surface levels of PD-1, LAG-3, and less frequently, BTLA and TIM-3, which is typical of exhausted/anergic cells (Figure 6F–H and unpublished data) [44,45].

To test whether exhaustion/anergy of tetramer+ TCR-switched T cells prevented a more dramatic form of autoimmune inflammation, we injected mice with PD-L1 and PD-L2 blocking or control antibodies twice a week for 4 consecutive weeks, starting 2 d before switch induction. The administration of these blocking antibodies has previously been shown to efficiently prevent anergy induction of conventional T as well as NKT cells, and to partially reverse the exhaustion of CD8+ T cells [44,45]. However, we did

not observe any dramatic differences in spleen weight or cellularity, or signs of increased inflammation, between animals receiving PD-L blocking or control antibodies (unpublished data). In response to PD-1 blockade, other inhibitory receptors such as LAG-3, BTLA, or TIM-3 might control the TCR-switched T cells.

Taken together, our results showed that expression of the Vα14i-TCR on mature conventional T cells is not sufficient to induce a NKT cell differentiation program. Still, it is likely that Vα14i-TCR signals induce auto-antigen-mediated activation, possibly to the point of exhaustion. We therefore present strong evidence that the Vα14i-TCR can constitutively recognize self-lipids in the naïve steady state situation in vivo.

Maintenance of Mature NKT Cells Is TCR-Independent

The evidence for autoreactivity of the Vα14i-TCR on mature peripheral T cells raised the old but still not completely resolved question whether and to what extent interactions with self-lipid-presenting APCs are required for NKT cell maintenance, cellular identity, and function. In order to evaluate the importance of constitutive TCR expression and signaling for NKT cells directly in vivo and for long periods of time, we ablated the TCR on mature T cells using poly(I:C) injection of *Mx-Cre* $C\alpha^{F/F}$ mice [40].

Two weeks after induced Cre-mediated recombination, around 30% of CD4 and 65% of CD8 T cells had lost functional TCR expression in these mice (Figure 7A and [40]). To unambiguously identify TCR-deficient NKT cells, we developed a robust staining strategy based on CD4, NK1.1, CD5, and CD62L expression (Figure S3A). This limited us to CD4+ NKT cells, but our staining identified over 50% of the total NKT cell populations in thymus and spleen (Figure S3B). Around 65% of the thus identified NKT cells had lost TCR surface expression 2 wk after Cre induction (Figure 7A,B).

Due to complete Cre-mediated recombination in lymphoid progenitors, T cell development is blocked at the double positive stage in *Mx-Cre* $C\alpha^{F/F}$ mice after induction of Cre [40]. This allowed us to study the T cell decay in the absence of cellular efflux from the thymus. In agreement with previous studies [40,46], we found that loss of the TCR leads to decay of naïve CD4+ $CD44^{low}$ and memory/effector-like CD4+ $CD44^{high}$ T cells with a half-life of 40 d and 297 d, respectively (Figure 7C,D). Interestingly, we observed essentially no decay of receptor-less NKT cells, with a calculated half-life of 322 d (Figure 7E), and could find significant numbers of TCR-deficient NKT cells even 45 wk after TCR deletion (unpublished data). To evaluate the role of TCR signals during in situ homeostatic proliferation, we administered BrdU for 4 wk via the drinking water, starting 2 wk after induced TCR ablation. Naïve CD4+ $CD44^{low}$ as well as CD4+ $CD44^{high}$ memory/effector-like T cells showed significantly decreased BrdU incorporation in TCR-deficient compared to TCR-expressing cells (Figure 7F,G). In contrast, TCR ablation did not affect NKT cell proliferation (Figure 7F,G). Interestingly, the BrdU incorporation was identical in TCR-deficient CD4+ $CD44^{high}$ T and NKT cells, indicating that in the absence of TCR signals the cytokine-driven expansion of CD4+ $CD44^{high}$ memory/effector-like T and NKT cells is similar (Figure 7F,G). Our results therefore indicate that long-term in situ NKT cell homeostasis is completely independent of TCR-induced signals.

The TCR Is Dispensable for the Identity and Cytokine-Secretion Ability of Mature NKT Cells

In absence of de novo T cell generation, we found elevated Egr2 expression in mature thymic, but not splenic, NKT cells compared to DP thymocytes and CD4+ T cells, respectively (Figure 8A). This indicates that NKT cells receive stronger TCR signals in the thymus, which is supported by the decreased Egr2 expression of mature thymic TCR-deficient NKT cells (Figure 8A). Surprisingly, in mature NKT cells in thymus and spleen, expression of the TCR-signal-induced key transcription factor PLZF is completely unaffected by TCR ablation (Figure 8B).

In order to more generally evaluate to what extent NKT cell TCR-expression is required for the maintenance of characteristic lineage-specific gene expression (resembling recently activated T cells), we extensively analyzed the cell-surface phenotype of NKT cells 6 wk after TCR ablation. Of all the analyzed markers, the only significant changes that we observed on splenic NKT cells upon TCR ablation were downregulation of NK1.1, CD4, CD5, and ICOS (Figures 8C,D and S3C–E). NK1.1 expression was also reduced in thymic TCR-deficient NKT cells, in addition to CXCR6 expression (unpublished data). CD5 and ICOS expression were also reduced in TCR-deficient splenic naïve as well as $CD62L^{low}$ CD4+ T cells (Figure S3C,D). CD4 was upregulated on TCR-deficient CD4+ naïve, but downregulated on NKT and CD4+ $CD44^{high}$ T cells (Figure S3E). Strikingly, all other cell surface markers characteristic for the NKT cell lineage, among them the transcription factors PLZF, GATA-3, T-bet, and Th-POK, as well as many cell surface markers whose expression is also induced upon TCR engagement, remained largely unaffected by loss of the NKT cell TCR (Figure 8D).

Treatment of mice with LPS, a cell wall component of gram-negative bacteria, leads to release of IFN-γ by NKT cells via stimulation with IL-12 and IL-18 produced by innate immune cells. This does not require acute TCR engagement [21]. However, it has been proposed that the ability of NKT cells to rapidly release IFN-γ in this context critically requires continuous weak TCR activation in the steady state [25]. We therefore analyzed IFN-γ release of TCR+ and TCR- NKT cells after in vivo injection of LPS, α-GalCer, and PBS (Figure 9A,B). As expected, Egr2 expression could only be detected in NKT cells that were activated through their TCR (Figure 9A). Accordingly, 90 min after α-GalCer injection, the majority of TCR+ NKT cells, but virtually none of the TCR- NKT cells or the CD4+ conventional T cells, produced IFN-γ protein (Figure 9B). Interestingly, NKT cell activation through LPS injection in vivo was able to induce similar IFN-γ production by TCR- NKT cells in comparison to their TCR+ counterparts (Figure 9B). Our results thus clearly demonstrate that homeostasis and key features defining the nature of NKT cells, namely the unique activated cell-surface phenotype and the innate capacity for instant production of IFN-γ, do not require continuous auto-antigen recognition in the mouse.

Discussion

The elucidation of NKT cell function and their intriguing semi-invariant TCR benefited enormously from Vα14i-TCR transgenic mouse models [11,32,47,48]. Over the last years, it became increasingly clear that premature expression of transgenic TCRα chains, including Vα14i [11,32], leads to various unwanted side-effects such as impaired β-selection and the generation of large numbers of DN T cells both in the periphery and in the thymus [26,27]. This drawback affects even TCR alleles generated through nuclear transfer of mature NKT cells [33]. For that reason, Baldwin et al. developed a system in which a transgenic *CAGGS*-promoter-driven TCRα-chain is expressed upon CD4-Cre-mediated excision of a *loxP*-flanked STOP cassette, mimicking the physiologic expression time point [26]. Likewise, Griewank and colleagues expressed the Vα14i-TCR

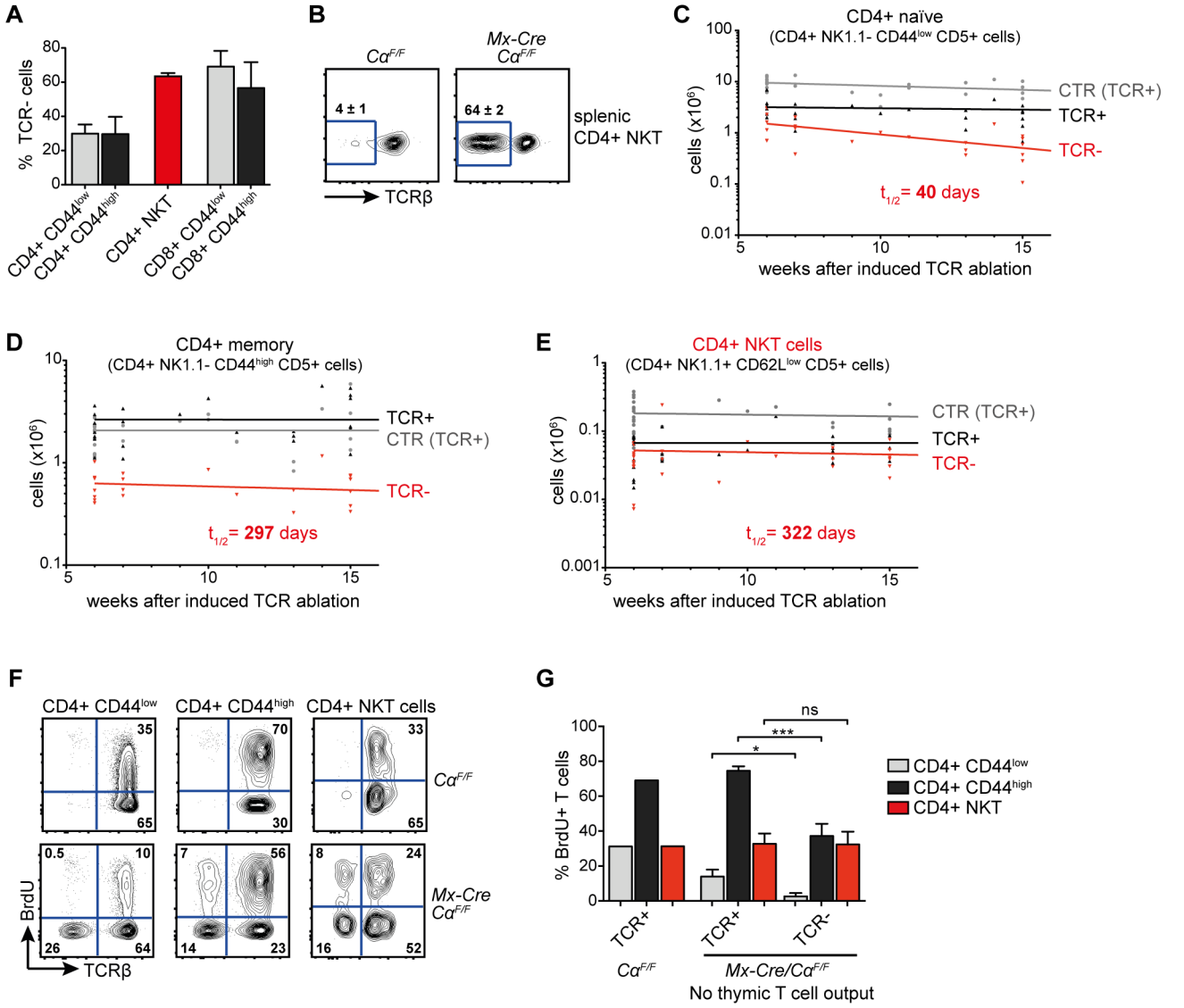

Figure 7. TCR signaling is not required for the steady state homeostasis of mature NKT cells. (A) Percentages of TCRβ− cells of the depicted T cell subsets 2 wk after poly(I:C) injection into *Mx-Cre* $C\alpha^{F/F}$ mice. Bars show means and SD (error bars) of 3–5 mice. (B) Surface TCRβ expression of splenic CD4+ NKT cells (NK1.1+ CD5+ $CD62L^{low}$) 2 wk after poly(I:C) injection. Numbers indicate means ± SD of three independent experiments with altogether five mice per genotype. (C, D) Total cell counts of splenic naïve conventional CD4+ T cells (CD5+ $CD44^{low}$ NK1.1−; C) or of memory/effector-like CD4+ T cells (CD5+ $CD44^{high}$ NK1.1−; D) from 26 control $C\alpha^{F/F}$ (CTR, TCR+) animals as well as from 24 *Mx-Cre* $C\alpha^{F/F}$ animals, all after poly(I:C) injection (TCR+, TCR−). (E) Splenic CD4+ NKT cell numbers from in total 32 control $C\alpha^{F/F}$ animals (CTR, TCR+) as well as TCRβ+ and TCRβ− CD4+ NKT cell numbers from in total 27 *Mx-Cre* $C\alpha^{F/F}$ animals, at the indicated time after poly(I:C) injection. (C–E) Half-lives were calculated with GraphPad Prism software using nonlinear regression, one-phase decay analysis. (F) BrdU was administered for 4 wk via the drinking water, starting 2 wk after poly(I:C) injection. Directly afterwards, animals were sacrificed and BrdU incorporation was measured by flow cytometry. Representative blots of 2 $C\alpha^{F/F}$ and 4 *Mx-Cre* $C\alpha^{F/F}$ mice are shown. (G) Bar chart showing proportion of cells that incorporated BrdU of the indicated T cell subtypes. Bars show means calculated from 2 $C\alpha^{F/F}$ and means and SD (error bars) 4 *Mx-Cre* $C\alpha^{F/F}$ mice. *** $p<0.001$; * $p<0.05$; ns, not significant; one-way ANOVA.

doi:10.1371/journal.pbio.1001589.g007

under direct control of *CD4* promoter and enhancer sequences [11]. These are clear improvements, but carry the inbuilt caveats of the respective heterologous expression construct. For example, it has been shown that a large proportion of activated mature T cells loses expression from such transgenic *CD4* promoter enhancer constructs [49].

Here, we present a novel approach, in which the expression of the transgenic Vα14i-TCRα-chain, and in the future any other TCRα-chain of interest, can be initiated via CD4-Cre at the DP stage in the thymus, and is under endogenous control of the *Tcrα* locus throughout the lifespan of the cell. In these mice, large numbers of bona fide CD4+ and DN NKT cells were generated. The reduced proportions of fully mature stage 3 NKT cells (NK1.1+, $CD69^{high}$, T-bet+), as well as the reduced numbers of NK cells, are most likely a consequence of limiting amounts of common differentiation and maintenance factors, such as IL-15 [14,37,50]. In addition, attenuated TCR-signaling due to increased competition for self-antigen/CD1d-complexes might delay the full maturation of NKT cells in the transgenic animals. TCR signals have been proposed to

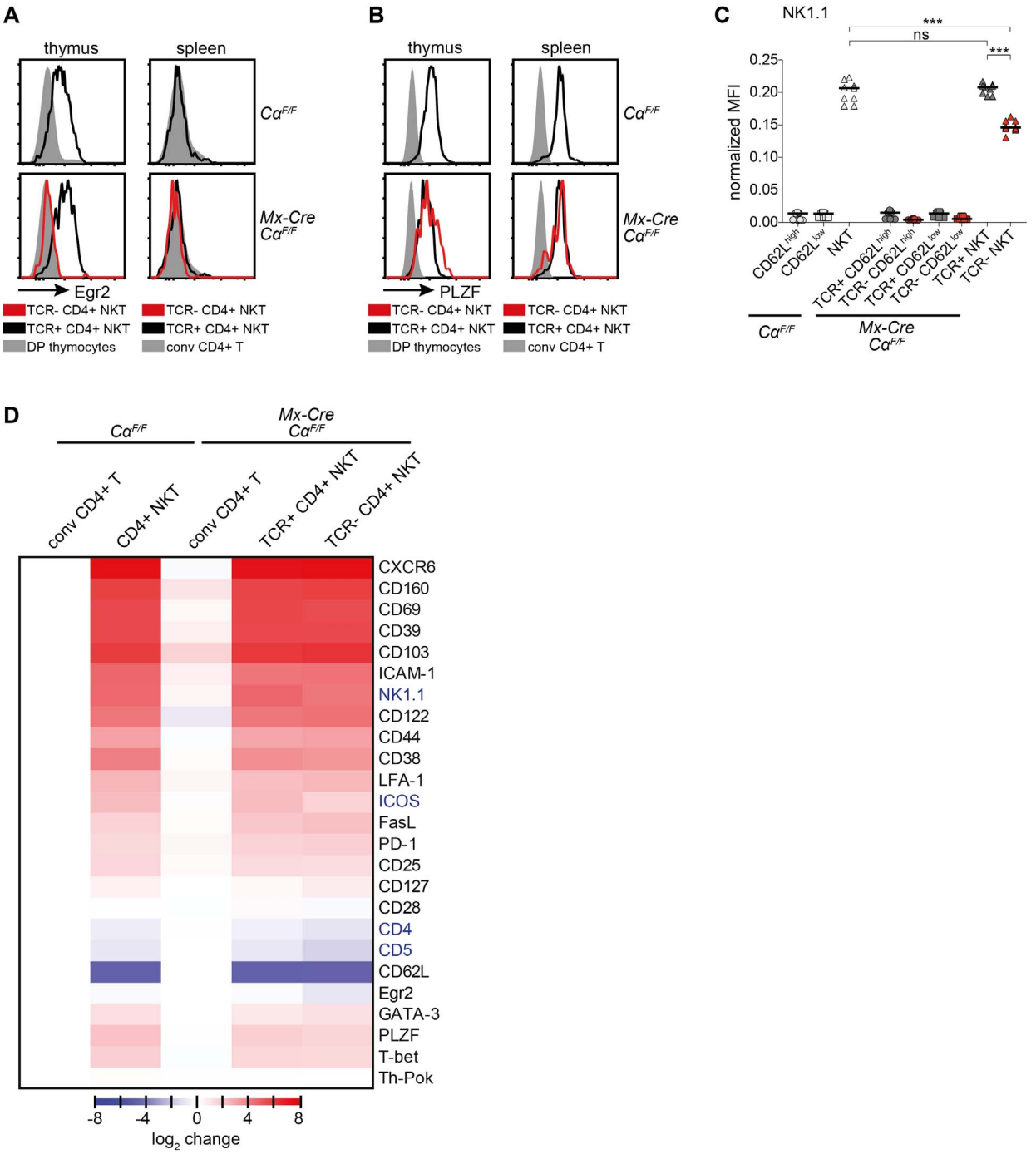

Figure 8. The maintenance of NKT lineage identity does not depend on TCR-signals. $C\alpha^{F/F}$ and *Mx-Cre* $C\alpha^{F/F}$ mice were injected with poly(I:C) and analyzed 6 wk later. (A, B) Intracellular expression of Egr2 (A) and PLZF (B) in T cells from the depicted mice. Plots are representative for at least three independent experiments. (C) Flow cytometric analysis of NK1.1 expression on splenic naïve (CD62L^{high} CD5+), memory/effector-like (CD62L^{low} CD5+) CD4+ T cells, and CD4+ NKT cells (NK1.1+ CD5+ CD62L^{low}), with or without TCR expression. Median fluorescence intensity, normalized to NK1.1 expression of NK cells (NK1.1+ TCRβ− CD5−). Bars indicate medians. *** $p<0.001$; ** $p<0.01$; * $p<0.05$; ns, not significant; one-way ANOVA. (D) Flow cytometric expression analysis of extra- and intracellular markers of splenic T cells. Median fluorescence intensities of at least four mice per analyzed protein were normalized to the expression on/in conventional CD4+ T cells (tetramer− TCRβ+) to account for interexperimental variations. Expression of NK1.1, CD122, FasL, and T-bet were normalized to NK cells (NK1.1+ TCRβ− CD5−) and then set to 1 for naïve T cells. Data are shown as heatmap, calculated by Perseus software. Blue letters, significantly reduced on splenic TCR− CD4+ NKT cells in comparison to TCR+ CD4+ NKT cells from $C\alpha^{F/F}$ and *Mx-Cre* $C\alpha^{F/F}$ mice; analyzed by one-way ANOVA.
doi:10.1371/journal.pbio.1001589.g008

play a role in the initiation of CD69 expression on NKT cells, as well as in the induction of IL-2Rβ, the β-chain of the IL-2 and IL-15 receptors [13].

Moreover, we observed the generation of tetramer+ CD8+ T cells. CD8+ NKT cells are found in the human, but not in wild-type mice. CD8 expression on Vα14i NKT cells does not interfere

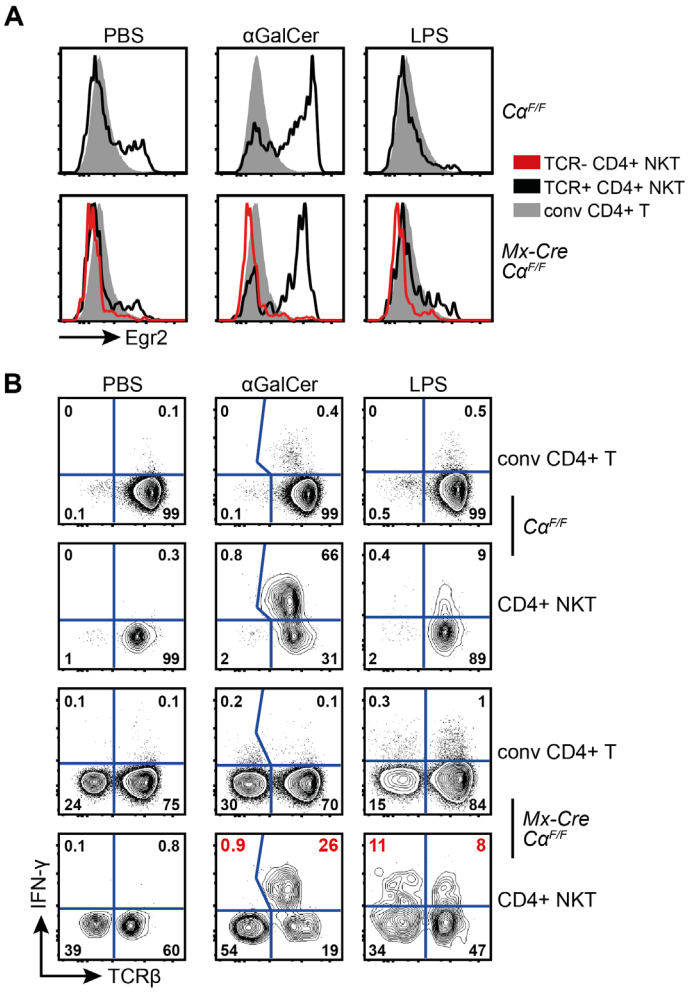

Figure 9. TCR-signals are not required for the innate activation of NKT cells. (A) Intracellular Egr2 expression of the depicted splenic T cells, 90 min after PBS or αGalCer injection, or 6 h after LPS injection. Plots are representative for at least three independent experiments. (B) Intracellular IFN-γ expression of the depicted cells stained directly ex vivo without addition of brefeldin or monensin. Splenic cells were isolated 90 min after PBS or αGalCer injection, or 6 h after LPS injection. Plots are representative for at least three independent experiments.
doi:10.1371/journal.pbio.1001589.g009

with negative selection, avidity for antigen presented by CD1d, or NKT cell function [28]. Instead, it was proposed that the absence of CD8+ NKT cells in the mouse is due to the constitutive expression of the transcription factor Th-Pok in all CD4+ as well as DN NKT cells [28]. Th-Pok has been shown to be crucial for the maturation and function of NKT cells, and directly represses CD8 expression [28]. This scenario fits well with the fact that the CD8+ tetramer+ T cells in the *CD4-Cre Vα14i*^{StopF}*/wt* (as well as in the Vα11p-*Vα14itg* animals) did not express Th-Pok. These cells also lack many other characteristic features of NKT cells, including PLZF expression. Therefore, we refer to them as tetramer+ CD8+ T cells.

Given the faithful recapitulation of endogenous TCRα-chain expression timing and strength in our knock-in mice, combined with the extremely high homologous recombination efficiency, we believe that our strategy should prove useful for the generation of further novel TCR-transgenic mouse models. By replacing RAG-mediated Vα14 to Jα18 recombination with Cre-mediated activation of Vα14i expression in *CD4-Cre Vα14i*^{StopF}*/wt* mice, we can directly couple conditional gain or loss of gene function with Vα14i-TCR expression in NKT cells. NKT cell-specific gene targeting in mice with physiological NKT cell numbers could be achieved through the generation of mixed bone marrow chimeras with *Jα18*$^{-/-}$ bone marrow, which cannot give rise to Vα14i-NKT cells.

Our studies were designed to elucidate whether or to what extent the expression of the autoreactive semi-invariant TCR would activate a peripheral mature naïve conventional T cell, convert it into an NKT cell, or induce gene expression typical of NKT cells. We took advantage of the conditional nature of the Vα14i-TCR knock-in transgene for a TCR switch experiment on conventional peripheral T cells. Naïve CD4+ T cells inherit a high plasticity [51]. Depending on TCR signaling strength and cytokine environment, they can differentiate in various subsets in periphery. This differentiation includes the induction of specific transcription factors, namely T-bet (Th1), GATA-3 (Th2), ROR-γt (Th17), and FoxP3 (peripherally derived regulatory T cells). For NKT cells, it is believed that strong TCR signaling, together with homotypic interactions involving the SLAM family (SLAMf) receptors 1 and 6, ultimately leads to PLZF induction during thymic development [11,13]. DP thymocytes, presenting auto-antigen via CD1d and also expressing SLAMf members, are crucial for thymic NKT cell selection [11]. These SLAMf receptors are expressed on peripheral lymphocytes in comparable levels to double positive

thymocytes (www.immgen.org). Therefore, lymphocytes, especially marginal zone B cells, which express CD1d to a similar level as DP thymocytes, should be able to present antigen and SLAMf-mediated co-stimulation, to naïve conventional T cells with a newly expressed Vα14i-TCR on their surface. The elevated levels of the TCR-induced transcription factor Egr2 in switched tetramer+ T cells suggest that they receive an (auto-)antigenic signal. This finding is in principle in agreement with our finding that tetramer+ TCR-switched T cells are enriched in cells that express Vβ2- and Vβ8.1-/8.2-containing Vα14i-TCRs. These TCRs were shown to have the highest avidity for NKT cell antigens [3]. Furthermore, Vβ7-containing Vα14i-TCRs were shown to be favored when endogenous ligand concentration are suboptimal in $CD1d^{+/-}$ mice [42]. In fact, in CD4+ tetramer+ TCR-switched T cells the relative enrichment for Vβ7-expressing cells was slightly higher than for Vβ2- and Vβ8.1-/8.2-expressing cells (unpublished data). However, the interpretation that this advantage is due to antigenic selection is at odds with the fact that Vβ7-expressing cells are not enriched in tetramer+ TCR-switched CD8+ T cells. We currently have no satisfactory explanation for this discrepancy. Both CD4+ and CD8+ Vα14i-TCR-expressing conventional T cells show features of activation and exhaustion/anergy, but do not develop into NKT cells, judged by absent PLZF and NK cell marker expression. This indicates that either mature T cells have lost the ability to enter the NKT cell lineage, the peripheral Vα14i-TCR signal is not strong enough, or as yet unidentified components of the thymic microenvironment are required to induce an NKT cell fate. Indeed, the high Egr2 expression of mature NKT cells that matured in the periphery and migrated back to the thymus (Figure 8A) suggests that stronger self-antigens are presented at this location. Interestingly, unlike TCR-switched tetramer+ T cells, Egr2 expression in mature splenic NKT cells was similar to that of conventional mature CD4+ T cells. Our data therefore suggest that in the periphery, the Vα14i-TCR can recognize self-lipids, but maturing NKT cells undergo a developmental program that prevents an auto-reactive inflammatory response. At this point, we cannot exclude the possibility that the observed cellular activation was antigen-independent. The fact that the internal control cells, the co-transferred tetramer− T cells, show no or significantly less signs of activation strongly argues for an involvement of antigen recognition or tonic signaling by the Vα14i-TCR. It also remains possible that the transient immune activation caused by the poly(I:C) administration contributes to the observed phenotypes. In all likelihood, this contribution is small, as we never observed any significant immune activation, not to mention loss of CD1d-expressing antigen-presenting B cells and dendritic cells, in *Mx-Cre* $C\alpha^{F}/wt$ control mice that received poly(I:C). Despite these caveats, our results clearly show that under our experimental conditions, Vα14i-TCR expression on conventional naïve T cells leads to their activation and general immune deregulation.

These findings seemed to support notions that NKT cell maintenance [52], their activated surface phenotype, and especially their rapid cytokine expression abilities might depend on constant antigen recognition [25]. However, by ablating the TCR on mature NKT cells in situ, we unequivocally demonstrated that long-term mouse NKT cell homeostasis and gene expression are nearly completely independent of TCR signals. In this regard, they are similar to memory T and B cells, which can maintain their numbers, identity, and functional capabilities in the absence of antigen [53,54]. Our results are hard to reconcile with a recent report suggesting that NKT cell maintenance requires lipid presentation by B cells [52]. While there might be some differences between mouse and man, a more likely scenario is that the observations of Bosma et al. reflect rather acute local activation than true homeostatic requirements. Most of the known functions of NKT cells critically depend on their ability to rapidly secrete large amounts of many different immune-modulatory cytokines shortly after their activation. Still, it is not fully understood how NKT cell activation is triggered in different disease settings, and especially to what extent signaling in response to TCR-mediated recognition of antigens versus activation by proinflammatory cytokines contributes to this. Various studies reported that CD1d-dependent signals were required for full NKT activation in vitro [19,20,55], although most of them contained the caveat of potentially incomplete blockade of CD1d function by blocking antibodies. Our experiments, in line with a recent report [21], show that even in the complete absence of TCR signaling for 4 wk, NKT cells can be robustly activated in vivo to produce IFN-γ upon LPS injection in similar amounts as their TCR+ counterparts. Thus, we demonstrate that in mouse NKT cells continuous steady-state TCR-signaling is not required to maintain the *Ifng* locus in a transcriptionally active state, as recently proposed for human NKT cells [25]. Therefore, our results clearly demonstrate that cellular identity and critical functional abilities of mature NKT cells, such as steady-state proliferation and innate cytokine secretion ability, although initially instructed by strong TCR signals, do not require further antigen recognition through their TCR.

Collectively, our data strongly support the view that Vα14i-TCR expression on developing NKT cells triggers a program that makes them unresponsive to peripheral self-antigens, which can continuously be recognized by their auto-reactive TCR. NKT cells are extremely potent immune-modulatory cells that upon activation can instantly secrete a large array of cytokines. Although they are selected by high affinity to auto-antigens, similar to regulatory T cells, they are not mainly suppressive cells. Therefore, it seems plausible that NKT cells are rendered "blind" to peripheral auto-antigens, rather than depend on continuous stimulation by self-lipids to maintain their cellular identity and innate functions. By keeping their activated state independent of self-antigen recognition, NKT cells can stay poised to secrete immune-activating cytokines while minimizing the risk of causing damage to self during normal physiology. On the other hand, the presence of the auto-reactive Vα14i-TCR serves to detect pathogenic states when a stronger signal is generated by the enhanced presentation of potentially more potent self-antigens or foreign lipids.

Materials and Methods

Genetically Modified Mice

To generate $Vα14i^{StopF}$ mice, B6 ES cells (Artemis) were transfected, cultured, and selected as previously described for Bruce 4 ES cells [56]. *Mx-Cre* [39], $C\alpha^{F}$ [40], *CD4-Cre* [57], *Nestin-Cre* [31], Vα11p-*Vα14i-tg* [32], and $Vα14i^{StopF}$ mice were kept on a C57BL/6 genetic background. As we did not observe any differences between *CD4-Cre* and $Vα14i^{StopF}/wt$ mice in NKT cell biology, they were sometimes grouped together as controls. Mice were housed in the specific pathogen-free animal facility of the MPIB. All animal procedures were approved by the Regierung of Oberbayern.

Cre Induction in Mx-Cre Animals

At the age of 6–8 wk (or 2 wk after cell transfer for the TCR switch experiment), animals were given a single i.p. injection (400 μg) of poly(I:C) (Amersham). All mice were analyzed 6–8 wk after injection, unless otherwise indicated.

Flow Cytometry and Heat Map Generation

Single-cell suspensions were prepared and stained with monoclonal antibodies: B220 (clone RA3-6B2), BTLA (8F4), CD11c (N418), CD122 (TM-b1), CD127 (A7R34), CD160 (eBioCNX46-3), CD25 (PC61.5), CD28 (37.51), CD38 (90), CD39 (24DMS1), CD4 (RM4-5), CD44 (IM7), CD45RB (C363.16A), CD5 (53-7.3), CD62L (MEL-14), CD69 (H1.2-F3), CD8α (53-6.7), CD8β (H35-17.2), CD95 (15A7), DX5 (DX5), Egr2 (erongr2), GATA-3 (TWAJ), Gr1 (RB6-8C5), ICOS (7E.17G9), IL-4 (11B11), IL-13 (eBio13A), IL-17A (eBio17B7), IFN-γ (XMG1.2), LAG-3 (eBioC9B7W), LFA-1 (M17/4), Ly49A/D (eBio12A8), Ly49C/I (14B11), Ly49G2 (eBio4D11), Mac1 (M1/70), NKG2A (16A11), NKG2D (CX5), NK1.1 (PK136), PD-1 (J43), ROR-γt (AFKJS-9), T-bet (eBio4B10), TCRβ (H57-597), Ter119 (TER-119), Th-POK (2POK), and TNF (MP6-XT22) (all from eBioscience). SiglecF (E50-2440) was from BD. TCRβ chains were stained with the mouse Vβ TCR screening panel (BD). PLZF antibody and the CXCL16-Fc fusion were generous gifts from Derek Sant'Angelo and Mehrdad Matloubian, respectively. mCD1d-tetramers were provided by the NIH tetramer core facility. For intracellular transcription factor stainings, cells were fixed and permeabilized with the FoxP3 staining kit (eBioscience). For intracellular cytokine stainings, mice were injected i.v. in the tail vein with 40 μg of LPS (Sigma) or 2 μg αGalCer (Funakoshi) in a total volume of 200 μl PBS. Afterwards, cells were treated according to manufacturer's instructions with the Cytofix/Cytoperm kit (BD). For multiplex measurement of cytokines in the serum, we used the mouse Th1/Th2 10plex Cytomix kit according to manufacturer's instructions (eBioscience). Samples were acquired on a FACSCanto2 (BD) machine, and analyzed with FlowJo software (Treestar). The heat map was generated using perseus (part of the MaxQuant software [58]).

BrdU Incorporation

Mice were fed with 0.5 mg/ml BrdU (Sigma) in the drinking water for 4 consecutive weeks. Directly afterwards, BrdU incorporation was analyzed with a BrdU Flow Kit (BD).

ELISA

Serum TNF levels were determined by ELISA as recommended by the manufacturer (BD).

Quantitative RT-PCR

RNA was isolated (QIAGEN RNeasy Micro Kit) and reverse transcribed (Promega) for quantitative real-time polymerase chain reaction (PCR) using probes and primers from the Universal Probe Library (Roche Diagnostics) according to the manufacturer's instructions.

Statistics

Statistical analysis of the results was performed by one-way ANOVA followed by Tukey's test, or by student *t* test, in Prism software (GraphPad). The *p* values are presented in figure legends where a statistically significant difference was found.

Supporting Information

Figure S1 Southern blot screening strategy for the *Vα14i*^{StopF} knock-in allele and NKT cell characterization in *Vα14i*–transgenic mice. (A) DNA of targeted neomycin-resistant embryonic stem cells was digested with BamHI. The Southern Blot probe contains the untranslated exon 4 of Cα and recognizes a 12.5 kb fragment for the knock-in in comparison to 8.9 kb for the wild-type allele. Representative Southern blot for 325 clones, six of eight showing homologous integration of the knock-in allele. (B) Absolute cell numbers in thymus and spleen of 7–13 mice of the indicated genotypes of CD8+ tetramer+ T cells. Bars indicate medians. *** $p<0.001$; ns, not significant, one-way ANOVA. (C) CD8α/CD8β expression of splenic CD8α+ NKT cells from *CD4-Cre Vα14i*^{StopF}*/wt* animals. Numbers indicate mean percentages ± SD of three mice. (D) Serum cytokine levels, measured by FlowCytomix, of three CTR mice and each five *CD4-Cre Vα14i*^{StopF}*/wt* and Vα11p-*Vα14itg* mice. (E, F) CD69 and intracellular T-bet expression of NK1.1+/NK1.1− NKT cells from CTR and *CD4-Cre Vα14i*^{StopF}*/wt* mice. Numbers in representative histogram indicate percentage of CD69^{high} or T-bet+ cells among the indicated NKT cells calculated from eight animals per genotype (CD69) or three animals per genotype (T-bet). Histograms are representative of three or more independent experiments with each at least seven mice in total. (G) CD69 expression of CD4+ conventional T cells (filled grey) and NKT cells (black) from Vα11p-*Vα14itg* mice. Number in representative histogram indicates percentage of CD69^{high} cells among the NKT cells, calculated from seven animals. Throughout the figure, NKT cells were gated as tetramer+ TCRβ+, conventional (conv) T cells as tetramer− TCRβ+; CTR, *CD4-Cre* or *Vα14i*^{StopF}*/wt*.
(TIF)

Figure S2 NKT-cell-depletion before cell transfer and additional analysis of the animals in the TCR-switch experiment. (A) Splenocytes of the indicated genotypes were stained before and after depletion of NKT cells by MACS. Numbers indicate percentages of tetramer+ and tetramer− T cells (TCRβ+). Plots are representative for over 15 independent experiments. (B) Staining with "unloaded" mCD1d-tetramer in comparison to PBS57-loaded mCD1d-tetramer of splenocytes from the same animal. Plots are representative for three independent experiments with five mice in total. (C) Expression of intracellular IFN-γ or TNF ex vivo 90 min after αGalCer injection. Data are representative of two independent experiments with two animals each. (D) Representative histograms of flow cytometric analysis of T cells in animals 8 wk after switch induction: CD4+ tetramer–, CD4+ tetramer+, CD8+ tetramer–, and CD8+ tetramer+ T cells (TCRβ+). Surface expression of the depicted markers in comparison to NK cells (gated as marker+, TCRβ−). Representative plots for at least three independent experiments with at least one mouse each.
(TIF)

Figure S3 Gating strategy for the TCR-ablation experiments. (A) Gating strategy to identify TCR− NKT cells. (B) Yield of the applied gating strategy. (C–E) Extracellular expression of the depicted proteins on CD4+ naïve (CD62L^{high} CD5+), CD4+ memory/effector-like (CD62L^{low} CD5+) T cells, and CD4+ NKT cells (NK1.1+ CD5+ CD62L^{low}). MFIs were normalized to the expression of CD4+ naïve T cells.
(TIF)

Table S1 Comparison of different Vα14i-transgenic mice.
(DOCX)

Acknowledgments

We are grateful to Reinhard Fässler for support. We wish to thank Julia Knogler and Barbara Habermehl for technical assistance. The PLZF and the CXCL16-Fc fusion protein were generous gifts from Derek Sant'Angelo and Mehrdad Matloubian, respectively. The Vα11p-*Vα14i-tg* mice were kindly provided by Stephanie Ganal and Andreas Diefenbach. We are grateful to Xiaojing Yue and Tilman Borggrefe for sharing data on CD4p-*Vα14i-tg* mice with us. We thank Albert Bendelac for input and plasmids for our first attempts to generate TCR-switch mouse models. We wish to thank the NIH tetramer core facility for providing us with mCD1d-PBS57-tetramers.

Author Contributions

The author(s) have made the following declarations about their contributions: Conceived and designed the experiments: JCV MSS. Performed the experiments: JCV KH NK MSS. Analyzed the data: JCV MYH MSS. Contributed reagents/materials/analysis tools: LB HY BP. Wrote the paper: JCV MSS.

References

1. Bendelac A, Savage PB, Teyton L (2007) The biology of NKT cells. Annu Rev Immunol 25: 297–336.
2. Gapin L (2010) iNKT cell autoreactivity: what is "self" and how is it recognized? Nat Rev Immunol 10: 272–277. doi:10.1038/nri2743.
3. Mallevaey T, Scott-Browne JP, Matsuda JL, Young MH, Pellicci DG, et al. (2009) T cell receptor CDR2 beta and CDR3 beta loops collaborate functionally to shape the iNKT cell repertoire. Immunity 31: 60–71. doi:10.1016/j.immuni.2009.05.010.
4. Wei D, Curran S, Savage PB, Teyton L, Bendelac A (2006) Mechanisms imposing the Vbeta bias of Valpha14 natural killer T cells and consequences for microbial glycolipid recognition. J Exp Med 203: 1197–1207.
5. Mallevaey T, Clarke AJ, Scott-Browne JP, Young MH, Roisman LC, et al. (2011) A molecular basis for NKT cell recognition of CD1d-self-antigen. Immunity 34: 315–326. doi:10.1016/j.immuni.2011.01.013.
6. Kronenberg M, Rudensky AY (2005) Regulation of immunity by self-reactive T cells. Nature 435: 598–604.
7. Bendelac A, Bonneville M, Kearney J (2001) Autoreactivity by design: innate B and T lymphocytes. Nat Rev Immunol 1: 177–186.
8. Facciotti F, Ramanjaneyulu GS, Lepore M, Sansano S, Cavallari M, et al. (2012) Peroxisome-derived lipids are self antigens that stimulate invariant natural killer T cells in the thymus. Nat Immunol 13: 474–480. doi:10.1038/ni.2245.
9. Zhou D, Mattner J, Cantu C, Schrantz N, Yin N, et al. (2004) Lysosomal glycosphingolipid recognition by NKT cells. Science 306: 1786–1789.
10. Fox LM, Cox DG, Lockridge JL, Wang X, Chen X, et al. (2009) Recognition of lyso-phospholipids by human natural killer T lymphocytes. PLoS Biol 7: e1000228. doi:10.1371/journal.pbio.1000228.
11. Griewank K, Borowski C, Rietdijk S, Wang N, Julien A, et al. (2007) Homotypic interactions mediated by Slamf1 and Slamf6 receptors control NKT cell lineage development. Immunity 27: 751–762. doi:10.1016/j.immuni.2007.08.020.
12. Moran AE, Holzapfel KL, Xing Y, Cunningham NR, Maltzman JS, et al. (2011) T cell receptor signal strength in Treg and iNKT cell development demonstrated by a novel fluorescent reporter mouse. J Exp Med 208: 1279–1289. doi:10.1084/jem.20110308.
13. Seiler MP, Mathew R, Liszewski MK, Spooner C, Barr K, et al. (2012) Elevated and sustained expression of the transcription factors Egr1 and Egr2 controls NKT lineage differentiation in response to TCR signaling. Nat Immunol 13: 264–271. doi:10.1038/ni.2230.
14. Matsuda JL, Gapin L, Sidobre S, Kieper WC, Tan JT, et al. (2002) Homeostasis of V alpha 14i NKT cells. Nat Immunol 3: 966–974. doi:10.1038/ni837.
15. McNab FW, Berzins SP, Pellicci DG, Kyparissoudis K, Field K, et al. (2005) The influence of CD1d in postselection NKT cell maturation and homeostasis. J Immunol 175: 3762–3768.
16. Kinjo Y, Tupin E, Wu D, Fujio M, Garcia-Navarro R, et al. (2006) Natural killer T cells recognize diacylglycerol antigens from pathogenic bacteria. Nat Immunol 7: 978–986. doi:10.1038/ni1380.
17. Kinjo Y, Wu D, Kim G, Xing G, Poles M, et al. (2005) Recognition of bacterial glycosphingolipids by natural killer T cells. Nature 434: 520–525. doi:nature03407
18. Kinjo Y, Illarionov P, Vela JL, Pei B, Girardi E, et al. (2011) Invariant natural killer T cells recognize glycolipids from pathogenic Gram-positive bacteria. Nat Immunol 12: 966–974. doi:10.1038/ni.2096.
19. Mattner J, Debord KL, Ismail N, Goff RD, Cantu C, et al. (2005) Exogenous and endogenous glycolipid antigens activate NKT cells during microbial infections. Nature 434: 525–529. doi:10.1038/nature03408.
20. Brigl M, Tatituri RVV, Watts GFM, Bhowruth V, Leadbetter EA, et al. (2011) Innate and cytokine-driven signals, rather than microbial antigens, dominate in natural killer T cell activation during microbial infection. J Exp Med 208: 1163–1177. doi:10.1084/jem.20102555.
21. Nagarajan NA, Kronenberg M (2007) Invariant NKT cells amplify the innate immune response to lipopolysaccharide. J Immunol 178: 2706–2713.
22. Tyznik AJ, Tupin E, Nagarajan NA, Her MJ, Benedict CA, et al. (2008) Cutting edge: the mechanism of invariant NKT cell responses to viral danger signals. J Immunol 181: 4452–4456.
23. Matsuda JL, Gapin L, Baron JL, Sidobre S, Stetson DB, et al. (2003) Mouse V alpha 14i natural killer T cells are resistant to cytokine polarization in vivo. Proc Natl Acad Sci USA 100: 8395–8400. doi:10.1073/pnas.1332805100.
24. Stetson DB, Mohrs M, Reinhardt RL, Baron JL, Wang Z-E, et al. (2003) Constitutive cytokine mRNAs mark natural killer (NK) and NK T cells poised for rapid effector function. J Exp Med 198: 1069–1076. doi:10.1084/jem.20030630.
25. Wang X, Bishop KA, Hegde S, Rodenkirch LA, Pike JW, et al. (2012) Human invariant natural killer T cells acquire transient innate responsiveness via histone H4 acetylation induced by weak TCR stimulation. J Exp Med 209: 987–1000. doi:10.1084/jem.20111024.
26. Baldwin TA, Sandau MM, Jameson SC, Hogquist KA (2005) The timing of TCR alpha expression critically influences T cell development and selection. J Exp Med 202: 111–121. doi:10.1084/jem.20050359.
27. Serwold T, Hochedlinger K, Inlay MA, Jaenisch R, Weissman IL (2007) Early TCR expression and aberrant T cell development in mice with endogenous prerearranged T cell receptor genes. J Immunol 179: 928–938.
28. Engel I, Hammond K, Sullivan BA, He X, Taniuchi I, et al. (2010) Co-receptor choice by V alpha14i NKT cells is driven by Th-POK expression rather than avoidance of CD8-mediated negative selection. J Exp Med 207: 1015–1029. doi:10.1084/jem.20090557.
29. Godfrey DI, Stankovic S, Baxter AG (2010) Raising the NKT cell family. Nat Immunol 11: 197–206. doi:10.1038/ni.1841.
30. Coquet JM, Chakravarti S, Kyparissoudis K, McNab FW, Pitt LA, et al. (2008) Diverse cytokine production by NKT cell subsets and identification of an IL-17-producing CD4-NK1.1- NKT cell population. Proc Natl Acad Sci USA 105: 11287–11292. doi:10.1073/pnas.0801631105.
31. Betz UA, Vosshenrich CA, Rajewsky K, Müller W (1996) Bypass of lethality with mosaic mice generated by Cre-loxP-mediated recombination. Curr Biol 6: 1307–1316.
32. Bendelac A, Hunziker R, Lantz O (1996) Increased interleukin 4 and immunoglobulin E production in transgenic mice overexpressing NK1 T cells. J Exp Med 184: 1285–1293.
33. Wakao H, Kawamoto H, Sakata S, Inoue K, Ogura A, et al. (2007) A novel mouse model for invariant NKT cell study. J Immunol 179: 3888–3895.
34. Yue X, Izcue A, Borggrefe T (2011) Essential role of Mediator subunit Med1 in invariant natural killer T-cell development. Proc Natl Acad Sci USA. doi:10.1073/pnas.1109095108.
35. Thapa P, Das J, McWilliams D, Shapiro M, Sundsbak R, et al. (2013) The transcriptional repressor NKAP is required for the development of iNKT cells. Nat Commun 4: 1582. doi:10.1038/ncomms2580.
36. Kovalovsky D, Uche OU, Eladad S, Hobbs RM, Yi W, et al. (2008) The BTB–zinc finger transcriptional regulator PLZF controls the development of invariant natural killer T cell effector functions. Nat Immunol 9: 1055–1064. doi:10.1038/ni.1641.
37. Gordy LE, Bezbradica JS, Flyak AI, Spencer CT, Dunkle A, et al. (2011) IL-15 regulates homeostasis and terminal maturation of NKT cells. J Immunol 187: 6335–6345. doi:10.4049/jimmunol.1003965.
38. Ranson T, Vosshenrich CAJ, Corcuff E, Richard O, Laloux V, et al. (2003) IL-15 availability conditions homeostasis of peripheral natural killer T cells. Proc Natl Acad Sci USA 100: 2663–2668. doi:10.1073/pnas.0535482100.
39. Kuhn R, Schwenk F, Aguet M, Rajewsky K (1995) Inducible gene targeting in mice. Science 269: 1427–1429.
40. Polic B, Kunkel D, Scheffold A, Rajewsky K (2001) How alpha beta T cells deal with induced TCR alpha ablation. Proc Natl Acad Sci USA 98: 8744–8749.
41. Bourgeois C, Hao Z, Rajewsky K, Potocnik AJ, Stockinger B (2008) Ablation of thymic export causes accelerated decay of naive CD4 T cells in the periphery because of activation by environmental antigen. Proc Natl Acad Sci USA 105: 8691–8696. doi:10.1073/pnas.0803732105.
42. Schümann J, Mycko MP, Dellabona P, Casorati G, Macdonald HR (2006) Cutting edge: influence of the TCR Vbeta domain on the selection of semi-invariant NKT cells by endogenous ligands. J Immunol 176: 2064–2068.
43. Brossay L, Tangri S, Bix M, Cardell S, Locksley R, et al. (1998) Mouse CD1-autoreactive T cells have diverse patterns of reactivity to CD1+ targets. J Immunol 160: 3681–3688.
44. Blackburn SD, Shin H, Haining WN, Zou T, Workman CJ, et al. (2009) Coregulation of CD8+ T cell exhaustion by multiple inhibitory receptors during chronic viral infection. Nat Immunol 10: 29–37. doi:10.1038/ni.1679.
45. Parekh VV, Lalani S, Kim S, Halder R, Azuma M, et al. (2009) PD-1/PD-L blockade prevents anergy induction and enhances the anti-tumor activities of glycolipid-activated invariant NKT cells. J Immunol 182: 2816–2826. doi:10.4049/jimmunol.0803648.
46. Witherden D, van Oers N, Waltzinger C, Weiss A, Benoist C, et al. (2000) Tetracycline-controllable selection of CD4(+) T cells: half-life and survival signals in the absence of major histocompatibility complex class II molecules. J Exp Med 191: 355–364.
47. Capone M, Cantarella D, Schümann J, Naidenko OV, Garavaglia C, et al. (2003) Human invariant V alpha 24-J alpha Q TCR supports the development of CD1d-dependent NK1.1+ and NK1.1- T cells in transgenic mice. J Immunol 170: 2390–2398.
48. Inoue K, Wakao H, Ogonuki N, Miki H, Seino K, et al. (2005) Generation of cloned mice by direct nuclear transfer from natural killer T cells. Curr Biol 15: 1114–1118.
49. Manjunath N, Shankar P, Stockton B, Dubey PD, Lieberman J, et al. (1999) A transgenic mouse model to analyze CD8(+) effector T cell differentiation in vivo. Proc Natl Acad Sci USA 96: 13932–13937.
50. Huntington ND, Puthalakath H, Gunn P, Naik E, Michalak EM, et al. (2007) Interleukin 15-mediated survival of natural killer cells is determined by interactions among Bim, Noxa and Mcl-1. Nat Immunol 8: 856–863. doi:10.1038/ni1487.

51. Zhu J, Yamane H, Paul WE (2010) Differentiation of effector CD4 T cell populations (*). Annu Rev Immunol 28: 445–489. doi:10.1146/annurev-immunol-030409-101212.
52. Bosma A, Abdel-Gadir A, Isenberg DA, Jury EC, Mauri C (2012) Lipid-antigen presentation by CD1d(+) B cells is essential for the maintenance of invariant natural killer T cells. Immunity 36: 477–490. doi:10.1016/j.immuni.2012.02.008.
53. Boyman O, Krieg C, Homann D, Sprent J (2012) Homeostatic maintenance of T cells and natural killer cells. Cell Mol Life Sci 69: 1597–1608. doi:10.1007/s00018-012-0968-7.
54. Maruyama M, Lam KP, Rajewsky K (2000) Memory B-cell persistence is independent of persisting immunizing antigen. Nature 407: 636–642. doi:10.1038/35036600.
55. Brigl M, Bry L, Kent SC, Gumperz JE, Brenner MB (2003) Mechanism of CD1d-restricted natural killer T cell activation during microbial infection. Nat Immunol 4: 1230–1237. doi:10.1038/ni1002.
56. Schmidt-Supprian M, Bloch W, Courtois G, Addicks K, Israel A, et al. (2000) NEMO/IKK gamma-deficient mice model incontinentia pigmenti. Mol Cell 5: 981–992. doi:S1097-2765(00)80263-4.
57. Lee P, Fitzpatrick D, Beard C, Jessup H, Lehar S, et al. (2001) A critical role for Dnmt1 and DNA methylation in T cell development, function, and survival. Immunity 15: 763–774.
58. Cox J, Mann M (2008) MaxQuant enables high peptide identification rates, individualized p.p.b.-range mass accuracies and proteome-wide protein quantification. Nat Biotechnol 26: 1367–1372. doi:10.1038/nbt.1511.

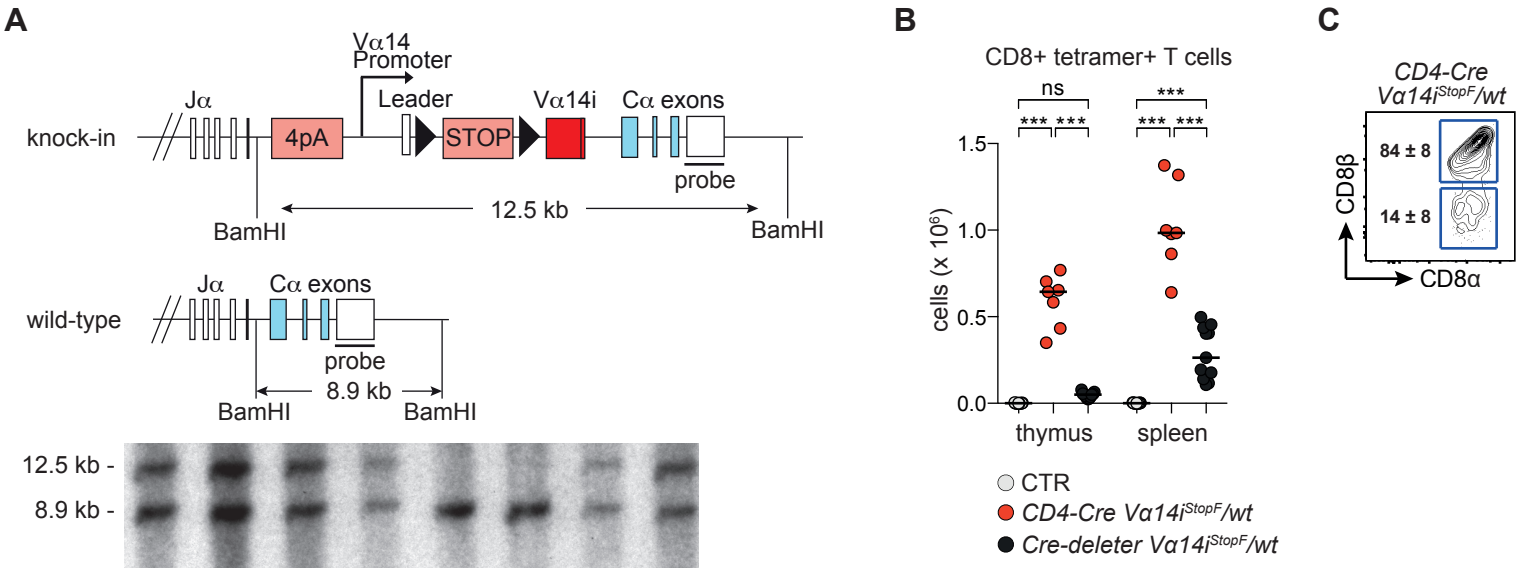

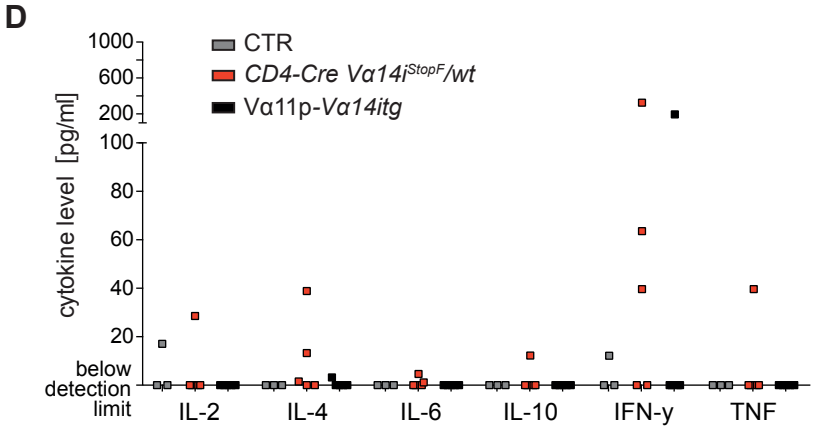

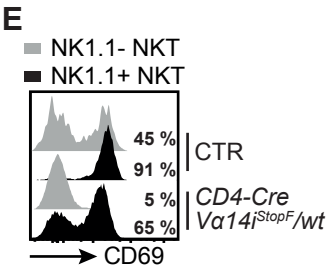

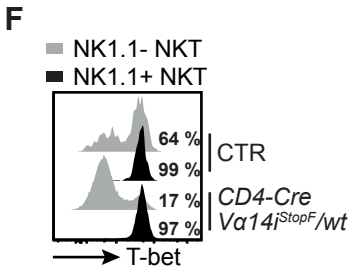

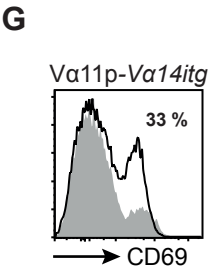

Supplementary Figure 1

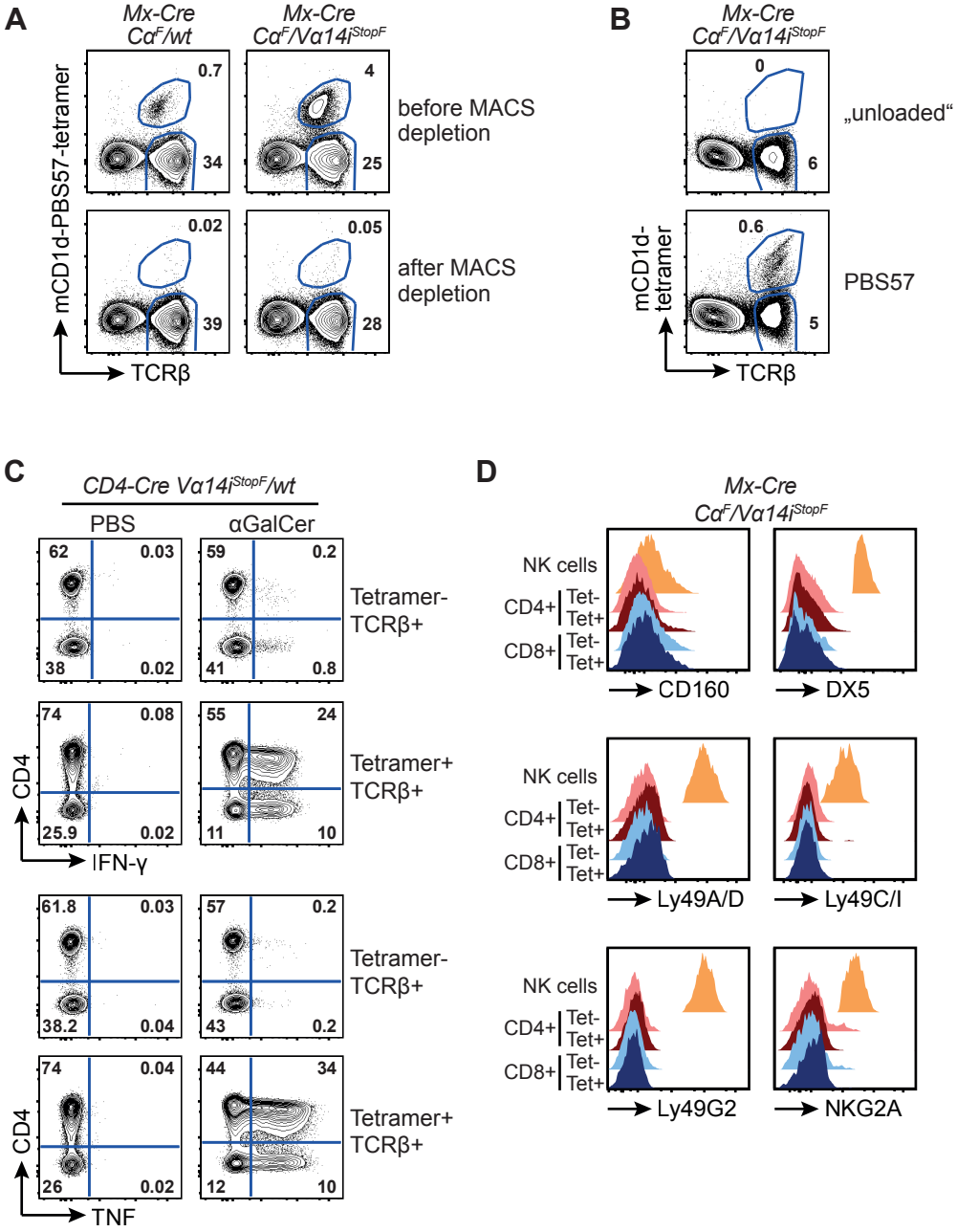

Supplementary Figure 2

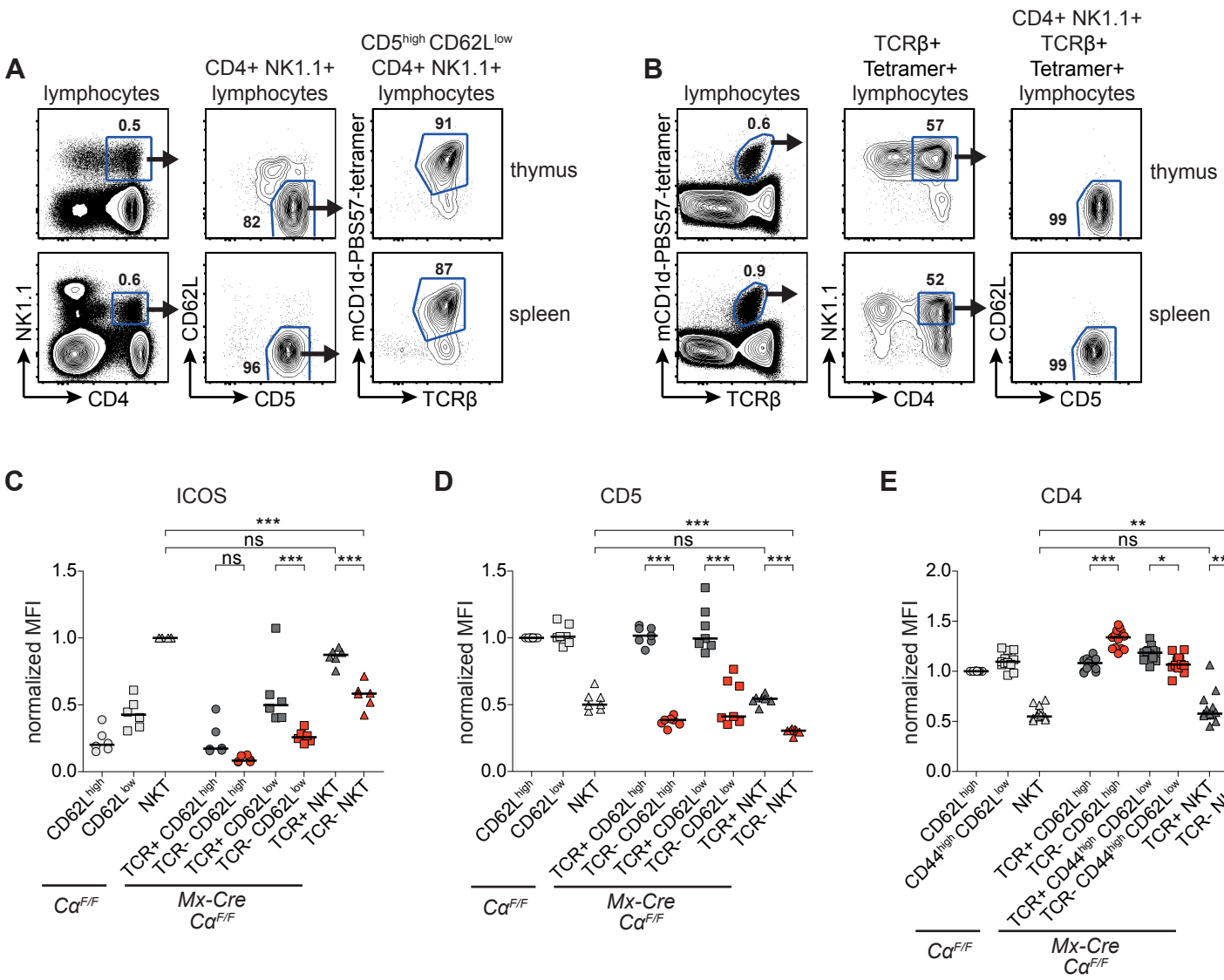

Supplementary Figure 3

Table S1: Comparison of different Vα14i-transgenic mice.

	control (n = 13)	*CD4-Cre Vα14iStop^F/wt* (n = 7)	*Cre-deleter Vα14iStop^F/wt* (n = 7)	Vα11p-*Vα14itg* (n = 11)	CD4p-*Vα14itg* (Yue et al.)	rec-*Vα14itg* (Thapa et al.)	Nuc. transfer-*Vα14itg* (Wakao et al.)
thymus							
total cells (x 10^6)	132 ± 39	54 ± 13	15 ± 3	15 ± 4	-	-	16 ± 10
% NKT cells	0.4	15.2	10.4	14.8	9.0	1.1	16
total NKT cells (x 10^6)	0.3	**7.9**	1.7	2.1	4.0	-	2.5*
NKT: % CD4+/DN/CD8+	68/32/-	67/24/8	44/53/3	36/61/4	-	-	-
CD+/DN/CD8+ NKT cells (x 10^6)	0.2/0.1/-	4.6/1.7/0.6	0.7/0.9/0.1	0.7/1.2/0.1	-	-	-
NKT: % of CD69^{high}	84	61	-	54	-	-	28
CD69^{high} NKT cells (x 10^6)	0.3	4.8	-	1.1	-	-	0.7*
NKT: % of NK1.1+	87	15	27	24	10**	66	23
NK1.1+ NKT cells (x 10^6)	0.3	1.2	0.5	0.5	0.4*/**	-	0.6*
DN tetramer- T cells (x 10^6)	0.1	0.1	0.5	1.0	-	-	-
spleen							
total cells (x 10^6)	74 ± 19	70 ± 14	57 ± 19	47 ± 7	-	-	60 ± 12
% NKT cells	0.6	19.1	13.5	8.3	4.5	3.8	12.0
total NKT cells (x 10^6)	0.3	**12.1**	6.1	3.7	5.7	-	7.2*
NKT: % CD4+/DNCD8+	80/20/-	72/19/9	46/49/5	25/66/9	-	-	-
CD+/DN/CD8+ NKT cells (x 10^6)	0.2/0.1/-	8.7/2.2/1.0	2.7/2.9/0.3	1.0/2.4/0.3	-	-	-
NKT: % of CD69^{high}	57	17	-	33	-	-	-
CD69^{high} NKT cells (x 10^6)	0.2	2.1	-	1.2	-	-	-
NKT: % of NK1.1+	72	20	31	44	-	-	-
NK1.1+ NKT cells (x 10^6)	0.2	2.5	1.9	1.7	-	-	-
DN tetramer- T cells (x 10^6)	0.3	0.2	1.3	0.9	-	-	-

Shown are average total cell counts and percentages (+/- SD) in thymus and spleen of the indicated mice. Grey results were not measured by us, but instead taken from the respective publications. *, calculated by multiplying the representative percentage with the average cell number. **, probably higher due to dim NK1.1 staining.

Paper II

Vahl J.C., Heger K., Ohkura N., Hein M.Y., Kretschmer K., Prazeres da Costa O., Buch T., Polic O., Sakaguchi S. and Schmidt-Supprian M. TCR ablation leads to loss of regulatory T cell identity.

Manuscript in preparation.

TCR ablation leads to loss of regulatory T cell identity

J. Christoph Vahl[1], Klaus Heger[1], Naganari Ohkura[2], Marco Y. Hein[1,6], Karsten Kretschmer[3], Olivia Prazeres da Costa[4], Thorsten Buch[4], Bojan Polic[5], Shimon Sakaguchi[2] and Marc Schmidt-Supprian[1,*]

[1]Max Planck Institute of Biochemistry, Am Klopferspitz 18, 82152 Martinsried, Germany.
[2]Department of Experimental Immunology, World Premier International Immunology Frontier Research Center, Osaka University, Suita 565-0871, Japan.
[3]Deutsche Forschungsgemeinschaft–Center for Regenerative Therapies, Dresden, Germany
[4]Institute for Medical Microbiology, Immunology & Hygiene, Technische Universität München, Munich, Germany.
[5]University of Rijeka School of Medicine, Rijeka, Croatia
[6]Present address: Proteomics and Signal Transduction, Max Planck Institute of Biochemistry, Am Klopferspitz 18, 82152 Martinsried, Germany.

Running Title: Role of T cell receptor signaling for Tregs

Corresponding author: Marc Schmidt-Supprian
Max Planck Institute of Biochemistry
Am Klopferspitz 18
D-82152 Martinsried
Phone: +498985782464
Fax: +498985782422
E-mail: supprian@biochem.mpg.de

Abbreviations used: DC, dendritic cell; DN, double negative; DP, double positive; FoxP3, Forkhead Box P3; ICOS, inducible T-cell Co-Stimulator; MFI, median fluorescence intensity; NKT, natural killer T; Nrp1, Neuropilin-1; T_{reg}, regulatory T; SP, single positive; TCR, T cell receptor.

ABSTRACT

Regulatory T (T_{reg}) cells are of critical importance to prevent the development of autoimmune responses. During their development in the thymus, T cells expressing T cell receptors (TCRs) with increased reactivity towards self are selected to become T_{reg} cells. Several observations suggest that mature T_{reg} cells continuously receive autoreactive TCR signals in the periphery, but the importance of this inherent autoreactivity is still unclear. To address this question, we ablated the TCR of mature T_{reg} cells *in vivo* and followed their fate over several weeks. Our experiments demonstrate that the homeostasis, cell-type-specific gene expression and suppressive function of T_{reg} cells depend on continuous triggering of their TCR.

INTRODUCTION

The generation of a peripheral T cell pool with a broad variety of T cell receptors (TCRs) is critical for a functional immune system. The random nature of somatic TCR gene assembly ensures that a large number of foreign antigens can be recognized, but self-reactive TCRs are also generated. Various cellular and molecular checkpoints exist to delete autoreactive T cells or render them ineffective. These checkpoints can be subdivided into central and peripheral tolerance mechanisms (Xing and Hogquist, 2012). During thymic T cell development, most T cells with a strong self-reactivity to peptide-MHC complexes are deleted.

Some cells displaying intermediate self-reactivity are instructed to develop into regulatory T (T_{reg}) cells, a process known as agonist selection (Josefowicz et al., 2012; Stritesky et al., 2012; Xing and Hogquist, 2012). Regulatory T cells are critical to control aberrant autoimmune activation in the periphery, since their absence or dysfunction leads to severe T cell-mediated pathologies in man and mouse (Josefowicz et al., 2012; Sakaguchi et al., 2008). Regulatory T cells act mostly by suppressing the expansion and function of effector T cells, through various direct and indirect mechanisms. The key lineage-defining transcription factor Forkhead Box P3 (FoxP3) controls the expression of gene programs necessary to induce and maintain T_{reg} cell identity and function. While the number genes whose expression is influenced by FoxP3 alone is limited, much larger and diverse sets of genes are regulated by FoxP3 in conjunction with other transcriptional regulators, depending on

the type of the immune response and the tissue where this response takes place. Recently, it was shown that establishment of a T_{reg} cell-specific hypomethylation pattern constitutes an additional independent requirement (Ohkura et al., 2012). Hypomethylation might also hard-wire a transcriptionally poised state in a set of T_{reg} cell core genes, rendering their expression less dependent on the flexible composition of activated transcription factors. Peripheral T_{reg} cell identity depends on continued FoxP3 expression, which is remarkably stable in the mouse. Furthermore, the majority of T_{reg} cells express high levels of CD25, the α-chain of the high affinity IL-2 receptor, and their survival and full FoxP3 expression depends on IL-2 (Fontenot et al., 2005a).

Similar to conventional T cells, the peripheral T_{reg} cell pool contains naïve and effector/tissue-homing subsets (Campbell and Koch, 2011; Fisson et al., 2003). Naïve T_{reg} cells are quiescent and express the adhesion/homing receptor CD62L and the chemokine receptor CCR7, allowing them to enter secondary lymphoid organs (Campbell and Koch, 2011). In contrast, effector T_{reg} cells are cycling, predominantly found in the $CD25^{low}$ subset and show increased expression of CD5, CD38, CD44, Ox40, GITR, CD69, and ICAM-1 in comparison to naïve T_{reg} cells (Campbell and Koch, 2011; Feuerer et al., 2009; Fisson et al., 2003; Fontenot et al., 2005b; Huehn et al., 2004; Stephens et al., 2007). It was proposed that the effector T_{reg} cell subset is comprised of short-lived cells that were recently activated upon (self-)antigen recognition (Campbell and Koch, 2011; Fisson et al., 2003).

Importantly, both lineage-defining characteristics of T_{reg} cells, namely FoxP3 expression and the specific hypomethylated state, are induced by strong, and in the latter case long lasting, TCR signals in developing T_{reg} cells. TCR-mediated activation of NF-κB, NF-AT and Nr4a family transcription factors is essential for T_{reg} cell development, at least in part through induction of FoxP3 expression (Isomura et al., 2009; Medoff et al., 2009; Schmidt-Supprian et al., 2003; 2004; Sekiya et al., 2013). Furthermore, a mutation in LAT abolishing its ability to bind to PLCγ1 severely interfered with T_{reg} cell, but not conventional T cell development (Koonpaew et al., 2006). Interruption of TCR signaling in developing thymic T_{reg} cells by ablation of Lck via Ox40-Cre led to reduced splenic, although increased lymph node FoxP3+ T_{reg} cell numbers. Lck-deficient T_{reg} cells displayed a striking deficiency in T_{reg} cell signature genes (Kim et al., 2009).

The importance of TCR-generated signals for the maintenance of mature T_{reg} cell pool size and lineage identity in the immunological periphery is less well understood. A reporter mouse for TCR signal strength suggested that T_{reg} cells continuously receive stronger TCR signals in comparison to conventional T cells not only during thymic development, but also in the periphery (Moran et al., 2011). Mice expressing MHCII only on cortical thymic epithelial cells showed normal proportions of *in vitro* suppressive CD4+ CD25+ T cells in peripheral lymph nodes (Bensinger et al., 2001), which would suggest that peripheral homeostasis of T_{reg} cells is to a large degree MHCII independent. Fittingly, T_{reg} cell-specific deletion of IKK2, a kinase that links TCR activation to the transcription factor NF-κB pathway and that is crucial during thymic T_{reg} cell development (Schmidt-Supprian et al., 2004), did not lead to changes in peripheral T_{reg} cell numbers (Chang et al., 2012). Furthermore, graded interference of TCR signaling by ZAP mutations of varying severity led to reduced T_{reg} cell numbers in the thymus, but not in the spleen (Siggs et al., 2007). Altogether, these observations indicated that the homeostasis of mature T_{reg} cells is independent of TCR signals. On the other hand, ablation of MHCII expression specifically on $CD11c^{high}$ dendritic cells (DCs) significantly reduced proportions and absolute cell numbers of T_{reg} cells in lymph nodes and spleen (Darrasse-Jèze et al., 2009). These results are in line with the fact that the homeostatic proliferation of adoptively transferred *in vitro* suppressive CD4+ CD25+ T cells requires MHCII expression (Gavin et al., 2002).

To directly address the importance of tonic TCR signaling for peripheral T_{reg} cell homeostasis and lineage identity, we monitored the effects of induced TCR ablation on mature T_{reg} cells over time. Our results show that TCR-less T_{reg} cells quickly lose their activated phenotype and further show impaired homeostasis and function. Therefore, we propose that TCR-derived signals are not only critical during thymic development, but also for the maintenance and function of peripheral regulatory T cells.

RESULTS

Inducible TCR ablation on regulatory T cells

In order to study the importance of constitutive TCR signaling for regulatory T cells, we conditionally ablated the TCRα-chain by using the previously described *Mx-Cre* $C\alpha^{F/F}$ system (Polic et al., 2001). Regulatory T cells, as well as conventional T cells, develop normally in these mice. Cre expression is controlled by the *Mx1*-promoter, which can be induced by injection of type-I-interferons or double-stranded RNA (poly(I:C)) in vivo (Polic et al., 2001). It was previously shown that upon Cre-dependent Cα-ablation, the surface expression of the TCRβ-chain and CD3 was noticeable down-regulated 5 d after poly(I:C) treatment, and both molecules were absent from the surface after 10 d (Polic et al., 2001). Intracellular FoxP3 staining of CD4+ $CD25^{high}$ splenocytes showed that 2 wk after poly(I:C) treatment, around ¼ of the FoxP3+ T_{reg} cells had lost TCR surface expression (Fig. 1A). Importantly, TCR-deficient T_{reg} cells still expressed high FoxP3 levels (Fig. 1A), indeed we did not observe at any time point FoxP3 downregulation in TCR-deficient T_{reg} cells. For further studies, the mice were bred to the FoxP3-eGFP reporter strain to facilitate the identification of TCR+ and TCR- T_{reg} cells (Bettelli et al., 2006).

Together, these experiments demonstrate that continuous TCR-generated signals are not obligate for the maintenance of FoxP3 expression of mature T_{reg} cells. For the following experiments, we analyzed T_{reg} cells 6 wk after induced TCR ablation unless otherwise indicated, so that they did not receive TCR signals for at least 1 month. At this time-point the effects of cellular activation by poly(I:C) injection should also have completely subsided.

Peripheral homeostasis of regulatory T cells is strongly impaired upon TCR deletion

The continued FoxP3 expression allowed us to unambiguously identify TCR-deficient T_{reg} cells. Upon poly(I:C) treatment, Cre-mediated recombination of conditional TCRα alleles is complete in lymphoid progenitors of *Mx-Cre* mice (Polic et al., 2001). Accordingly, 6 wk after poly(I:C) treatment, the thymi of *Mx-Cre* $C\alpha^{F/F}$ mice were almost devoid of mature TCRβ+ T cells as well as of TCR^{int} $CD69^{high}$ cells that are undergoing positive selection (Fig. 1B). Many of the remaining TCR^{int} $CD69^{high}$ cells

are recirculating NKT cells (Vahl et al., 2013). Furthermore, T_{reg} cells were almost absent from the thymi of the poly(I:C)-treated *Mx-Cre* $C\alpha^{F/F}$ mice, in line with the previously described fast emigration of T_{reg} cells upon selection (Toker et al., 2013) (Fig. 1B). Therefore, we could employ these mice to study the homeostasis of peripheral T_{reg} cells in the absence of cellular influx from the thymus.

Interestingly, the half-life of T_{reg} cells was significantly reduced in comparison to their TCR+ counterparts in the absence of TCR signals, down to around 46 days (Fig. 1C). Their half-life was comparable to that of TCR-deficient naïve CD4+ cells (40 - 46 days, (Polic et al., 2001; Vahl et al., 2013). On the other hand, TCR-deficient NKT cells and CD4+ $CD44^{high}$ memory/effector T cells, whose homeostasis depends on cytokines and not on TCR signals (Polic et al., 2001; Vahl et al., 2013), have a dramatically longer half-life at around 300 d. However, the total number of peripheral T_{reg} cells was not changed 6 and 15 wk after poly(I:C) injection in *Mx-Cre* $C\alpha^{F/F}$ mice, which was in contrast to the total numbers of naïve CD4+ as well as CD8+ T cells (Supplementary Fig. 1). Thus, the peripheral T_{reg} cell pool size is kept stable in the absence of thymic output (Fig. 1C & Supplementary Fig. 1).

Previously, it has been demonstrated that cytokines, most importantly IL-2 and IL-7, influence the homeostasis of T_{reg} cells (Burchill et al., 2007; Setoguchi et al., 2005). Interestingly, when we analyzed expression of CD25, the α-chain of the high affinity IL-2 receptor, we observed that all TCR-deficient T_{reg} cells expressed high levels of CD25 (Fig. 1D). In contrast, the expression of CD122, the β-chain of the receptors for IL-2 and IL-15, and CD127, a component of the IL-7 receptor, were not significantly altered upon TCR deletion, whereas the expression of the IL-15 receptor α-chain was only partially reduced (Fig. 1D). Therefore, the homeostatic defects of TCR-deficient T_{reg} cells are mostly likely not due to defective cytokine signaling.

The decrease of peripheral TCR-deficient T_{reg} cells (Fig. 1C) could be a consequence of impaired survival or proliferation, or both. To answer this question, we first addressed T_{reg} cell proliferation. Previously, it has been shown that peripheral T_{reg} cells, especially the $CD25^{low}$ subset, vigorously cycle in the steady-state in comparison to conventional T cells (Fisson et al., 2003; Fontenot et al., 2005b). Interestingly, both the proliferation marker Ki-67 as well as CD71, a marker for dividing T cells (Bayer et al., 1998), were not expressed by TCR-deficient T_{reg} cells (Fig. 1E). In order to study the proliferation of T_{reg} cells in the absence of TCR signals

over a longer period of time, we fed mice containing TCR-deficient and –proficient T_{reg} cells with BrdU via drinking water for 4 weeks and analyzed BrdU incorporation directly afterwards. As expected, the vast majority of $CD25^{low}$ T_{reg} cells, as well as a significant proportion of TCR+ $CD25^{high}$ T_{reg} cells, had incorporated BrdU (Fig. 1F). However, in line with the absent Ki-67 and CD71 expression, BrdU-incorporation of TCR-deficient T_{reg} cells was significantly reduced in comparison to their TCR-sufficient counterparts, indicating that their proliferation requires tonic TCR signals (Fig. 1F).

To study whether TCR-deficiency directly impairs the survival of T_{reg} cells, we extracted splenic lymphocytes and stained them for 1 h for presence of activated caspases, a marker for apoptotic cells. Interestingly, a significantly higher percentage of TCR-deficient T_{reg} cells contained activated caspases after this incubation time (Fig. 1G), indicating that at least under these culture conditions, TCR-deficient T_{reg} cells have an increased tendency to enter into apoptosis.

Together, these results demonstrate that the absence of TCR signals abrogates T_{reg} cell homeostasis, due to impaired proliferation and probably increased apoptosis.

TCR-deficient T_{reg} cells lose their activated phenotype

A direct comparison of the $CD25^{high}$/$CD25^{low}$ T_{reg} cell subsets revealed that the $CD25^{low}$ subset is enriched for cells expressing effector/tissue-homing markers (Fontenot et al., 2005b). Therefore, as the TCR-deficient T_{reg} cells were exclusively $CD25^{high}$ (Fig. 1D), we compared the gene expression of these cells to TCR-expressing $CD25^{high}$ T_{reg} cells unless noted otherwise.

T_{reg} cells leaving the thymus express high levels of the chemokine receptor CCR7 as well as of CD62L, similar to conventional naïve T cells, which allow them to recirculate between secondary lymphoid organs (Campbell and Koch, 2011). TCR ablation did not did not reduce the proportions of T_{reg} cells expressing CCR7 and CD62L, suggesting that TCR-deficient Treg cells can recirculate efficiently (Fig. 2A). In contrast, we observed that activation/effector markers such as 4-1BB, CD49b, CD69, CD103 and KLRG-1 were almost not expressed on TCR-deficient T_{reg} cells (Fig. 2B). In addition, we could not detect PD-1 expression on TCR- T_{reg} cells, a marker for the recently discovered follicular T_{reg} cell subset that is important for the

control of follicular helper T cells and germinal center B cells (Linterman et al., 2011; Sage et al., 2012).

To further elucidate the impact of TCR ablation on Treg cell identity, we monitored the expression of several well-described T_{reg} cell markers on TCR-deficient T_{reg} cells in comparison to naïve conventional CD4+ T cells, $CD25^{high}$ or $CD25^{low}$ TCR+ T_{reg} cells. Interestingly, our analysis revealed that CD44, highly expressed on effector T_{reg} cells and intermediately expressed on naïve T_{reg} cells (Campbell and Koch, 2011), was further downregulated on TCR-deficient T_{reg} cells to the level observed on naïve conventional T cells (Fig. 2C). Furthermore, surface expression of the costimulatory molecules CD28, ICOS and Ox40, as well as of CD5, CD38, and ICAM-1, was significantly decreased (Fig. 2C). Additional analysis of intracellular transcription factor expression showed that c-Rel and Egr2, both of which have been linked to TCR activation, were downregulated (Fig. 2D). Furthermore, T_{reg} cells expressing increased levels of T-bet were not found among the TCR-deficient cells (Supplementary Fig. 2). A comprehensive overview on the marker proteins analyzed by flow cytometry is shown in Supplementary Fig. 2. Together, these findings demonstrate that T_{reg} cells revert to a naïve phenotype in absence of TCR-derived signals.

Dramatic changes in gene expression upon TCR ablation

To analyze the consequences of loss of TCR signals for T_{reg} cell phenotype and homeostasis in an unbiased and global fashion, we analyzed gene expression changes caused by the absence of TCR signals through Affymetrix microarrays. We FACS-purified TCR+/TCR- FoxP3-eGFP+ $CD25^{high}$ T_{reg} cells to exclude effector/tissue-homing $CD25^{low}$ T_{reg} cells that were not present among the TCR-deficient T_{reg} cells as mentioned above. In total, we found 915 genes to be at least 3-fold differentially expressed between TCR+ and TCR- T_{reg} cells. The vast majority of these genes (802 = 88%) were significantly downregulated and included as expected the TCRα-chain and molecules induced by TCR-signaling such as Egr2 and Egr3. We confirmed the downregulation of surface molecules such as 4-1BB (encoded by *Tnfrsf9*), CD38, ICOS and PD-1 (encoded by *Pdc1*) that we already observed by flow cytometry.

Next, we analyzed the expression of a set of T_{reg} cell signature genes, as described by Hill and colleagues (Hill et al., 2007), and could detect 559 of 603 of these genes in our microarrays. Interestingly, 76 (14 %) of the T_{reg} cell signature genes were at least 3-fold differently expressed when compared to control T_{reg} cells (Fig. 3B), and 325 (58 %) T_{reg} cell signature genes were at least 2-fold differentially expressed (data not shown), indicating that a substantial proportion of the characteristic T_{reg} cell gene expression pattern relies on TCR-derived signals.

The transcription factor FoxP3, central in T_{reg} cell biology, has been shown to regulate T_{reg} cell gene expression through forming complexes and interacting with various other transcription factors, including Aiolos, Eos, Foxo1, IRF4, NFAT, Ror-γt, Runx1, T-bet and various others (Fu et al., 2012; Rudra et al., 2012). Recently, a genome-wide list of FoxP3 target genes has been established (Zheng et al., 2007). Although FoxP3 expression itself was unaltered (Fig. 1A, B), the expression of several genes specifically repressed or upregulated by FoxP3 (33 of 99 genes = 30 %) was significantly changed, with all of them being downregulated (Fig. 3C). Among these significantly downregulated genes were the four transcription factor-encoding genes *Crem*, *Ikzf2*, *Irf6* and *Prdm1* (data not shown), whose expression is directly initiated by FoxP3 in wild-type T_{reg} cells and which were suggested to play an important role in the FoxP3-induced developmental and functional reprogramming of T_{reg} cells (Zheng et al., 2007). In addition, we discovered downregulation of further important transcription factors including Aiolos, Eomes, Eos, IRF4 and T-bet (Fig. 3A, B and data not shown).

Together, the results from the gene expression analysis confirm and extend our findings from the flow cytometric analysis, showing that TCR ablation causes dramatic changes for T_{reg} cells. Importantly, the overwhelming majority of differentially expressed mRNAs were downregulated in TCR-deficient T_{reg} cells, indicating that a large part of the Treg cell specific gene expression pattern is induced through their autoreactivity TCR. Furthermore, although FoxP3 is still present in TCR-deficient T_{reg} cells, its functionality is probably impaired due to the decreased expression or even absence of several of its important co-factors.

The lineage-specific epigenetic pattern is not affected by TCR ablation

Recently, it was proposed that besides FoxP3 expression, the establishment of a specific hypomethylation pattern (nTreg-Me) is of critical importance during thymic T_{reg} cell development (Ohkura et al., 2012). These hypomethylated regions were consistently found in the gene loci of FoxP3, GITR, CTLA4 and Eos, and partially in Helios (Ohkura et al., 2012). Long-lasting TCR stimulation of developing thymocytes was shown to induce nTreg-Me, whereas FoxP3 expression was a consequence of strong TCR activation (Ohkura et al., 2012). This demethylation is performed independently of cell-division through members of the family of Tet dioxygenases (Toker et al., 2013). Interestingly, we observed that the expression of two of these Tet family members, Tet1 and Tet2, was significantly reduced upon TCR deletion in T_{reg} cells (Fig. 3B and data not shown). This suggested that continuous TCR activation might play a role in maintaining the lineage-specific hypomethylation pattern of peripheral T_{reg} cells. To test this possibility, we FACS-purified TCR-deficient and proficient T_{reg} cells from multiple animals, similar as for the Affymetrix gene array, 6 and 15 weeks after TCR ablation by poly(I:C) injection, and performed bisulfite sequencing. Against our expectations, we found no changes in the nTreg-Me 6 weeks and also 15 weeks after induced TCR deletion (Fig. 4A). These results indicate that while establishment of the T_{reg} cell-specific methylation pattern is induced through TCR signals, its maintenance is independent of continuous TCR signals. In line with these results, the expression levels of the proteins that contain hypomethylated regulatory regions were, albeit reduced, still significantly higher in TCR-deficient T_{reg} cells than in naïve conventional T cells (Fig. 1A & 4B). These results suggest that in absence of TCR signals, some genes in T_{reg} cells remain highly expressed due to the stable nTreg-Me.

TCR-deficient T_{regs} lose at least half of their suppressive protein arsenal

Various mechanisms are implicated in the suppressive ability of T_{reg} cells (Fontenot et al., 2005a; Josefowicz et al., 2012; Sakaguchi et al., 2008; Shevach, 2009). First, it was suggested that T_{reg} cells are able to consume large amounts of the cytokine IL-2, which is important for the survival and proliferation of activated T cells. Furthermore, T_{reg} cells directly act on activated T cells through release of suppressive cytokines

(IL-10 and IL-35), granzymes, perforin and Galectin-1. Moreover, T_{reg} cell-expression of molecules including CTLA-4, CD39, CD73, LAG-3, LFA-1 and Neuropilin-1 (Nrp1) was shown to be important in the modulation of the costimulatory abilities of antigen-presenting cells.

Interestingly, we found that for 8 of 18 (44 %) tested putative suppressor genes, TCR-deficient T_{reg} cells expressed significantly reduced transcript levels. This was the case for CD73, CTLA-4, IL-10, Ebi3, Fgl-2, LFA-1, Nrp1 and PD-1L2 (Fig. 3B and data not shown). Perforin was the only significantly upregulated suppressor gene (Fig. 3A). To test whether this could be confirmed on the protein level, we analyzed the expression of putative suppressor molecules by flow cytometry. Our results confirmed the downregulation of CTLA-4 (Fig. 4B), CD73, LFA-1 and Nrp1 that was already seen on the mRNA level (Fig. 5A). Furthermore, we found significant reduction of surface expression of GITR (Fig. 4B), but not of CD39 (Fig. 5A). LAG-3 was significantly reduced in comparison to TCR+ $CD25^{high}$ T_{reg} cells from the same animals, but not in comparison to control animals.

To study the ability of T_{reg} cells to release IL-10 upon activation, we stimulated them *in vitro* with PMA/ionomycin and assessed IL-10 production by flow cytometry. A significantly smaller percentage of TCR-deficient T_{reg} cells produced IL-10 in comparison to their TCR-expressing counterparts (Fig. 5B). In total, we demonstrated that half of the proteins implicated in T_{reg} cell-mediated suppression (9 of 18) were significantly downregulated after TCR ablation. We therefore conclude that the suppressive function of T_{reg} cells depends on constant TCR generated signals to a large extent.

DISCUSSION

T_{reg} cells are mostly generated in the thymus and are crucial to control autoimmune responses in the periphery. Upon egress from the thymus, control of peripheral T_{reg} cell homeostasis has been mostly attributed to cytokine signaling (Burchill et al., 2007; Setoguchi et al., 2005). Conversely, we found that despite the fact that TCR-deficient T_{reg} cells expressed high levels of cytokine receptors for IL-2 and IL-7 and should be able to properly compete for these cytokines with conventional T cells, their half-life was strongly reduced. The expression of the IL-15 receptor was slightly

reduced, but this is unlikely to account for the reduced half-life, as peripheral T_{reg} cell homeostasis was not affected in IL-15-deficient animals (Burchill et al., 2007). Furthermore, we showed that the impaired homeostasis of these cells is a due to a proliferative block and potentially also to decreased survival. Therefore, our study demonstrates that the inherent T_{reg} cell autoreactivity is of crucial importance for T_{reg} cell homeostasis. Interestingly, the size of the peripheral T_{reg} cell pool was not affected when the thymic T cell production was blocked, in line with the previously reported finding that T_{reg} cells are under homeostatic control and quickly fill empty niches (Benoist and Mathis, 2012).

Regulatory T cells can be broadly separated into two different subsets *in vivo* (Campbell and Koch, 2011; Fisson et al., 2003; Huehn et al., 2004). The majority of T_{reg} cell displays a naïve phenotype, is slowly cycling and held in a resting state. In contrast, the smaller subset is composed of highly proliferative cells with a effector phenotype that express homing receptors allowing them to migrate to non-lymphoid sites in the body (Campbell and Koch, 2011). It was speculated that the effector subsets consists of cells that were recently activated upon auto-antigen recognition (Campbell and Koch, 2011; Fisson et al., 2003). Further strengthening this hypothesis, we failed to detect TCR-deficient T_{reg} cells expressing the characteristic activated/effector T cell markers 4-1BB, CD49b, CD69, CD103 and KLRG1, as well as the newly described PD-1-expressing follicular T_{reg} cell subset, 6 weeks after TCR deletion. Moreover, we did not detect actively cycling cells among the TCR-deficient T_{reg} cells. Interestingly, we also found significant changes in the gene expression of the naïve T_{reg} cell subset, including downregulation of CTLA-4, CD38, CD44, ICAM, ICOS and Ox40, and upregulation of CD45RB. This indicates that also the naïve T_{reg} cell subset is composed of autoreactive cells that are consistently activated, and this activation is fundamental for their gene expression.

Various molecules are implicated in the T_{reg} cell suppressor function (Josefowicz et al., 2012; Shevach, 2009). However, there is probably no single mechanism that is active in each scenario. This is notion is supported by the fact that no knockout has been described to date that causes a similar dramatic phenotype as FoxP3-deficiency. Thus, probably depending on the type of immune response regulated and the location in the body, one or several different suppression mechanisms are important. In this regard, subsets of T_{reg} cells expressing transcription factors typical for helper T cells,

such as Bcl-6 (Linterman et al., 2011) IRF4 (Zheng et al., 2009), STAT-3 (Chaudhry et al., 2009) and T-bet (Koch et al., 2009), are each important in different disease settings. Still, it is not well understood how T_{reg} cell TCR engagement is involved in suppression of their target cells. It was recently shown that at least *in vitro*, directly *ex vivo* isolated T_{reg} cells are able to suppress without previous activation (Szymczak-Workman et al., 2009). It has been speculated that auto-antigen recognition is key to maintain polyclonal T_{reg} cells in an activated state allowing them to control various different immune responses independently of TCR specificity (Shevach, 2009). We did not only find that T_{reg} cells expressing helper T cell transcription factors such as IRF4 and T-bet were absent from the TCR-deficient population, but also that the TCR-deficient T_{reg} cell subset lost expression of many proteins implicated in their suppressive function, including CTLA-4, GITR, LFA-1 and IL-10. These results strongly suggest that constant TCR-generated signals are crucial to maintain the suppressive abilities of these cells. The loss of suppressive function and shortened half-live of TCR-deficient Treg cells did not lead to manifestation of an autoimmune phenotype. However, our system just allowed partial TCR deletion in T_{reg} cells, and the size of the TCR-expressing T_{reg} cell pool was kept stable despite the block of thymic T_{reg} cell development and the decay of TCR-deficient T_{reg} cells. For that reason, it is likely that the TCR-expressing T_{reg} cell subset is able protect these mice from autoimmunity in most of the cases.

TCR signaling is essential for T_{reg} cell development through induction of FoxP3 expression and the establishment of hypomethylated regions. Recently, it was shown that upon TCR stimulation, c-Rel directly binds the *FoxP3* promoter and also a highly conserved noncoding sequence, CNS3, in the *Foxp3* locus (Long et al., 2009). This regulatory CNS3 element was shown to play a role in the maintenance of FoxP3 expression after its induction. Surprisingly, we found that in the absence of TCR expression, causing a significant downregulation of c-Rel, FoxP3 expression of T_{reg} cells was remarkably stable. Therefore, continuous TCR signals are clearly dispensable for the maintenance of FoxP3 expression in mature T_{reg} cells, which instead is probably stabilized by the T_{reg} cell-specific demethylation of regulatory regions of the *Foxp3* locus. However, despite the presence of FoxP3, the expression of a large proportion of its target genes was significantly downregulated in response to TCR ablation. These findings indicate that a crucial role of FoxP3 is to repress

TCR activation-induced genes and thereby to desensitize T_{reg} cells from their autoreactive TCR.

In summary, our study demonstrates that T_{reg} cells continuously receive signals through their autoreactive TCR, and that these signals are essential for T_{reg} cell survival, activation status and suppressive function. Despite this ongoing activation, only few T_{reg} cells acquire an effector phenotype, whereas the majority of T_{reg} cells are still "naïve". Most likely, this is due to differential activation strength, depending on receptor affinity, costimulation and also the cytokine environment. Only upon proper activation, naïve T_{reg} cells acquire an effector phenotype, migrate to the specific location of an immune response, and quickly decay after its end.

MATERIALS AND METHODS

Genetically modified mice

Mx-Cre (Kuhn et al., 1995), $C\alpha^F$ (Polic et al., 2001), and *FoxP3-eGFP* (Bettelli et al., 2006) mice were kept on a C57BL/6 genetic background. At the age of 6-8 wk, the animals were given a single dose (400 μg) of poly(I:C) (Amersham). All mice were analyzed 6 wk after injection, unless otherwise indicated. Mice were housed in the specific pathogen–free animal facility of the MPIB. All animal procedures were approved by the Regierung of Oberbayern.

Flow Cytometry & Heat Map Generation

Single-cell suspensions were prepared and stained with monoclonal antibodies: 4-1BB (17B5), Aiolos (8B2), CCR7 (4B12), CD103 (2E7), CD122 (TM-b1), CD126 (D7715A7), CD127 (A7R34), CD25 (PC61.5), CD28 (37.51), CD200 (OX90), CD38 (90), CD39 (24DMS1), CD4 (RM4-5), CD44 (IM7), CD45RB (C363.16A), CD5 (53-7.3), CD62L (MEL-14), CD69 (H1.2-F3), CD71 (R17217), CD73 (eBioTY/11.8), CD8α (53-6.7), CD83 (Michel-17), c-Rel (1RELAH5), CTLA-4 (UC10-4B9), Egr2 (erongr2), Eomes (Dan11mag), Eos (ESB7C2), Fas (15A7), FasL (MFL3), FolR4 (eBio12A5), FoxP3 (FJK-16s), GARP (YGIC86), GATA-3 (TWAJ), GITR (DTA-1), Helios (22F6), ICAM-1 (YN1/1.7.4), IL-10 (JES3-16E3), IL-15Rα (DNT15Ra), IRF4 (3E4), ITGAL (M17/4), ICOS (7E.17G9), Ki-67 (SolA15), KLRG-1 (2F1), LAG-3 (eBioC9B7W), Ly6C (HK1.4), Nur77 (12.14), Ox40 (Ox86), PD-1 (J43), Runx1 (RXDMC), T-bet (eBio4B10) and TCRβ (H57-597) (all from eBioscience). CD49b

(HMa2) and Nrp1 (AF566) were purchased from BioLegend or R&D Systems, respectively. For intracellular transcription factor stainings, cells were fixed and permeabilized with the FoxP3 staining kit (eBioscience). For intracellular cytokine stainings, cells were activated for 5 h with phorbol-12-myristat-13-acetat (PMA) and ionomycin (both from Sigma), and monensin (eBioscience) was added for the last 3 h of culture. Afterwards, cells were fixed and permeabilized with the Cytofix/Cytoperm kit (BD). To detect active caspases, cells were stained for 1 h with the CaspGLOW Red Active Caspase Kit (BioVision) as recommended by the manufacturer. Samples were acquired on a FACSCanto2 (BD) machine, and analyzed with FlowJo software (Treestar). To evaluate the relative expression of regulatory T cell marker genes, the median fluorescence intensities (MFI) of at least five mice per genotypes were calculated with FlowJo, and the MFI for the CD4+ naïve conventional ($CD44^{low}$ FoxP3- TCRβ+) T cells of $C\alpha^{F/F}$ control mice was set to 1 for each set.

BrdU incorporation

Mice were fed with 0.5 mg/ml BrdU (Sigma) in the drinking water for 4 consecutive weeks. Directly afterwards, BrdU incorporation was measured with the BrdU Flow Kit (BD).

Cell sorting & gene expression analysis

TCR+ (FoxP3+ CD4+ $CD25^{high}$ cells from $C\alpha^{F/F}$ *FoxP3-eGFP* control animals) and TCR- (FoxP3+ TCR- CD4+ $CD25^{high}$ cells from *Mx-Cre* $C\alpha^{F/F}$ *FoxP3-eGFP* animals) T_{reg} cells were sorted 6 weeks after poly(I:C) injection with a FACSAria (BD). To reduce variability, cells from several mice were pooled for sorting, and 4 replicates for the control animals as well as 5 replicates for the *Mx-Cre* animals were generated. mRNA from 3-5 x 10^5 cells was purified with a RNeasy Micro kit (Qiagen), amplified, labeled and hybridized to Affymetrix M430 V2 microarrays.

CpG methylation analysis by bisulfite sequencing

TCR+ and TCR- T_{reg} cells cells were sorted 6 wk and 15 wk after poly(I:C) injection similar as for the gene expression analysis. The CpG methylation status was analyzed as previously described (Ohkura et al., 2012).

Statistics

Statistical analysis of the results was performed by one-way ANOVA followed by Tukey's test or by student t test. *P* values are presented in figure legends where a statistically significant difference was found.

ACKNOWLEDGEMENTS

This study was supported by Emmy Noether grant SCHM2440 from the Deutsche Forschungsgemeinschaft (DFG). J.C.V. and K.H. received PhD stipends from the Ernst Schering Foundation and the Boehringer Ingelheim foundation, respectively. We are grateful to Reinhard Fässler for support. We wish to thank Julia Knogler and Barbara Habermehl for technical assistance.

FIGURE LEGENDS

Figure 1. Regulatory T cells homeostasis is impaired upon TCR deletion

(A) Surface TCRβ and intracellular FoxP3 expression of splenic CD4+ $CD25^{high}$ T_{reg} cells from the indicated animals 2 wk after poly(I:C) injection. Plots are representative for 5 independent experiments.

(B) Expression of CD69 and FoxP3 in comparison to TCRβ of total thymocytes, 6 wk after poly(I:C) injection. Plots are representative for 5 independent experiments.

(C) Splenic regulatory T cell numbers from in total 24 control (CTR) $C\alpha^{F/F}$ animals as well as TCRβ+ and TCRβ- T_{reg} cell numbers from in total 23 *Mx-Cre* $C\alpha^{F/F}$ animals, at the indicated time after poly(I:C) injection. Half-lifes were calculated with GraphPad Prism software using non-linear regression, one-phase decay analysis. The lines for the TCR+ T_{reg} cell subsets lie directly on top of each other.

(D) Extracellular expression of the respective cytokine receptor subunits on splenic FoxP3-eGFP+ T_{reg} cells of the depicted animals, 6 wk after poly(I:C) injection. Numbers indicate mean percentage ± SD of at least 6 mice per genotype.

(E) Extracellular expression of CD71, and intracellular expression of Ki-67, on/in splenic FoxP3-eGFP+ T_{reg} cells of the depicted animals, 6 wk after poly(I:C) injection. Plots are representative for at least 3 independent experiments.

(F) BrdU was administered for 4 wk via the drinking water, starting 2 wk after poly(I:C) injection. Directly afterwards, mice were sacrificed, and BrdU incorporation in $CD25^{low}$/$CD25^{high}$ FoxP3-eGFP+ T_{reg} cells of the depicted animals was measured

by flow cytometry. Bar chart depicts means and SD (error bars) of one experiment with 2 $C\alpha^{F/F}$ as well as 4 *Mx-Cre* $C\alpha^{F/F}$ animals.

(G) Splenic FoxP3-eGFP+ T_{reg} cells of the depicted animals were stained in vitro for 1 h for the presence of active caspases. Numbers indicate mean percentage ± SD of 2 $C\alpha^{F/F}$ animals or 4 *Mx-Cre* $C\alpha^{F/F}$ animals. Scatter plot shows the percentage of active caspase-stained FoxP3-eGFP+ T_{reg} cells from control 2 $C\alpha^{F/F}$ or from 4 *Mx-Cre* $C\alpha^{F/F}$ animals. Bars indicate means.

Figure 2. Regulatory T cells lose their activated phenotype upon TCR deletion

(A) Extracellular expression of CCR7 or CD62L on splenic FoxP3-eGFP+ $CD25^{high}$ T_{reg} cells from the depicted animals, 6 wk after poly(I:C) injection. Black numbers in representative plots indicate mean percentage ± SD of at least 6 mice per genotype. Red numbers indicate percentage among TCR+ or TCR- T_{reg} cells, respectively.

(B) Extracellular expression of the depicted markers on splenic FoxP3-eGFP+ $CD25^{high}$ T_{reg} cells from the depicted animals, 6 wk after poly(I:C) injection. Black numbers in representative plots indicate mean percentage ± SD of at least 6 mice per marker per genotype.

(C, D) Extracellular (C) or intracellular (D) expression of the depicted markers of the indicated splenic T cell subsets, all from *Mx-Cre* $C\alpha^{F/F}$ animals 6 wk after poly(I:C) injection. Numbers in representative histograms indicate means of the median fluorescence intensities (MFIs), normalized to CD4+ $CD44^{low}$ naïve conventional T cells of $C\alpha^{F/F}$ animals. Means were calculated from at least 5 mice per genotype.

Figure 3. Regulatory T cell mRNA expression is severely changed upon TCR deletion

The mRNA expression of splenic TCR+ $CD25^{high}$ T_{reg} cells from 4 $C\alpha^{F/F}$ control animals and TCR- $CD25^{high}$ T_{reg} cells from 5 *Mx-Cre* $C\alpha^{F/F}$ animals, 6 wk after poly(I:C) injection, was compared by Affymetrix microarray.

(A) Volcano plot representation (fold change vs. t test *p* value) of all analyzed genes. For better visibility, significantly changed genes discussed in the text are marked in red.

(B) Heatmap showing the expression of 76 at least 3-fold differentially expressed genes of the T_{reg} cell signature. The values of the 4 control animals were averaged, and are displayed together with the values of the 5 individual *Mx-Cre* $C\alpha^{F/F}$ animals.

(C) FoxP3 specifically up- or downregulates the expression of a set of target genes in the periphery only or in the thymus and the periphery. Bar chart shows the expression of these FoxP3 target genes after TCR deletion.

Figure 4. T_{reg} cell-specific methylation pattern is unaltered upon TCR deletion
(A) CpG methylation status of splenic $CD25^{high}$ TCR+/TCR- T_{reg} cells of the depicted animals, 6 wk or 15 wk after poly(I:C) injection.
(B) Extracellular (GITR) or intracellular (CTLA-4; Eos; Helios) expression of the depicted markers of the indicated splenic T cell subsets, all from *Mx-Cre* $C\alpha^{F/F}$ animals 6 wk after poly(I:C) injection. Numbers in representative histograms indicate means of the median fluorescence intensities (MFIs), normalized to CD4+ $CD44^{low}$ naïve conventional T cells of $C\alpha^{F/F}$ animals. Means were calculated from at least 5 mice per genotype.

Figure 5. Regulatory T cells show reduced expression of several suppressor markers and reduced IL-10 production upon TCR deletion
(A) Extracellular expression of the depicted markers of the indicated splenic T cell subsets, all from *Mx-Cre* $C\alpha^{F/F}$ animals 6 wk after poly(I:C) injection. Numbers in representative histograms indicate means of the median fluorescence intensities (MFIs), normalized to CD4+ $CD44^{low}$ naïve conventional T cells of $C\alpha^{F/F}$ animals. Means were calculated from at least 5 mice per genotype.
(B) Intracellular IL-2 and IL-10 expression of splenic FoxP3-eGFP+ T_{reg} cells, activated in vitro with PMA/Ionomycin for 5 h. Cells were extracted from mice and activated 6 wk after poly(I:C) injection. Numbers indicate mean percentages of TCR+ or TCR- T_{reg} cells expressing the respective cytokine. Data are representative for 4 animals per genotype.

Supplementary Figure 1. Total splenic cell counts of CD4+ and CD8+, naïve ($CD44^{low}$) and memory/effector ($CD44^{high}$), as well as T_{reg} cells, of the depicted animals, 6 wk or 15 wk after poly(I:C) injection. Data represents means and SD (error bars) of three independent experiments with at least 6 mice per genotype and time point.

Supplementary Figure 2. Flow cytometric expression analysis of extra- and intracellular markers of splenic T cells, 6 wk after poly(I:C) injection. Median fluorescence intensities of at least 5 mice per analyzed protein were normalized to the expression on/in conventional CD4+ T cells to account for interexperimental variations. Data are shown as heatmap, calculated by Perseus software. Blue letters, significantly reduced on/in TCR- T_{reg} cells in comparison to TCR+ $CD25^{high}$ T_{reg} cells from both $C\alpha^{F/F}$ control as well as *Mx-Cre* $C\alpha^{F/F}$ animals. Red letter, significantly increased; analyzed by one-way ANOVA.

REFERENCES

Bayer, A.L., Baliga, P., and Woodward, J.E. (1998). Transferrin receptor in T cell activation and transplantation. J Leukoc Biol *64*, 19–24.

Benoist, C., and Mathis, D. (2012). Treg cells, life history, and diversity. Cold Spring Harb Perspect Biol *4*, a007021.

Bensinger, S.J., Bandeira, A., Jordan, M.S., Caton, A.J., and Laufer, T.M. (2001). Major histocompatibility complex class II-positive cortical epithelium mediates the selection of CD4(+)25(+) immunoregulatory T cells. J Exp Med *194*, 427–438.

Bettelli, E., Carrier, Y., Gao, W., Korn, T., Strom, T.B., Oukka, M., Weiner, H.L., and Kuchroo, V.K. (2006). Reciprocal developmental pathways for the generation of pathogenic effector TH17 and regulatory T cells. Nature *441*, 235–238.

Burchill, M.A., Yang, J., Vogtenhuber, C., Blazar, B.R., and Farrar, M.A. (2007). IL-2 receptor beta-dependent STAT5 activation is required for the development of Foxp3+ regulatory T cells. J Immunol *178*, 280–290.

Campbell, D.J., and Koch, M.A. (2011). Phenotypical and functional specialization of FOXP3+ regulatory T cells. Nat Rev Immunol *11*, 119–130.

Chang, J.-H., Xiao, Y., Hu, H., Jin, J., Yu, J., Zhou, X., Wu, X., Johnson, H.M., Akira, S., Pasparakis, M., et al. (2012). Ubc13 maintains the suppressive function of regulatory T cells and prevents their conversion into effector-like T cells. Nat Immunol *13*, 481–490.

Chaudhry, A., Rudra, D., Treuting, P., Samstein, R.M., Liang, Y., Kas, A., and Rudensky, A.Y. (2009). CD4+ regulatory T cells control TH17 responses in a Stat3-dependent manner. Science *326*, 986–991.

Darrasse-Jèze, G., Deroubaix, S., Mouquet, H., Victora, G.D., Eisenreich, T., Yao, K.-H., Masilamani, R.F., Dustin, M.L., Rudensky, A., Liu, K., et al. (2009). Feedback control of regulatory T cell homeostasis by dendritic cells in vivo. J Exp Med *206*, 1853–1862.

Feuerer, M., Hill, J.A., Mathis, D., and Benoist, C. (2009). Foxp3+ regulatory T cells: differentiation, specification, subphenotypes. Nat Immunol *10*, 689–695.

Fisson, S., Darrasse-Jèze, G., Litvinova, E., Septier, F., Klatzmann, D., Liblau, R., and Salomon, B.L. (2003). Continuous activation of autoreactive CD4+ CD25+ regulatory T cells in the steady state. J Exp Med *198*, 737–746.

Fontenot, J.D., Rasmussen, J.P., Gavin, M.A., and Rudensky, A.Y. (2005a). A function for interleukin 2 in Foxp3-expressing regulatory T cells. Nat Immunol *6*, 1142–1151.

Fontenot, J.D., Rasmussen, J.P., Williams, L.M., Dooley, J.L., Farr, A.G., and Rudensky, A.Y. (2005b). Regulatory T cell lineage specification by the forkhead

transcription factor foxp3. Immunity *22*, 329–341.

Fu, W., Ergun, A., Lu, T., Hill, J.A., Haxhinasto, S., Fassett, M.S., Gazit, R., Adoro, S., Glimcher, L., Chan, S., et al. (2012). A multiply redundant genetic switch "locks in" the transcriptional signature of regulatory T cells. Nat Immunol.

Gavin, M.A., Clarke, S.R., Negrou, E., Gallegos, A., and Rudensky, A. (2002). Homeostasis and anergy of CD4(+)CD25(+) suppressor T cells in vivo. Nat Immunol *3*, 33–41.

Hill, J.A., Feuerer, M., Tash, K., Haxhinasto, S., Perez, J., Melamed, R., Mathis, D., and Benoist, C. (2007). Foxp3 Transcription-Factor-Dependent and -Independent Regulation of the Regulatory T Cell Transcriptional Signature. Immunity *27*, 786–800.

Huehn, J., Siegmund, K., Lehmann, J.C.U., Siewert, C., Haubold, U., Feuerer, M., Debes, G.F., Lauber, J., Frey, O., Przybylski, G.K., et al. (2004). Developmental stage, phenotype, and migration distinguish naive- and effector/memory-like CD4+ regulatory T cells. J Exp Med *199*, 303–313.

Isomura, I., Palmer, S., Grumont, R., Bunting, K., Hoyne, G., Wilkinson, N., Banerjee, A., Proietto, A., Gugasyan, R., Li, W., et al. (2009). c-Rel is required for the development of thymic Foxp3+ CD4 regulatory T cells. J Exp Med.

Josefowicz, S.Z., Lu, L.-F., and Rudensky, A.Y. (2012). Regulatory T cells: mechanisms of differentiation and function. Annu Rev Immunol *30*, 531–564.

Kim, J.K., Klinger, M., Benjamin, J., Xiao, Y., Erle, D.J., Littman, D.R., and Killeen, N. (2009). Impact of the TCR signal on regulatory T cell homeostasis, function, and trafficking. PLoS ONE *4*, e6580.

Koch, M.A., Tucker-Heard, G., Perdue, N.R., Killebrew, J.R., Urdahl, K.B., and Campbell, D.J. (2009). The transcription factor T-bet controls regulatory T cell homeostasis and function during type 1 inflammation. Nat Immunol *10*, 595–602.

Koonpaew, S., Shen, S., Flowers, L., and Zhang, W. (2006). LAT-mediated signaling in CD4+CD25+ regulatory T cell development. J Exp Med *203*, 119–129.

Kuhn, R., Schwenk, F., Aguet, M., and Rajewsky, K. (1995). Inducible gene targeting in mice. Science *269*, 1427–1429.

Linterman, M.A., Pierson, W., Lee, S.K., Kallies, A., Kawamoto, S., Rayner, T.F., Srivastava, M., Divekar, D.P., Beaton, L., Hogan, J.J., et al. (2011). Foxp3+ follicular regulatory T cells control the germinal center response. Nat Med *17*, 975–982.

Long, M., Park, S.-G., Strickland, I., Hayden, M.S., and Ghosh, S. (2009). Nuclear factor-kappaB modulates regulatory T cell development by directly regulating expression of Foxp3 transcription factor. Immunity *31*, 921–931.

Medoff, B.D., Sandall, B.P., Landry, A., Nagahama, K., Mizoguchi, A., Luster, A.D.,

and Xavier, R.J. (2009). Differential requirement for CARMA1 in agonist-selected T-cell development. Eur J Immunol *39*, 78–84.

Moran, A.E., Holzapfel, K.L., Xing, Y., Cunningham, N.R., Maltzman, J.S., Punt, J., and Hogquist, K.A. (2011). T cell receptor signal strength in Treg and iNKT cell development demonstrated by a novel fluorescent reporter mouse. J Exp Med *208*, 1279–1289.

Ohkura, N., Hamaguchi, M., Morikawa, H., Sugimura, K., Tanaka, A., Ito, Y., Osaki, M., Tanaka, Y., Yamashita, R., Nakano, N., et al. (2012). T Cell Receptor Stimulation-Induced Epigenetic Changes and Foxp3 Expression Are Independent and Complementary Events Required for Treg Cell Development. Immunity.

Polic, B., Kunkel, D., Scheffold, A., and Rajewsky, K. (2001). How alpha beta T cells deal with induced TCR alpha ablation. Proc Natl Acad Sci USA *98*, 8744–8749.

Rudra, D., Deroos, P., Chaudhry, A., Niec, R.E., Arvey, A., Samstein, R.M., Leslie, C., Shaffer, S.A., Goodlett, D.R., and Rudensky, A.Y. (2012). Transcription factor Foxp3 and its protein partners form a complex regulatory network. Nat Immunol.

Sage, P.T., Francisco, L.M., Carman, C.V., and Sharpe, A.H. (2012). The receptor PD-1 controls follicular regulatory T cells in the lymph nodes and blood. Nat Immunol.

Sakaguchi, S., Yamaguchi, T., Nomura, T., and Ono, M. (2008). Regulatory T cells and immune tolerance. Cell *133*, 775–787.

Schmidt-Supprian, M., Courtois, G., Tian, J., Coyle, A., Israel, A., Rajewsky, K., and Pasparakis, M. (2003). Mature T cells depend on signaling through the IKK complex. Immunity *19*, 377–389.

Schmidt-Supprian, M., Tian, J., Grant, E., Pasparakis, M., Maehr, R., Ovaa, H., Ploegh, H.L., Coyle, A., and Rajewsky, K. (2004). Differential dependence of CD4+CD25+ regulatory and natural killer-like T cells on signals leading to NF-kappaB activation. Proc Natl Acad Sci USA *101*, 4566–4571.

Sekiya, T., Kashiwagi, I., Yoshida, R., Fukaya, T., Morita, R., Kimura, A., Ichinose, H., Metzger, D., Chambon, P., and Yoshimura, A. (2013). Nr4a receptors are essential for thymic regulatory T cell development and immune homeostasis. Nat Immunol.

Setoguchi, R., Hori, S., Takahashi, T., and Sakaguchi, S. (2005). Homeostatic maintenance of natural Foxp3(+) CD25(+) CD4(+) regulatory T cells by interleukin (IL)-2 and induction of autoimmune disease by IL-2 neutralization. J Exp Med *201*, 723–735.

Shevach, E.M. (2009). Mechanisms of foxp3+ T regulatory cell-mediated suppression. Immunity *30*, 636–645.

Siggs, O.M., Miosge, L.A., Yates, A.L., Kucharska, E.M., Sheahan, D., Brdicka, T., Weiss, A., Liston, A., and Goodnow, C.C. (2007). Opposing functions of the T cell receptor kinase ZAP-70 in immunity and tolerance differentially titrate in response to nucleotide substitutions. Immunity *27*, 912–926.

Stephens, G.L., Andersson, J., and Shevach, E.M. (2007). Distinct subsets of FoxP3+ regulatory T cells participate in the control of immune responses. J Immunol *178*, 6901–6911.

Stritesky, G.L., Jameson, S.C., and Hogquist, K.A. (2012). Selection of self-reactive T cells in the thymus. Annu Rev Immunol *30*, 95–114.

Szymczak-Workman, A.L., Workman, C.J., and Vignali, D.A.A. (2009). Cutting edge: regulatory T cells do not require stimulation through their TCR to suppress. J Immunol *182*, 5188–5192.

Toker, A., Engelbert, D., Garg, G., Polansky, J.K., Floess, S., Miyao, T., Baron, U., Düber, S., Geffers, R., Giehr, P., et al. (2013). Active Demethylation of the Foxp3 Locus Leads to the Generation of Stable Regulatory T Cells within the Thymus. J Immunol.

Vahl, J.C., Heger, K., Knies, N., Hein, M.Y., Boon, L., Yagita, H., Polic, B., and Schmidt-Supprian, M. (2013). NKT Cell-TCR Expression Activates Conventional T Cells in Vivo, but Is Largely Dispensable for Mature NKT Cell Biology. PLoS Biol *11*, e1001589.

Xing, Y., and Hogquist, K.A. (2012). T-cell tolerance: central and peripheral. Cold Spring Harb Perspect Biol *4*.

Zheng, Y., Chaudhry, A., Kas, A., Deroos, P., Kim, J.M., Chu, T.-T., Corcoran, L., Treuting, P., Klein, U., and Rudensky, A.Y. (2009). Regulatory T-cell suppressor program co-opts transcription factor IRF4 to control T(H)2 responses. Nature *458*, 351–356.

Zheng, Y., Josefowicz, S.Z., Kas, A., Chu, T.-T., Gavin, M.A., and Rudensky, A.Y. (2007). Genome-wide analysis of Foxp3 target genes in developing and mature regulatory T cells. Nature *445*, 936–940.

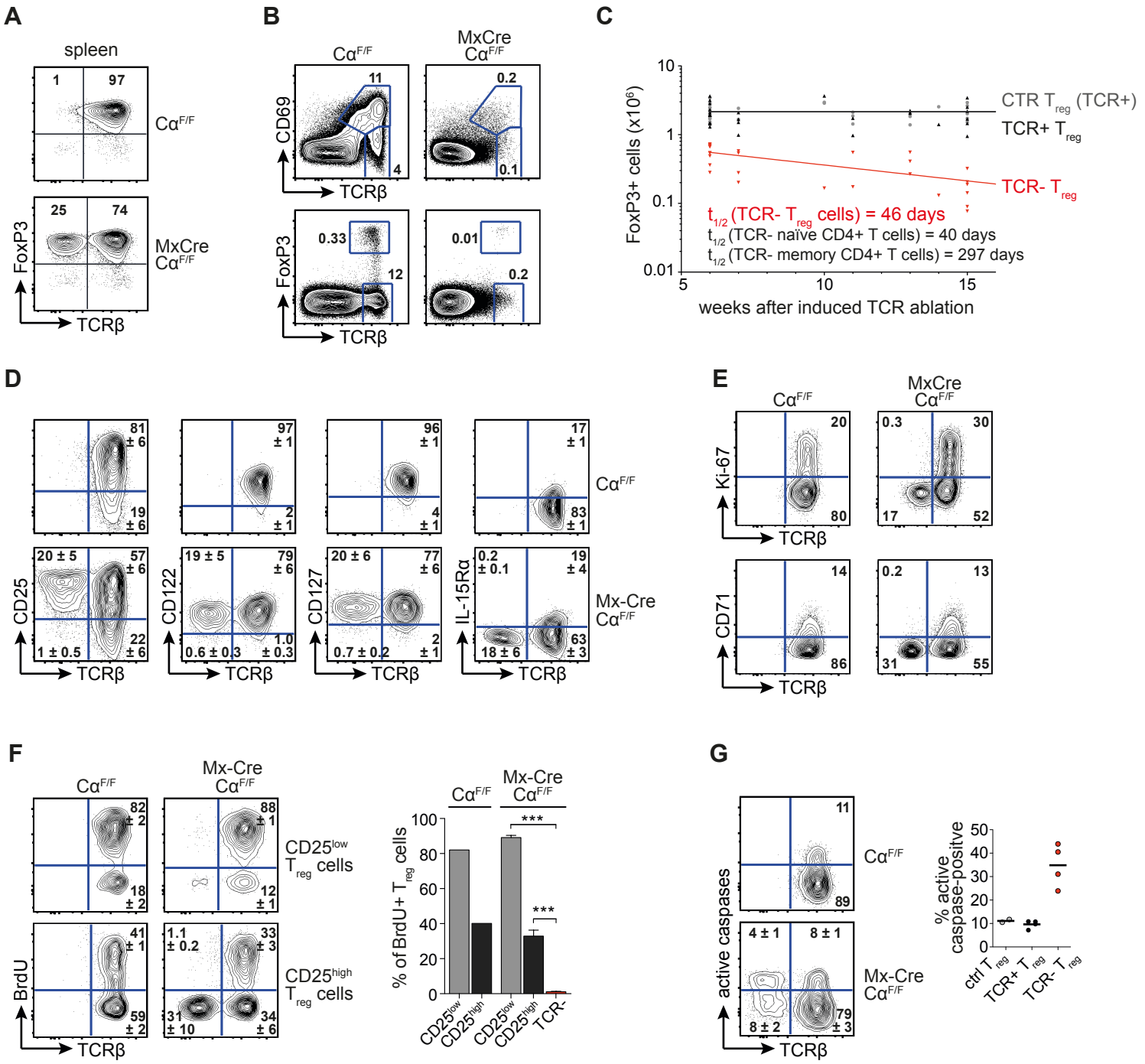

Figure 1. Regulatory T cells homeostasis is impaired upon TCR deletion.

(**A**) Surface TCRβ and intracellular FoxP3 expression of splenic CD4+ CD25^{high} Treg cells from the indicated animals 2 wk after poly(I:C) injection. Plots are representative for 5 independent experiments.

(**B**) Expression of CD69 and FoxP3 in comparison to TCRβ of total thymocytes, 6 wk after poly(I:C) injection. Plots are representative for 5 independent experiments.

(**C**) Splenic regulatory T cell numbers from in total 24 control (CTR) *Cα$^{F/F}$* animals as well as TCRβ+ and TCRβ- Treg cell numbers from in total 23 *Mx-Cre Cα$^{F/F}$* animals, at the indicated time after poly(I:C) injection. Half-lifes were calculated with GraphPad Prism software using non-linear regression, one-phase decay analysis. The lines for the TCR+ Treg cell subsets lie directly on top of each other.

(**D**) Extracellular expression of the respective cytokine receptor subunits on splenic FoxP3-eGFP+ Treg cells of the depicted animals, 6 wk after poly(I:C) injection. Numbers indicate mean percentage ± SD of at least 6 mice per genotype.

(**E**) Extracellular expression of CD71, and intracellular expression of Ki-67, on/in splenic FoxP3 eGFP+ Treg cells of the depicted animals, 6 wk after poly(I:C) injection. Plots are representative for at least 3 independent experiments.

(**F**) BrdU was administered for 4 wk via the drinking water, starting 2 wk after poly(I:C) injection. Directly afterwards, mice were sacrificed, and BrdU incorporation in CD25^{low}/CD25^{high} FoxP3-eGFP+ Treg cells of the depicted animals was measured by flow cytometry. Bar chart depicts means and SD (error bars) of one experiment with 2 *Cα$^{F/F}$* as well as 4 *Mx-Cre Cα$^{F/F}$* animals.

(**G**) Splenic FoxP3-eGFP+ Treg cells of the depicted animals were stained in vitro for 1 h for the presence of active caspases. Numbers indicate mean percentage ± SD of 2 *Cα$^{F/F}$* animals or 4 *Mx-Cre Cα$^{F/F}$* animals. Scatter plot shows the percentage of active caspase-stained FoxP3-eGFP+ Treg cells from control 2 *Cα$^{F/F}$* or from 4 *Mx-Cre Cα$^{F/F}$* animals. Bars indicate means.

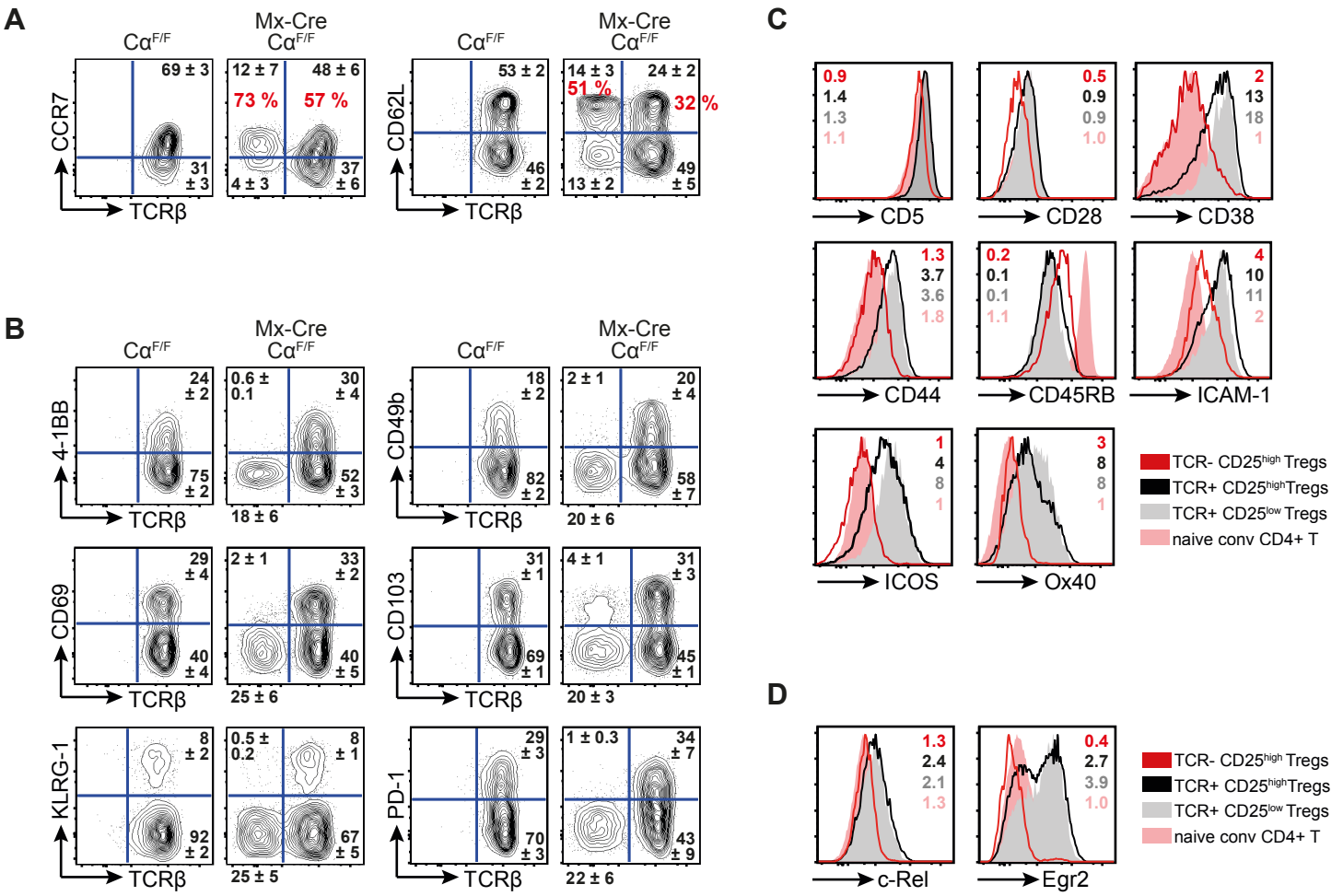

Figure 2. Regulatory T cells lose their activated phenotype upon TCR deletion.
(**A**) Extracellular expression of CCR7 or CD62L on splenic FoxP3-eGFP+ CD25^{high} Treg cells from the depicted animals, 6 wk after poly(I:C) injection. Black numbers in representative plots indicate mean percentage ± SD of at least 6 mice per genotype. Red numbers indicate percentage among TCR+ or TCR- Treg cells, respectively.
(**B**) Extracellular expression of the depicted markers on splenic FoxP3-eGFP+ CD25^{high} Treg cells from the depicted animals, 6 wk after poly(I:C) injection. Black numbers in representative plots indicate mean percentage ± SD of at least 6 mice per marker per genotype.
(**C, D**) Extracellular (C) or intracellular (D) expression of the depicted markers of the indicated splenic T cell subsets, all from *Mx-Cre Cα$^{F/F}$* animals 6 wk after poly(I:C) injection. Numbers in representative histograms indicate means of the median fluorescence intensities (MFIs), normalized to CD4+ CD44^{low} naïve conventional T cells of *Cα$^{F/F}$* animals. Means were calculated from at least 5 mice per genotype.

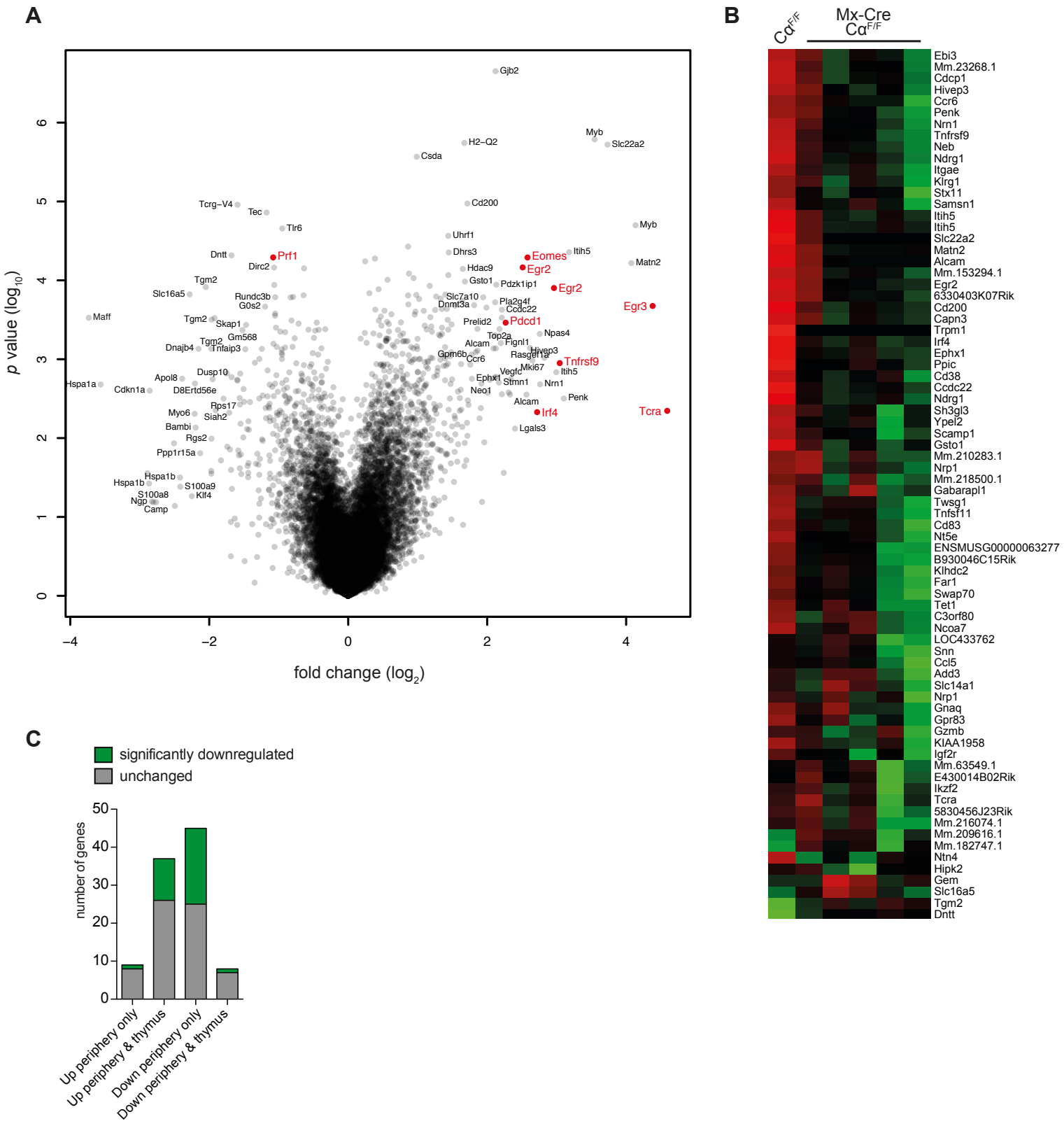

Figure 3. Regulatory T cell mRNA expression is severely changed upon TCR deletion
The mRNA expression of splenic TCR+ CD25^{high} Treg cells from 4 *Cα$^{F/F}$* control animals and TCR- CD25^{high} Treg cells from 5 *Mx-Cre Cα$^{F/F}$* animals, 6 wk after poly(I:C) injection, was compared by Affymetrix microarray.
(**A**) Volcano plot representation (fold change vs. t test p value) of all analyzed genes. For better visibility, significantly changed genes discussed in the text are marked in red.
(**B**) Heatmap showing the expression of 76 at least 3 fold differentially expressed genes of the Treg cell signature. The values of the 4 control animals were averaged, and are displayed together with the values of the 5 individual *Mx-Cre Cα$^{F/F}$* animals.
(**C**) FoxP3 specifically up- or downregulates the expression of a set of target genes in the periphery only or in the thymus and the periphery. Bar chart shows the expression of these FoxP3 target genes after TCR deletion.

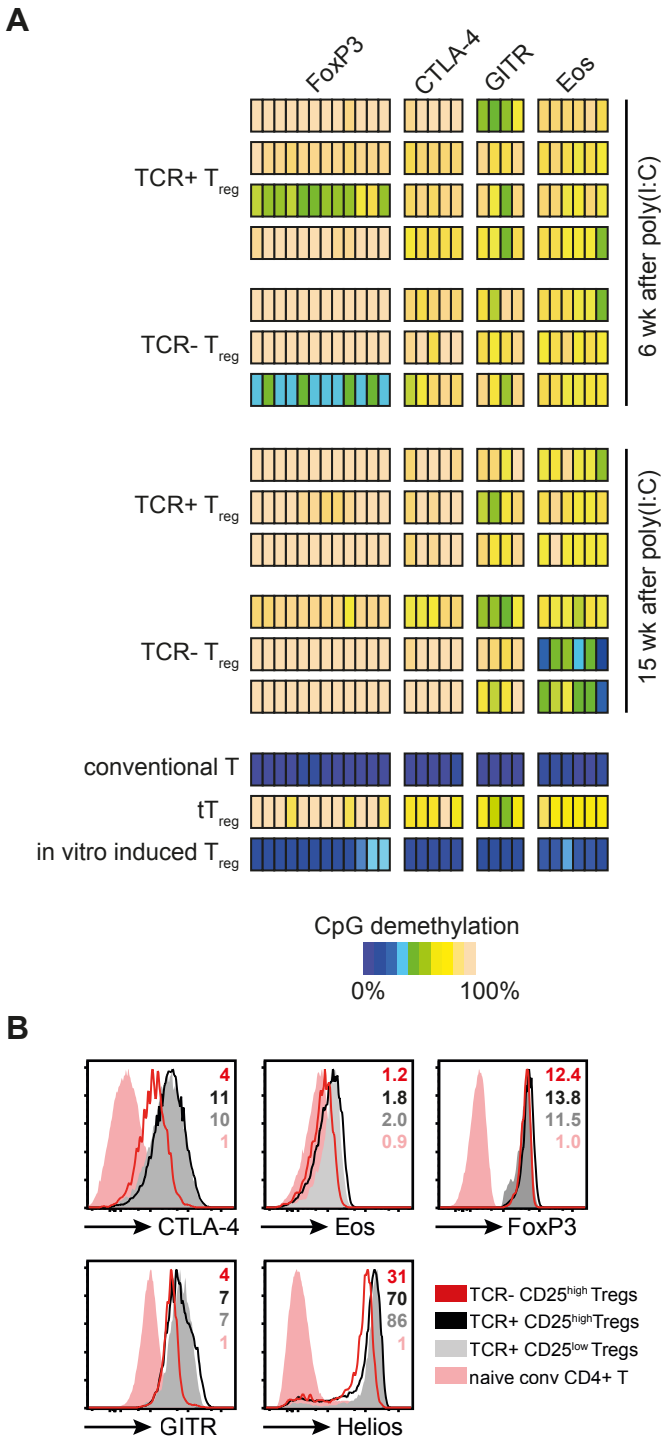

Figure 4. Treg cell-specific methylation pattern is unaltered upon TCR deletion.
(**A**) CpG methylation status of splenic CD25^{high} TCR+/TCR- Treg cells of the depicted animals, 6 wk or 15 wk after poly(I:C) injection.
(**B**) Extracellular (GITR) or intracellular (CTLA 4; Eos; Helios) expression of the depicted markers of the indicated splenic T cell subsets, all from *Mx-Cre Cα$^{F/F}$* animals 6 wk after poly(I:C) injection. Numbers in representative histograms indicate means of the median fluorescence intensities (MFIs), normalized to CD4+ CD44^{low} naïve conventional T cells of *Cα$^{F/F}$* animals. Means were calculated from at least 5 mice per genotype.

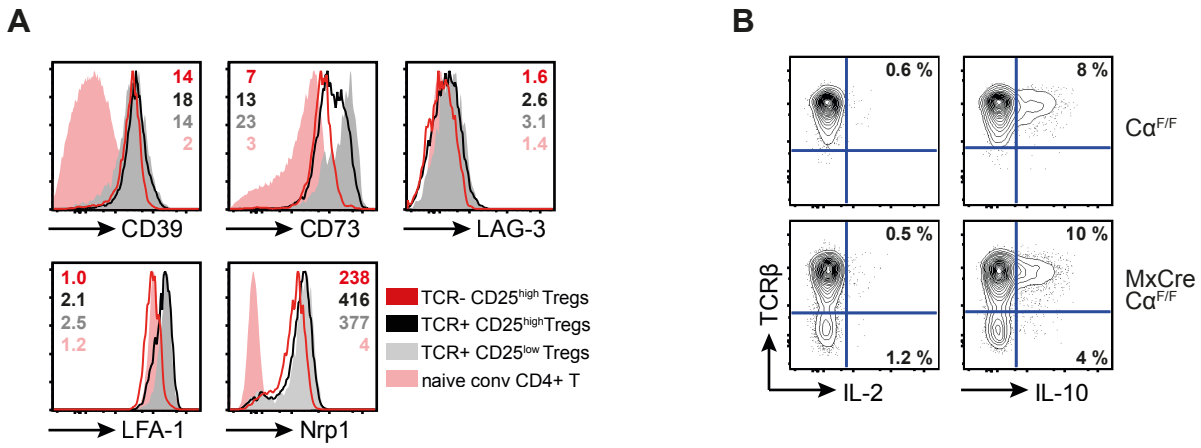

Figure 5. Regulatory T cells show reduced expression of several suppressor markers and reduced IL-10 production upon TCR deletion.

(**A**) Extracellular expression of the depicted markers of the indicated splenic T cell subsets, all from *Mx-Cre Cα$^{F/F}$* animals 6 wk after poly(I:C) injection. Numbers in representative histograms indicate means of the median fluorescence intensities (MFIs), normalized to CD4+ CD44^{low} naïve conventional T cells of *Cα$^{F/F}$* animals. Means were calculated from at least 5 mice per genotype.

(**B**) Intracellular IL-2 and IL-10 expression of splenic FoxP3-eGFP+ Treg cells, activated in vitro with PMA/Ionomycin for 5 h. Cells were extracted from mice and activated 6 wk after poly(I:C) injection. Numbers indicate mean percentages of TCR+ or TCR- Treg cells expressing the respective cytokine. Data are representative for 4 animals per genotype.

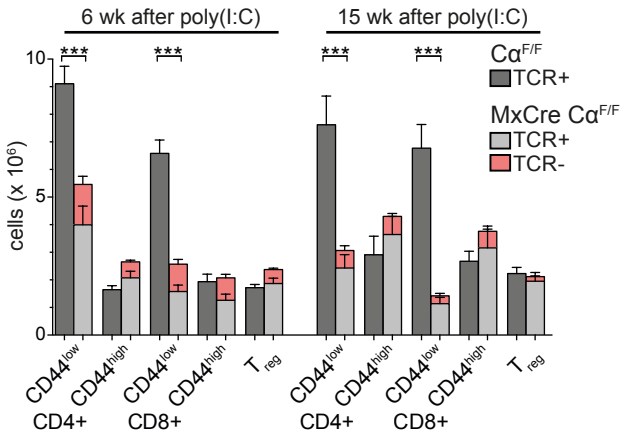

Supplementary Figure 1. Total splenic cell counts of CD4+ and CD8+, naïve ($CD44^{low}$) and memory/effector ($CD44^{high}$), as well as Treg cells, of the depicted animals, 6 wk or 15 wk after poly(I:C) injection. Data represents means and SD (error bars) of three independent experiments with at least 6 mice per genotype and time point.

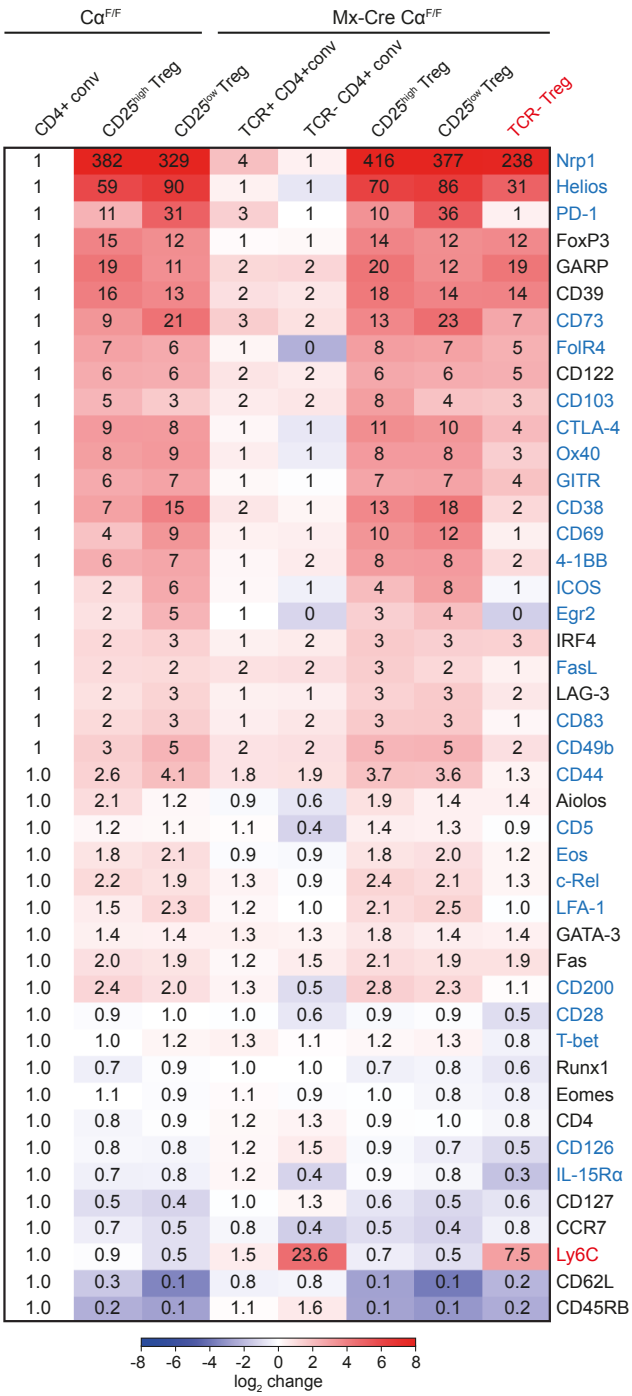

Supplementary Figure 2. Flow cytometric expression analysis of extra- and intracellular markers of splenic T cells, 6 wk after poly(I:C) injection. Median fluorescence intensities of at least 5 mice per analyzed protein were normalized to the expression on/in conventional CD4+ T cells to account for interexperimental variations. Data are shown as heatmap, calculated by Perseus software. Blue letters, significantly reduced on/in TCR- Treg cells in comparison to TCR+ CD25^{high} Treg cells from both *Cα$^{F/F}$* control as well as *Mx-Cre Cα$^{F/F}$* animals. Red letter, significantly increased; analyzed by one way ANOVA.

Paper III

Chu Y., **Vahl J.C.**, Kumar D., Heger K., Bertossi A., Wójtowicz E., Soberon V., Schenten D., Mack B., Reutelshöfer M., Beyaert R., Amann K., van Loo G. and Schmidt-Supprian M. (2011). B cells lacking the tumor suppressor TNFAIP3/A20 display impaired differentiation and hyperactivation and cause inflammation and autoimmunity in aged mice.
Blood 117: 2227–2236.

B cells lacking the tumor suppressor TNFAIP3/A20 display impaired differentiation and hyperactivation and cause inflammation and autoimmunity in aged mice

Yuanyuan Chu,[1] J. Christoph Vahl,[1] Dilip Kumar,[1] Klaus Heger,[1] Arianna Bertossi,[1] Edyta Wójtowicz,[1] Valeria Soberon,[1] Dominik Schenten,[2] Brigitte Mack,[3] Miriam Reutelshöfer,[4] Rudi Beyaert,[5] Kerstin Amann,[4] Geert van Loo,[5] and Marc Schmidt-Supprian[1]

[1]Max Planck Institute of Biochemistry, Martinsried, Germany; [2]Yale University School of Medicine, New Haven, CT; [3]Department of Otorhinolaryngology, Head and Neck Surgery, Grosshadern Medical Center, Ludwig-Maximilians-University of Munich, Munich, Germany; [4]Universitätsklinikum Erlangen, Pathologisches Institut, Abt Nephropathologie, Erlangen, Germany; and [5]Department for Molecular Biomedical Research, VIB and Department of Biomedical Molecular Biology, Ghent University, Ghent, Belgium

The ubiquitin-editing enzyme A20/*TNFAIP3* is essential for controlling signals inducing the activation of nuclear factor-κB transcription factors. Polymorphisms and mutations in the *TNFAIP3* gene are linked to various human autoimmune conditions, and inactivation of A20 is a frequent event in human B-cell lymphomas characterized by constitutive nuclear factor-κB activity. Through B cell-specific ablation in the mouse, we show here that A20 is required for the normal differentiation of the marginal zone B and B1 cell subsets. However, loss of A20 in B cells lowers their activation threshold and enhances proliferation and survival in a gene-dose–dependent fashion. Through the expression of proinflammatory cytokines, most notably interleukin-6, A20-deficient B cells trigger a progressive inflammatory reaction in naive mice characterized by the expansion of myeloid cells, effector-type T cells, and regulatory T cells. This culminates in old mice in an autoimmune syndrome characterized by splenomegaly, plasma cell hyperplasia, and the presence of class-switched, tissue-specific autoantibodies. (*Blood*. 2011;117(7):2227-2236)

Introduction

B cells play essential roles during protective immune responses to invading pathogens. On encounter of foreign antigen and with cognate T-cell help, B lymphocytes proliferate and form distinct histologic structures, termed germinal center (GC). In the GC, they undergo somatic hypermutation and class-switch recombination. During somatic hypermutation, they introduce random mutations into their immunoglobulin variable regions while they exchange the heavy chain constant region during class-switch recombination to allow for different effector functions. After a selection process by antigen, B cells differentiate into memory B cells and plasma cells (PCs), which secrete antibodies.[1] The deregulation of this process is heavily implicated in human disease. Production of class-switched antibodies against self-antigens causes or contributes to various autoimmune syndromes and unrestrained B-cell proliferation and survival can result in lymphomas.[1,2] It is thought that the majority of human lymphomas derive from the GC, probably because the DNA damage inherent to the GC reaction facilitates mutations and chromosomal translocations.[1,3]

Recently, the ubiquitin-editing enzyme A20, encoded by the tumor necrosis factor-α-inducible gene 3 (*TNFAIP3*), has been associated with both autoimmunity and lymphomagenesis. Polymorphisms and mutations in or near the *TNFAIP3* genomic locus have been linked with various human autoimmune syndromes with a strong humoral component, such as systemic lupus erythematosus (SLE),[4,5] rheumatoid arthritis,[6,7] and celiac disease.[8] Loss of A20 function through mutations, chromosomal deletions, and/or promoter methylation is a frequent event in several human lymphomas,[9-12] all of which are characterized by constitutive activation of nuclear factor-κB (NF-κB).[13] These factors regulate a plethora of genes encoding for proinflammatory mediators, antiapoptotic proteins, cell adhesion molecules and, for negative feedback control, inhibitory proteins, such as p100, IκBα, and A20.[14,15]

During the transmission of NF-κB activating signals from cell-surface receptors such as the B-cell receptor (BCR), CD40, or Toll-like receptors (TLRs), signal transduction occurs via the attachment of polyubiquitin chains to key proteins, including MALT1 or TRAF6. Polyubiquitin chains, linked via K63 or linear assembly, serve to recruit different kinase complexes. In the case of canonical NF-κB, induced proximity allows the upstream kinase TAK1 to phosphorylate its target IKK2, which then effects NF-κB activation. A20, whose transcription is induced by NF-κB, dampens signaling through 2 main activities. First, as deubiquitinase A20 removes K63-linked polyubiquitin chains from essential signaling intermediates, such as TRAF6. Second, A20 induces, in concert with other proteins, degradation of some of its molecular targets, through addition of K48-linked ubiquitin chains.[14,16] Degradation of RIP1 limits TNF-induced signaling,[14] whereas degradation of the K63-chain-specific E2 ligases Ubc13/UbcH5c generally affects the assembly of K63-linked polyubiquitin chains.[17]

Submitted September 8, 2010; accepted October 28, 2010. Prepublished online as *Blood* First Edition paper, November 18, 2010; DOI 10.1182/blood-2010-09-306019.

An Inside *Blood* analysis of this article appears at the front of this issue.

The online version of this article contains a data supplement.

The publication costs of this article were defrayed in part by page charge payment. Therefore, and solely to indicate this fact, this article is hereby marked "advertisement" in accordance with 18 USC section 1734.

To date, the main molecular action of A20 is to prevent prolonged NF-κB activation in response to stimulation of TNF-R, TLR-, or NOD-like receptors and the TCR.[14,16] Signal containment by A20 is crucial for immune homeostasis because A20-deficient mice die early on due to an uncontrolled inflammatory disease. The inflammation is triggered via MyD88-dependent TLRs by the commensal intestinal flora.[18] To study the cell-type-specific and cell-intrinsic roles of A20 in the mouse, we recently generated a conditional *Tnfaip3* allele ($A20^F$).[19] Given the implication of A20/TNFAIP3 in B-cell lymphomas and autoimmune diseases, we used B lineage-specific ablation of A20 to study its role in B-cell development, function, and disease.

Methods

Genetically modified mice

All mice described in this study are published and were originally generated using C57BL/6 ES cells, or backcrossed to C57BL/6 at least 6 times. Mice were housed in the specific pathogen-free animal facility of the Max Planck Institute. All animal procedures were approved by the Regierung of Oberbayern.

Flow cytometry

Single-cell suspensions were prepared[20] and stained with monoclonal antibodies: AA4.1(AA4.1), B220(RA3-6B2), CD1d(1B1), CD19(eBio1D3), CD22(2D6), CD23(B3B4), CD25(PC61.5), CD3(17A2), CD38(90) CD4(RM4-5), CD44(IM7), CD5(53-7.3), CD62L(MEL-14), CD69(H1.2F3), CD8(53-6.7), FoxP3(FJK-16s), GR-1(RB6-8C5), IgD(11-26), IgM(II/41), IL-10(JES5-16E3), IL-17A(eBio17B7), IL-4(11B11), IL-6(MP5-20F3), INF-γ(XMG1.2), Mac-1(M1/70), TCR-β(H57-597), TNF-α(MP6-XT22), CD95(15A7), CD21(7G6), CD86(GL-1), CD80(16-10A1), c-kit(2B8) (eBioscience), Ly-6G(1A8), Siglec-F(E50-2440), CD138(281-2) (BD Biosciences), and PNA (Vector Laboratories).

For intranuclear FoxP3 stainings (eBioscience) according to the manufacturer's instructions, dead cells were excluded with ethidium monoazide bromide. Samples were acquired on FACSCalibur and FACSCantoII (BD Biosciences) machines and analyzed with FlowJo software (TreeStar). For intracellular cytokine stainings, cells were stimulated for 5 hours at 37°C with 10nM phorbol myristate acetate (Calbiochem), 1mM ionomycin (Calbiochem), and 10nM brefeldin-A (Applichem). Cells were treated with Fc-block (eBioscience), and washed and surface-stained before fixation with 2% paraformaldehyde and permeabilization with 0.5% saponin. For in vitro culture, cells were purified by MACS (Miltenyi Biotec; > 85%-90% pure). Final concentrations of the activating stimuli: 2.5 μg/mL αCD40 (HM40–3, eBioscience), 10 μg/mL αIgM (Jackson ImmunoResearch Laboratories), 0.1μM CpG (InvivoGen), 20 μg/mL lipopolysaccharide (LPS; Sigma-Aldrich), and 4 ng/mL IL-4 (R&D Systems). Enzyme-linked immunosorbent assays were conducted using antibody pairs to IL-6 (BD Biosciences) and TNF (BD Biosciences). Cell-cycle analyses by propidium iodide (PI) and carboxyfluorescin diacetate succimidyl ester (CFDASE) were conducted as described.[20]

Real-time PCR

RNA was isolated (QIAGEN RNeasy Mini Kit) and reverse transcribed (Promega) for quantitative real-time polymerase chain reaction (PCR) using probes and primers from the Universal Probe Library (Roche Diagnostics) according to the manufacturer's instructions.

Biochemistry

B-cell whole-cell, cytoplasmic, and nuclear lysates were essentially prepared as published.[20] PVDF membranes were blotted with the following antibodies: p-IκBα, p-ERK, ERK, p-JNK, JNK, p-Akt, Akt, p-p38, p38, p100/p52 (Cell Signaling); IκBα, PLCγ2, RelB, RelA, c-Rel, Lamin B (Santa Cruz Biotechnology); tubulin (Upstate Biotechnology); p105/50 (Abcam); and A20.[19]

Immunofluorescence and immunohistochemistry

For immunofluorescence stainings, frozen 10-μm sections were thawed, air-dried, methanol-fixed, and stained for 1 hour at room temperature in a humidified chamber with B220-fluorescein isothiocyanate (eBioscience), biotinylated rat anti-CD3 (BD Biosciences), biotinylated rat anti-CD138 (BD Biosciences), and rabbit anti–laminin (gift from Michael Sixt) followed by Cy3-streptavidin and Cy5-conjugated anti–rabbit antibodies (Jackson ImmunoResearch). Immunohistochemically, MZB cells were identified by anti-CD1d (eBioscience) and metallophilic macrophages by anti-MOMA1 (Serotec). Detection of IgG immune complexes in paraformaldehyde-fixed kidney sections was performed using peroxidase-labeled anti–mouse IgG antibodies and 3-amino-9-ethylcarbazole staining (Vector Laboratories). For the detection of tissue-specific autoantibodies, frozen sections from organs of $Rag2^{-/-}$ mice were incubated with sera of aged and control mice and an anti–mouse IgG-Cy3 conjugate (Jackson ImmunoResearch Laboratories).

Images were acquired on a Zeiss Axiophot microscope (10×/0.3 or 20×/0.75 objectives; Carl Zeiss) using a Zeiss AxioCamMRm camera (Carl Zeiss) for monochromatic pictures and a Zeiss AxioCamMRC5 for RGB pictures. The following software programs were employed: Axiovision release 4.8 (Carl Zeiss), Photoshop CS4 and Illustrator CS4 (Adobe Systems).

Immunizations, ELISA

Mice were immunized intraperitoneally with 10 μg NP-Ficoll (Biosearch Technologies) and bled by the tail vein. Serum immunoglobulin concentrations and NP-specific antibodies were determined by ELISA.[21] The detection of antinuclear and anticardiolipin autoantibodies was performed using ELISA kits (Varelisa). Rheumatoid factor: ELISA plates were coated with rabbit IgG (Jackson ImmunoResearch Laboratories).

Results

Loss of A20 leads to defects in the generation and/or localization of mature B-cell subsets

To inactivate A20 specifically in B lineage cells at different developmental time points and to distinguish the specific effects of A20 ablation from potential artifacts inherent to individual cre-transgenic strains,[22] we initially investigated the consequences of CD19cre- and Mb1cre-mediated ablation of A20 in parallel (supplemental Figure 1A, available on the *Blood* Web site; see the Supplemental Materials link at the top of the online article). Because we did not observe any significant differences between $CD19cre/A20^{F/F}$ and $Mb1cre/A20^{F/F}$ mice in our experiments, we refer to them collectively as $B^{A20-/-}$ mice ($B^{A20+/-}$ for heterozygous deletion). Most of the experiments presented here were conducted using CD19cre. Efficient loss of the NF-κB–inducible A20 protein in B cells of these mice was confirmed by Western blot in both resting conditions and after treatment with LPS (Figure 1A).

Loss of A20 does not affect early B-cell development in the bone marrow, except for a minor increase in immature B cells. In contrast, the number of mature recirculating B cells is significantly reduced (supplemental Figure 1C-E). $B^{A20-/-}$ mice have enlarged spleens, coinciding with a minor increase in total B-cell numbers (supplemental Figure 1B; Figure 1B), suggesting that other cell types are also expanded. Mature follicular B-cell numbers are unaffected by A20 deficiency, but immature transitional B cells accumulate (Figure 1C-D) without any apparent block within the transitional compartment (supplemental Figure 2A). The numbers of marginal zone B (MZB) cells, defined by CD1d and CD21 expression (Figure 1C), are elevated because of an expansion of $CD23^+$ MZB precursor cells (Figure 1E; supplemental Figure 2B).

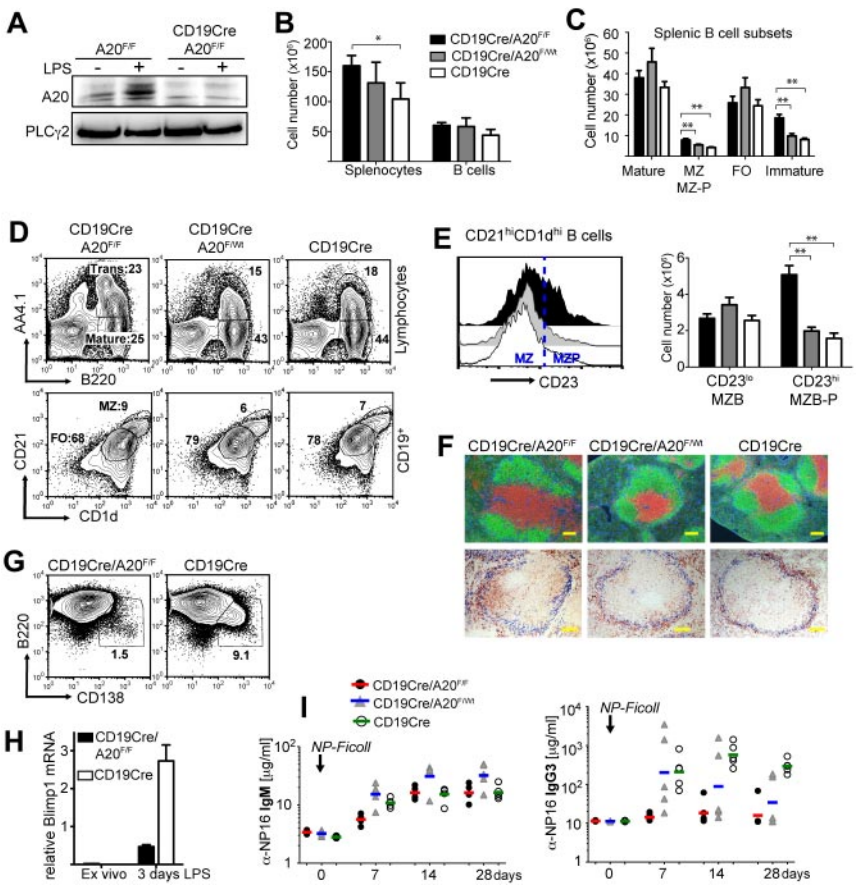

Figure 1. Conditional knockout of A20 in B cells induces severe defects in B-cell development and differentiation. (A) A20 protein expression in CD43-depleted B cells after 4-hour culture with or without 10 μg/mL LPS. (B-E) Absolute cell numbers were calculated from 5 to 7 age-matched mice per genotype. Data are mean ± SD. (B) Absolute splenocyte and B-cell numbers of the indicated genotypes. (C) Absolute cell numbers of splenic mature (B220^{+}AA4.1^{-}), marginal zone/marginal zone precursor (MZ; MZ-P: B220^{+}CD1d^{high}CD21^{high}), follicular (B220^{+}AA4.1^{-}CD1d^{-}CD23^{+}), and transitional (B220^{+}AA4.1^{+}) B cells. (D) Representative proportions of transitional (Trans: B220^{+}AA4.1^{+}) and mature (B220^{+}AA4.1^{-}) B cells of total lymphocytes (top panels) and of follicular (FO: CD1d^{int}CD21^{int}) and marginal zone/marginal zone precursor (MZ: CD1d^{high}CD21^{high}) B cells of CD19^{+} B cells (bottom panels) in the spleen. (E) CD23 expression on B220^{+}CD1d^{hi}CD21^{hi} B cells (left panel). Absolute cell numbers of marginal zone (B220^{+}CD1d^{hi}CD21^{hi}CD23^{lo}) and marginal zone precursor (B220^{+}CD1d^{hi}CD21^{hi}CD23^{hi}) B cells (right panel). (F) Top panels: Immunofluorescence of spleen sections: green represents αB220, B cells; red, αCD3, T cells; and blue, laminin. Bottom panels: Immunohistochemistry of spleen sections: blue represents MOMA-1, metallophilic macrophages; and brown, CD1d-expressing cells. Bar represents 100 μm. (G) Proportions of B220^{lo}CD138^{hi} plasma blasts in splenic B cells 3 days after LPS treatment. (H) Blimp1 mRNA expression relative to porphobilinogen deaminase was determined by real-time PCR in splenic B cells 3 days after LPS treatment. (I) Antigen-specific IgM and IgG3 serum titers in response to T-independent immunizations with 10 μg NP-Ficoll determined by ELISA. Lines represent geometric means for 5 mice per experimental group. *$P < .05$ (1-way analysis of variance). **$P < .001$ (1-way analysis of variance).

Inspection of the splenic follicular organization by immunofluorescence revealed normal B- and T-cell compartments in B$^{A20-/-}$ spleens (Figure 1F). However, in B$^{A20-/-}$ spleen sections, CD1d-expressing MZB cells are mostly located inside the follicle, whose border is defined by MOMA-1-expressing metallophilic macrophages located adjacent to the marginal sinus. In contrast, on B$^{A20+/-}$ and control spleen sections, CD1d-expressing cells are properly located in the marginal zone (Figure 1F). Immunofluorescent detection of laminin and B cells indicates that the B$^{A20-/-}$ splenic marginal zone is essentially devoid of B cells (supplemental Figure 2B), further demonstrating that A20-deficient MZB cells are not at their proper location. To test MZB cell function, we treated splenocyte cultures with LPS for 3 days and monitored the differentiation of short-lived plasma cells. At early times after activation of splenic B cells by LPS MZB cells, and to much lesser extent follicular B cells, differentiate into short-lived plasma cells.[23] As opposed to control B cells, A20-deficient splenic B cells show a profound defect in their ability to differentiate into Blimp1-expressing plasmablasts after LPS stimulation in vitro (Figure 1G-H), indicating the absence or paucity of functional MZB cells. Further underscoring this notion, B$^{A20-/-}$ mice display a significant reduction in the production of class-switched, antigen-specific IgG3 after immunizations with the TI-II antigen NP-Ficoll (Figure 1I), a response exquisitely dependent on the presence of MZB cells.[24] These results are in line with a significant reduction of total IgG3 serum levels in naive B$^{A20-/-}$ mice. IgG1 levels are also lower in these mice, whereas IgG2c and IgG2b levels are unchanged and IgM and IgA serum levels are strongly elevated (Figure 2A; supplemental Table 1). Supporting a role for A20 in B-cell differentiation and/or proper localization, peritoneal B1, especially B1a cells, are reduced in B$^{A20-/-}$ mice (Figure 2B; supplemental Figure 2E). In addition, thymic B cells are reduced in B$^{A20-/-}$ mice, although they appear elevated in B$^{A20+/-}$ mice (supplemental Figure 2D). Together, our results uncover several surprising deficiencies in the generation, differentiation, and/or maintenance of mature B-cell subsets in absence of A20. The affected subsets include MZB and B1 cells, which are thought to mediate the innate functions of the B lineage.[25]

A20-deficiency enhances GC B-cell formation in gut-associated lymphoid tissues

Given A20's role as negative regulator of NF-κB signaling, we expected A20-deficient B cells to be hyper-reactive to stimulation. We did not observe significant spontaneous GC formation in the spleens of the mice analyzed, indicating that spontaneous B-cell activation, if present in these mice, is not strong enough to induce GCs. In naive mice, gut-associated lymphoid tissue (GALT) is the place where B cells are constantly triggered by bacterial antigens to enter the GC.[26] The percentages and, to a lesser extent, absolute cell numbers of GC B cells in mesenteric lymph nodes and Peyer patches are increased in B$^{A20-/-}$ and B$^{A20+/-}$ mice (Figure 2C; and data not shown). This shows that, during B-cell activation by bacterial antigens in the GALT, strong hemizygous effects of A20 deficiency become apparent.

B cell–specific lack of A20 induces the spontaneous expansion of regulatory T, effector-type T, and myeloid cells

The increase in transitional and MZB precursor cell numbers is not sufficient to explain the higher splenocyte numbers in young B$^{A20-/-}$ mice (Figure 1B). Further detailed analyses showed that

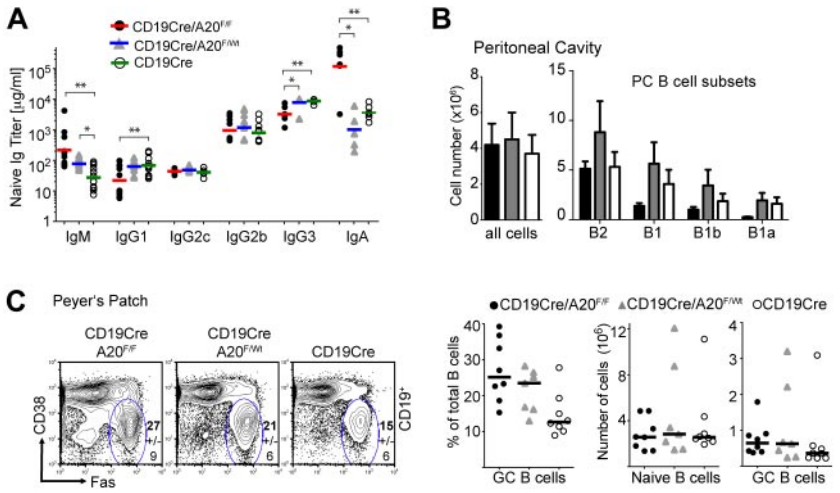

Figure 2. A20-deficiency impairs B1 cell generation but enhances GC formation in the GALT. (A) Titers of immunoglobulin isotypes were determined by ELISA; n = 6 to 12 per genotype. (B) Absolute cell numbers of B-cell subsets in the peritoneal cavity: B2 ($CD19^{+}B220^{+}$), B1 ($CD19^{high}B220^{low}$), B1a ($CD19^{high}B220^{low}CD5^{+}$), and B1b ($CD19^{high}B220^{low}CD5^{-}$) cell numbers were calculated from 5 to 7 age-matched mice per genotype. Data are mean ± SD. (C) Left panel: Proportions of GC ($CD19^{+}PNA^{hi}Fas^{hi}CD38^{lo}$) of total B cells in Peyer patches. Data are mean ± SD of 8 mice per genotype. Right panel: Proportions of GC B cells depicted as individual data points (left chart), absolute cell numbers for naive B cells (mantle zone B cells: $CD19^{+}PNA^{-}$ $Fas^{-}CD38^{hi}$; middle chart), and GC B cells (right chart). Bars represent medians of 8 mice per group (same as in the left panel). $^{*}P < .05$ (1-way analysis of variance). $^{**}P < .001$ (1-way analysis of variance).

homozygous and heterozygous ablation of A20 in B cells induces elevated numbers of T and myeloid cells. The sizes of many splenic T-cell compartments are increased in $B^{A20-/-}$ mice, especially the regulatory (Figure 3A-B), memory-type and effector-type CD4 (Figure 3B), and effector-type CD8 T cells (Figure 3C). Similar effects on T cells were observed in the lymph nodes (data not shown). The analysis of ex vivo T-cell cytokine production by intracellular staining revealed comparable proportions of IL-17–, interferon-γ– and TNF-producing cells between $B^{A20-/-}$ and control mice (Figure 3E). We were unable to detect any IL-4-producing cells (not shown). These analyses suggest the absence of detectable T-cell differentiation into specific T-helper lineages. The cell numbers of all splenic myeloid subsets analyzed were higher in $B^{A20-/-}$ compared with control mice, with significant increases in dendritic cells and eosinophils (Figure 3D). Importantly, heterozygous loss of A20 in B cells induces an intermediate phenotype (Figures 3A-D) in most aspects of this immune deregulation. $B^{A20+/-}$ mice contain even higher proportions of splenic regulatory and effector T cells than $B^{A20-/-}$ mice (Figure 3A). However, the higher absolute cell numbers of total CD4 T cells in $B^{A20-/-}$ mice leads to the greatest absolute cell numbers also in these subsets (Figure 3B). $B^{A20-/-}$ and $B^{A20+/-}$ mice contain elevated proportions of IL-10–producing B cells (supplemental Figure 2C), excluding the possibility that absence of this immune-regulatory B-cell subset[27] causes the perturbation in immune homeostasis. To validate that CD19cre mediates inactivation of A20 alleles only in B cells, we performed PCR on DNA purified from splenic cell subsets of $B^{A20-/-}$ mice. The purified T cells, dendritic cells, macrophages, and granulocytes contain less than 0.2% A20-knockout cells, which could be contaminating B cells (supplemental Figure 3). Our findings therefore indicate that the absence or gene-dose reduction of A20, specifically in B cells, induces an immune deregulation reminiscent of sterile inflammation, possibly held in check by regulatory lymphocyte subsets.

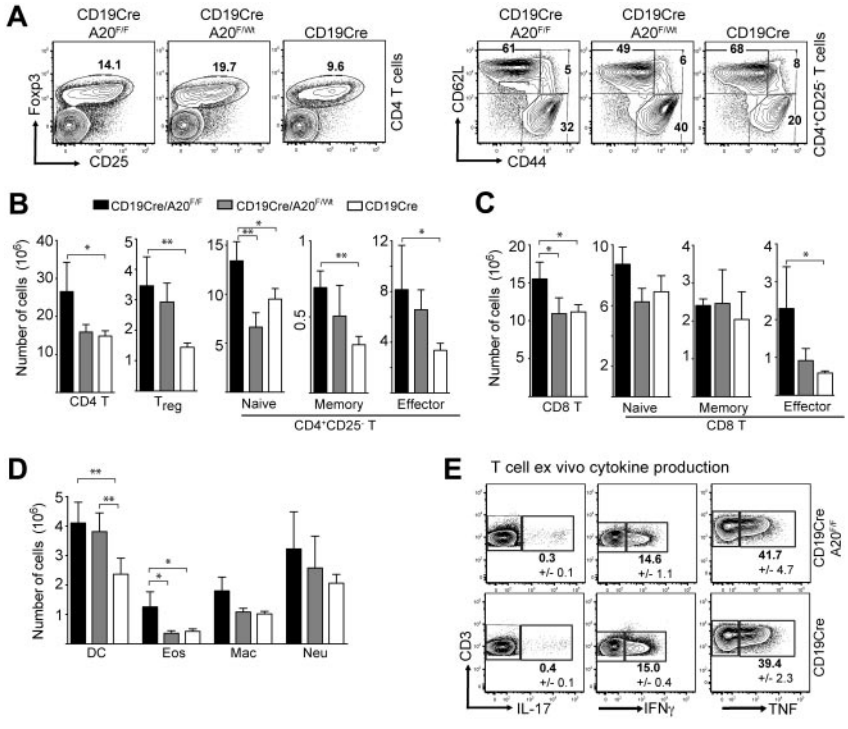

Figure 3. Ablation of A20 in the B-lineage has B cell-extrinsic effects on immune homeostasis. (A) Dot-plots showing percentages of $CD4^{+}Foxp3^{+}$ regulatory T cells and $CD4^{+}CD25^{-}$ T cells (naïve indicates $CD44^{int}CD62L^{hi}$; memory, $CD44^{hi}CD62L^{hi}$; and effector, $CD44^{hi}CD62L^{lo}$) in the spleen. Numbers indicate the mean of 4 to 6 mice for each genotype. (B-D) Absolute cell numbers of CD4 T (B), CD8 T (C), and myeloid cell (D) subsets in $B^{A20-/-}$, $B^{A20+/-}$, and CD19cre mice (n = 6 per group; 8-12 weeks old). Data are mean ± SD. Treg indicates $Foxp3^{+}$; naive, $CD44^{int}CD62L^{hi}$; memory, $CD44^{hi}CD62L^{hi}$; effector/memory, $CD44^{hi}CD62L^{lo}$; DC, dendritic cell ($CD11c^{+}$); Eos, eosinophils ($Gr1^{int}SiglecF^{+}$); Mac, macrophages ($Mac1^{+}Gr1^{lo}$); and Neu, neutrophils ($Gr1^{hi}Ly6G^{+}$). (E) Intracellular cytokine staining of ex vivo isolated splenocytes (gated on T cells). Numbers represent mean plus or minus SD of 3 mice per genotype. $^{*}P < .05$ (1-way analysis of variance). $^{**}P < .001$ (1-way analysis of variance).

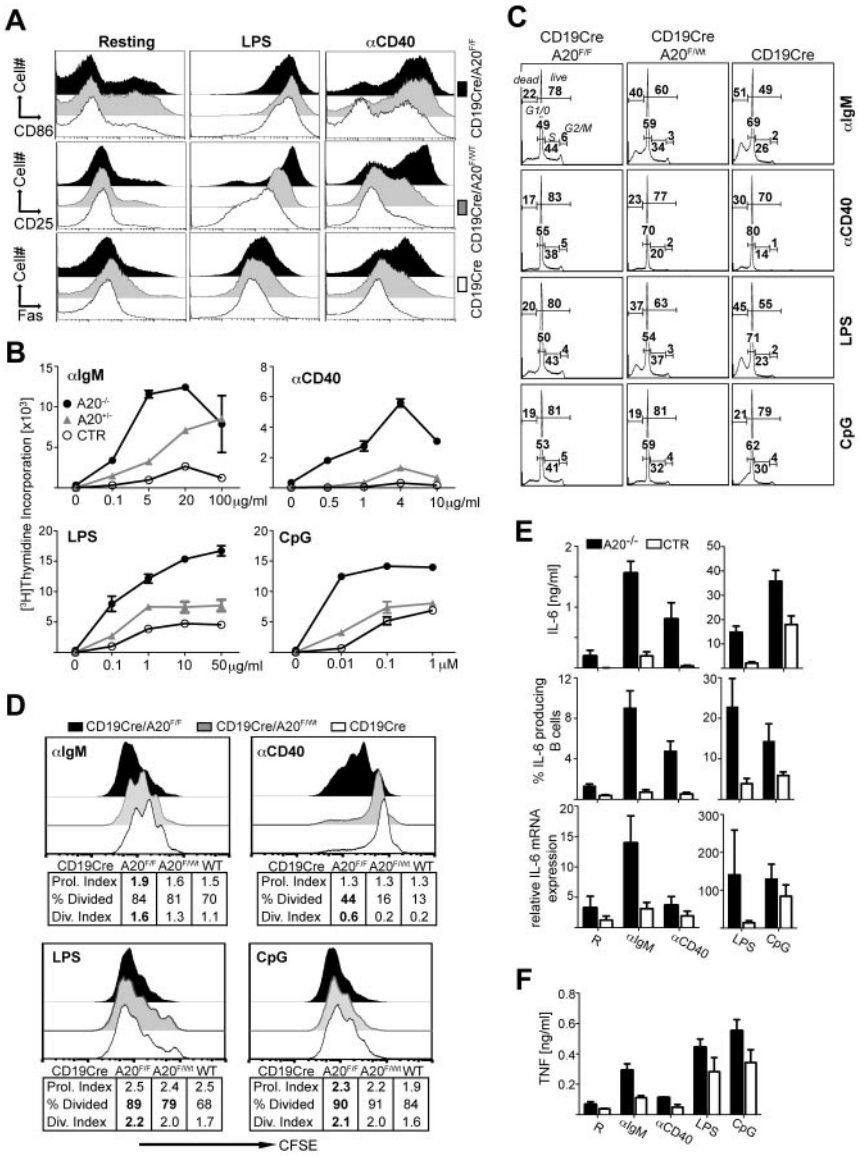

Figure 4. A20-deficiency amplifies B-cell responses. (A) Expression levels of the respective B-cell activation marker after overnight stimulation with LPS or αCD40. The dot-plots are representative of 3 to 6 independent experiments. (B) [^{3}H]Thymidine incorporation during a 10-hour pulse 48 hours after stimulation of B-cell cultures with αIgM, αCD40, LPS, or CpG. Data are mean ± SD of triplicate measurements. The experiment was repeated with similar results. (C) Cell cycle profile analysis by propidium iodide staining of B cells 2 days after stimulation with the indicated mitogens. Percentages of dead (sub G_0) and live cells are indicated at the top of each histogram. The distribution within the cell cycle was calculated with the FlowJo software Version 8.7.3 using the Watson model (values do not add up to 100%). Data are means of 2 independent experiments. (D) Assessment of proliferation by the carboxyfluorescein succinimidyl ester dilution assay: histograms represent carboxyfluorescein succinimidyl ester intensities 3 days after stimulation. The tables under each histogram show the proliferation index (Prol. Index: average number of divisions of the proliferating cells), the percentage of dividing cells (% Divided: the proportion of cells that initially started to divide), and the division index (Div. Index: average number of divisions of all cells); values were calculated with the FlowJo software. Data represent the means of 5 independent experiments, and bold values are significantly different ($P < .05$) from wild-type according to 1-way analysis of variance analysis. (E) Evaluation of IL-6 production in overnight activated B cells by ELISA (top panels), intracellular FACS (middle panels), and real-time PCR (bottom panels). For intracellular FACS, B cells were stimulated for 3 days. cDNA was quantified relative to porphobilinogen deaminase. Data are mean ± SD of 3 independent experiments. (F) Quantification of TNF production by overnight-stimulated B cells via ELISA. Data are mean ± SD of 3 independent experiments.

A20 regulates B-cell responses in vitro in a gene-dose–dependent fashion

Our observations of enhanced GC B-cell formation in the GALT in B$^{A20-/-}$ and B$^{A20+/-}$ mice suggested the possibility that their B cells are more easily activated in this context. To analyze this in more detail, we first quantified the relative A20 mRNA expression at different time points after activation with αIgM, αCD40, LPS, CpG DNA, and TNF. All these stimuli induced a strong increase in A20 mRNA, peaking at approximately 1 hour (supplemental Figure 4A), prompting us to test the in vitro responses of purified A20-deficient and A20$^{+/-}$ B cells to these mitogens. B cells up-regulate certain cell surface molecules (activation markers) upon activation, among them B7.1/CD80, B7.2/CD86, MHC II, CD25, and Fas. The expression of these markers was already slightly higher in unstimulated B cells purified from B$^{A20-/-}$ and B$^{A20+/-}$ mice compared with control B cells (Figure 4A; supplemental 4B). This is probably because of the latent immune activation we observed in these mice. Upon activation with the indicated mitogens, A20-deficient B cells produced higher surface levels of many activation markers (Figure 4A; supplemental Figure 3B). B cells carrying one functional A20 allele showed an intermediate phenotype regarding expression of these activation markers (Figure 4A). We then monitored αIgM-, αCD40-, LPS-, and CpG DNA-induced proliferation by 3 assays: Both [^{3}H]thymidine incorporation (Figure 4B) and cell cycle analysis (Figure 4C) showed increased proliferative activity in the A20-deficient B-cell cultures in response to all stimuli, and quantification of live cells revealed increased survival after all stimuli, except for CpG DNA (Figure 4C). By CFSE dilution assay (Figure 4D), we determined that the absence of A20 increased the proportion of B cells that initially start to divide (% divided) in response to αCD40 and LPS. Only CpG DNA and BCR crosslinking enhanced the proliferation of dividing A20-deficient B cells (Proliferation Index; Figure 4D). Combination of stimuli, such as LPS and αIgM, or the addition of IL-4, did not yield additive effects (supplemental Figure 4C). In all stimulations, the magnitude of the A20$^{+/-}$ B-cell response was in between A20$^{-/-}$ and control B cells (Figure 4B-D). Taken together, our studies show that reduction of A20 function magnifies B-cell responses through 3 mechanisms, depending on the activating stimulus: lowering the threshold for initial activation (αCD40, LPS), protecting activated B cells against apoptosis (αIgM, αCD40, LPS), and enhancing the proliferation of cells that were activated to divide (αIgM, CpG).

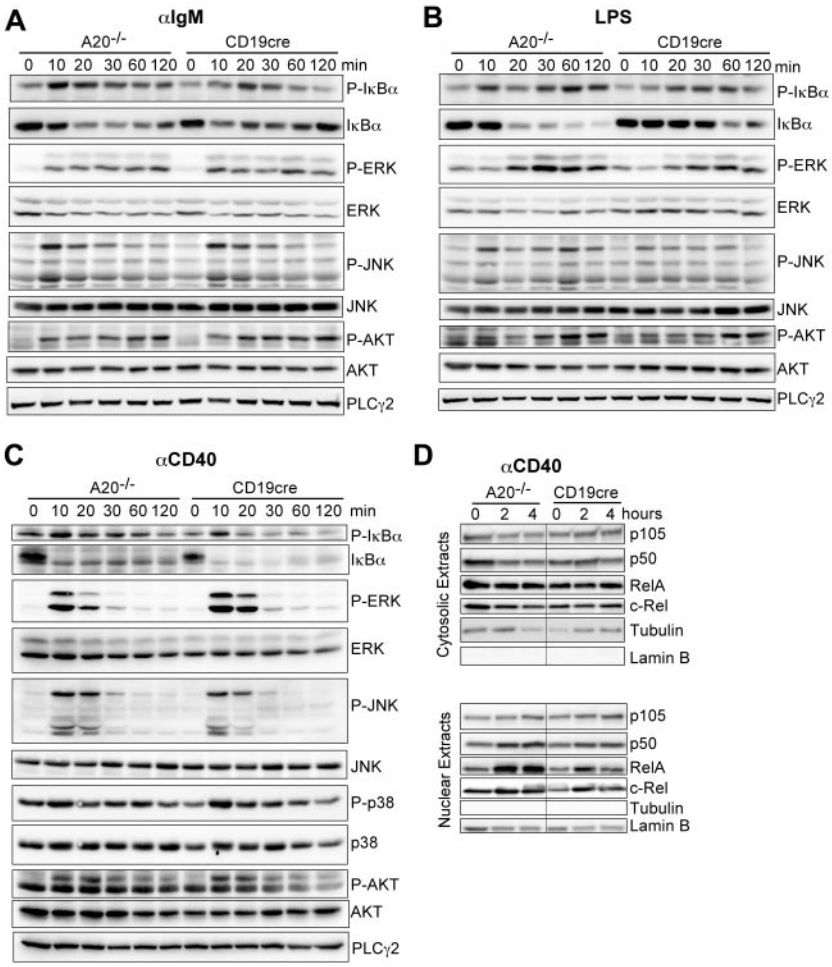

Figure 5. A20 controls canonical NF-κB activation in response to B-cell mitogens. (A-C) Western blot of whole cell lysates stimulated for the indicated time points with (A) 10 μg/mL αIgM, (B) 20 μg/mL LPS, and (C) 10 μg/mL αCD40. (D) Western blots on cytoplasmic and nuclear extracts after stimulation with αCD40. Results are representative of 2 or 3 independent experiments.

A20-deficient B cells exhibit spontaneous IL-6 secretion and highly elevated IL-6 secretion on activation

In light of the T effector and myeloid cell expansion, we wondered whether the higher excitability of A20-deficient B cells leads to secretion of proinflammatory cytokines, which in turn affect the differentiation and expansion of immune cells. IL-6 is a pleiotropic cytokine with inflammatory activity, and its levels are up-regulated in various autoimmune diseases, such as rheumatoid arthritis and SLE.[28] Activated A20-deficient B cells produced dramatically more IL-6 mRNA and protein than control B cells in response to all mitogens (Figure 4E). We could again detect an intermediate phenotype in $A20^{+/-}$ B cells (supplemental Figure 4D). Indeed, A20-deficient B cells spontaneously produced and released IL-6 into the cell culture medium in the absence of stimulation in comparable amounts to the IL-6 secretion in αIgM-stimulated control B cells (Figure 4E). A20-deficient B cells also produced slightly more TNF in response to all stimuli (Figure 4F). In accord with these findings, we detected more IL-6 and TNF-producing cells in ex vivo isolated A20-deficient compared with control B cells (supplemental Figure 4E). The evaluation of IL-6 production in immune cell subsets of 3- to 4-month-old $B^{A20-/-}$ mice by intracellular flow cytometry and real-time PCR revealed that, in addition to B cells, dendritic cells and, to a lesser extent, macrophages also produce IL-6 (supplemental Figure 5). This suggests that secondary activation of myeloid cells by A20-deficient B cells exacerbates the immune deregulation in $B^{A20-/-}$ mice.

A20 negatively regulates canonical NF-κB, but not MAPK or AKT activation, in response to engagement of the BCR, CD40, and TLRs

We established that A20 is a gene-dose–dependent negative regulator of B-cell activation in response to triggering of the BCR, CD40, and TLRs. A20 was reported to limit the activation of canonical NF-κB in response to various stimuli in other cell types.[14,16] Therefore, we wanted to confirm that the hyper-reactivity of A20-deficient B cells also correlates with enhanced canonical NF-κB activity in response to the stimuli used in our study. Indeed, the absence of A20 selectively enhances the activation of the canonical NF-κB pathway, evidenced by prolonged increased IκBα phosphorylation and degradation (Figure 5A-C). The activation of MAPK pathways or AKT phosphorylation was unaltered in response to αIgM, LPS, and αCD40 (Figure 5A-C). The increased IκBα phosphorylation correlated well with an increase in nuclear translocation of p50 and RelA 2 and 4 hours after activation with αCD40 (Figure 5D). We detected elevated expression of p100 and RelB, substrates of the alternative NF-κB pathway and transcriptional targets of canonical NF-κB in whole cell extracts of A20-deficient B cells (data not shown) in accord with the higher canonical NF-κB activity in these cells. Taken together, although we do not rule out that A20 has additional functions, we demonstrate that deficiency for A20 in B cells strongly enhances activation of the canonical NF-κB pathway in response to BCR cross-linking (antigen), T-cell costimulation (αCD40), and microbial components (TLRs).

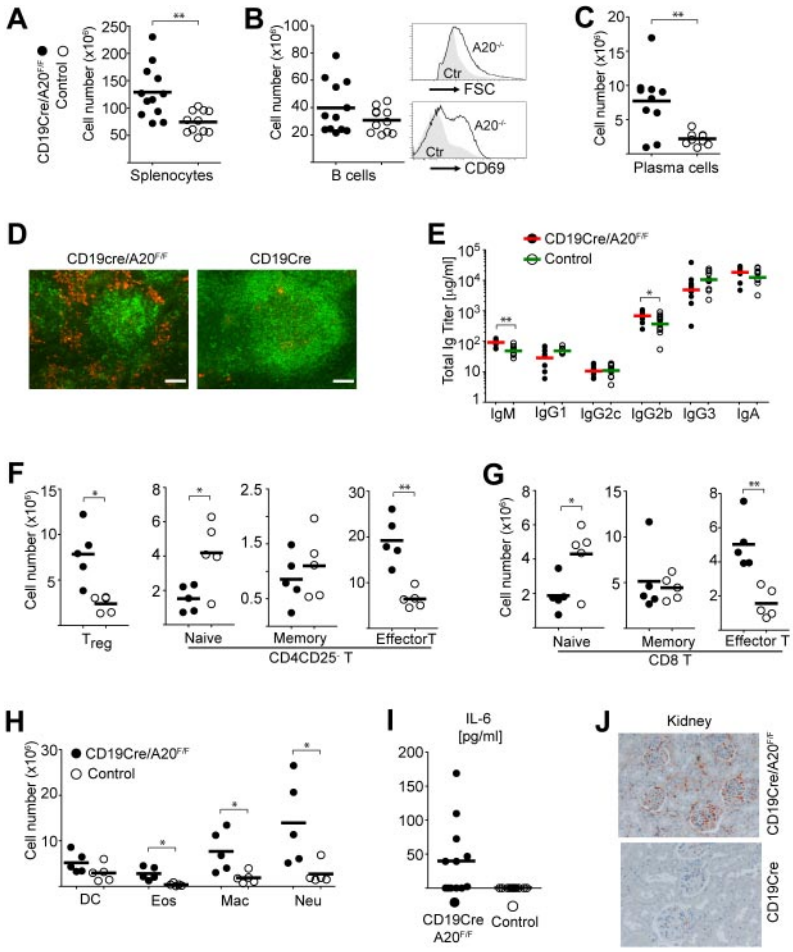

Figure 6. Splenomegaly and plasma cell hyperplasia in old B$^{A20-/-}$ mice. Cohort description: age range, 60 to 85 weeks; mean age of experimental group, 68 weeks; mean age of control group, 66 weeks. (A) Absolute cell numbers of splenocytes (n(B$^{A20-/-}$) = 10, n(control) = 9). (B) Left panel: Absolute cell numbers of B cells (CD19^{+}; n(B$^{A20-/-}$) = 12, n(control) = 11). Right panel: Representative size and CD69 expression of splenic B220^{+} B cells. (C) Absolute cell numbers of splenic plasma cells (B220^{lo}CD138^{hi}; n(B$^{A20-/-}$) = 10, n(control) = 9). (D) Representative immunofluorescence analysis of plasma cells in the spleen, plasma cells (red represents αCD138), B cells (green represents αB220). Bar represents 100 μm. (E) Titers of immunoglobulin isotypes in aged mice were determined by ELISA; n(B$^{A20-/-}$) = 12, n(control) = 11. (F-H) Absolute splenic cell numbers for the following cellular subsets: CD4 T cells. (F) Treg (CD4^{+}CD25^{+}); CD4^{+} naive (CD25^{-}CD44^{int}CD62L^{hi}), memory-type (CD25^{-}CD44^{hi}CD62L^{hi}), and effector T (CD4^{+}CD44^{hi}CD62L^{lo}); CD8-T cells. (G) Naive (CD44^{int}CD62L^{hi}), memory-type (CD44^{hi}CD62L^{hi}), and effector T (CD44^{hi}CD62L^{lo}); myeloid cells (H): DC indicates dendritic cell (CD11c^{+}); Eos, eosinophils (Gr1^{int}SiglecF^{+}); Mac, macrophages (Mac1^{+}Gr1^{lo}); and Neu, neutrophils (Gr1^{hi}Ly6G^{+}). n(B$^{A20-/-}$) = 5, n(control) = 5. (I) Serum IL-6 (pg/mL) in aged mice was measured by ELISA; n(B$^{A20-/-}$) = 12, n(control) = 11. (J) Representative stainings of IgG immune complexes in kidneys of B$^{A20-/-}$ and control mice. Original magnification × 20. *$P < .05$ (1-way analysis of variance). **$P < .001$ (1-way analysis of variance).

Loss of A20 in B cells leads to autoimmune pathology in old mice

To assess the impact of the chronic proinflammatory state induced by B cell-specific loss of A20 in old age, we aged a cohort of B$^{A20-/-}$ and control mice. Histologic analysis of organs from 20-week-old B$^{A20-/-}$ mice did not yield any signs of inflammation (not shown). B$^{A20-/-}$ mice, more than one year old, on the contrary, were characterized by splenomegaly (Figure 6A; supplemental Figure 6A-B). Although total B-cell numbers were not significantly elevated in old B$^{A20-/-}$ compared with control mice, all A20$^{-/-}$ B cells appeared activated, as judged by the larger cell size and elevated levels of the activation marker CD69 (Figure 6B). In addition, we observed a marked expansion of PCs in the spleen (Figure 6C; supplemental Figure 6C), but not in the bone marrow (data not shown). Immunofluorescence analysis of the enlarged spleens revealed a diffuse pattern of PCs surrounding altered and disrupted B-cell follicles (Figure 6D). Analysis of the serum isotype titers in aged B$^{A20-/-}$ mice revealed higher IgM titers compared with controls, as seen in young mice. However, in contrast to the latter, in old B$^{A20-/-}$ mice the levels of the pathogenic IgG2b isotype[29] are elevated (Figure 6E; supplemental Table 2). The increase of effector and regulatory T cells, already apparent in young B$^{A20-/-}$ mice, has further expanded in old mice, at the expense of the respective naive compartments (Figure 6F-G). In addition, the expansion of myeloid cell subsets was much more pronounced (Figure 6H). The progressive nature of the inflammation in the B$^{A20-/-}$ mice is also reflected in elevated levels of serum IL-6 in aged B$^{A20-/-}$ mice (Figure 6I), which could not be detected in the 20-week-old B$^{A20-/-}$ mice (not shown). Histologic analysis of organs from aged mice revealed inflammatory infiltrates in the liver and kidney of most of the old B$^{A20-/-}$ mice (supplemental Figure 6D). Examinations of the renal pathology revealed no extensive glomerular damage but clear IgG immune complex depositions in aged B$^{A20-/-}$ mice (Figure 6J).

Given this finding, we tested the sera of all old B$^{A20-/-}$ and control mice for indicators of self-recognition. Class-switched antibodies against nuclear self-antigens (ANAs) are the most common autoantibodies observed in autoimmune conditions in mice and humans.[30] Sera from B$^{A20-/-}$ mice did not contain significantly higher ANA levels than sera from the controls, and we also did not detect enhanced reactivity to endogenous red blood cells (Figure 7A). In addition, we observed increased levels of rheumatoid factor of the IgM isotype in some B$^{A20-/-}$ mice, but not of the IgG isotype (Figure 7A). However, we detected significantly elevated amounts of anticardiolipin IgG antibodies in aged B$^{A20-/-}$ mice (Figure 7A), demonstrating systemic class-switched autoimmune reactivity. To evaluate whether antiphospholipid antibodies are already detectable in younger mice, we screened the sera of 3-month-old mice. We detected elevated anticardiolipin IgG antibodies in sera from B$^{A20-/-}$ mice (and B$^{A20+/-}$ mice) compared with control sera, but the differences were not statistically significant (Figure 7C).

To screen for further autoreactivity against potentially tissue-specific self-antigens, we incubated organ sections of Rag2$^{-/-}$ mice with the sera of the aged mice. We detected autoreactive class-switched IgG antibodies in the sera of B$^{A20-/-}$, but not of

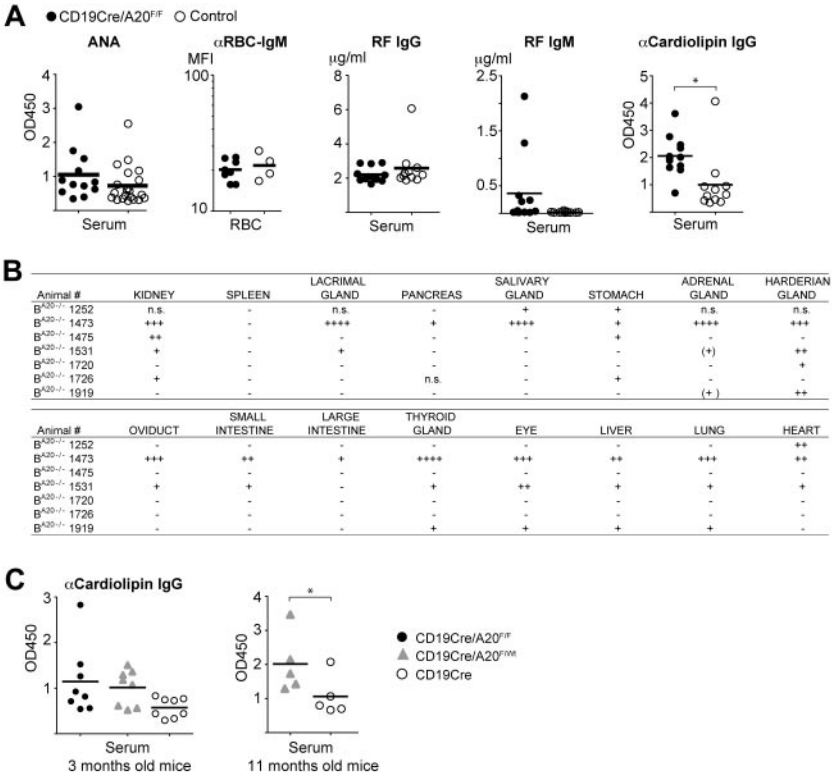

Figure 7. Autoimmune manifestations in old $B^{A20-/-}$ mice. (A) Analysis of autoantibodies in aged mice. ANA indicates that antinuclear IgG antibodies were detected by ELISA, n($B^{A20-/-}$) = 12, n(control) = 21; αRBC-IgM, antierythrocyte IgM was detected by FACS and represented as mean fluorescence intensity, n($B^{A20-/-}$) = 8, n(control) = 4. IgG and IgM rheumatoid factor (RF) was measured by ELISA; n($B^{A20-/-}$) = 12, n(control) = 11. α-Cardiolipin IgG antibodies were detected by ELISA; n($B^{A20-/-}$) = 12, n(control) = 11. *$P < .05$ (2-tailed unpaired Student t test). **$P < .001$ (2-tailed unpaired Student t test). (B) Table depicting the self-reactivity of sera from individual $B^{A20-/-}$ mice against the indicated organs from $Rag2^{-/-}$ mice. +, ++, and +++ indicate the severity of autoreactivity; and n.s., not screened. (C) Levels of α-cardiolipin IgG autoantibodies in 3-month-old mice (left panel; n = 8 per genotype) and in 11-month-old mice (right panel; n = 5 per genotype) were detected by ELISA. *$P < .05$ (1-tailed unpaired Student t test).

control mice, directed predominantly against kidney, harderian gland, stomach, thyroid gland, eye, liver, and lung (Figure 7B; supplemental Figure 6E). Pancreas, salivary, lacrimal, and adrenal glands were also recognized by sera from few $B^{A20-/-}$ mice but with a lower penetrance compared with the organs mentioned earlier (Figure 7B). Notably, the kidney was recognized by autoantibodies in the sera of the majority of $B^{A20-/-}$ mice. Therefore, we conclude that A20-deficient B cells induce chronic progressive inflammation, which results in significant autoimmune manifestations and pathologic alterations in old mice.

Discussion

The prevalent inactivation of the ubiquitin-editing enzyme A20 in human B-cell lymphoma and the linkage of polymorphisms in the A20/*TNFAIP3* gene to human autoimmune diseases raise the question of its function in the B-lineage, especially during B-cell activation.

The major molecular function of A20 uncovered to date is the negative regulation of canonical NF-κB activation.[14] We confirm that, also in B cells, A20 limits activation of this signaling pathway by all relevant physiologic inducers. Constitutive activation of canonical NF-κB in B cells induces B-cell hyperplasia, especially pronounced in MZB cells.[20] In contrast, we uncovered that A20 activity is required for the correct localization of MZB cells and for MZB cell function. Therefore, we conclude that proper differentiation of A20-deficient MZB cells does not take place. In addition, A20 is needed for the generation or cellular maintenance of peritoneal B1, bone marrow recirculating and thymic B cells, either directly or by mediating their correct localization. Reduced cellular maintenance could be caused by lower sensitivity to survival signals available in naive mice, but also by increased terminal differentiation because of their hyperactivatable state. The elevated IgA serum levels could be a consequence of the enhanced GC reactivity in the GALT of $B^{A20-/-}$ mice. Another possible explanation is that the lower levels of B1a cells could, at least in part, be caused by their enhanced differentiation to IgA-producing plasma cells in response to inducing signals, such as IL-15,[31] a cytokine known to induce NF-κB activation. This phenomenon could also contribute to the elevated IgM levels. Because B1 cells are thought to be the main source of naturally occurring autoantibodies in naive mice,[32] this could signify that also natural autoantibody IgM titers, which are not pathogenic but rather play a protective role, are enhanced in the $B^{A20-/-}$ mice. The accumulation of A20-deficient precursor populations (transitional B cells and MZB cell precursors) points to blocks in development, although we cannot exclude a role for impaired negative selection.

Taken together, our data on B-cell development and in vitro activation studies suggest the following: A20 activity is required to limit acute B-cell activation induced by stimuli connected to invasion by pathogens. Its absence reduces the activation threshold and enhances survival and proliferation in response to such stimuli. On the other side, the absence of A20 does not render B cells more responsive to maintenance signals required for mature resting cells.

Increased B cell–mediated IL-6 secretion resulting from sporadic local activation and, at least in the case of A20 deficiency, spontaneous production and release of IL-6 is a probable underlying cause of the effector T-cell differentiation and myeloid cell hyperplasia that we observed in $B^{A20-/-}$ and $B^{A20+/-}$ mice. Subsequent cytokine secretion by activated myeloid cells most probably amplifies this response. Indeed, Tsantikos et al recently showed that effector T-cell activation, myeloid cell expansion, and the development of autoimmune disease in Lyn-deficient mice, which strikingly resemble $B^{A20-/-}$ and $B^{A20+/-}$ mice in this regard, are entirely dependent on the secretion of IL-6.[33] Interestingly, the authors also observed expansion of $CD4^+CD25^+$ T cells but did not investigate whether they represent activated or regulatory

T cells.[33] The enhanced numbers of Tregs we observe in the B$^{A20-/-}$ and B$^{A20+/-}$ mice appear paradoxical in the context of elevated IL-6 levels.[34] We suggest that they expand and/or are induced in reaction to the IL-6-driven inflammation. However, the presence of IL-6 increases the resistance of effector T cells to suppression by regulatory T cells,[35] both systemically and locally. Expansion of Tregs has also been observed in the BWF1 mouse model for human SLE.[36] Whether, and to what extent, an expanded Treg population serves to keep the sterile inflammation in check is an intriguing question to be tested in future studies.

While this manuscript was in preparation, a study by Tavares et al on the same topic was published.[37] The authors also found a convincing gene-dose–dependent effect of A20 ablation on B-cell activation. They detected elevated levels of antibodies in the serum of CD19cre/A20$^{F/F}$ mice that recognize self-antigens on a protein array. However, in their approach, anti–mouse Ig was used to detect autoantibodies, which also recognizes IgM. Indeed, both studies find highly elevated titers of IgM in naive B$^{A20-/-}$ mice (in our case, a 10-fold difference in the geometric mean). Naturally occurring autoantibodies are mostly of the IgM isotype.[38,39] Therefore, the increased recognition of self observed by Tavares et al[37] could reflect, at least to some degree, this increase in natural autoantibodies. This possibility is substantiated by the fact that only IgM$^+$ dsDNA-recognizing plasma cells were detected and that IgM immune complex deposits were revealed in naive 6-month-old mice, in the absence of any sign of pathology.[37] Given that the role of IgM autoantibodies is also discussed as being protective,[38,39] it is unclear whether the autoreactivity observed in younger mice contributes to the development of, or helps to prevent, disease.

We observed significant autoreactivity of class-switched antibodies only in old mice, together with autoimmune pathology and inflammation. The chronic inflammation induced by the A20-deficient B cells perhaps contributes to a progressive break in B-cell tolerance resulting in the production of class-switched, autoreactive antibodies. The immune senescence of old age might also contribute to this break in tolerance.[32] The inflammatory microenvironment in the spleen, and potentially in other affected organs, together with the elevated presence of the pleiotropic cytokine IL-6, may serve as a niche for the (autoreactive) plasma cells. However, we do not detect significant levels of IgG ANAs, the hallmark of SLE.[30] Instead, we observe general IgG autoreactivity to cardiolipin, a common autoantigen in autoimmune disease[30,40] in old B$^{A20-/-}$ mice. The presence of tissue-specific class-switched autoantibodies strongly underscores the loss of tolerance. Some pathologic features of the old B$^{A20-/-}$ mice are reminiscent of human Castleman disease, namely, massive infiltrations of plasma cells and the elevated presence of IL-6.[28,41] It is indeed possible that the disturbed B-cell development, including the elevated levels of naturally occurring auto-IgM, are preventing a more severe syndrome. Heterozygous B$^{A20+/-}$ mice display inflammation and B-cell hyper-reactivity, but no developmental defects. Therefore, they might represent a good tool for modeling the reduced expression or function of A20 that should underlie the link between mutations and polymorphisms in A20/*TNFAIP3* and human autoimmune disease. Indeed, initial analyses revealed elevated class-switched antibodies against cardiolipin in a cohort of 11-month-old B$^{A20+/-}$ mice (Figure 7C).

We demonstrate here that selective loss of A20 in B cells is sufficient to cause an inflammatory syndrome with autoimmune manifestations in old mice. This condition is characterized by a progressive chronic inflammation, elevated levels of IL-6, dramatic plasma cell expansion, and the presence of class-switched systemic and tissue-specifc autoantibodies. The exquisite dose effects of monoallelic loss of A20 make it a prime target for deregulation by proinflammatory miRNAs and oncomirs in disease contexts. Our results demonstrate that B-cell hyper-reactivity caused by reduced A20 function can contribute to the observed link between inherited genetic mutations or polymorphisms in A20/*TNFAIP3* and various human autoimmune diseases.

Acknowledgments

The authors thank Reinhard Fässler for support; Julia Knogler and Barbara Habermehl for technical assistance; Reinhard Voll and Michael Sixt for advice; Guru Krishnamoorthy for help with thymidine incorporation assays; Ludger Klein for tissues of Rag2$^{-/-}$ mice; Claudia Uthoff-Hachenberg for ELISA reagents; and Michael Sixt, Charo Robles, Vigo Heissmeyer, Stefano Casola, Sergei Koralov, Manu Derudder, and Dinis Calado for critical reading of the manuscript.

This work was supported by the Deutsche Forschungsgemeinschaft (SFB684) and an Emmy Noether grant (M.S.-S.). J.C.V. and K.H. received PhD stipends from the Ernst Schering Foundation and the Boehringer Ingelheim Fonds, respectively. G.v.L. is a FWO postdoctoral researcher with an Odysseus Grant, K.A. was supported by the IZKF Erlangen (project A31) and D.S. by the Cancer Research Institute.

Authorship

Contribution: Y.C. and M.S.-S. designed and performed research, analyzed data, and wrote the paper; J.C.V., D.K., K.H., A.B., E.W., V.S., B.M., and M.R. performed research; D.S. and K.A. analyzed data; and R.B. and G.v.L. contributed new reagents.

Conflict-of-interest disclosure: The authors declare no competing financial interests.

Correspondence: Marc Schmidt-Supprian, Max Planck Institute of Biochemistry, Am Klopferspitz 18, D-82152 Martinsried, Germany; e-mail: supprian@biochem.mpg.de.

References

1. Klein U, Dalla-Favera R. Germinal centres: role in B-cell physiology and malignancy. *Nat Rev Immunol.* 2008;8(1):22-33.
2. Goodnow CC. Multistep pathogenesis of autoimmune disease. *Cell.* 2007;130(1):25-35.
3. Kuppers R. Mechanisms of B-cell lymphoma pathogenesis. *Nat Rev Cancer.* 2005;5(4):251-262.
4. Graham RR, Cotsapas C, Davies L, et al. Genetic variants near TNFAIP3 on 6q23 are associated with systemic lupus erythematosus. *Nat Genet.* 2008;40(9):1059-1061.
5. Musone SL, Taylor KE, Lu TT, et al. Multiple polymorphisms in the TNFAIP3 region are independently associated with systemic lupus erythematosus. *Nat Genet.* 2008;40(9):1062-1064.
6. Plenge RM, Cotsapas C, Davies L, et al. Two independent alleles at 6q23 associated with risk of rheumatoid arthritis. *Nat Genet.* 2007;39(12):1477-1482.
7. Thomson W, Barton A, Ke X, et al. Rheumatoid arthritis association at 6q23. *Nat Genet.* 2007;39(12):1431-1433.
8. Trynka G, Zhernakova A, Romanos J, et al. Coeliac disease-associated risk variants in TNFAIP3 and REL implicate altered NF-kappaB signalling. *Gut.* 2009;58(8):1078-1083.
9. Schmitz R, Hansmann ML, Bohle V, et al. TNFAIP3 (A20) is a tumor suppressor gene in Hodgkin lymphoma and primary mediastinal B cell lymphoma. *J Exp Med.* 2009;206(5):981-989.
10. Chanudet E, Huang Y, Ichimura K, et al. A20 is targeted by promoter methylation, deletion and inactivating mutation in MALT lymphoma. *Leukemia.* 2010;24(2):483-487.

11. Honma K, Tsuzuki S, Nakagawa M, et al. TNFAIP3 is the target gene of chromosome band 6q23.3-q24.1 loss in ocular adnexal marginal zone B cell lymphoma. *Genes Chromosomes Cancer.* 2008;47(1):1-7.
12. Novak U, Rinaldi A, Kwee I, et al. The NF-κB negative regulator TNFAIP3 (A20) is inactivated by somatic mutations and genomic deletions in marginal zone lymphomas. *Blood.* 2009;113(20): 4918-4921.
13. Packham G. The role of NF-kappaB in lymphoid malignancies. *Br J Haematol.* 2008;143(1):3-15.
14. Hymowitz SG, Wertz IE. A20: from ubiquitin editing to tumour suppression. *Nat Rev Cancer.* 2010;10(5):332-341.
15. Karin M, Cao Y, Greten FR, Li ZW. NF-kappaB in cancer: from innocent bystander to major culprit. *Nat Rev Cancer.* 2002;2(4):301-310.
16. Vereecke L, Beyaert R, van Loo G. The ubiquitin-editing enzyme A20 (TNFAIP3) is a central regulator of immunopathology. *Trends Immunol.* 2009; 30(8):383-391.
17. Shembade N, Ma A, Harhaj EW. Inhibition of NF-kappaB signaling by A20 through disruption of ubiquitin enzyme complexes. *Science.* 2010; 327(5969):1135-1139.
18. Turer EE, Tavares RM, Mortier E, et al. Homeostatic MyD88-dependent signals cause lethal inflammation in the absence of A20. *J Exp Med.* 2008;205(2):451-464.
19. Vereecke L, Sze M, Guire CM, et al. Enterocyte-specific A20 deficiency sensitizes to tumor necrosis factor-induced toxicity and experimental colitis. *J Exp Med.* 2010;207(7):1513-1523.
20. Sasaki Y, Derudder E, Hobeika E, et al. Canonical NF-kappaB activity, dispensable for B cell development, replaces BAFF-receptor signals and promotes B-cell proliferation upon activation. *Immunity.* 2006;24(6):729-739.
21. Schmidt-Supprian M, Tian J, Ji H, et al. I kappa B kinase 2 deficiency in T cells leads to defects in priming, B cell help, germinal center reactions, and homeostatic expansion. *J Immunol.* 2004; 173(3):1612-1619.
22. Schmidt-Supprian M, Rajewsky K. Vagaries of conditional gene targeting. *Nat Immunol.* 2007; 8(7):665-668.
23. Fairfax KA, Kallies A, Nutt SL, Tarlinton DM. Plasma cell development: from B-cell subsets to long-term survival niches. *Semin Immunol.* 2008; 20(1):49-58.
24. Guinamard R, Okigaki M, Schlessinger J, Ravetch JV. Absence of marginal zone B cells in Pyk-2-deficient mice defines their role in the humoral response. *Nat Immunol.* 2000;1(1):31-36.
25. Allman D, Pillai S. Peripheral B-cell subsets. *Curr Opin Immunol.* 2008;20(2):149-157.
26. Casola S, Rajewsky K. B cell recruitment and selection in mouse GALT germinal centers. *Curr Top Microbiol Immunol.* 2006;308:155-171.
27. Bouaziz JD, Yanaba K, Tedder TF. Regulatory B cells as inhibitors of immune responses and inflammation. *Immunol Rev.* 2008;224:201-214.
28. Nishimoto N, Kishimoto T. Inhibition of IL-6 for the treatment of inflammatory diseases. *Curr Opin Pharmacol.* 2004;4(4):386-391.
29. Ehlers M, Fukuyama H, McGaha TL, Aderem A, Ravetch JV. TLR9/MyD88 signaling is required for class switching to pathogenic IgG2a and 2b autoantibodies in SLE. *J Exp Med.* 2006;203(3): 553-561.
30. Vinuesa CG, Sanz I, Cook MC. Dysregulation of germinal centres in autoimmune disease. *Nat Rev Immunol.* 2009;9(12):845-857.
31. Hiroi T, Yanagita M, Ohta N, Sakaue G, Kiyono H. IL-15 and IL-15 receptor selectively regulate differentiation of common mucosal immune system-independent B-1 cells for IgA responses. *J Immunol.* 2000;165(8):4329-4337.
32. Cancro MP, Hao Y, Scholz JL, et al. B cells and aging: molecules and mechanisms. *Trends Immunol.* 2009;30(7):313-318.
33. Tsantikos E, Oracki SA, Quilici C, Anderson GP, Tarlinton DM, Hibbs ML. Autoimmune disease in Lyn-deficient mice is dependent on an inflammatory environment established by IL-6. *J Immunol.* 2010;184(3):1348-1360.
34. Kimura A, Kishimoto T. IL-6: regulator of Treg/Th17 balance. *Eur J Immunol.* 2010;40(7):1830-1835.
35. Pasare C, Medzhitov R. Toll pathway-dependent blockade of CD4+CD25+ T cell-mediated suppression by dendritic cells. *Science.* 2003; 299(5609):1033-1036.
36. Abe J, Ueha S, Suzuki J, Tokano Y, Matsushima K, Ishikawa S. Increased Foxp3(+) CD4(+) regulatory T cells with intact suppressive activity but altered cellular localization in murine lupus. *Am J Pathol.* 2008;173(6):1682-1692.
37. Tavares RM, Turer EE, Liu CL, et al. The ubiquitin modifying enzyme A20 restricts B cell survival and prevents autoimmunity. *Immunity.* 2010; 33(2):181-191.
38. Shoenfeld Y, Toubi E. Protective autoantibodies: role in homeostasis, clinical importance, and therapeutic potential. *Arthritis Rheum.* 2005; 52(9):2599-2606.
39. Witte T. IgM antibodies against dsDNA in SLE. *Clin Rev Allergy Immunol.* 2008;34(3):345-347.
40. Font J, Cervera R, Lopez-Soto A, et al. Anticardiolipin antibodies in patients with autoimmune diseases: isotype distribution and clinical associations. *Clin Rheumatol.* 1989;8(4):475-483.
41. Kishimoto T. IL-6: from its discovery to clinical applications. *Int Immunol.* 2010;22(5):347-352.

Cell purification and flow cytometry
The purification of lymphocyte and leukocyte subsets was achieved by a two step procedure. Splenic cell suspensions were first separated into CD43-expressing and CD43-negative fractions by MACS (Miltenyi). The CD43-negative fraction was stained with antibodies against B220 (eBioscience) and CD19 (eBioscience) and $B220^{+}CD19^{+}$ B cells were purified using a FACSAria (BD). The CD43-positive fraction was stained with antibodies against B220, TCRβ, CD11c, Gr-1 and Mac1 (all eBioscience). The following subsets were purified by FACS: T cells ($B220^{-}TCR\beta^{+}$), dendritic cells ($B220^{-}TCR\beta^{-}CD11c^{+}$), granulocytes ($B220^{-}TCR\beta^{-}CD11c^{-}Gr1^{+}Mac1^{lo}$) and macrophages ($B220^{-}TCR\beta^{-}CD11c^{-}Gr1^{lo}Mac1^{hi}$). All cell populations were over 99% pure.

For intracellular ex vivo IL-6 stainings of lymphocytes and leukocyte subsets, cells were stimulated for 5 h at 37°C with 10 nM brefeldin-A (Applichem).

PCR to identify A20 knock-out cells
PCR was performed using the primers a (CATTTAACCCTTCTGAGTTTCCA), b (CCGGGCTTTAACCACTCTC), c (CCACCCCTATTACTACGTGACC) and the following touchdown program: (1) 95°C 3min, (2) 95°C 30s, (3) 65°C 45s, (4) 72°C 60s, while steps (2)–(4) are repeated 10 times, the annealing temperature is decreased by 1°C/cycle, until 55°C is reached; (5) 95°C 30s, (6) 55°C 45s, (7) 72°C 60s, (5)–(7) are repeated 20 times; (8) 72°C 5min, (9) 4°C 15min. The PCR was conducted with either all three primers or only two (b, c) to specifically amplify the A20-knockout allele. PCR was performed on DNA isolated from the purified cell subsets. To estimate the sensitivity of the PCR for the knockout allele, we diluted DNA from CD19cre/$A20^{F/F}$ B cells at different ratios in DNA from $A20^{F/F}$ macrophages.

Immunohistochemistry
Spleen, kidney, liver were fixed in 4% PFA, processed, and embedded in paraffin. 2-µm sections for PAS stainings were prepared according to routine protocols. For the detection of tissue-specific autoantibodies, frozen sections from organs of *Rag2*$^{-/-}$ mice were incubated with sera of aged and control mice and an anti–mouse IgG–Cy3 conjugate (Jackson ImmunoResearch).

Table S1. Immunoglobulin titers in young mice

IgM			IgG1			IgG2c			IgG2b			IgG3			IgA		
KO	**Het**	**WT**	**KO**	**Het**	**WT**	**KO**	**Het**	**WT**	**KO**	**Het**	**WT**	**KO**	**Het**	**WT**	**KO**	**Het**	**WT**
841	150	31	66	81	178	56	71	59	3493	1178	981	2959	10141	9547	480439	1923	3237
131	70	71	33	72	80	32	47	46	1588	4593	3269	1177	9541	9553	285393	6048	8266
4220	121	81	97	82	66	42	41	46	2886	4480	2141	5473	10099	8299	124031	1923	5450
581	71	41	96	94	198	39	49	37	2815	3059	1301	2389	9961	6361	137648	327	3593
581	50	21	70	61	194	45	45	41	2123	4868	965	3235	2287	9421	351497	753	1733
201	90	90	53	122	115	52	44	25	544	1874	896	7495	9829	9787	3237	194	2628
63	75	14	6	66	31				482	479	467						
73	79	12	6	30	60				446	470	469						
172	63	8	10	63	25				483	478	449						
85	49	20	7	28	29				485	455	464						
70	52	54	10	49	54				455	485	414						
69	116	10	8	71	32				494	488	442						
216	***77***	***28***	***22***	***63***	***68***	***44***	***49***	***41***	***957***	***1187***	***796***	***3214***	***7762***	***8734***	***117737***	***1012***	***3655***

Numbers represent individual values (μg/ml) as determined by ELISA. Geometric means are shown in bold and italics in the last row.
KO = CD19cre/A20$^{F/F}$, Het = CD19cre/A20$^{F/Wt}$, WT = A × CD19cre; B × other.

Table S2. Immunoglobulin titers in old mice

IgM		IgG1		IgG2c		IgG2b		IgG3		IgA	
KO	WT	KO	WT	KO	WT	KO	WT	KO	WT	KO	WT
95	36	16	56	17	10	1085	346	7912	9512	26417	24875
97	40	36	43	10	18	991	552	5752	23912	21417	8208
116	37	64	73	14	17	956	239	38552	5192	4750	18625
59	59	69	58	14	7	615	385	2952	16472	24750	16958
80	28	50	56	9	7	249	506	5432	20952	23083	10708
57	70	37	41	8	7	403	266	1752	2312	23917	10292
124	38	48	41	19	19	828	737	312	4632	23917	19875
122	60	6	46	11	17	920	917	7512	9832	18917	3208
104	87	16	43	6	16	544	616	4232	19752	28917	26542
107	53	33	42	6	11	781	196	10472	20232	23917	8208
82	49	10	39	13	13	928	648	6552	10712	16417	
95		37		9	4	598	54	5192		8083	
92	***48***	***28***	***48***	***10***	***11***	***689***	***371***	***4861***	***10568***	***18419***	***12573***

Numbers represent individual values (μg/ml) as determined by ELISA. Geometric means are shown in bold and italics in the last row.
KO = CD19cre/A20$^{F/F}$, WT = A × CD19cre; B × other.

Figure S1. Loss of A20 B-lineage cells leads to decreased numbers of recirculating B cells in the bone marrow

(A) Scheme of B cell development and developmental time-frame (depicted as arrow), during which Mb1cre and CD19cre mouse strains express the cre recombinase. CD19cre induces partial recombination in preB and immature B cells: dotted line. (B) Representative spleen sizes of 8–12-week-old age-matched mice. (C) Representative dotplots showing proportions of pre/pro ($B220^{+}IgM^{-}$), immature ($B220^{lo}IgM^{+}$) and mature/recirculating ($B220^{hi}IgM^{+}$) B cells of lymphocytes (upper panels) and pro (proB: $CD25^{-}$c-Kit^{+}) and pre (preB: $CD25^{+}$c-Kit^{-}) B cells of $B220^{+}IgM^{-}$ cells (lower panels) in the bone marrow. (D) Absolute cell numbers of lymphocyte subsets in the bone marrow: total bone marrow cells, B cells ($B220^{+}$), proB, preB, immature B and recirculating B cells (defined as in C). Values represent means and s.d. calculated from 5–6 mice per genotype. (E) Effects of Mb1cre-mediated ablation of A20 on B-lineage cells in the bone marrow: upper two sets of panels as in (C), lower panels: percentages of large ($B220^{hi}IgM^{+}CD25^{+}$c-$Kit^{-}FSC^{hi}$) preB of total preB cells. * = $p < 0.05$; ** = $p < 0.001$; one-way anova

Figure S2. Loss of A20 B-lineage cells leads to an accumulation of transitional B cells in the spleen

(A) Representative dotplots showing proportions (left) and bar charts with absolute cell numbers (right) of $B220^{+}AA4.1^{+}$ transitional B cell subsets in the spleen: $IgM^{hi}CD23^{-}$ T1, $IgM^{hi}CD23^{+}$ T2 and $IgM^{lo}CD23^{+}$ T3 (anergic). Values represent means and s.d. calculated from 5–6 mice per genotype. (B) Upper panels: representative dotplots showing proportions of $CD19^{+}CD21^{hi}CD1d^{hi}$ B cells in the spleen: $CD23^{lo}$ MZ and $CD23^{hi}$ MZ precursor B cells. Values represent means and s.d. calculated from 5–6 mice per genotype. Lower panels: immunofluorescence of spleen sections demonstrating the marginal sinus (depicted as dotted yellow line) as border between the marginal and follicular zone: green = αB220, B cells; red = αCD3, T cells; blue = laminin. Magnification: 20×. (C) Representative dotplots showing proportions of IL-10 producing B cells ($B220^{+}IL10^{+}$) after 5h stimulation with PMA/ionomycin/BFA/LPS. Values represent means and s.d. of 3 mice per genotype. (D) Representative dotplots showing proportions of B cells in the thymus ($B220^{+}TCR\beta^{-}$). Values represent means and s.d. of 3 mice per genotype. (E) Representative dotplots showing proportions of B cell subsets in the peritoneal cavity (absolute cell numbers are shown in Fig. 2B): $B220^{hi}CD19^{+}$ B2 and $B220^{lo}CD19^{hi}$ B1 cells of total lymphocytes (upper panels) and $CD43^{lo}CD5^{-}$ B1b and $CD43^{+}CD5^{+}$ B1a cells of B1 cells (lower panels). * = $p < 0.05$; ** = $p < 0.001$; one-way anova

Figure S3. Fidelity of CD19cre for specific recombination of conditional A20 alleles only in B cells

(A) Scheme of the conditional A20 allele before (upper panel) and after (lower panel) cre-mediated recombination. The location of the primers (a–c) employed for the genotyping PCR are shown and the length of the respective PCR amplification products. Squares indicate exons (E3–E7) and triangles loxP sites. (B) Upper panels: representative PCR results for two PCR reactions on DNA from purified splenic cell subsets: the three primer PCR (a, b, c) amplifies A20 loxP-flanked and knockout alleles,

whereas the two primer PCR (a, c) amplifies only DNA from A20-knockout alleles. Splenic cell subsets (T cells = $B220^{-}TCR\beta^{+}$, dendritic cells/DC = $B220^{-}TCR\beta^{-}CD11c^{+}$, macrophages/Mac = $B220^{-}TCR\beta^{-}CD11c^{-}Gr1^{lo}Mac1^{hi}$ and granulocytes/Gr = $B220^{-}TCR\beta^{-}CD11c^{-}Gr1^{+}Mac1^{lo}$) were MACS purified followed by cell sorting and were over 99% pure. Identical results were obtained for all the cellular subsets sorted from three individual CD19cre/$A20^{F/F}$ mice. Lower panels: evaluation of the sensitivity of the two PCRs. A20-knockout cells were diluted at different ratios with $A20^{F/F}$ cells. The PCRs are able to amplify the knockout allele at a dilution of 1 to 500. The amplification product for the knockout allele that could be observed with the DNA from purified T cells, DCs, macrophages and granulocyte was weaker than the amplification product from the 1:500 A20-knockout to $A20^{F/F}$ dilution in all cases. This band therefore represents most likely the presence of less than 0.2% contaminating B cells in the respective purified cell-type. However, this analysis does not allow us to rule out the presence of less than 0.2% A20-knockout cells within each cell-type.

Figure S4. A20 regulates B cell activation in a dose-dependent fashion
(A) Realtime PCR quantifying the amount of A20 mRNA relative to PBGD mRNA in wild-type B cells stimulated with the indicated mitogens for 1, 4 and 12 h. Means and s.d. of triplicate measurements are shown. (B) Expression levels of the B cell activation marker after o/n stimulation with αIgM, LPS, CpG or αCD40. The dotplots are representative of 3 independent experiments. (C) Assessment of proliferation by the CFSE dilution assay: histograms show CFSE intensities 3 days after stimulation with the indicated mitogens. The table depicts the proliferation index (Proliferation index: average number of divisions of the proliferating cells), the percentage of dividing cells (% Divided: the proportion of cells that initially started to divide) and the division index (Div. Index: average number of divisions of all cells). Numbers represent the means of 3 to 4 (αCD40/IL-4) independent experiments. (D) IL-6 levels were measured in the supernatant after o/n stimulation with αIgM, LPS, CpG or αCD40. (E) Representative dotplots showing proportions of TNFα- or IL-6–producing B cells ($B220^{+}$ $TNF\alpha^{+}$ or $B220^{+}$ $IL\text{-}6^{+}$) after 5h stimulation with PMA/ionomycin/BFA. Values represent means and s.d. of 3 mice per genotype.

Figure S5. IL-6 producing cell-types in CD19cre/$A20^{F/F}$ mice
(A) Realtime PCR analysis of IL-6 expression in FACS-purified splenic cell subsets of CD19cre/$A20^{F/F}$ and CD19cre control mice. Splenic cell subsets (T cells = $B220^{-}TCR\beta^{+}$, dendritic cells/DC = $B220^{-}TCR\beta^{-}CD11c^{+}$, macrophages/Mac = $B220^{-}TCR\beta^{-}CD11c^{-}Gr1^{lo}Mac1^{hi}$ and granulocytes/Gr = $B220^{-}TCR\beta^{-}CD11c^{-}Gr1^{+}Mac1^{lo}$) were MACS purified followed by cell sorting and were over 99% pure. IL6 cDNA was quantified relative to PBGD. Values represent means and s.d. of 3 independent experiments. (B) Proportions of IL-6 expressing cells of individual immune cell subsets in the spleen of CD19cre/$A20^{F/F}$ and CD19cre control mice identified by intracellular FACS. Values represent means and s.d. of 3 independent experiments.

Figure S6. Chronic inflammation and autoreactivity in aged $B^{A20-/-}$ mice
(A) Representative spleen size of old CD19cre/$A20^{F/F}$ and age-matched CD19cre control mice. (B) Spleen weight (n($B^{A20-/-}$) = 10, n(control) = 9). (C) Representative dotplot showing proportions of plasma cells ($B220^{lo}CD138^{hi}$), mean and s.d. for n = 9 mice per genotype are shown. (D) Representative PAS stainings of liver and kidney sections from aged mice. Magnification: 10×. (E) Representative immunofluorescence staining of tissue-specific IgG autoantibodies directed against kidney, harderian gland, stomach and lacrimal gland. Staining was performed by incubating sera from aged mice on sections of tissues isolated from $Rag2^{-/-}$ mice. Magnification: 20×.

Fig. S1

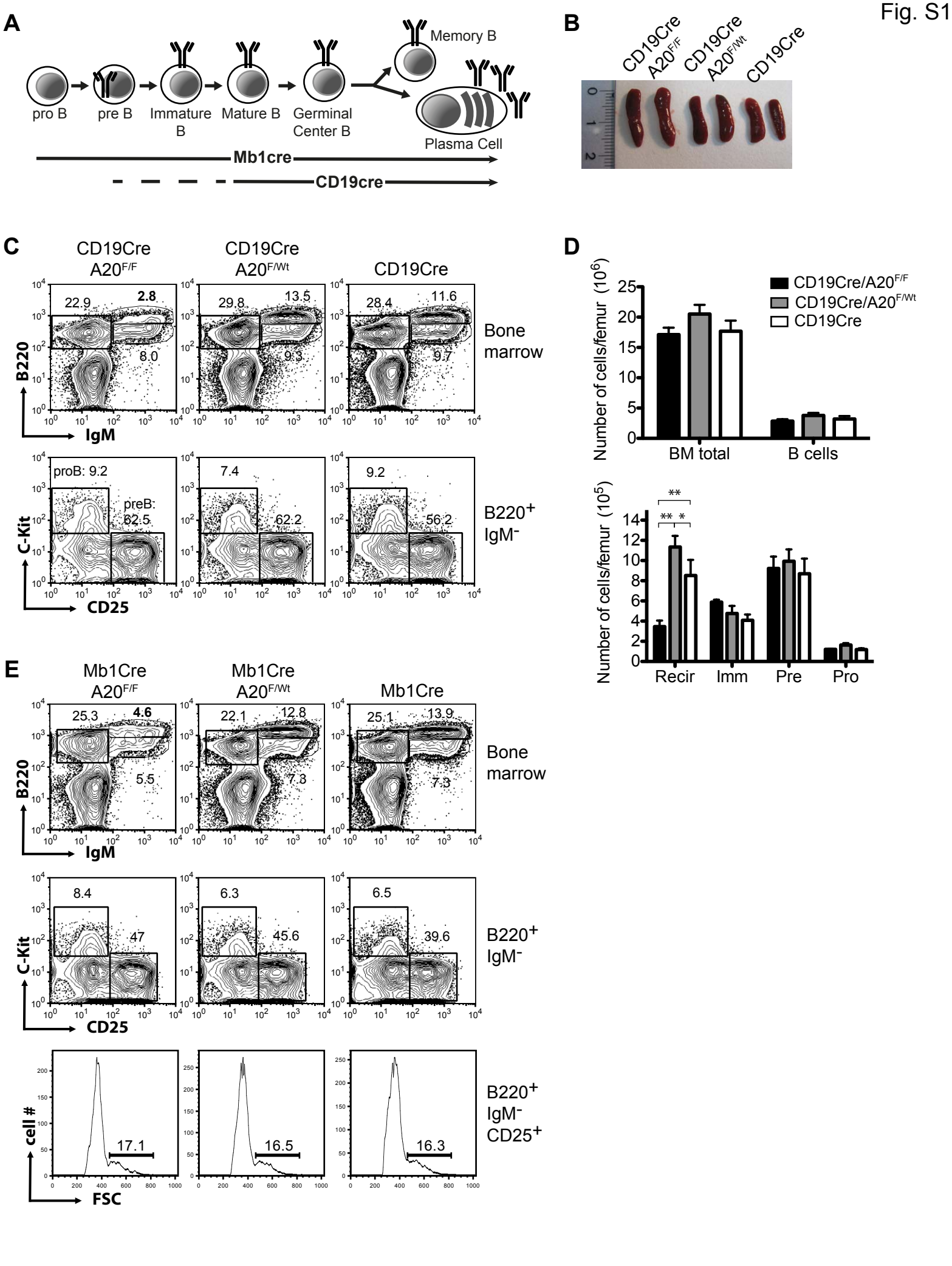
A
pro B
pre B
Immature B
Mature B
Germinal Center B
Memory B
Plasma Cell
Mb1cre
CD19cre
B
CD19Cre A20F/F
CD19Cre A20F/Wt
CD19Cre
C
CD19Cre A20F/F
CD19Cre A20F/Wt
CD19Cre
22.9
2.8
8.0
29.8
13.5
9.3
28.4
11.6
9.7
Bone marrow
B220
IgM
proB: 9.2
preB: 62.5
7.4
62.2
9.2
56.2
B220+ IgM-
C-Kit
CD25
D
CD19Cre/A20F/F
CD19Cre/A20F/Wt
CD19Cre
Number of cells/femur (10^6)
BM total
B cells
Number of cells/femur (10^5)
Recir
Imm
Pre
Pro
E
Mb1Cre A20F/F
Mb1Cre A20F/Wt
Mb1Cre
25.3
4.6
5.5
22.1
12.8
7.3
25.1
13.9
7.3
Bone marrow
8.4
47
6.3
45.6
6.5
39.6
B220+ IgM-
17.1
16.5
16.3
B220+ IgM- CD25+
cell #
FSC

A

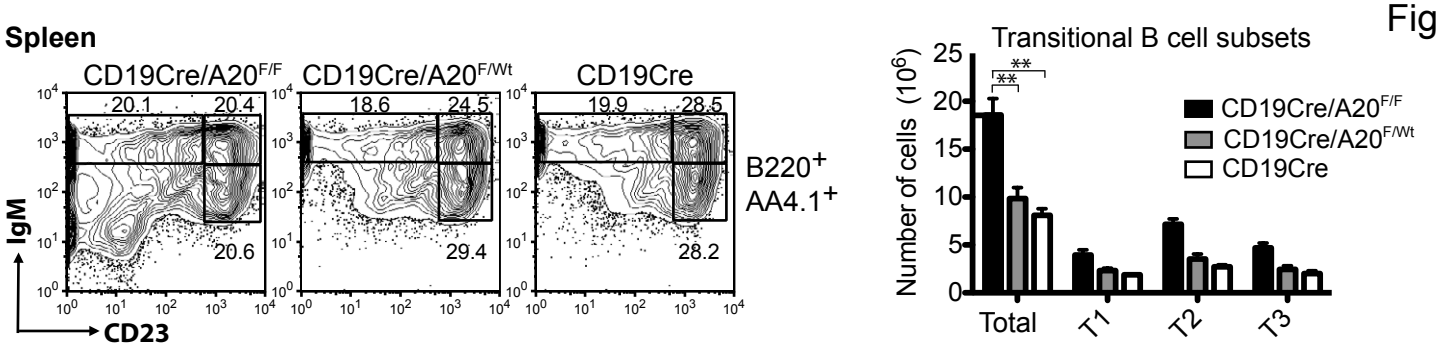
Spleen
CD19Cre/A20F/F
CD19Cre/A20F/Wt
CD19Cre
20.1
20.4
20.6
18.6
24.5
29.4
19.9
28.5
28.2
IgM
CD23
B220+
AA4.1+
Transitional B cell subsets
Number of cells (10^6)
**
**
CD19Cre/A20F/F
CD19Cre/A20F/Wt
CD19Cre
Total
T1
T2
T3

B

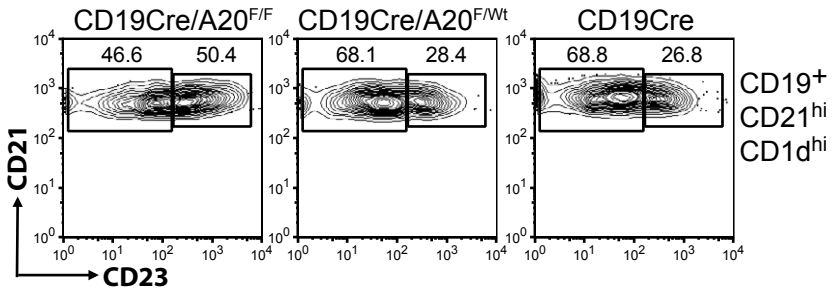
Spleen
CD19Cre/A20F/F
CD19Cre/A20F/Wt
CD19Cre
46.6
50.4
68.1
28.4
68.8
26.8
CD21
CD23
CD19+
CD21hi
CD1dhi

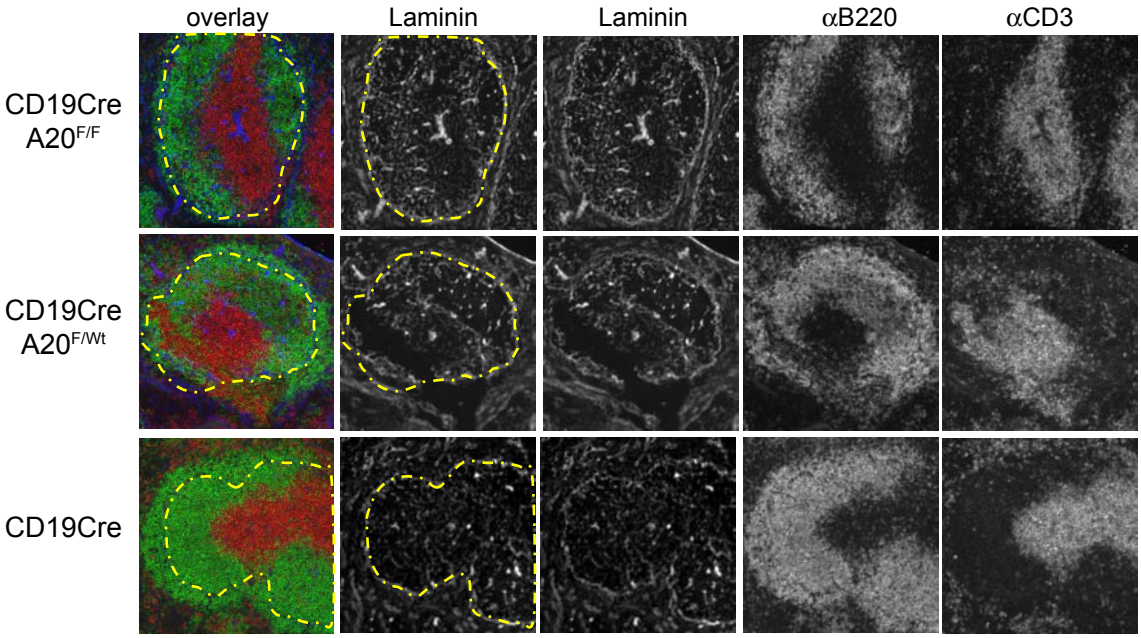
overlay
Laminin
Laminin
αB220
αCD3
CD19Cre
A20F/F
CD19Cre
A20F/Wt
CD19Cre

C

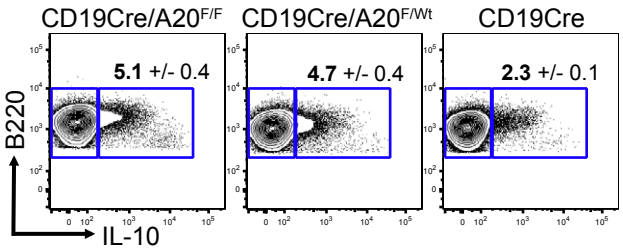
Spleen
CD19Cre/A20F/F
CD19Cre/A20F/Wt
CD19Cre
5.1 +/- 0.4
4.7 +/- 0.4
2.3 +/- 0.1
B220
IL-10

D

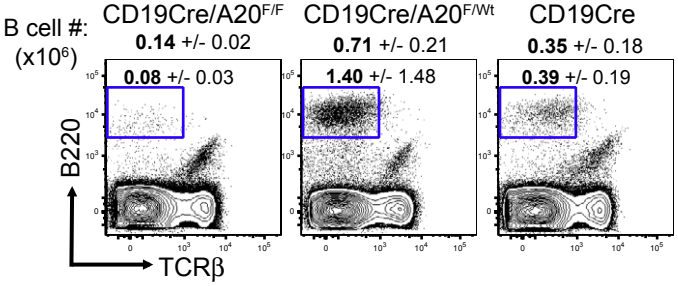
Thymus
B cell #:
(x10^6)
CD19Cre/A20F/F
CD19Cre/A20F/Wt
CD19Cre
0.14 +/- 0.02
0.71 +/- 0.21
0.35 +/- 0.18
0.08 +/- 0.03
1.40 +/- 1.48
0.39 +/- 0.19
B220
TCRβ

E

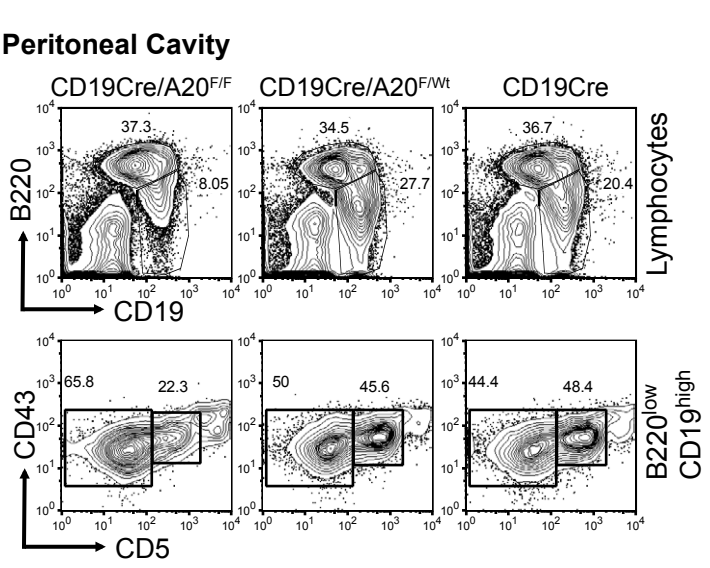
Peritoneal Cavity
CD19Cre/A20F/F
CD19Cre/A20F/Wt
CD19Cre
37.3
8.05
34.5
27.7
36.7
20.4
B220
CD19
Lymphocytes
65.8
22.3
50
45.6
44.4
48.4
CD43
CD5
B220low
CD19high

Fig. S3

A

loxP-flanked A20 allele

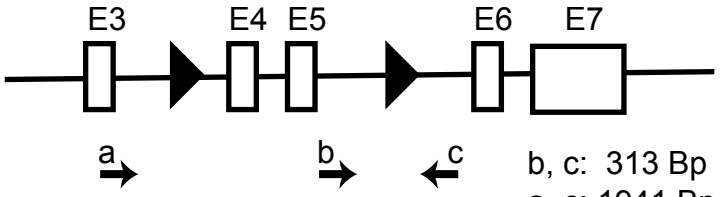

b, c: 313 Bp
a, c: 1941 Bp, not amplified

A20-knockout allele

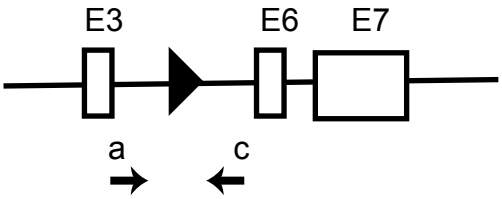

a, c: 210 Bp

B

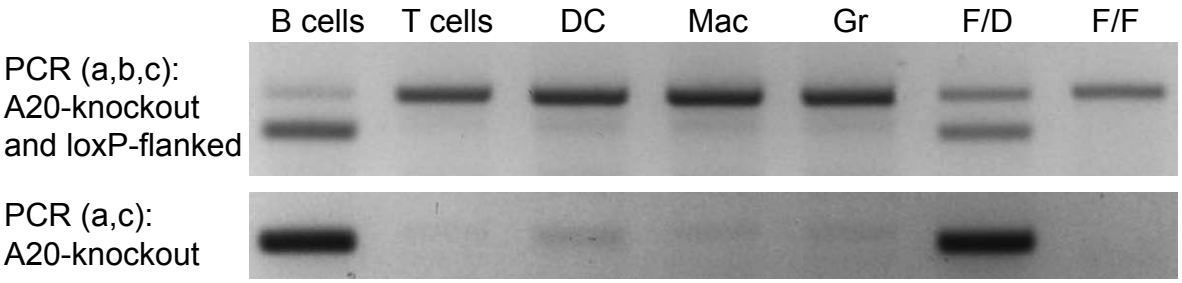

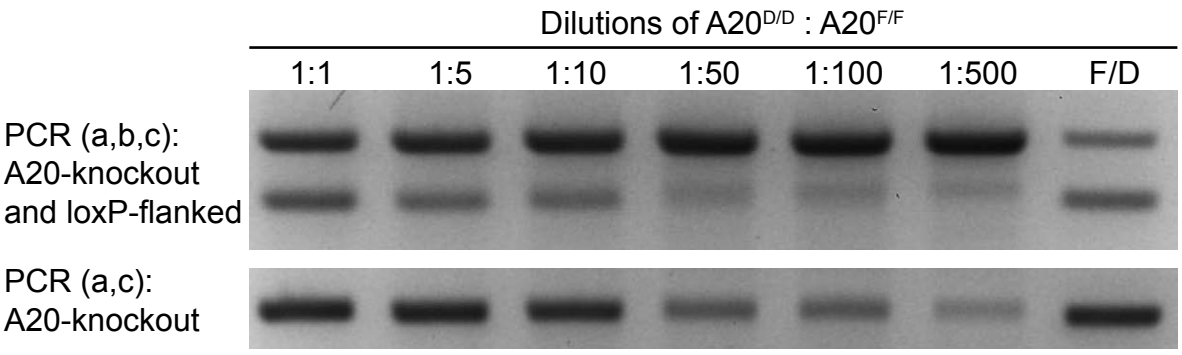

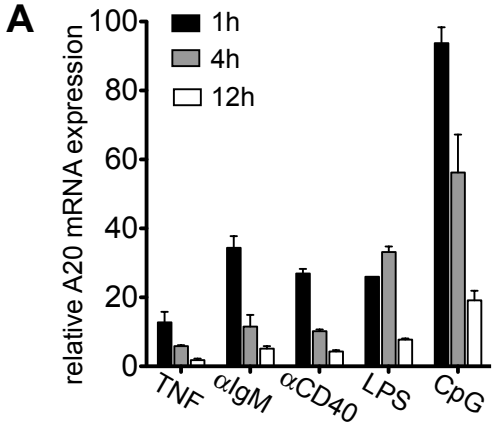

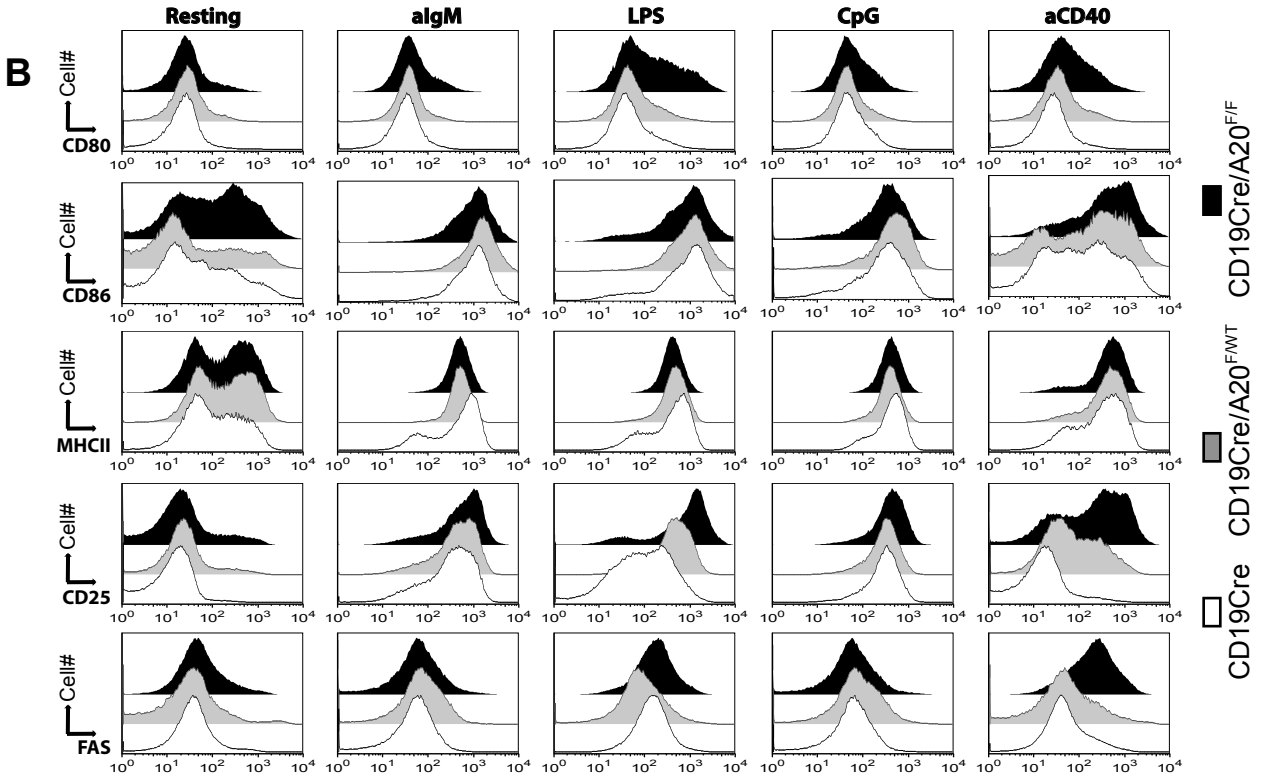

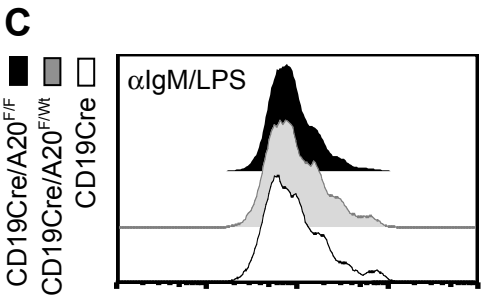

		CD19Cre	A20F/F	A20F/Wt	WT
αIgM/IL-4	Prol. Index	1.9	1.6	1.5
	% Divided	90	94	92
	Div. Index	1.9	1.7	1.7
αCD40/IL-4	Prol. Index	1.4	1.2	1.2
	% Divided	66	24	34
	Div. Index	0.9	0.3	0.4
LPS/IL-4	Prol. Index	2.2	2.1	2.2
	% Divided	86	76	70
	Div. Index	1.9	1.6	1.5
αIgM/LPS	Prol. Index	2.2	2.3	2.4
	% Divided	89	95	94
	Div. Index	2.0	2.2	2.2

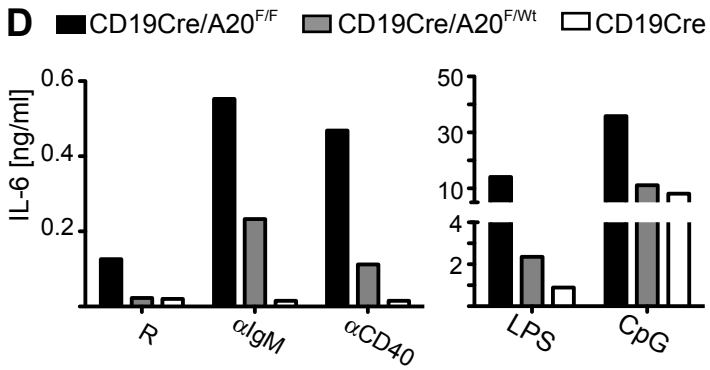

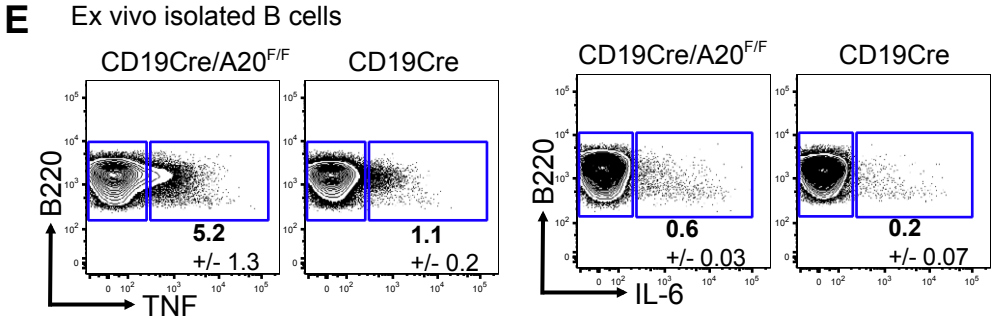

Fig. S5

A

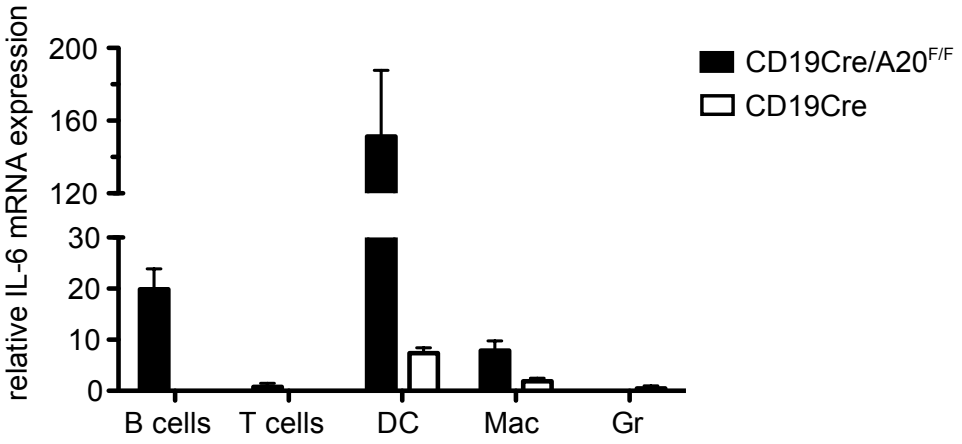
relative IL-6 mRNA expression
200
160
120
30
20
10
0
B cells
T cells
DC
Mac
Gr
CD19Cre/A20F/F
CD19Cre

B

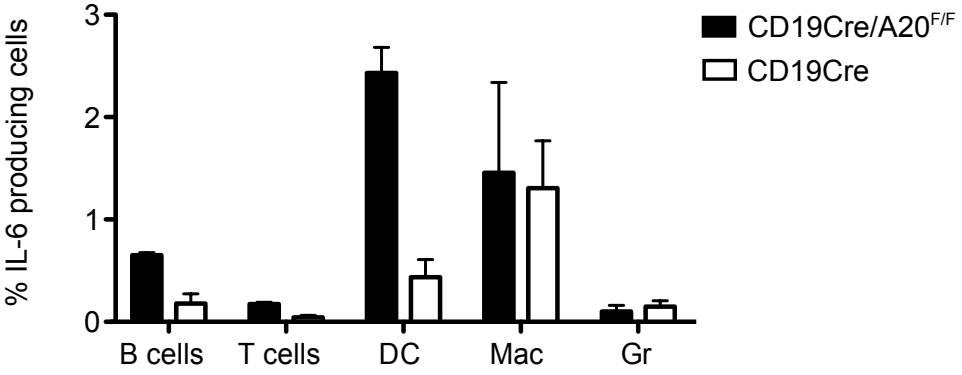
% IL-6 producing cells
3
2
1
0
B cells
T cells
DC
Mac
Gr
CD19Cre/A20F/F
CD19Cre

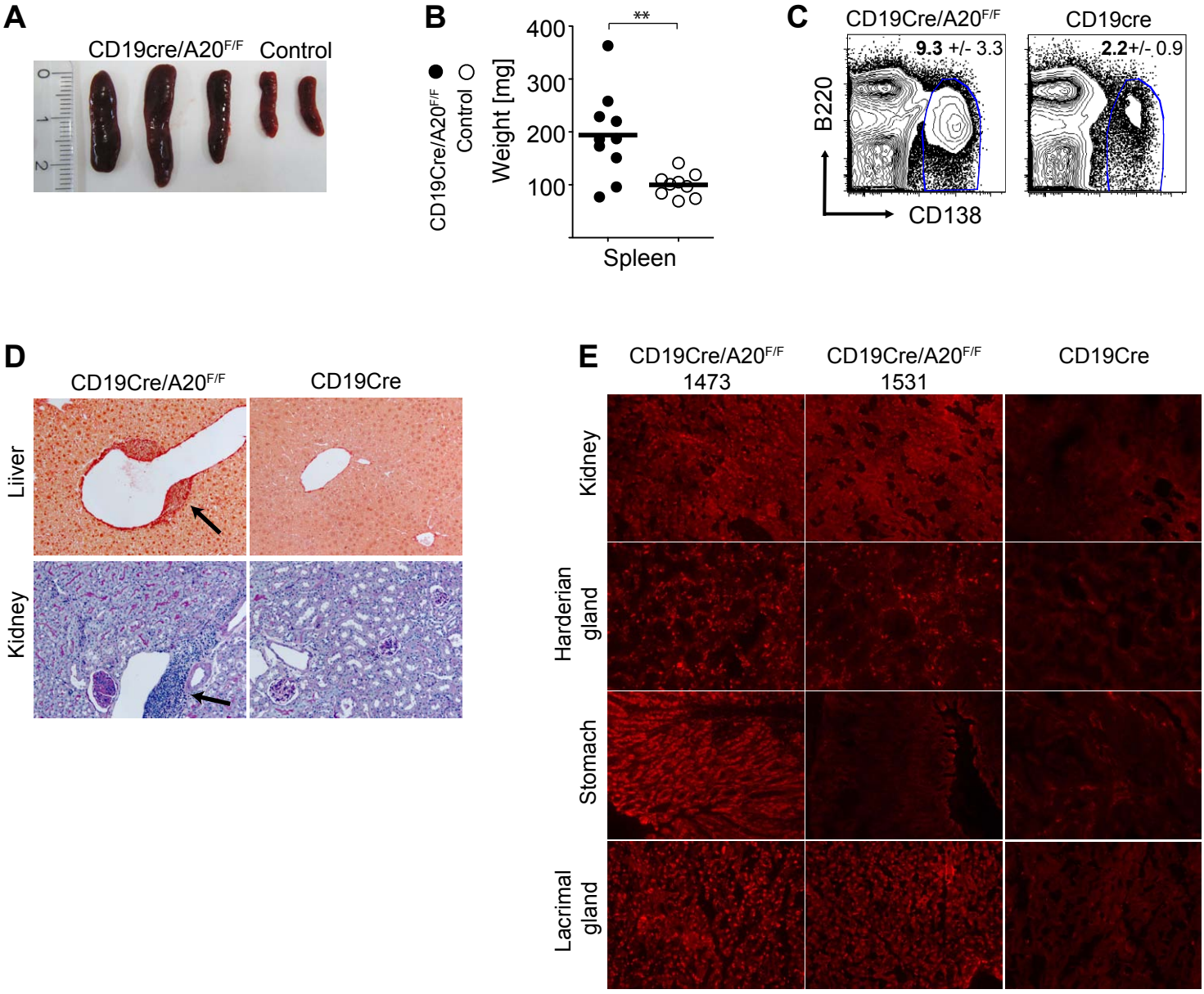
A
CD19cre/A20F/F
Control
B
CD19Cre/A20F/F
Control
Weight [mg]
400
300
200
100
**
Spleen
C
CD19Cre/A20F/F
CD19cre
9.3 +/- 3.3
2.2+/-. 0.9
B220
CD138
D
CD19Cre/A20F/F
CD19Cre
Liiver
Kidney
E
CD19Cre/A20F/F
1473
CD19Cre/A20F/F
1531
CD19Cre
Kidney
Harderian gland
Stomach
Lacrimal gland